Université de Haute-Alsace
Faculté des Sciences et Techniques

Habilitation à Diriger des Recherches
Discipline : Mathématiques

Couplage d'équations et résolution numérique des problèmes d'interaction fluide-structure

Cornel Marius MUREA

Date de soutenance : le 8 février 2007

Jury :

B. BRIGHI	Professeur à l'Université de Haute-Alsace, Directeur
G.-H. COTTET	Professeur à l'Université Joseph Fourier, Grenoble, Rapporteur
J.-M. CROLET	Professeur à l'Université de Franche-Comté, Président
J.Y. DREAN	Professeur à l'Université de Haute-Alsace, Rapporteur interne
L. FORMAGGIA	Professeur à Politecnico di Milano, Rapporteur
M. SOULI	Professeur à l'Université de Lille, Rapporteur

À ma fille Marie-Laetitia,
avec amour et tendresse

Remerciements

Je remercie Monsieur G.-H. Cottet, Professeur à l'Université Joseph Fourier, Grenoble, Monsieur L. Formaggia, Professeur à Politecnico di Milano, Monsieur M. Souli, Professeur à l'Université de Lille pour l'honneur qu'ils m'ont fait en acceptant de juger mon travail en qualité de rapporteurs. Je remercie également Monsieur J.Y. Drean, Professeur à l'Université de Haute-Alsace, d'avoir accepté la tache difficile d'évaluer ce travail en tant que rapporteur interne.

La présence dans le jury de Monsieur J.-M. Crolet, Professeur à l'Université de Franche-Comté est à la fois un honneur et un plaisir. Je le remercie chaleureusement d'avoir accepté de présider le jury.

Je remercie Monsieur B. Brighi, Professeur à l'Université de Haute-Alsace, qui m'a accordé sa confiance en se portant garant scientifique de mes travaux. Je le remercie pour sa gentillesse et son aide.

Je suis très reconnaissant envers Monsieur Yvon Maday, Professeur à l'Université Pierre et Marie Curie, pour l'accueil qu'il m'a réservé pendant le post-doc et pour m'avoir donné des précieux conseils pendant les premières écoles d'été CEMRACS et à l'occasion de colloques à Nice et Evian.

Je souhaite remercie également en tant que co-auteurs Monsieur C. Vázquez (La Coruña), Monsieur G. Hentschel (Atlanta), Monsieur Th. Hangan (Mulhouse) et Monsieur I. Mbaye (Mulhouse) avec lesquels il a été très agréable de travailler.

Je tiens à remercier tous mes collègues de Mulhouse pour la bonne ambiance.

Je remercie ma femme Silvia pour son soutien et son aide. Je dédie ce travail à ma fille Marie-Laetitia qui me rend le plus heureux des papas.

Je remercie ma mère et ma soeur pour leur soutien et leur encouragements.

Contents

Synthèse[1]

Les premiers quatre chapitres traitent de l'interaction fluide-structure stationnaire. On étudie l'interaction évolutive en temps dans les chapitres cinq et six. Les deux derniers chapitres sont consacrés aux écoulements à frontière libre avec tension de surface qui ont certaines similitudes avec les problèmes d'interaction fluide-structure.

Exemples d'interaction fluide-structure

Dans ce travail on étudie l'interaction entre un fluide incompressible et une structure élastique. D'une coté, le déplacement de la structure dépend des forces de surface exercées par le fluide. De l'autre coté, le domaine occupé par le fluide dépend du déplacement de la structure et les vitesses et la pression du fluide dépendent de la vitesse de l'interface ou des forces de surface exercées par la structure. Donc, le domaine occupé par le fluide est inconnu a priori. On précise que la structure n'est pas rigide.

L'interaction fluide-structure concerne multiples activités comme par exemple :

- **bio-mécanique** (écoulement du sang dans les artères, conception des coeurs artificiels),
- **construction d'automobiles** (absorbeur des chocs hydrauliques, conception des senseurs, lubrification),
- **génie civil** (oscillations des longs ponts ou des hautes structures métalliques sous l'action du vent),
- **aero-élasticité** (déformation des ailes d'avion).

Modèles géométriques et mathématiques

Dans le premier chapitre on étudie l'écoulement externe tridimensionnel autour d'un câble cylindrique déformable qui est fixé aux extrémités.

[1]Pour marquer la différence, mes travaux sont cités dans la synthèse de la manière "chapitre 1", "chapitre 2", etc. Les autres références bibliographiques sont cités [1], [2], etc.

Les chapitres deux, trois, quatre, cinq traitent de l'écoulement bidimensionnel dans un canal qui a une paroi élastique.

On suppose que le fluide est gouverné par : les équations de Stokes stationnaires (chapitres 1–4) ou Navier-Stokes d'évolution (chapitre 5). Pour la structure on utilise des modèles de type : poutre dans les chapitres 1–4 (voir [38])

$$EI\frac{\partial^4 u}{\partial x_1^4}(x_1) = \eta(x_1), \quad x_1 \in (0, L)$$

ou plaque dans le chapitre 5 (voir [18])

$$\rho^S h^S \frac{\partial^2 u}{\partial t^2}(x_1, t) + \frac{E(h^S)^3}{12(1-\nu^2)}\frac{\partial^4 u}{\partial x_1^4}(x_1, t) = \eta(x_1, t), \quad (x_1, t) \in (0, L) \times (0, T).$$

Ce dernier modèle est bien adapté aux structures minces en flexion.

L'interaction évolutive en temps entre les équations bidimensionnelles de Navier Stokes et une poutre élastique a été étudié en [24].

Pour la simulation bidimensionnelle de l'écoulement du sang dans les artères, les équations de Navier-Stokes en coordonnées axisymétriques couplées avec un modèle monodimensionnel de type membrane axisymétrique

$$\rho^S h^S \frac{\partial^2 u}{\partial t^2}(x_1, t) - h^S Gk\frac{\partial^2 u}{\partial x_1^2}(x_1, t) + \frac{Eh^S}{12(1-\nu^2)R^2}u(x_1, t) = \eta(x_1, t)$$

sont utilisées en [6], [15].

Dans [47], [48], [43] on ajoute un terme visco-élastique $\frac{\partial^3 u}{\partial x_1^2 \partial t}(x_1, t)$ au modèle de la structure, mais les équations bidimensionnelles de Navier-Stokes sont employées pour le fluide sans utiliser l'axisymétrie de la géométrie. Le terme visco-élastique est utilisé dans [42] pour obtenir l'estimation de l'énergie, dans [9] pour régulariser la solution et dans [15] pour stabiliser les schémas numériques.

Toujours pour des simulations bidimensionnelles, dans [10] les équations de Navier-Stokes axisymétriques sont utilisés pour le fluide alors que pour la structure, les équations de Navier bidimensionnelles sont employées sans utiliser l'axisymétrie de la géométrie.

Pour les simulations tridimensionnelles, les équations de Navier-Stokes sont couplées : avec des modèles monodimensionnels pour la structure sous l'hypothèse d'axisymétrie [29], avec des modèles bidimensionnels de type coques cylindriques [31] ou avec des équations d'élasticité linéaire tridimensionnelles [27]. Le dernier modèle est adapté quand la structure est épaisse, mais pour des structures minces et en grands déplacements, il faut prendre des modèles de type coque [39].

Domaines en mouvement

Dans les problèmes d'interaction fluide-structure, une méthode très utilisée pour prendre en compte le mouvement du domaine occupé par le fluide est le cadre ALE (Arbitrary

Lagrangian Eulerian) [48].

C'est la méthode employée dans les chapitres 1–5, avec la particularité suivante : quand la géométrie est simple, on peut utiliser une transformation ALE explicite qui facilite surtout l'étude de la sensibilité par rapport aux mouvements du domaine. En particulier, on peut obtenir la formulation exacte du jacobien de la transformation.

Le plus sauvent, on obtient la transformation ALE en minimisant une énergie de déformation d'un corps élastique [37], ou en supposant que chaque côté du maillage est un ressort [1]. Cette dernière méthode a été utilisée dans le chapitre 6.

D'autres cadres généraux pour résoudre les équations d'un fluide dans un domaine en mouvement sont : la frontière immergée [44], level set [49] et la méthode de la particule [13], [12].

Couplage d'équations

Les équations du fluide et celles de la structure sont couplées par deux types de conditions aux limites à l'interface

- continuité de vitesses : le fluide adhère aux parois ou d'une manière équivalente, les vitesses du fluide et de la structure sont égales à l'interface,
- continuité de forces de surface : les forces agissant à l'interface sur la structure sont égales et de sens contraire aux celles qui agissent sur le fluide.

Le fil directeur de mes travaux est de prendre comme "contrôle" une partie des conditions aux limites à l'interface et "d'observer" si les deux conditions de couplage sont vérifiées.

Dans le premier chapitre on étudie un problème stationnaire d'interaction fluide-câble en 3D. L'inconnue principale est la force de surface à l'interface $\boldsymbol{\lambda}$. On peut résoudre le problème structure et on trouve le déplacement u. On calcule ensuite la solution des équations de Stokes dans un domaine qui dépend de u avec des conditions aux limites de type Neumann à l'interface. On essaye à trouver $\boldsymbol{\lambda}$, tel que la vitesse du fluide à l'interface vérifie la condition de couplage Dirichlet dans le cas stationnaire $\mathbf{v}|_{\Gamma_u} = 0$. C'est un problème de type contrôlabilité où l'observation et le contrôle sont définies sur l'interface (voir Figure 1).

En utilisant une transformation ALE explicite et en traitant l'observation par la méthode de moindres carrés, on obtient un problème de type contrôle optimal où le contrôle se trouve dans les coefficients. La fonction coût à minimiser est

$$\inf \frac{1}{2} \left\| \widehat{v}|_{\Gamma_0} \right\|^2 .$$

Principalement, on prouve que la fonction coût est semi-continue inférieurement et en conséquence, on peut démontrer l'existence d'un contrôle optimal.

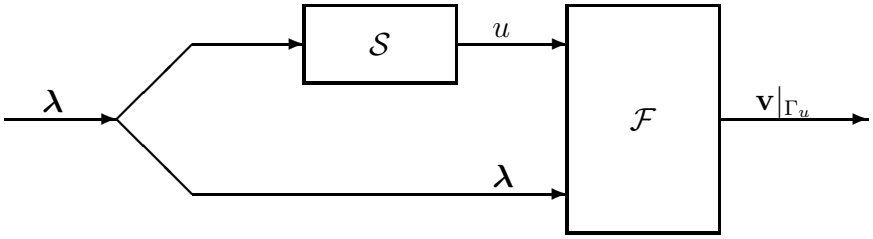

Figure 1: Schéma utilisé dans le chapitre 1

On utilise une démarche similaire dans le chapitre 2, où on résout le problème du fluide avec les conditions aux limites à l'interface

$$v_1 = 0, \quad e_2 \cdot \sigma^F \mathbf{n} = \lambda_2,$$

c'est à dire qu'on prescrit la composante horizontale de la vitesse du fluide et la composante verticale des forces de surface. On cherche a minimiser la composante verticale de la vitesse du fluide à l'interface (voir Figure 2).

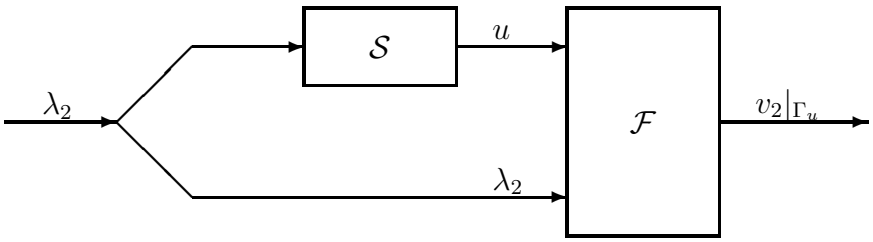

Figure 2: Schéma utilisé dans le chapitre 2

On prouve la différentiabilité de la fonction coût, et on donne la forme analytique du gradient. On présente également des résultats numériques.

Dans le chapitre 4, pour résoudre le problème du fluide, on prescrit la composante normale de la vitesse du fluide et la composante normale des forces de surface. C'est une formulation rarement utilisée pour résoudre les équations de Stokes. On cherche à minimiser la composante tangentielle de la vitesse du fluide à l'interface (voir Figure 3). On prouve que le problème fluide est bien défini et on présente des résultats numériques.

Dans les chapitres 3 (cas stationnaire) et 5 (cas d'évolution), en utilisant la décomposition modale $\boldsymbol{\alpha}$ des forces de surface à l'interface, on résout le problème structure. On calcule ensuite la vitesse $\mathbf{v}$ et la pression p du fluide en utilisant des conditions de Dirichlet sur la vitesse à l'interface. Les forces exercées par le fluide sur l'interface sont $\boldsymbol{\beta} = -\sigma^F(\mathbf{v}, p)\,\mathbf{n}$ (voir Figure 4). Le cadre de type point fixe est : trouver $\boldsymbol{\alpha} = \boldsymbol{\beta}$,

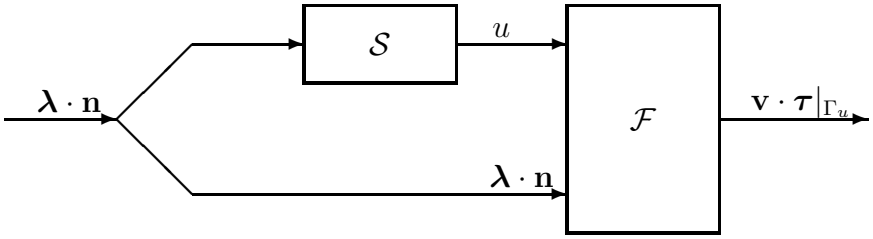

Figure 3: Schéma utilisé dans le chapitre 4

cependant nous considérons le problème sous la forme

$$\inf \frac{1}{2} \|\boldsymbol{\alpha} - \boldsymbol{\beta}\|^2 .$$

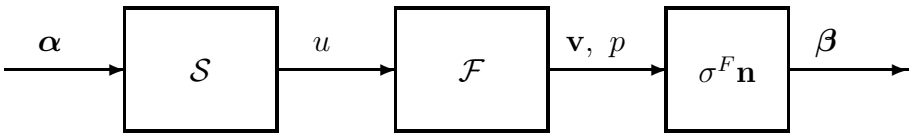

Figure 4: Schéma utilisé dans les chapitre 3 et 5

Dans le chapitre 3 on étudie la sensibilité du problème et on donne la forme analytique du gradient sans faire appel à l'état adjoint. Des résultats numériques sont obtenus.

Dans le chapitre 5, on doit résoudre à chaque pas de temps un problème de minimisation similaire à celui du chapitre 3. On présente des résultats numériques pour des pas de temps relativement grand. L'algorithme proposé est stable numériquement.

L'approche point fixe est généralement utilisée pour prouver l'existence d'une solution des problèmes d'interaction fluide structure (voir [32], [35], [2] pour le cas stationnaire et [34], [17], [4] pour le cas d'évolution). L'inconnue principale dans ces travaux est le déplacement de l'interface. Pour un modèle monodimensionnel l'existence a été prouvée en [19].

On n'a pas cité ici les résultats d'existence dans le cas où la structure est rigide et le mouvement est composé d'une translation et d'une rotation.

Points fixes, la méthode de Newton ou les moindres carrés ?

On va voir dans cette section différents algorithmes itératifs pour l'approximation du problème couplé fluide-structure.

Soit $G : \mathbb{R}^n \to \mathbb{R}^n$ une application non linéaire. Pour approcher les points fixes $G(x_*) = x_*$, on peut utiliser l'algorithme suivant

$$x_0 \in \mathbb{R}^n, \quad x_{k+1} = G(x_k). \tag{1}$$

Si l'application est une contraction et si x_0 est bien choisi, la suite $\{x_k\}$ converge linéairement.

On peut poser $F : \mathbb{R}^n \to \mathbb{R}^n$, $F(x) = x - G(x)$ et alors le problème $G(x_*) = x_*$ est équivalent à $F(x_*) = 0$. La méthode de Newton pour approcher les racines de F est :

$$x_0 \in \mathbb{R}^n, \quad x_{k+1} = x_k - \left(\nabla F(x_k)^T\right)^{-1} F(x_k). \tag{2}$$

Si la racine x_* de F existe, si le jacobien $\nabla F(x_*)^T$ est inversible et si x_0 est bien choisi, alors l'algorithme de Newton converge d'une manière quadratique.

Le principal désavantage des algorithmes 1 et 2 est que le point de départ x_0 doit être "proche" de la solution x_*.

Dans les problèmes d'interaction fluide-structure d'évolution, en général, on prend la solution ou une extrapolation des solutions au pas de temps précédent comme point de départ pour résoudre le problème couplé à l'instant de temps courant. Dans le chapitre 5, Figure 5.2 page 149 et Figure 5.6 page 153, on observe que $\|F(x_0)\|$ est très grand, qui veut dire que le point d'initialisation x_0 n'est pas "proche" de la solution x_*. Ce phénomène est dû à plusieurs facteurs :

- le fluide est très sensible au changement du domaine,
- le fluide est pulsatif, c'est-à-dire le débit a une croissance suivie d'une décroissance très importante dans un intervalle de temps court. C'est le cas d'écoulement sanguin, des chocs dans le système hydraulique d'une voiture, ou d'une explosion à l'intérieur d'un container métallique.
- le pas de la discrétisation en temps est agrandi.

La méthode de point fixe n'est pas applicable pour les problèmes de type contrôlabilité étudiés dans les chapitres 1, 2, 4 puisque le contrôle (par exemple les forces de surface à l'interface) et l'observation (les vitesses à l'interface) n'ont ni la même nature physique, ni la même régularité mathématique. Dans ce cas, on doit résoudre des problèmes non linéaires de type $F(x_*) = 0$ où $F : \mathbb{R}^m \to \mathbb{R}^n$ et $n, m \in \mathbb{N}$.

L'approche utilisé dans les chapitre 1–5 et de traiter l'observation par la méthode de moindres carrés et d'obtenir des problèmes d'optimisation du type

$$\inf_x f(x) = \frac{1}{2} \|F(x)\|^2 .$$

Dans ce cas particulier de la fonction coût et pour $n = m$, on a

$$\nabla f(x) = (\nabla F(x))\, F(x). \tag{3}$$

Pour résoudre numériquement le problème d'optimisation, on peut utiliser l'algorithme de Broyden, Fletcher, Goldforb, Shano (BFGS) :

Pas 0. Soient $x_0 \in \mathbb{R}^n$, H_0 une matrice symétrique positive définie et $\epsilon > 0$. On pose $k = 0$.

Pas 1. $\nabla f(x_k) = (\nabla F(x_k))\, F(x_k)$.

Pas 2. Si $\|\nabla f(x_k)\| < \epsilon$ stop.

Pas 3. $d_k = -H_k \nabla f(x_k)$.

Pas 4. $x_{k+1} = x_k + \theta_k d_k$, $\theta_k > 0$ où

$$f(x_{k+1}) \approx \min_{\theta \geq 0} f(x_k + \theta d_k).$$

Pas 5. $\delta_k = x_{k+1} - x_k$.

Pas 6. $\nabla f(x_{k+1})$ et $\gamma_k = \nabla f(x_{k+1}) - \nabla f(x_k)$.

Pas 7.

$$H_{k+1} = H_k + \left(1 + \frac{\gamma_k^T H_k \gamma_k}{\delta_k^T \gamma_k}\right) \frac{\delta_k \delta_k^T}{\delta_k^T \gamma_k} - \frac{\delta_k \gamma_k^T H_k + H_k \gamma_k \delta_k^T}{\delta_k^T \gamma_k}$$

Pas 8. $k \leftarrow k + 1$ et aller au **Pas 2**.

L'algorithme BFGS converge d'une manière super-linéaire vers un minimum local x_* de f qui vérifie

$$\nabla f(x_*) = 0 \Longleftrightarrow (\nabla F(x_*))\, F(x_*) = 0. \tag{4}$$

Si la matrice $\nabla F(x_*)$ est inversible, alors à partir de la relation précédente on obtient

$$\nabla f(x_*) = 0 \Longleftrightarrow F(x_*) = 0.$$

Autrement dit, les algorithmes de minimisation, celui de Newton et de type point fixe *convergent vers les mêmes solutions* !

Il faut préciser une chose qui pourrait surprendre : un minimum local x_* (qui vérifie donc $\nabla f(x_*) = 0$ et sous l'hypothèse que $\nabla F(x_*)$ est inversible) est un minimum global car $f(x_*) = \frac{1}{2} \|F(x_*)\|^2 = 0$. Il reste le cas $\nabla F(x_*)$ non inversible, mais dans cette situation, l'algorithme de Newton, lui non plus, n'est pas applicable.

Concernant la vitesse de convergence dans un cadre général, la méthode de Newton est plus rapide que l'algorithme BFGS, qui est plus rapide que l'algorithme de type point fixe.

Mais, contrairement aux deux autres méthodes, l'algorithme BFGS est moins sensible au point de départ x_0, ce qui représente l'avantage majeur de cette approche. Un autre aspect positif est qu'on peut utiliser des maillages qui ne sont pas compatibles à l'interface, comme par exemple dans les méthode de type "mortar" [5].

On va analyser maintenant l'effort de calcul pour effectuer une itération avec l'algorithme BFGS respectivement avec la méthode de Newton. La direction de descente dans la méthode de Newton est donnée par l'expression

$$d_k = -\left(\nabla F(x_k)^T\right)^{-1} F(x_k)$$

alors que dans l'algorithme BFGS, on a

$$d_k = -H_k \left(\nabla F(x_k)\right) F(x_k).$$

On voit que dans la méthode de Newton on doit inverser le jacobien $\nabla F(x_k)^T$, ce qui nécessite un effort de calcul supplémentaire.

Les étapes 5,6,7 dans l'algorithme BFGS ne sont pas coûteuses. Pour l'optimisation unidimensionnelle, au Pas 4, on peut utiliser des méthodes dites économiques ou on peut prendre $\theta_k = 1$ si c'est possible. La stratégie de type point fixe a été utilisée dans [39]. Pour accélérer la convergence on peut utiliser : la relaxation [43], [29], [48], la "transpiration" [23], [24], [14] ou la méthode d'Aitken [31], [15].

La méthode de Newton avec le jacobien approché par des différences finies a été utilisé dans [50]. Dans [31] le jacobien est remplacé par un opérateur plus simple et dans [26], [27] le jacobien est évalué exactement.

Une approche décomposition de domaine avec préconditionnement est proposé dans [15] et [16].

La méthode BFGS a été utilisée dans les chapitre 2 et 3 où le jacobien est calculé exactement, et dans le chapitre 5 où le jacobien est approché par différences finies.

Sensibilité par rapport au mouvement du domaine

On a vu dans la section précédente des méthodes qui emploient la formule exacte du jacobien. L'évaluation exacte de cette formule est une tâche difficile, parce qu'elle cache une dérivée par rapport au domaine.

Des études sur la sensibilité sont présentées dans [25], [26] et [27].

En utilisant une transformation ALE explicite et des techniques basées sur le théorème des fonctions implicites comme dans les travaux [8] et [11], on donne dans les chapitres 2 et 3 la formulation exacte du gradient de la fonction coût. Dans le chapitre 2 on fait appel à l'état adjoint.

En utilisant la décomposition modale pour la structure dans le chapitre 3, on donne la formulation exacte des dérivées. Pour évaluer les dérivées par rapport au domaine de la solution du problème de Stokes stationnaire, il faut résoudre des système linéaires où la matrice est identique à celle du problème de Stokes. Cela rend facile la mise en oeuvre numérique de cette méthode.

Stabilité en temps

Dans la plupart des cas, pour résoudre numériquement les problèmes d'interaction fluide-structure, on emploie des "procédures partagées", i.e. on utilise séparément des solveurs pour le fluide et pour la structure.

Les algorithmes dites "staggered" ont été appliqués avec succès dans les problèmes d'aero-élasticité [45], [20], [21], [46]. A chaque pas en temps, seulement une partie des conditions de couplage fluide-structure est vérifiée ("losely coupled"). En général, ces algorithmes utilisent des schémas implicites pour l'un de deux sous-problèmes, par exemple pour le fluide et des schémas explicites pour l'autre sous-problème, par exemple pour la structure. Il existe des variantes où on utilise des schémas implicites pour les deux sous-problèmes. Il faut préciser que globalement les algorithmes dites "staggered" sont explicites et on obtient la stabilité seulement si le pas en temps est petit.

La relation entre la stabilité des schémas numériques et les lois de conservation géométrique est étudiée dans [20], [22].

Les tests numériques concernant l'écoulement sanguin dans les artères montrent que les algorithmes explicites sont instables, d'où la nécessité d'utiliser des méthodes implicites, c'est-à-dire, tel qu'à chaque pas en temps on résout un problème non linéaire fluide-structure pour lequel toutes les conditions de couplages à l'interface sont vérifiées.

La preuve de la stabilité d'un schéma totalement implicite est présentée dans [33] pour un problème monodimensionnel. Un schéma totalement implicite est employée dans [39] pour une application aux composants hydrauliques automobiles. Dans [43] on peut trouver la preuve de la stabilité inconditionnelle de deux algorithmes totalement implicites basés sur des schémas implicites centrés ou non centrés pour la structure couplés avec la méthode d'Euler implicite pour le fluide.

La stabilité des schémas d'ordre deux en temps est analysée dans [30].

Dans [7], il est montré que, même avec un pas de temps très petit, les algorithmes explicites ne sont pas stables.

Nous avons déjà cité les algorithmes de type point fixe, de type Newton à jacobien exact ou approché, le cadre de décomposition de domaine, ou la méthode BFGS qui nous permet la construction des schémas implicites en temps.

Les résultats numériques rapportés dans [43] et [7] obtenus en employant la méthode du point fixe avec relaxation suggèrent que les instabilités apparaissent quand la structure est légère et mince ou quand le rapport entre l'hauteur et la longueur du domaine fluide est petit.

Dans [39], les résultats théoriques montrent que les algorithmes de type point fixe divergent si la structure est légère ou si le pas de la discrétisation en temps est petit.

La méthode de Newton converge en peu d'itérations, mais elle est sensible au point d'initialisation. Les résultats d'existence pour les problèmes d'interaction fluide-structure continues ne garantissent pas l'existence d'une solution pour le problème discret. Si $F(x) = 0$, $x \in \mathbb{R}^n$ n'a pas des solutions, la méthode de Newton diverge.

La méthode BFGS converge moins vite que celle de Newton, mais elle a la propriété de convergence globale, en ce sens qu'elle converge à partir de presque n'importe quel point de départ. On a vu dans une section précédente que la solution du problème d'optimisation de type moindres carrés est en général un minimum global. Cette approche nous a permis d'utiliser dans le chapitre 5 des pas de temps relativement plus

grands, donc de réduire l'effort de calcul total.

Écoulements à frontière libre avec tension de surface

Dans les chapitres 7 et 8, on veut déterminer numériquement l'évolution d'un domaine bidimensionnel avec application au développement cellulaire.

L'écoulement du fluide dans le domaine en mouvement dépend de la tension de surface à la frontière libre. Cette tension est proportionnelle à la courbure de la frontière. La vitesse de la frontière est égale à celle du fluide. La divergence de la vitesse du fluide n'est pas nulle. Ces problèmes ont certaines similitudes avec les problèmes d'interaction fluide-structure.

Pour le fluide on utilise l'équation de Darcy dans le chapitre 7 et les équations de Stokes dans le chapitre 8. La courbure est approchée par l'inverse du rayon du cercle passant par trois noeud consécutifs appartenant à la frontière, ou en utilisant des fonctions spline cubiques.

Les algorithmes employés dans les chapitres 7 et 8 sont de type "front-tracking". Des résultats numériques sont présentés.

Quand on utilise le modèle de Darcy, le problème à frontière libre est similaire aux équations Hele-Shaw avec tension de surface. Pour résoudre numériquement ce problème, il existe une approche efficace appelée $\theta-L$ introduit dans [36]. Cette méthode n'est plus appropriée si on remplace les équations de Darcy par les équations non linéaires de Navier-Stokes.

D'autres cadres généraux pour résoudre les équations d'un fluide dans un domaine en mouvement sont : la frontière immergée [44], level set [49] et la méthode de la particule [13].

Perspectives

Simulation numérique et contrôle des problèmes d'interaction fluide-structure tridimensionnels. Applications au système cardio-vasculaire.

Le but de cette étude est de développer de nouvelles méthodes mathématiques et informatiques simulant numériquement le comportement du système cardio-vasculaire pour s'approcher au mieux du comportement réel du système.

La paroi de l'artère sera modélisée par des équations de type coque mince.

L'écoulement du sang sera modélisé par des équations de Navier-Stokes avec des conditions aux limites sur la pression à l'entrée et à la sortie et une condition de type Dirichlet sur l'interface sang-artère.

Le couplage des deux systèmes d'équations sera une partie importante de cette étude.

Les couplages fluide-structure de type implicite, c'est-à-dire qu'à chaque pas de temps on doit résoudre un problème fortement non linéaire, est très coûteux en temps de calcul sur ordinateur. La résolution du système non linéaire peut ce faire à l'aide des méthodes de type Newton ou quasi-Newton.

Dans un article récent [28], les méthodes semi-implicites ont donnés de bons résultats numériques tout en étant moins gourmandes en temps de calcul sur ordinateur. Il s'agit de calculer la position de l'interface fluide-structure d'une manière explicite et d'utiliser le même maillage pour le fluide pendant toutes les sous-itérations à l'instant de temps courant.

1. Création des maillages tridimensionnels sang et artère à l'aide du logiciel MODULEF (INRIA, France). On utilisera des tétraèdres pour le sang et des triangles pour la paroi artérielle. Les deux maillages sont compatibles à l'interface. Cette étape a été réalisé pour des domaines cylindriques.

2. La résolution du problème structure (artère) utilisera les éléments finis et la décomposition modale. On utilisera également le module OpenFEM du SCILAB (INRIA, France). Les matrices de masse et de raideur seront récupérées, ainsi que les seconds membres. Ensuite on calcule les valeurs propres généralisées des deux matrices. Cette étape a été réalisée en utilisant ARNOLDI et Scilab (voir Fig. 5), mais les résultats ne sont pas satisfaisants. On envisage l'utilisation du logiciel ABAQUS récemment acheté par l'Université de Haute-Alsace.

3. La résolution du problème fluide (sang) utilisera les éléments finis (codes gratuits LifeV Lausanne, Suisse).

4. Le couplage sera effectué grâce à la méthode de Newton ou quasi-Newton où les dérivées par rapport au changement du domaine de calcul seront approchées par la méthode des différences finies.

5. Étude de la discrétisation en temps. La stabilité en temps des méthodes numériques sera analysée. Simulations numériques complexes.

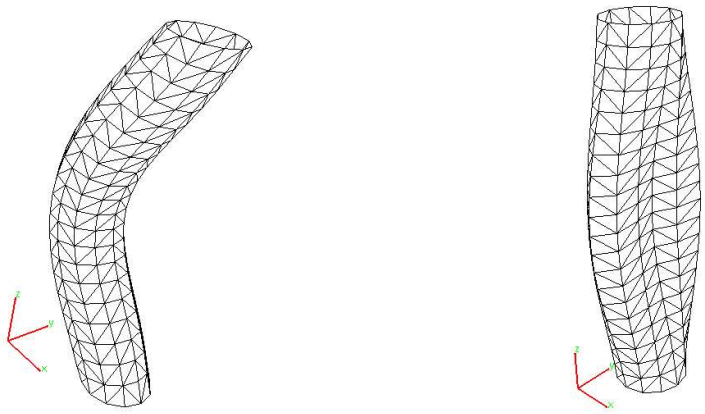

Figure 5: Deux modes propres d'une coque cylindrique

6. Identification des paramètres les plus significatifs qui gouvernent le couplage sang-artère. Étude de la contrôlabilité du système couplé.

Schémas semi-implicites et couplage fluide-structure par la méthode du Lagrangien augmenté

Actuellement, je travail sur un problème 2D d'interaction entre les équations d'élasticité linéaire et les équations de Navier-Stokes.

Pour l'approximation de la structure, l'algorithme de Newmark est employé. Pour les équations de Navier-Stokes on utilise la méthode ALE, la dérivée en temps sera approcher par le schéma d'Euler implicite et le terme non-linéaire est traité d'une manière semi-implicite.

La position de l'interface fluide-structure est calculée d'une manière explicite. A chaque pas en temps, on utilise la méthode du Lagrangien augmenté pour traiter l'égalité de vitesses à l'interface.

Dans la Figure 6, on peut voir les vitesses de la structure et du fluide à l'instant t=1s.

La différence dans la norme L^2 entres les vitesses du fluide et de la structure à l'interface est plus petite que 0.29. On essaye de diminuer cette erreur.

La stabilité en temps sera analysée.

Autres projets

Simulation 3D du développement cellulaire (en collaboration avec Prof. G. Hentschel, Atlanta). Déformations des bandes élastiques (en collaboration avec Prof. Th. Hangan, Mulhouse).

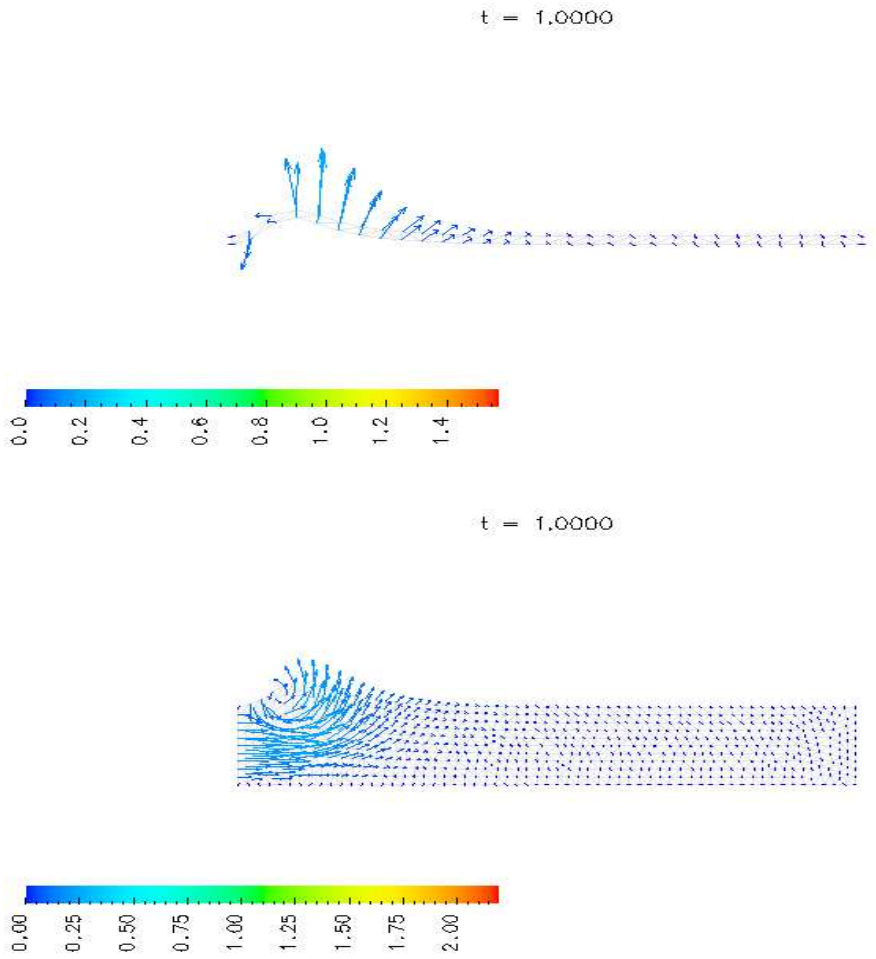

Figure 6: Vitesses de la structure (haut) et du fluide (bas) à l'instant t=1 s

Bibliography

[1] Batina J.T. (1990) Unsteady Euler Airfoil Solutions Using Unstructured Dynamic Meshes, AIAA Journal, vol. 28, no. 8, pp. 1381-1388

[2] Bayada G., Chambat M., Cid B., Vazquez C. (2004) On the existence of solution for a non-homogeneus Stokes-rod coupled problem, Nonlinear Analysis: Theory, Methods and Applications, 59:1-19

[3] Bayada G., Durany J., Vázquez C. (1995) Existence of a Solution for a Lubrication Problem in Elastic Journal Bearings with Thin Bearing, Math. Meth. Appl. Sci. 18:455–466

[4] Beirao da Veiga H. (2004) On the existence of strong solution to a coupled fluid-structure evolution problem, J. Math. Fluid Mech. 6:21–52

[5] Bernardi C., Maday Y, Patera A. (1989) A new non-conforming approach to domain decomposition: the mortar element method, in *Nonlinear Partial Differential Equations and Their Applications*, H. Brezis, J.L. Lions, eds., Pitman

[6] Canić S., Mikelić A. (2003) Effective equations modeling the flow of a viscous incompressible fluid through a long elastic tube arising in the study of blood flow through small arteries. SIAM J. Appl. Dyn. Syst. 2, no. 3, 431–463.

[7] Causin P., Gerbeau J.-F., Nobile F. (2004) Added-mass effect in the design of partitioned algorithms for fluid-structure problems, to appear in Comput. Methods Appl. Mech. Engrg.

[8] Céa J. (1986) Conception optimale ou identification de formes: calcul rapide de la dérivée directionnelle de la fonction coût, RAIRO Model. Math. Anal. Numer. 20(3):371–402

[9] Chambolle A., Desjardins B., Esteban M. J., Grandmont C. (2005) Existence of weak solutions for an unsteady fluid-plate interaction problem. (à paraître dans J. Math. Fluid Mech.)

[10] Chen H., Sheu T. (2003) Finite-element simulation of incompressible fluid flow in an elastic vessel, Int. J. Numer. Meth. Fluids 42:131–146

[11] Chenais D., Monnier J., Vila J.P. (2001) Shape optimal design problem with convective and radiative heat transfer: analysis and implementation, J. Optim. Theory Appl. 110(1):75–117

[12] Cottet G.-H. (2002) A particle model for fluid-structure interaction. C. R. Math. Acad. Sci. Paris 335, no. 10, 833–838

[13] Cottet G.-H. (2003) Particle methods for CFD, Lecture notes for Summer school "Advances for CFD for industrial and geophysical turbulence", Autrans

[14] Deparis S., Fernandez M.A., Formaggia L. (2003) Acceleration of a fixed point algorithm for fluid-structure interaction using transpiration conditions, M2AN Math. Model. Numer. Anal. 37(4):601–616

[15] Deparis S. (2004) Numerical Analysis of Axisymmetric Flows and Methods for Fluid-Structure Interaction Arising in Blood Flow Simulation, PhD, Ecole Polytechnique Féderale de Lausanne, Switzerland

[16] Deparis S., Discacciati M., Quarteroni A. (2004) A domain decomposition framework for fluid-structure interaction problems. In Proceedings of the Third International Conference on Computational Fluid Dynamics (ICCFD3), Toronto

[17] Desjardins B., Esteban M. , Grandmont C., Le Tallec P. (2001) Weak solutions for a fluid-elastic structure interaction model, Rev. Mat. Complut. 14(2):523–538

[18] Duvaut G., Lions J.-L. (1972) Les inéquations en mécanique et en physique. Dunod, Paris

[19] Errate D., Esteban M.J., Maday Y. (1994) Couplage fluide-structure. Un modèle simplifié en dimension 1. C. R. Acad. Sci. Paris Sér. I Math. 318, no. 3, 275–281

[20] Farhat C., Lesoinne M., Le Tallec P. (1998) Load and motion transfer algorithms for fluid/structure interaction problems with non-matching discrete interfaces: momentum and energy conservation, optimal discretization and application to aeroelasticity. Comput. Methods Appl. Mech. Engrg. 157, no. 1-2, 95–114

[21] Farhat C., Lesoinne M. (2000) Two efficient staggered algorithms for the serial and parallel solution of three-dimensional nonlinear transient aeroelastic problems, Comput. Methods Appl. Mech. Engrg. 182(3-4):499–515

[22] Farhat C., Geuzaine Ph., Grandmont C. (2001) The discrete geometric conservation law and the nonlinear stability of ALE schemes for the solution of flow problems on moving grids, J. Comput. Phys. 174(2):669–694

[23] Fernández M.A., Le Tallec P., (2003) Linear fluid-structure stability analysis with transpiration. Part I: formulation and mathematical analysis. Comput. Methods Appl. Mech. Engrg., vol. 192, num. 43, pp. 4805-4835

[24] Fernández M.A., Le Tallec P., (2003) Linear fluid-structure stability analysis with transpiration. Part II: numerical analysis and applications. Comput. Methods Appl. Mech. Engrg., vol. 192, num. 43, pp. 4837-4873

[25] Fernandez M. A., Moubachir M. (2002) Sensitivity analysis for an incompressible aeroelastic system, Math. Models Methods Appl. Sci. 12(8):1109–1130

[26] Fernandez M. A., Moubachir M. (2003) An exact block-Newton algorithm for solving fluid-structure interaction problems, C. R. Math. Acad. Sci. Paris 336(8):681–686

[27] Fernández M.A., Moubachir M. (2005) A Newton method using exact jacobians for solving fluid-structure coupling. Comput. & Structures, vol. 83, num. 2-3, pp. 127-142

[28] M.A. Fernández, J.-F. Gerbeau, C. Grandmont, A projection semi-implicit scheme for the coupling of an elastic structure with an incompressible fluid Publied on line in International Journal for Numerical Methods in Engineering, 2006.

[29] Formaggia L., Gerbeau J. F., Nobile F., Quarteroni A. (2001) On the coupling of 3D and 1D Navier-Stokes equations for flow problems in compliant vessels, Comput. Methods Appl. Mech. Engrg. 191(6-7):561–582

[30] Formaggia, L., Nobile F. (2004) Stability analysis of second-order time accurate schemes for ALE-FEM. Comput. Methods Appl. Mech. Engrg. 193, no. 39-41, 4097–4116

[31] Gerbeau J. F., Vidrascu M. (2003) A quasi-Newton algorithm on a reduced model for fluid - structure interaction problems in blood flows, M2AN Math. Model. Numer. Anal. 37(4):631–647

[32] Grandmont C. (1998) Existence et unicité de solutions d'un problème de couplage fluide-structure bidimensionnel stationnaire, C. R. Acad. Sci. Paris Sér. I Math. 326(5):651–656

[33] Grandmont C., Maday Y., Guimet V. (1998) Results about some decoupling techniques for the approximation of the unsteady fluid-structure interaction. ENUMATH 97 (Heidelberg), 319-326, World Sci. Publishing, River Edge, NJ

[34] Grandmont C., Maday Y. (2000) Existence for an unsteady fluid-structure interaction problem, M2AN Math. Model. Numer. Anal. 34(3):609–636

[35] Grandmont C. (2002) Existence for a three-dimensional steady state fluid-structure interaction problem, J. Math. Fluid Mech. 4(1):76–94

[36] Hou T.Y., Lowengrub J.S., Shelley M.J. (1994) Removing the stiffness from interfacial flows with surface tension. J. Comput. Phys. 114:312–328

[37] Le Tallec P., Gallice G., Martin C., (1993) Maillages adaptifs pour la résolution numérique des équations de Navier-Stokes, 25e Congrès National d'Analyse Numérique, Giens, France

[38] Le Tallec P. (2000) Introduction à la dynamique des structures, Cours Ecole Polytechnique, Ellipses

[39] Le Tallec P., Mouro J. (2001) Fluid-structure interaction with large structural displacements, Comput. Methods Appl. Mech. Engrg. 190(24-25):3039–3067

[40] Lions J.-L., Pironneau O. (2000) Virtual control, replicas and decomposition of operators, C. R. Acad. Sci. Paris Sér. I Math. 330(1):47–54

[41] Lions J.-L., Maday Y., Turinici G. (2001) Résolution d'EDP par un schéma en temps pararéel. C. R. Acad. Sci. Paris, Série I 332, 7, pp. 661

[42] Maday Y., Maury B., Metier P. (1999) Interaction de fluides potentiels avec une membrane élastique, in ESAIM Proc. 10, Soc. Math. Appl. Indust., Paris, pp. 23–33

[43] Nobile F. (2001) Numerical approximation of fluid-structure interaction problems with application to haemodynamics, PhD, Ecole Polytechnique Féderale de Lausanne, Switzerland

[44] Peskin C.S. (2002) The immersed boundary method. *Acta Numer.* 11: 479–517.

[45] Piperno S., Farhat C., Larrouturou B. (1995) Partitioned procedures for the transient solution of coupled aeroelastic problems. I. Model problem, theory and two-dimensional application, Comput. Methods Appl. Mech. Engrg. 124:79–112

[46] Piperno S., Farhat C. (2001) Partitioned procedures for the transient solution of coupled aeroelastic problems. II. Energy transfer analysis and three-dimensional application, Comput. Methods Appl. Mech. Engrg. 190:3147–3170

[47] Quarteroni A., Tuveri M., Veneziani A. (2000) Computational vascular fluid dynamics: problems, models and methods. *Comput. Visual. Sci.* 2:163–197.

[48] Quarteroni A., Formaggia L. (2003) Mathematical Modelling and Numerical Simulation of the Cardiovascular System, in Modelling of Living Systems, ed. N. Ayache, Handbook of Numerical Analysis Series, eds. P.G. Ciarlet and J.L. Lions, Elsevier

[49] Sethian J. A. (1996) Level set methods: evolving interfaces in geometry, fluid mechanics, computer vision and material science, Cambridge University Press

[50] Steindorf J., Matthies H.G. (2002) Partioned but strongly coupled iteration schemes for nonlinear fluid-structure interaction, Comput. & Structures, 80:1991–1999

Publications citées dans la synthèse

Chapitre 1. C.M. Murea, Y. Maday, Existence of an optimal control for a nonlinear fluid-cable interaction problem, Rapport de recherche CEMRACS 96, Interaction fluide-structure, Luminy

Chapitre 2. C.M. Murea, C. Vazquez, Sensitivity and approximation of coupled fluid-structure equations by virtual control method, *Appl. Math. Optim.*, **52** (2005), no. 2, 183–218

Chapitre 3. C.M. Murea, The BFGS algorithm for a nonlinear least squares problem arising from blood flow in arteries, *Comput. Math. Appl.*, **49** (2005), pp. 171–186

Chapitre 4. C.M. Murea, Optimal control approach for the fluid-structure interaction problems, *Proceedings of the Fourth European Conference on Elliptic and Parabolic Problems*, Rolduc and Gaeta, 2001, J. Bemelmans et al (eds.), World Scientific Publishing Co. Pte. Ltd., pp. 442–450, 2002

Chapitre 5. C.M. Murea, Numerical simulation of a pulsatile flow through a flexible channel, *ESAIM: Math. Model. Numer. Anal.* **40** (2006), no 6, 1101-1125

Chapitre 6. C.M. Murea, Dynamic meshes generation using the relaxation method with applications to fluid-structure interaction problems, *An. Univ. Bucureşti Mat.*, **47** (1998), No. 2, pp. 177–186

Chapitre 7. C.M. Murea, G. Hentschel, Finite element methods for investigating the moving boundary problem in biological development, *Progress in Nonlinear Differential Equations and Their Applications*, Vol. 64, pp. 357–371, Birkhauser Verlag, Basel, 2005

Chapitre 8. C.M. Murea, G. Hentschel, A Finite Element Method for Growth in Biological Development, *Math. Biosci. Eng.* **4** (2007) 2, 339–353

Publications non citées dans la synthèse

9. C.M. Murea, J.-M. Crolet, A stable algorithm for a fluid-structure interaction problem in 3D, in *Contact Mechanics II, Computational Techniques*, M.H. Aliabadi, C. Alessandri (eds.), pp. 325–332, Computational Mechanics Publications, Southampton, Boston, 1995

10. C.M. Murea, Sur la convergence d'un algorithme pour la résolution découplée d'un système de type Kuhn-Tucker, *An. Univ. Bucureşti Mat.*, **46** (1997), No. 1, pp. 35–40, Zbl 894.65027

11. C.M. Murea, Domain decomposition method for a flow through two porous media, *Bull. Math. Soc. Sc. Math. Roumaine*, **41** (1998), No. 4, pp. 257-265, MR1880365 (2002j:65121)

12. C.M. Murea, J.-M. Crolet, Etude d'un problème parabolique avec multiplicateur de Lagrange, *Proceedings of the anual meeting of the Romanian Society of Mathematical Sciences 97*, pp. 237–242, Bucharest, 1998

13. C.M. Murea, Optimization of satellite antenna, *An. Univ. Bucureşti Mat.*, **48** (1999), pp. 207–216

14. C.M. Murea, J.-M. Crolet, Formulation hybride pour un problème d'interaction fluide structure, *Rev. Roumaine Mat. Pure App.*, **44** (1999), No. 3, pp. 435–445, MR1839512 (2002d:74021)

15. C.M. Murea, J.-M. Crolet, Optimal control approach for a flow in unsaturated porous media, dans *Computational Methods for Flow and Transport in Porous Media*, J.-M. Crolet (ed.), Kluwer Academic Publishers, pp. 107–114, 2000

16. C.M. Murea, La méthode du lagrangien augmenté pour un problème d'interaction fluide-structure, *Rev. Anal. Numér. Théor. Approx.*, **29** (2002), No. 1, pp. 49–56

17. Th. Hangan, C. Murea, Elastic helices, special volume of *Rev. Roumaine Mat. Pure App.* **50** (2005), no. 5-6, 527–531

18. C.M. Murea, C. Vazquez, Numerical control of normal velocity by normal stress for interaction between an incompressible fluid and an elastic curved arch, *Proceedings (CDROM) ECCOMAS CFD 2006*, P. Wesseling, E. Onate , J. Périaux (Eds), September 5-8, 2006, Egmond aan Zee, The Netherlands

Pré-publications

19. I. Mbaye, C. Murea, Numerical procedure with analytic derivative for unsteady fluid-structure interaction

20. I. Mbaye, C. Murea, Approximation par la méthode des moindres carrés d'un problème bidimensionnel stationnaire d'interaction fluide-structure

Part I

Steady fluid-structure interaction

Chapter 1

Existence of an optimal control for a nonlinear fluid-cable interaction problem

This chapter is based on the paper:

C.M. Murea, Y. Maday, Rapport de recherche CEMRACS 96, *Interaction Fluide Structure*, C.I.R.M., Luminy, France, 1996

Abstract. A three-dimensional fluid-cable interaction is studied. The fluid is governed by the Stokes equations and the cable is governed by the beam equations without shearing stress. Only steady equations are studied in this paper. The fluid equations are described using arbitrary lagrangian eulerian coordinates.

The contact surface between fluid and cable is unknown a priori, therefore it is a free boundary like problem.

The fluid-cable interaction is modeled by an optimal control system with Neumann like boundary control and Dirichlet like boundary observation. The control appears also in the coefficients of the fluid equations.

It's a nonlinear and non-convex optimal control problem.

The existence of a solution is proved.

1.1 Introduction

We study the behavior of a three-dimensional cable under the action of an external flow.

The real system to be modeled is the behavior of an electric cable with fixed extremities under the wind action. We are interested by the displacement of the cable and by the velocity and the pressure of the fluid.

The contact surface between fluid and cable is unknown a priori, therefore it is a free boundary like problem.

We suppose that the fluid is governed by the Stokes equations and the cable is governed by the beam equations without shearing stress. Only steady equations will be studied in this paper.

The fluid and cable equations are coupled via two boundary conditions: equality of the fluid's and cable's velocities at the contact surface (which is a Dirichlet like boundary condition) and equality of the forces at the contact surface (which is a Neumann like boundary condition).

The coupled fluid-cable problem is modeled by an optimal control variational system. It's a Neumann like boundary control with Dirichlet like boundary observation. The control appears also in the coefficients of the fluid equations.

This mathematical model permits to solve numerically the coupled fluid-cable problem via partitioned procedures (i.e. in a decoupled way, more precisely the fluid and the cable equations are solved separately).

The aim of this paper is to prove the existence of an optimal control for this fluid-cable interaction problem.

1.2 Notations

Let us consider a cable of cross section S. We assume that $S \subseteq \mathbb{R}^2$ has the following properties: non-empty, open, bounded, connected, with Lipschitz boundary and $(0,0) \in S$.

The displacement of the cable will be described using the displacement of the median thread noted here by:

$$u = (u_1, u_2, u_3) : [0, L] \to \mathbb{R}^3.$$

For instant, we assume that $u_1 = 0$.

The three-dimensional domain occupied by the cable is

$$\Omega_u^S = \left\{(x_1, x_2, x_3) \in \mathbb{R}^3; x_1 \in]0, L[\,, (x_2 - u_2(x_1), x_3 - u_3(x_1)) \in S\right\} \tag{1.1}$$

and the domain occupied by the fluid is

$$\Omega_u^F = \mathbb{R}^3 \setminus \overline{\Omega_u^S}. \tag{1.2}$$

The contact surface between fluid and cable is

$$\Gamma_u = \left\{(x_1, x_2, x_3) \in \mathbb{R}^3; x_1 \in]0, L[\,, (x_2 - u_2(x_1), x_3 - u_3(x_1)) \in \partial S\right\} \tag{1.3}$$

which is the free boundary of our problem.

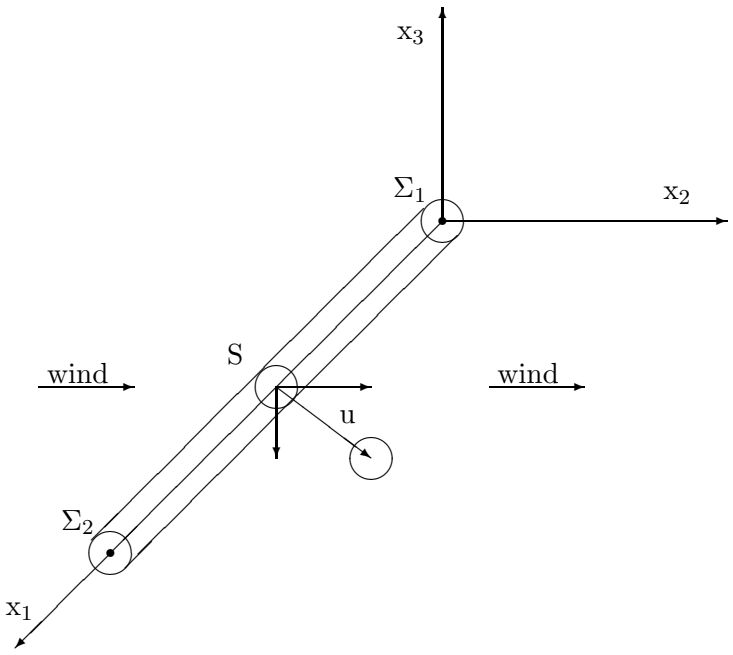

Figure 1.1: The geometrical configuration of the fluid-cable interaction

The extremities of the cable are noted:

$$\begin{aligned} \Sigma_1 &= \left\{(0, x_2, x_3) \in \mathbb{R}^3; (x_2, x_3) \in S\right\}, \\ \Sigma_2 &= \left\{(L, x_2, x_3) \in \mathbb{R}^3; (x_2, x_3) \in S\right\} \end{aligned} \tag{1.4}$$

which are fixed.

1.3 Variational formulation for the cable equations

Now, we present the variational formulation for the cable equations. We have supposed that the cable is governed by the beam equations without shearing stress (see [4]).

Let $D_2 \in \mathbb{R}_+^*$ be given. We set

$$\left\{ \begin{array}{c} a_S : H_0^2(]0, L[) \times H_0^2(]0, L[) \to \mathbb{R} \\ a_S(\phi, \psi) = D_2 \cdot \int_{]0,L[} \frac{d^2\phi}{dx_1^2}(x_1) \frac{d^2\psi}{dx_1^2}(x_1)\, dx_1 \end{array} \right. \tag{1.5}$$

The form a_S is evidently symmetric, bilinear, continuous. In addition, applying the Poincaré inequality (see [8, vol. 3, chap. IV, p. 920]), we obtain that a_S is $H_0^2(]0, L[)$-elliptic.

Let $H^{-2}(]0,L[)$ be the dual of the $H_0^2(]0,L[)$. In this section, we denote by $\langle\cdot,\cdot\rangle$ the duality pairing between $H^{-2}(]0,L[)$ and $H_0^2(]0,L[)$.

As a simple consequence of the Lax-Milgram Theorem (see [8, vol. 4, chap. VII, p. 1217]), we have the following result:

Proposition 1.1 *Let $f_i^S \in H^{-2}(]0,L[)$ and $\eta_i \in L^2(]0,L[)$ for $i=2,3$. Then, the problem:*
Find u_2, u_3 in $H_0^2(]0,L[)$ such that

$$a_S(u_i,\psi)=\int_{]0,L[}\eta_i(x_1)\,\psi(x_1)\,dx_1+\left\langle f_i^S,\psi\right\rangle,\quad \forall\psi\in H_0^2(]0,L[),\ i=2,3 \tag{1.6}$$

has a unique solution.

In order to couple the 3D Stokes equations of the fluid with the beam equations described using the median thread, which is a curve in $\mathbb{R}^3$, we shall need the following result:

Proposition 1.2 *There is a linear and continuous operator D mapping $L^2(]0,L[\times\partial S)$ onto $L^2(]0,L[)$ such that:*

$$(Dg)(x_1)=\int_{\partial S}g(x_1,\sigma)\,d\sigma,\qquad \text{a.e. } x_1\in]0,L[. \tag{1.7}$$

Proof. Let g be an element of $L^2(]0,L[\times\partial S)$. Applying the Fubini's Theorem (see [12, p. 140] for example), we have $g(x_1,\cdot)\in L^1(\partial S)$, a.e. $x_1\in]0,L[$ and the map

$$x_1\in]0,L[\mapsto\int_{\partial S}g(x_1,\sigma)\,d\sigma$$

is Lebesgue measurable.

From the Schwarz inequality (see [12, p. 62]), it follows that

$$\left(\int_{\partial S}g(x_1,\sigma)\,d\sigma\right)^2\le\left(\int_{\partial S}1d\sigma\right)\int_{\partial S}g^2(x_1,\sigma)\,d\sigma,\qquad \text{a.e. } x_1\in]0,L[.$$

Integrating the above inequality on $]0,L[$, we have

$$\int_{]0,L[}\left(\int_{\partial S}g(x_1,\sigma)\,d\sigma\right)^2\le L\left(\int_{\partial S}1d\sigma\right)\int_{]0,L[}\left(\int_{\partial S}g^2(x_1,\sigma)\,d\sigma\right)dx_1.$$

Using once again the Fubini's Theorem, we obtain

$$\int_{]0,L[}\left(\int_{\partial S} g^2(x_1,\sigma)\,d\sigma\right)dx_1=\int_{]0,L[\times\partial S} g^2(x_1,\sigma)\,d\sigma dx_1=\|g\|^2_{0,]0,L[\times\partial S}$$

therefore $Dg\in L^2(]0,L[)$ and

$$\|Dg\|^2_{0,]0,L[}\leq L\left(\int_{\partial S}1d\sigma\right)\|g\|^2_{0,]0,L[\times\partial S}\,. \tag{1.8}$$

The operator D is linear from the linearity of the Lebesgue integral.
The inequality (1.8) implies the continuity of the linear operator D. □

1.4 Mixed formulation for the fluid equations in moving exterior domain

Let u_2 and u_3 be the solutions of the equation (1.6) and Ω_u^F be the domain occupied by the fluid given by the relations (1.2) and (1.1).

Let us consider the Sobolev space with weights:

$$W^1\left(\Omega_u^F\right)=\left\{w\in\mathcal{D}'\left(\Omega_u^F\right);\ \frac{w(x)}{\left(1+\|x\|^2\right)^{1/2}}\in L^2\left(\Omega_u^F\right);\ \frac{\partial w}{\partial x_i}\in L^2\left(\Omega_u^F\right);\ i=1,2,3\right\}$$

where $\|x\|=\left(\sum_{i=1}^3 x_i^2\right)^{1/2}$ is the eulerian norm in $\mathbb{R}^3$.

We set

$$|w|_{1,\Omega_u^F}=\left(\sum_{i=1}^3\int_{\Omega_u^F}\left|\frac{\partial w}{\partial x_i}(x)\right|^2dx\right)^{1/2}$$

which is a semi-norm and

$$\|w\|_{1,\Omega_u^F}=\left(\int_{\Omega_u^F}\frac{|w(x)|^2}{1+\|x\|^2}\,dx+|w|^2_{1,\Omega_u^F}\right)^{1/2}$$

which is a norm.

We denote by $W_0^1\left(\Omega_u^F\right)$ the closure of $\mathcal{D}\left(\Omega_u^F\right)$ in $W^1\left(\Omega_u^F\right)$ for the norm $\|\cdot\|_{1,\Omega_u^F}$.

From the Theorem 1 [8, vol. 6, chap. XI B, p. 650], we have that the semi-norm $|\cdot|_{1,\Omega_u^F}$ is a norm for the spaces $W^1\left(\Omega_u^F\right)$ and $W_0^1\left(\Omega_u^F\right)$. Moreover, it's equivalent to $\|\cdot\|_{1,\Omega_u^F}$.

In view of the Remark 2 [8, vol. 6, chap. XI B, p. 651], the spaces $W^1\left(\Omega_u^F\right)$ and $W_0^1\left(\Omega_u^F\right)$ are identical with the Beppo-Levi spaces $BL\left(\Omega_u^F\right)$ and $\hat{\mathcal{D}}^1\left(\Omega_u^F\right)$ respectively.

So, the spaces $W^1\left(\Omega_u^F\right)$ and $W_0^1\left(\Omega_u^F\right)$ are the Hilbert spaces for the scalar product:

$$(\phi,\ \psi) = \sum_{i=1}^{3} \int_{\Omega_u^F} \frac{\partial \phi}{\partial x_i} \frac{\partial \psi}{\partial x_i} dx$$

(see also the Remark 7 [8, vol. 5, chap. IX A, p. 264]).

In view of the Sobolev Embedding Theorem (see [1]), we have

$$H_0^2\left(]0, L[\right) \hookrightarrow \mathcal{C}^1\left([0, L]\right)$$

therefore the boundary Γ_u is Lipschitz, so we can define the space $H^{1/2}\left(\Gamma_u\right)$.

From the Theorem 2 [8, vol. 6, chap. XI B, p. 652], there exists the trace application mapping $W^1\left(\Omega_u^F\right)$ onto $H^{1/2}\left(\Gamma_u\right)$ denoted by

$$w \longrightarrow w_{|\Gamma_u}$$

which is continuous and surjective and

$$W_0^1\left(\Omega_u^F\right) = \left\{ w \in W^1\left(\Omega_u^F\right);\ w_{|\Gamma_u \cup \overline{\Sigma}_1 \cup \overline{\Sigma}_2} = 0 \right\}$$

Let us consider the following Hilbert space:

$$W_u = \left\{ w \in \left(W^1\left(\Omega_u^F\right)\right)^3;\ w = 0 \text{ on } \overline{\Sigma}_1 \cup \overline{\Sigma}_2 \right\}$$

equipped with the scalar product

$$(v, w) = \sum_{i,j=1}^{3} \int_{\Omega_u^F} \frac{\partial v_i}{\partial x_j} \frac{\partial w_i}{\partial x_j} dx$$

where $v = (v_1, v_2, v_3)$ and $w = (w_1, w_2, w_3)$ are in W_u.

Also, let us consider the Hilbert space:

$$Q_u = L^2\left(\Omega_u^F\right)$$

equipped with the habitual scalar product.

We use the notation $div\ w = \frac{\partial w_1}{\partial x_1} + \frac{\partial w_2}{\partial x_2} + \frac{\partial w_3}{\partial x_3}$ for all $w = (w_1, w_2, w_3)$ in $\left(W^1\left(\Omega_u^F\right)\right)^3$.

Lemma 1.1 *For all u_2 and u_3 in $H_0^2\left(]0, L[\right)$, the operator div mapping W_u onto Q_u is surjectif.*

Proof. Let u_2 and u_3 be in $H_0^2(]0,L[)$.

Let us denote:

$$L_0^2\left(\Omega_u^F\right) = \left\{ q \in L^2\left(\Omega_u^F\right);\ \int_{\Omega_u^F} q\ dx = 0 \right\}$$

It is known (see [8, vol. 5, chap IX A, p. 267, Remark 8] for example) that $div\left(W_0^1\left(\Omega_u^F\right)\right)^3 = L_0^2\left(\Omega_u^F\right)$. Evidently we have $\left(W_0^1\left(\Omega_u^F\right)\right)^3 \subseteq W_u$, so

$$L_0^2\left(\Omega_u^F\right) \subseteq div\left(W_u\right) \subseteq L^2\left(\Omega_u^F\right) \tag{1.9}$$

Since the operator div is linear, we obtain that $div\left(W_u\right)$ is a vectorial subspace.

Knowing that the co-dimension of $L_0^2\left(\Omega_u^F\right)$ in $L^2\left(\Omega_u^F\right)$ is one, the inclusions (1.9) imply: $div\left(W_u\right) = L_0^2\left(\Omega_u^F\right)$ or $div\left(W_u\right) = L^2\left(\Omega_u^F\right)$.

In order to finish the proof of this Lemma, we shall prove that $div\left(W_u\right) \neq L_0^2\left(\Omega_u^F\right)$.

To obtain a contradiction, we suppose that

$$div\left(W_u\right) = L_0^2\left(\Omega_u^F\right) = div\left(W_0^1\left(\Omega_u^F\right)\right)^3 \tag{1.10}$$

Let w be in W_u such that $\sum_{i=1}^3 \int_{\Gamma_u} w_i n_i\ d\sigma > 0$, where n is the unit outward normal to Γ_u.

From (1.10) we obtain that there is ψ in $\left(W_0^1\left(\Omega_u^F\right)\right)^3$ such that $div\ \psi = div\ w$.

From the Green's formula we have

$$0 = \int_{\Omega_u^F} div\left(w-\psi\right)\ dx = \sum_{i=1}^3 \int_{\overline{\Sigma}_1 \cup \overline{\Sigma}_2 \cup \Gamma_u} \left(w_i - \psi_i\right) n_i\ d\sigma = \sum_{i=1}^3 \int_{\Gamma_u} w_i n_i\ d\sigma > 0$$

and we have obtained a contradiction. Then the proof of this Lemma is finished. □

Remark 1.1 *As good as for a bounded domain, the Green's formula holds for an exterior domain, i.e. complement of a compact (see [8, vol. 6, chap. XI B, p. 694]).*

We set

$$\begin{cases} a_F : \left(H_0^2(]0,L[)\right)^3 \times W_u \times W_u \to \mathbb{R} \\ a_F(u,v,w) = \displaystyle\sum_{i,j=1}^3 \int_{\Omega_u^F} \frac{\partial v_i}{\partial x_j} \frac{\partial w_i}{\partial x_j} dx \end{cases} \tag{1.11}$$

and

$$\begin{cases} b_F : \left(H_0^2(]0,L[)\right)^3 \times W_u \times Q_u \to \mathbb{R} \\ b_F(u,w,q) = -\displaystyle\int_{\Omega_u^F} (div\ w)\, q\ dx \end{cases} \tag{1.12}$$

Proposition 1.3 *For all u_2, u_3 in $H_0^2(]0,L[)$, $\lambda = (\lambda_1, \lambda_2, \lambda_3)$ in $(L^2(\Gamma_u))^3$, the problem:*
Find $(v,\ p) \in W_u \times Q_u$ such that

$$\begin{cases} a_F(u,v,w) + b_F(u,w,p) = \sum_{i=1}^{3} \int_{\Gamma_u} \lambda_i w_i \, d\sigma, & \forall w \in W_u \\ b_F(u,v,q) = 0, & \forall q \in Q_u \end{cases} \tag{1.13}$$

has a unique solution.

Proof. For all u_2, u_3 in $H_0^2(]0,L[)$, the bilinear form $a_F(u,\cdot,\cdot)$ is continuous and W_u-elliptic for the norm $|\cdot|_{1,\Omega_u^F}$.

Using the Lemma 1.1 and a property of the surjectif operators [6, Theorem II.19, p. 29], we obtain that the inf-sup condition holds for the bilinear form $b_F(u,\cdot,\cdot)$.

Now, the conclusion of our proposition is a simple consequence of the results of Babuska [3] and Brezzi [7]. □

Remark 1.2 *The system (1.13) represents the mixed formulation for the Stokes equations in an exterior domain: v and p are the velocity and the pressure of the fluid, λ are the forces on the surface Γ_0.*

1.5 Mixed formulation for the fluid equations in a fixed exterior domain

In order to obtain the mixed formulation for the fluid equations in a fixed exterior domain, the arbitrary lagrangian eulerian coordinates have been used. The formulation in a fixed domain permits us to obtain the existence of the solution for the cable-fluid coupled problem.

We set

$$\Omega_0^S = \{(x_1,x_2,x_3) \in \mathbb{R}^3;\ x_1 \in]0,L[\,,\ (x_2,x_3) \in S\}\,,$$
$$\Omega_0^F = \mathbb{R}^3 \setminus \overline{\Omega_0^S},$$
$$\Gamma_0 = \{(x_1,x_2,x_3) \in \mathbb{R}^3;\ x_1 \in]0,L[\,,\ (x_2,x_3) \in \partial S\}\,.$$

Let $u_2,\ u_3$ in $H_0^2(]0,L[)$ be given. We have $H_0^2(]0,L[) \hookrightarrow \mathcal{C}^1([0,L])$ and we extend $u_2,\ u_3$ by zero in the exterior of the interval $[0,L]$. Without risk of confusion, we use the same notations $u_2,\ u_3$ for the extended functions, so

$$u_2(x_1) = u_3(x_1) = 0, \quad \forall x_1 \notin [0,L]$$

Therefore we have $u_i \in \mathcal{C}^1(\mathbb{R})$ and we denote by u_i' the first derivate of u_i for $i = 2, 3$.

Let us consider the following one-to-one continuous differentiable transformation:

$$\begin{array}{c} T_u : \mathbb{R}^3 \to \mathbb{R}^3 \\ T_u\left(\widehat{x}_1, \widehat{x}_2, \widehat{x}_3\right) = \left(\widehat{x}_1, \widehat{x}_2 + u_2\left(\widehat{x}_1\right), \widehat{x}_3 + u_3\left(\widehat{x}_1\right)\right) \end{array} \tag{1.14}$$

which admits the continuous differentiable inverse below:

$$\begin{array}{c} T_u^{-1} : \mathbb{R}^3 \to \mathbb{R}^3 \\ T_u^{-1}\left(x_1, x_2, x_3\right) = \left(x_1, x_2 - u_2\left(x_1\right), x_3 - u_3\left(x_1\right)\right) \end{array} \tag{1.15}$$

We have

$$\begin{array}{c} T_u\left(\Omega_0^F\right) = \Omega_u^F \\ T_u\left(\Gamma_0\right) = \Gamma_u \\ T_u\left(\widehat{x}\right) = \widehat{x},\ \forall \widehat{x} \in \overline{\Sigma}_1 \cup \overline{\Sigma}_2 \end{array}$$

We denote by

$$\begin{array}{rcl} Jac\, T_u\left(\widehat{x}\right) & = & \begin{pmatrix} 1 & 0 & 0 \\ u_2'\left(\widehat{x}_1\right) & 1 & 0 \\ u_3'\left(\widehat{x}_1\right) & 0 & 1 \end{pmatrix} \\ Jac\, T_u^{-1}\left(x\right) & = & \begin{pmatrix} 1 & 0 & 0 \\ -u_2'\left(x_1\right) & 1 & 0 \\ -u_3'\left(x_1\right) & 0 & 1 \end{pmatrix} \end{array}$$

the Jacobi matrices of the transformations T_u and T_u^{-1} respectively.

We set $T_u\left(\widehat{x}\right) = x$, where $x = \left(x_1, x_2, x_3\right) \in \Omega_u^F$ and $\widehat{x} = \left(\widehat{x}_1, \widehat{x}_2, \widehat{x}_3\right) \in \Omega_0^F$ and $T_u\left(\widehat{\sigma}\right) = \sigma$ where $\sigma \in \Gamma_u$ and $\widehat{\sigma} \in \Gamma_0$.

If A is a square matrix, we denote by $det\left(A\right),\ A^{-1},\ A^t$ its determinant, the inverse and the transpose matrix, respectively.

Lemma 1.2 *We have:*

$$\left\{ \begin{array}{rcl} \phi \in L^1\left(\Omega_u^F\right) & \Leftrightarrow & \widehat{\phi} = \phi \circ T_u \in L^1\left(\Omega_0^F\right) \\ \displaystyle\int_{\Omega_u^F} \phi\left(x\right) dx & = & \displaystyle\int_{\Omega_0^F} \widehat{\phi}\left(\widehat{x}\right) d\widehat{x} \end{array} \right. \tag{1.16}$$

$$\left\{ \begin{array}{rcl} \widehat{\phi} \in L^1\left(\Gamma_0\right) & \Rightarrow & \phi\, \omega_u \in L^1\left(\Gamma_u\right) \\ \displaystyle\int_{\Gamma_0} \widehat{\phi}\left(\widehat{\sigma}\right) d\widehat{\sigma} & = & \displaystyle\int_{\Gamma_u} \phi\left(\sigma\right) \omega_u\left(\sigma\right) d\sigma \end{array} \right. \tag{1.17}$$

where $\phi = \left(\widehat{\phi} \circ T_u^{-1}\right)$, $\omega_u\left(\sigma\right) = \left\| det\left(Jac\, T_u^{-1}\left(\sigma\right)\right) \left(\left(Jac\, T_u^{-1}\left(\sigma\right)\right)^{-1}\right)^t n\left(\sigma\right) \right\|_{\mathbb{R}^3}$ *and* $n\left(\sigma\right)$ *is the unit outward normal to* Γ_u *in* σ,

$$\left\{\begin{array}{lcl} \phi \in W^1\left(\Omega_u^F\right) & \Leftrightarrow & \widehat{\phi} = \phi \circ T_u \in W^1\left(\Omega_0^F\right) \\ \left(\begin{array}{c} \frac{\partial \phi}{\partial x_1}(x) \\ \frac{\partial \phi}{\partial x_2}(x) \\ \frac{\partial \phi}{\partial x_3}(x) \end{array}\right) & = & \left(\left(Jac\, T_u(\widehat{x})\right)^{-1}\right)^t \left(\begin{array}{c} \frac{\partial \widehat{\phi}}{\partial \widehat{x}_1}(\widehat{x}) \\ \frac{\partial \widehat{\phi}}{\partial \widehat{x}_2}(\widehat{x}) \\ \frac{\partial \widehat{\phi}}{\partial \widehat{x}_3}(\widehat{x}) \end{array}\right) \end{array}\right. \tag{1.18}$$

Proof. Since $det\left(Jac\, T_u(\widehat{x})\right) = det\left(Jac\, T_u^{-1}(x)\right) = 1$ for all x and $\widehat{x}$ in $\mathbb{R}^3$, the assertion (1.16) is a consequence of the change-of-variable formula for the unbounded domains (see [2, Theorem VIII.5.1, p. 352]).

The proof of (1.17) can be founded in [13, Prop. 2.47, p. 78].

Let us prove (1.18). Let $\phi \in W^1\left(\Omega_u^F\right)$ be given.

From the change-of-variable formula (1.16), we have

$$\int_{\Omega_u^F} \frac{|\phi(x)|^2}{1+\|x\|^2} dx = \int_{\Omega_0^F} \frac{\left|\widehat{\phi}(\widehat{x})\right|^2}{1+\|\widehat{x}\|^2} d\widehat{x}$$

Let $\psi \in \mathcal{D}\left(\Omega_0^F\right)$ and $supp\ \psi \subseteq \mathcal{O}$ where $\mathcal{O}$ is a open and bounded set in Ω_0^F.

Since T_u is a diffeomorphism, we have than $T_u(\mathcal{O})$ is a open and bounded set in Ω_u^F.

From the Remark 7 [8, vol. 5, chap IX A, p. 264], we have $\phi \in H^1\left(T_u(\mathcal{O})\right)$ and using [6, Prop. IX.6, p. 156], we obtain that $\widehat{\phi} \in H^1(\mathcal{O})$ and

$$\int_{\mathcal{O}} (\phi \circ T_u)(\widehat{x}) \frac{\partial \psi}{\partial \widehat{x}_j}(\widehat{x})\, d\widehat{x} = -\sum_{i=1}^{3} \int_{\mathcal{O}} \frac{\partial \phi}{\partial x_i}(T_u(\widehat{x})) \frac{\partial T_{u,i}}{\partial \widehat{x}_j}(\widehat{x})\, \psi(\widehat{x})\, d\widehat{x}$$

The above equality holds also if we change $\mathcal{O}$ by Ω_0^F because $supp\ \psi \subseteq \mathcal{O} \subseteq \Omega_0^F$ then the equality from the second row of the system (1.18) holds.

Since $Jac\, T_u$ is in $\left(L^\infty\left(\Omega_0^F\right)\right)^9$, we have that $\frac{\partial \widehat{\phi}}{\partial \widehat{x}_j}$ are in $L^2\left(\Omega_0^F\right)$ for $j = 1, 2, 3$, so $\widehat{\phi} \in W^1\left(\Omega_0^F\right)$. $\square$

Let us consider the following Hilbert space:

$$\widehat{W} = \left\{\widehat{w} \in \left(W^1\left(\Omega_0^F\right)\right)^3;\ \widehat{w} = 0 \text{ on } \overline{\Sigma}_1 \cup \overline{\Sigma}_2\right\}$$

equipped with the scalar product

$$(\widehat{v}, \widehat{w}) = \sum_{i,j=1}^{3} \int_{\Omega_0^F} \frac{\partial \widehat{v}_i}{\partial \widehat{x}_j} \frac{\partial \widehat{w}_i}{\partial \widehat{x}_j} d\widehat{x} \tag{1.19}$$

where $\widehat{v} = (\widehat{v}_1, \widehat{v}_2, \widehat{v}_3)$ and $\widehat{w} = (\widehat{w}_1, \widehat{w}_2, \widehat{w}_3)$ are in $\widehat{W}$.

Also, let us consider the Hilbert space:

$$\widehat{Q} = L^2\left(\Omega_0^F\right)$$

equipped with the habitual scalar product.

We set

$$\begin{gathered}
\widehat{a}_F : \left(H_0^2\left(]0, L[\right)\right)^3 \times \widehat{W} \times \widehat{W} \to \mathbb{R} \\
\widehat{a}_F\left(u, \widehat{v}, \widehat{w}\right) \\
= \sum_{i=1}^{3} \int_{\Omega_0^F} \left(\frac{\partial \widehat{v}_i}{\partial \widehat{x}_1} - u_2' \frac{\partial \widehat{v}_i}{\partial \widehat{x}_2} - u_3' \frac{\partial \widehat{v}_i}{\partial \widehat{x}_3}\right)\left(\frac{\partial \widehat{w}_i}{\partial \widehat{x}_1} - u_2' \frac{\partial \widehat{w}_i}{\partial \widehat{x}_2} - u_3' \frac{\partial \widehat{w}_i}{\partial \widehat{x}_3}\right) d\widehat{x} \\
+ \sum_{i=1}^{3} \int_{\Omega_0^F} \left(\frac{\partial \widehat{v}_i}{\partial \widehat{x}_2}\frac{\partial \widehat{w}_i}{\partial \widehat{x}_2} + \frac{\partial \widehat{v}_i}{\partial \widehat{x}_3}\frac{\partial \widehat{w}_i}{\partial \widehat{x}_3}\right) d\widehat{x}
\end{gathered} \tag{1.20}$$

and

$$\begin{cases}
\widehat{b}_F : \left(H_0^2\left(]0, L[\right)\right)^3 \times \widehat{W} \times \widehat{Q} \to \mathbb{R} \\
\widehat{b}_F\left(u, \widehat{w}, \widehat{q}\right) = -\displaystyle\int_{\Omega_0^F} \left(\frac{\partial \widehat{w}_1}{\partial \widehat{x}_1} + \frac{\partial \widehat{w}_2}{\partial \widehat{x}_2} + \frac{\partial \widehat{w}_3}{\partial \widehat{x}_3} - u_2' \frac{\partial \widehat{w}_2}{\partial \widehat{x}_1} - u_3' \frac{\partial \widehat{w}_3}{\partial \widehat{x}_1}\right) \widehat{q}\, d\widehat{x}
\end{cases} \tag{1.21}$$

Proposition 1.4 *For all u_2, u_3 in $H_0^2\left(]0, L[\right)$, $\widehat{\lambda} = \left(\widehat{\lambda}_1, \widehat{\lambda}_2, \widehat{\lambda}_3\right)$ in $\left(L^2\left(\Gamma_0\right)\right)^3$, the problem:*
Find $(\widehat{v},\ \widehat{p}) \in \widehat{W} \times \widehat{Q}$ such that

$$\begin{cases}
\widehat{a}_F\left(u, \widehat{v}, \widehat{w}\right) + \widehat{b}_F\left(u, \widehat{w}, \widehat{p}\right) = \displaystyle\sum_{i=1}^{3} \int_{\Gamma_0} \widehat{\lambda}_i \widehat{w}_i\, d\widehat{\sigma}, & \forall \widehat{w} \in \widehat{W} \\
\widehat{b}_F\left(u, \widehat{v}, \widehat{q}\right) = 0, & \forall \widehat{q} \in \widehat{Q}
\end{cases} \tag{1.22}$$

has a unique solution.

Proof.

Existence: Let u_2, u_3 in $H_0^2\left(]0, L[\right)$ and $\widehat{\lambda} = \left(\widehat{\lambda}_1, \widehat{\lambda}_2, \widehat{\lambda}_3\right)$ in $\left(L^2\left(\Gamma_0\right)\right)^3$ be given. We set $\lambda\left(\sigma\right) = \left(\widehat{\lambda} \circ T_u^{-1}\right)\left(\sigma\right) \omega_u\left(\sigma\right)$ where

$$\omega_u\left(\sigma\right) = \left\| det\left(Jac\, T_u^{-1}\left(\sigma\right)\right)\left(\left(Jac\, T_u^{-1}\left(\sigma\right)\right)^{-1}\right)^t n\left(\sigma\right)\right\|_{\mathbb{R}^3}$$

and $n\left(\sigma\right)$ is the unit outward normal to Γ_u in σ.

From the Lemma 1.2, we obtain that λ is well defined and $\lambda \in \left(L^2\left(\Gamma_0\right)\right)^3$.

According to the Proposition 1.3, there exits an unique solution (v,p) of the mixed system (1.13) and we set $\widehat{v} = v \circ T_u,\ \widehat{p} = p \circ T_u$.

From the Lemma 1.2, we have that $\widehat{v} \in \widehat{W}$ and $\widehat{p} \in \widehat{Q}$. Using the change-of-variable formula, we obtain that (1.22) holds.

Uniqueness: Let $(\widehat{v}^1,\ \widehat{p}^1)$ and $(\widehat{v}^2,\ \widehat{p}^2)$ be two solutions of the (1.22).

We set $v^1 = \widehat{v}^1 \circ T_u^{-1}$, $p^1 = \widehat{p}^1 \circ T_u^{-1}$, $v^2 = \widehat{v}^2 \circ T_u^{-1}$ and $p^2 = \widehat{p}^2 \circ T_u^{-1}$. Using once again the change-of-variable formula, we have that (v^1,p^1) and (v^2,p^2) are solutions for (1.13), but this problem has a unique solution, then $(v^1,p^1) = (v^2,p^2)$.

It follows that

$$\widehat{v}^1 = \left(\widehat{v}^1 \circ T_u^{-1}\right) \circ T_u = \left(\widehat{v}^2 \circ T_u^{-1}\right) \circ T_u = \widehat{v}^2$$

and in the same way, $\widehat{p}^1 = \widehat{p}^2$.

So, the conclusion of the proposition holds. □

1.6 Existence of an optimal control for the fluid-cable interaction problem

The coupled fluid-cable problem will be modeled by an optimal control variational system.

In this section, the existence of an optimal control for the fluid-cable interaction problem will be proved.

Let f_i^S in $H^{-2}\left(]0,L[\right)$, $i = 2,3$ and $\widehat{K}$ compact in $\left(L^2\left(\Gamma_0\right)\right)^3$ be given. Let D be the operator defined by the Proposition 1.2.

We denote by $\widehat{v}_{|\Gamma_0}$ the trace on Γ_0 of $\widehat{v} \in \widehat{W}$ and by $\|\cdot\|_{0,\Gamma_0}$ the habitual norm in $\left(L^2\left(\Gamma_0\right)\right)^3$.

We consider the following optimal control problem $\mathcal{P}$:

$$\inf \frac{1}{2} \left\|\widehat{v}_{|\Gamma_0}\right\|_{0,\Gamma_0}^2$$

subject to

a) $\widehat{\lambda} \in \widehat{K}$

b) $u_2, u_3 \in H_0^2\left(]0,L[\right)$

c) $a_S\left(u_i,\psi\right) = -\displaystyle\int_{]0,L[} \left(D\widehat{\lambda}_i\right)\left(x_1\right)\psi\left(x_1\right)dx_1 + \left\langle f_i^S,\psi\right\rangle, \quad \forall \psi \in H_0^2\left(]0,L[\right),\ i = 2,3$

d) $(\widehat{v},\widehat{p}) \in \widehat{W} \times \widehat{Q}$

e)
$$\begin{cases} \widehat{a}_F\left(u,\widehat{v},\widehat{w}\right) + \widehat{b}_F\left(u,\widehat{w},\widehat{p}\right) = \displaystyle\sum_{i=1}^{3} \int_{\Gamma_0} \widehat{\lambda}_i \widehat{w}_i\, d\widehat{\sigma}, & \forall \widehat{w} \in \widehat{W} \\ \widehat{b}_F\left(u,\widehat{v},\widehat{q}\right) = 0, & \forall \widehat{q} \in \widehat{Q} \end{cases}$$

It's an optimal control problem with Neumann like boundary control ($\widehat{\lambda}$) and Dirichlet like boundary observation ($\widehat{v}_{|\Gamma_0}$). The control appears also in the coefficients of the fluid equations (relation e)).

The relation a) represents the control constraint and the second relation of the system e) represents the state constraint.

This mathematical model permits to solve numerically the coupled fluid-cable problem via partitioned procedures (i.e. in a decoupled way, more precisely the fluid and the cable equations are solved separately).

The relations b) and c) represent the cable equations and the relations d) and e) represent the fluid equations.

In the classical approaches, the fluid and structure equations are coupled by two boundary conditions: equality of the fluid's and structure's velocities at the contact surface (which is a Dirichlet like boundary condition) and equality of the forces at the contact surface (which is a Neumann like boundary condition).

In our approach, we start with a guess for the contact forces (step a). The displacement of the structure can be computed (steps b and c). We suppose that domain occupied by the fluid is completely determined by the displacement of the structure. Knowing the actual domain of the fluid and the contact forces, we can compute the velocity and the pressure of the fluid (steps d and e).

In this way, the Neumann like contact boundary condition is trivially accomplished: we use the same value $\widehat{\lambda}$ for the contact forces on Γ_0 in the equations c) (for the cable) and in the equations e) (for the fluid).

The Dirichlet like contact boundary condition $\widehat{v}_{|\Gamma_0} = 0$ is treated by the Least Squares Method

$$\inf \frac{1}{2} \left\| \widehat{v}_{|\Gamma_0} \right\|^2_{0,\Gamma_0}$$

We denote by $|\cdot|_{1,\Omega_0^F}$ the norm induced by the scalar product (1.19). We have that $\widehat{W}$ is a Hilbert space for this scalar product.

If A is a matrix, we denote by A^t the transpose matrix and if y is a column vector of $\mathbb{R}^3$

$$y = \begin{pmatrix} y_1 \\ y_2 \\ y_3 \end{pmatrix},$$

we denote by y^t the transpose vector $y^t = (y_1, y_2, y_3)$.

Lemma 1.3 *Let B be a bounded set in $H_0^2(]0, L[)$.*

Then the following inequalities hold:

$$\exists m_B > 0, \forall u_2, u_3 \in B, \forall \widehat{w} \in \widehat{W}, \quad m_B \left|\widehat{w}\right|^2_{1,\Omega_0^F} \leq \widehat{a}_F\left(u, \widehat{w}, \widehat{w}\right)$$
$$\exists M_B > 0, \forall u_2, u_3 \in B, \forall \widehat{w}^1, \widehat{w}^2 \in \widehat{W}, \ \widehat{a}_F\left(u, \widehat{w}^1, \widehat{w}^2\right) \leq M_B \left|\widehat{w}^1\right|_{1,\Omega_0^F} \left|\widehat{w}^2\right|_{1,\Omega_0^F}$$

Proof. The equality (1.20) can be rewritten in the form

$$\widehat{a}_F(u,\widehat{v},\widehat{w}) = \sum_{i=1}^{3}\int_{\Omega_0^F}\left(\frac{\partial\widehat{v}_i}{\partial\widehat{x}_1},\frac{\partial\widehat{v}_i}{\partial\widehat{x}_2},\frac{\partial\widehat{v}_i}{\partial\widehat{x}_3}\right)L_u^t(\widehat{x}_1)\,L_u(\widehat{x}_1)\left(\frac{\partial\widehat{w}_i}{\partial\widehat{x}_1},\frac{\partial\widehat{w}_i}{\partial\widehat{x}_2},\frac{\partial\widehat{w}_i}{\partial\widehat{x}_3}\right)^t d\widehat{x} \tag{1.23}$$

where for all $\widehat{x}_1$ in $[0,L]$ we denote:

$$L_u(\widehat{x}_1) = \begin{pmatrix} 1 & -u_2'(\widehat{x}_1) & -u_3'(\widehat{x}_1) \\ 0 & 1 & 0 \\ 0 & 0 & 1 \end{pmatrix} = \left(\left(Jac\,T_u^{-1}(\widehat{x})\right)^{-1}\right)^t$$

Evidently, L is an invertible matrix and we have:

$$L_u^{-1}(\widehat{x}_1) = \begin{pmatrix} 1 & u_2'(\widehat{x}_1) & u_3'(\widehat{x}_1) \\ 0 & 1 & 0 \\ 0 & 0 & 1 \end{pmatrix}$$

We denote by $\|y\| = (y^t y)^{1/2}$ the euclidean norm of $\mathbb{R}^3$. Now, we evaluate the euclidean norm of the matrix L^{-1}.

$$\begin{aligned} \left\|L_u^{-1}(\widehat{x}_1)\right\| &= \max_{\|y\|\le 1}\left\|L_u^{-1}(\widehat{x}_1)\,y\right\| \\ &= \max_{\|y\|\le 1}\sqrt{\left(y_1+u_2'(\widehat{x}_1)\,y_2+u_3'(\widehat{x}_1)\,y_3\right)^2+y_2^2+y_3^2} \\ &\le \max_{\|y\|\le 1}\sqrt{\left(1+\left(u_2'(\widehat{x}_1)\right)^2+\left(u_3'(\widehat{x}_1)\right)^2\right)\left(y_1^2+y_2^2+y_3^2\right)+y_2^2+y_3^2} \\ &\le \sqrt{2+\left(u_2'(\widehat{x}_1)\right)^2+\left(u_3'(\widehat{x}_1)\right)^2} \end{aligned}$$

We have

$$\begin{aligned} |u_i'(\widehat{x}_1)| &= \left|\int_0^{\widehat{x}_1} u_i''(s)\,ds\right| \le \int_0^{\widehat{x}_1}|u_i''(s)|\,ds \\ &\le \int_0^L |u_i''(s)|\,ds \le \sqrt{L}\left(\int_0^L\left(u_i''(s)\right)^2 ds\right)^{1/2} \le \sqrt{L}\,\|u_i\|_{2,]0,L[} \end{aligned} \tag{1.24}$$

The set B is bounded in $H_0^2(]0,L[)$, then

$$\exists\alpha_B>0,\forall u_2,u_3\in B,\forall\widehat{x}_1\in[0,L],\quad \left\|L_u^{-1}(\widehat{x}_1)\right\|\le\sqrt{\alpha_B}$$

It follows that

$$\begin{aligned} &\forall u_2,u_3\in B,\forall\widehat{x}_1\in[0,L],\forall y\in\mathbb{R}^3, \\ &\|L_u(\widehat{x}_1)\,y\|^2 = y^t L_u^t(\widehat{x}_1)\,L_u(\widehat{x}_1)\,y \ge \frac{1}{\alpha_B}\|y\|^2 \end{aligned}$$

Using the last inequality, we obtain from (1.23) the following relation:

$$\forall u_2, u_3 \in B, \forall \widehat{w} \in \widehat{W},$$
$$\frac{1}{\alpha_B} |\widehat{w}|_{1,\Omega_0^F} = \frac{1}{\alpha_B} \sum_{i=1}^{3} \sum_{j=1}^{3} \int_{\Omega_0^F} \left| \frac{\partial \widehat{w}_i}{\partial \widehat{x}_j} (\widehat{x}) \right|^2 d\widehat{x} \leq \widehat{a}_F (u, \widehat{w}, \widehat{w})$$

In the same way, we have

$$\forall u_2, u_3 \in B, \forall \widehat{x}_1 \in [0, L], \quad \|L_u (\widehat{x}_1)\| \leq \sqrt{\alpha_B}$$

and then

$$\forall u_2, u_3 \in B, \forall \widehat{x}_1 \in [0, L], \forall y, z \in \mathbb{R}^3,$$
$$z^t L_u^t (\widehat{x}_1) L_u (\widehat{x}_1) y \leq \alpha_B z^t y$$

Using the last inequality, we obtain from (1.23) the following relation:

$$\forall u_2, u_3 \in B, \forall \widehat{w}^1, \widehat{w}^2 \in \widehat{W},$$
$$\widehat{a}_F \left(u, \widehat{w}^1, \widehat{w}^2\right) \leq \alpha_B \sum_{i=1}^{3} \sum_{j=1}^{3} \int_{\Omega_0^F} \frac{\partial \widehat{w}_i^1}{\partial \widehat{x}_j} \frac{\partial \widehat{w}_i^2}{\partial \widehat{x}_j} d\widehat{x} \leq \alpha_B \left|\widehat{w}^1\right|_{1,\Omega_0^F} \left|\widehat{w}^2\right|_{1,\Omega_0^F}$$

We set $m_B = 1/\alpha_B$, $M_B = \alpha_B$ and then the proof of this lemma is finished. □

Lemma 1.4 *Let u_2 and u_3 be given in $H_0^2(]0, L[)$. Then*

$$\exists \delta_u > 0, \forall \widehat{w} \in \widehat{W}, \forall \widehat{q} \in \widehat{Q}, \quad \delta_u |\widehat{w}|_{1,\Omega_0^F} \|\widehat{q}\|_{0,\Omega_0^F} \leq \widehat{b}_F (u, \widehat{w}, \widehat{q})$$

Proof. Using the change-of-variable formula (1.18), we obtain that

$$\begin{aligned}
\frac{\partial w_1}{\partial x_1}(x) &= \frac{\partial \widehat{w}_1}{\partial \widehat{x}_1}(\widehat{x}) - u_2'(\widehat{x}_1) \frac{\partial \widehat{w}_1}{\partial \widehat{x}_2}(\widehat{x}) - u_3'(\widehat{x}_1) \frac{\partial \widehat{w}_1}{\partial \widehat{x}_3}(\widehat{x}) \\
\frac{\partial w_2}{\partial x_2}(x) &= \frac{\partial \widehat{w}_2}{\partial \widehat{x}_2}(\widehat{x}) \\
\frac{\partial w_3}{\partial x_3}(x) &= \frac{\partial \widehat{w}_3}{\partial \widehat{x}_3}(\widehat{x})
\end{aligned}$$

From the Lemma 1.1 and the above equalities, we obtain that the operator mapping $\widehat{W}$ onto $\widehat{Q}$

$$\widehat{w} \longmapsto \frac{\partial \widehat{w}_1}{\partial \widehat{x}_1} + \frac{\partial \widehat{w}_2}{\partial \widehat{x}_2} + \frac{\partial \widehat{w}_3}{\partial \widehat{x}_3} - u_2' \frac{\partial \widehat{w}_1}{\partial \widehat{x}_2} - u_3' \frac{\partial \widehat{w}_1}{\partial \widehat{x}_3}$$

is surjectif.

In a standard way, from the property of the surjectif operators [6, Theorem II.19, p. 29], we obtain the conclusion of this Lemma. □

Lemma 1.5 *Let u_2, u_3, $\overline{u}_2$, $\overline{u}_3$ be given in $H_0^2(]0,L[)$. We denote $u=(0,u_2,u_3)$ and $\overline{u}=(0,\overline{u}_2,\overline{u}_3)$. Then there exists a constant β not depending upon u, $\overline{u}$ such that*

$$\forall \widehat{w}\in\widehat{W},\forall \widehat{q}\in\widehat{Q},\quad \widehat{b}_F\left(u,\widehat{w},\widehat{q}\right)\geq \widehat{b}_F\left(\overline{u},\widehat{w},\widehat{q}\right)-\beta\left\|u-\overline{u}\right\|_{2,]0,L[}\left|\widehat{w}\right|_{1,\Omega_0^F}\left\|\widehat{q}\right\|_{0,\Omega_0^F}$$

Proof. We have

$$\widehat{b}_F\left(u,\widehat{w},\widehat{q}\right)-\widehat{b}_F\left(\overline{u},\widehat{w},\widehat{q}\right)=-\int_{\Omega_0^F}\left(u_2-\overline{u}_2\right)'\frac{\partial\widehat{w}_1}{\partial\widehat{x}_2}\widehat{q}\,d\widehat{x}-\int_{\Omega_0^F}\left(u_3-\overline{u}_3\right)'\frac{\partial\widehat{w}_1}{\partial\widehat{x}_2}\widehat{q}\,d\widehat{x}$$

Using the inequality (1.24) and after the Cauchy-Schwartz inequality, we obtain

$$\int_{\Omega_0^F}\left(u_i-\overline{u}_i\right)'\frac{\partial\widehat{w}_1}{\partial\widehat{x}_i}\widehat{q}\,d\widehat{x}\leq\sqrt{L}\left\|u_i-\overline{u}_i\right\|_{2,]0,L[}\left\|\frac{\partial\widehat{w}_1}{\partial\widehat{x}_i}\right\|_{0,\Omega_0^F}\left\|\widehat{q}\right\|_{0,\Omega_0^F}\qquad\text{for } i=2,3$$

and the proof of this Lemma is finished. □

Theorem 1.1 *For all f_i^S in $H_0^2(]0,L[)$, $i=2,3$ and $\widehat{K}$ compact in $\left(L^2(\Gamma_0)\right)^3$, the problem $\mathcal{P}$ has at least one optimal solution $\left[\widehat{\lambda}^*,u^*,\widehat{v}^*,\widehat{p}^*\right]$, where $\widehat{\lambda}^*$ is the density of the forces on the contact surface, $u^*=(0,u_2^*,u_3^*)$ is the displacement of the cable, $\widehat{v}^*$ and $\widehat{p}^*$ are the velocity and the pressure of the fluid in the arbitrary lagrangian eulerian coordinates. In order to obtain the velocity and the pressure in the real domain we must use the transformation $v^*=\widehat{v}^*\circ T_{u^*}^{-1}$ and $p^*=\widehat{p}^*\circ T_{u^*}^{-1}$.*

Proof. I) The cost functional of the problem $\mathcal{P}$ is evidently positiv, then there exits a real number d such that

$$\inf\frac{1}{2}\left\|\widehat{v}_{|\Gamma_0}\right\|_{0,\Gamma_0}^2=d \tag{1.25}$$

The observation $\widehat{v}$ was computed from the control $\widehat{\lambda}$ using the relations a) - e) of the problem $\mathcal{P}$.

Let $\left\{\widehat{\lambda}^k\right\}_{k\in\mathbb{N}}$ be a minimizing sequence, i.e.

$$\lim_{k\to\infty}\frac{1}{2}\left\|\widehat{v}_{|\Gamma_0}^k\right\|_{0,\Gamma_0}^2=d \tag{1.26}$$

where $\widehat{v}^k$ was computed from $\widehat{\lambda}^k$ using the following relations:

$a')$ $\widehat{\lambda}^k\in\widehat{K}$

$b')$ $u_2^k,u_3^k\in H_0^2(]0,L[)$

$c')$ $a_S\left(u_i^k,\psi\right)=-\int_{]0,L[}\left(D\widehat{\lambda}_i^k\right)(x_1)\,\psi(x_1)\,dx_1+\left\langle f_i^S,\psi\right\rangle,\quad\forall\psi\in H_0^2(]0,L[),\ i=2,3$

$d')$ $\left(\widehat{v}^k,\widehat{p}^k\right)\in\widehat{W}\times\widehat{Q}$

$e')$ $\begin{cases}\widehat{a}_F\left(u^k,\widehat{v}^k,\widehat{w}\right)+\widehat{b}_F\left(u^k,\widehat{w},\widehat{p}^k\right)=\sum_{i=1}^3\int_{\Gamma_0}\widehat{\lambda}_i^k\widehat{w}_i\,d\widehat{\sigma}, & \forall\widehat{w}\in\widehat{W}\\ \widehat{b}_F\left(u^k,\widehat{v}^k,\widehat{q}\right)=0, & \forall\widehat{q}\in\widehat{Q}\end{cases}$

The set $\widehat{K}$ is compact, then there exits a subsequence of $\left\{\widehat{\lambda}^k\right\}_{k\in\mathbb{N}}$ strongly convergent in $\left(L^2(\Gamma_0)\right)^3$. Without risk of confusion, we use the same notation $\left\{\widehat{\lambda}^k\right\}_{k\in\mathbb{N}}$ for this subsequence. We denote $\widehat{\lambda}^*$ its limit, so

$$\widehat{\lambda}^k \to \widehat{\lambda}^* \text{ strongly in } \left(L^2(\Gamma_0)\right)^3$$

II) Let $u^* = (0, u_2^*, u_3^*)$ be the displacement of the cable computed using the variational equations b) - c) for the density of the contact forces $\widehat{\lambda}^*$. Since $\left\{\widehat{\lambda}^k\right\}_{k\in\mathbb{N}}$ is strongly convergent in $\left(L^2(\Gamma_0)\right)^3$ to $\widehat{\lambda}^*$, from b') and c') we obtain that $u^k = \left(0, u_2^k, u_3^k\right)$ is strongly convergent to u^* in $\left(H_0^2(]0, L[)\right)^3$. Consequently, there exists a compact B in $H_0^2(]0, L[)$ such that u_2^k, u_3^k belong to B for all k. Also, u_2^*, u_3^* belong to B.

III) From e') we have

$$\widehat{a}_F\left(u^k, \widehat{v}^k, \widehat{v}^k\right) = \sum_{i=1}^{3} \int_{\Gamma_0} \widehat{\lambda}_i^k \widehat{v}_i^k \, d\widehat{\sigma}$$

and using the Lemma 1.3 and the Cauchy-Schwartz inequality, we obtain

$$m_B \left|\widehat{v}^k\right|_{1,\Omega_0^F}^2 \leq \left\|\widehat{\lambda}^k\right\|_{0,\Gamma_0} \left\|\widehat{v}_{|\Gamma_0}^k\right\|_{0,\Gamma_0}$$

From the Trace Theorem, we have for all $\widehat{w}$ in $\widehat{W}$

$$\left\|\widehat{w}_{|\Gamma_0}\right\|_{0,\Gamma_0} \leq c\left(\Omega_0^F\right) |\widehat{w}|_{1,\Omega_0^F}$$

where $c\left(\Omega_0^F\right)$ is a constant only depending upon Ω_0^F which is fixed.

It follows that

$$m_B \left|\widehat{v}^k\right|_{1,\Omega_0^F}^2 \leq c\left(\Omega_0^F\right) \left\|\widehat{\lambda}^k\right\|_{0,\Gamma_0} \left|\widehat{v}^k\right|_{1,\Omega_0^F}$$

Since $\widehat{\lambda}^k$ is strongly convergent, then $\left\|\widehat{\lambda}^k\right\|_{0,\Gamma_0}$ is bounded which implies that $\left|\widehat{v}^k\right|_{1,\Omega_0^F}$ is bounded, too.

From the first equality of the system e') and the Lemma 1.3, we have

$$\begin{aligned}\widehat{b}_F\left(u^k, \widehat{w}, \widehat{p}^k\right) &= \sum_{i=1}^{3} \int_{\Gamma_0} \widehat{\lambda}_i^k \widehat{w}_i \, d\widehat{\sigma} - \widehat{a}_F\left(u^k, \widehat{v}^k, \widehat{w}\right) \\ &\leq \sum_{i=1}^{3} \int_{\Gamma_0} \widehat{\lambda}_i^k \widehat{w}_i \, d\widehat{\sigma} + M_B \left|\widehat{v}^k\right|_{1,\Omega_0^F} |\widehat{w}|_{1,\Omega_0^F}\end{aligned}$$

From the Cauchy Schwartz inequality and the trace theorem, it follows

$$\sum_{i=1}^{3} \int_{\Gamma_0} \widehat{\lambda}_i^k \widehat{w}_i \, d\widehat{\sigma} \leq \left\|\widehat{\lambda}^k\right\|_{0,\Gamma_0} \left\|\widehat{w}_{|\Gamma_0}\right\|_{0,\Gamma_0} \leq c\left(\Omega_0^F\right) \left\|\widehat{\lambda}^k\right\|_{0,\Gamma_0} |\widehat{w}|_{1,\Omega_0^F}$$

From the above inequalities, we obtain

$$\widehat{b}_F\left(u^k,\widehat{w},\widehat{p}^k\right)\leq c\left(\Omega_0^F\right)\left\|\widehat{\lambda}^k\right\|_{0,\Gamma_0}|\widehat{w}|_{1,\Omega_0^F}+M_B\left|\widehat{v}^k\right|_{1,\Omega_0^F}|\widehat{w}|_{1,\Omega_0^F} \tag{1.27}$$

From the Lemmas 1.4 and 1.5, we have

$$\begin{aligned}&\delta_{u^*}|\widehat{w}|_{1,\Omega_0^F}\left\|\widehat{p}^k\right\|_{0,\Omega_0^F}-\beta\left\|u^k-u^*\right\|_{2,]0,L[}|\widehat{w}|_{1,\Omega_0^F}\left\|\widehat{p}^k\right\|_{0,\Omega_0^F}\\&\leq\widehat{b}_F\left(u^*,\widehat{w},\widehat{p}^k\right)-\beta\left\|u^k-u^*\right\|_{2,]0,L[}|\widehat{w}|_{1,\Omega_0^F}\left\|\widehat{p}^k\right\|_{0,\Omega_0^F}\\&\leq\widehat{b}_F\left(u^k,\widehat{w},\widehat{p}^k\right)\end{aligned} \tag{1.28}$$

Using the inequalities (1.27) and (1.28), we obtain for all k in $\mathbb{N}$ and $\widehat{w}$ in $\widehat{W}$

$$\begin{aligned}&\left(\delta_{u^*}-\beta\left\|u^k-u^*\right\|_{2,]0,L[}\right)\left\|\widehat{p}^k\right\|_{0,\Omega_0^F}|\widehat{w}|_{1,\Omega_0^F}\\&\leq\left(c\left(\Omega_0^F\right)\left\|\widehat{\lambda}^k\right\|_{0,\Gamma_0}+M_B\left|\widehat{v}^k\right|_{1,\Omega_0^F}\right)|\widehat{w}|_{1,\Omega_0^F}\end{aligned}$$

Since $\delta_{u^*}>0$ is fixed, $\left|\widehat{v}^k\right|_{1,\Omega_0^F}$ and $\left\|\widehat{\lambda}^k\right\|_{0,\Gamma_0}$ are bounded and

$$\lim_{k\to\mathbb{N}}\left\|u^k-u^*\right\|_{2,]0,L[}=0$$

we obtain that $\left\|\widehat{p}^k\right\|_{0,\Omega_0^F}$ is bounded.

The spaces $\widehat{W}$ and $\widehat{Q}$ are Hilbert, then there exists a subsequence $\left\{\widehat{v}^{k_l}\right\}_{l\in\mathbb{N}}$ weakly convergent in $\widehat{W}$ and $\left\{\widehat{p}^{k_l}\right\}_{l\in\mathbb{N}}$ weakly convergent in $\widehat{Q}$. We denote by $\widehat{v}^{**}$ and $\widehat{p}^{**}$ the limits of these subsequences.

IV) We have from the previous steps

$$\begin{array}{rcll}\widehat{\lambda}^k&\to&\widehat{\lambda}^*&\text{strongly in }\left(L^2\left(\Gamma_0\right)\right)^3\\u^k&\to&u^*&\text{strongly in }\left(H_0^2\left(]0,L[\right)\right)^3\\\widehat{v}^{k_l}&\to&\widehat{v}^{**}&\text{weakly in }\widehat{W}\\\widehat{p}^{k_l}&\to&\widehat{p}^{**}&\text{weakly in }\widehat{Q}\end{array}$$

We denote by $(\widehat{v}^*,\widehat{p}^*)$ the solution of the problem (1.22) computed for the displacement u^* and for the forces $\widehat{\lambda}^*$ on the surface Γ_0.

We shall prove that $\widehat{v}^{**}=\widehat{v}^*$, $\widehat{p}^{**}=\widehat{p}^*$, the whole sequence $\left\{\widehat{v}^k\right\}_{k\in\mathbb{N}}$ is weakly convergent to $\widehat{v}^*$ in $\widehat{W}$ and the whole sequence $\left\{\widehat{p}^k\right\}_{k\in\mathbb{N}}$ is weakly convergent to $\widehat{p}^*$ in $\widehat{Q}$. In order to prove this, we shall show that the following equalities hold:

$$\begin{aligned}\forall\widehat{w}\in\widehat{W},\quad&\lim_{l\to\mathbb{N}}\widehat{a}_F\left(u^{k_l},\widehat{v}^{k_l},\widehat{w}\right)=\widehat{a}_F\left(u^*,\widehat{v}^{**},\widehat{w}\right)\\\forall\widehat{w}\in\widehat{W},\quad&\lim_{l\to\mathbb{N}}\widehat{b}_F\left(u^{k_l},\widehat{w},\widehat{p}^{k_l}\right)=\widehat{b}_F\left(u^*,\widehat{w},\widehat{p}^{**}\right)\\\forall\widehat{q}\in\widehat{Q},\quad&\lim_{l\to\mathbb{N}}\widehat{b}_F\left(u^{k_l},\widehat{v}^{k_l},\widehat{q}\right)=\widehat{b}_F\left(u^*,\widehat{v}^{**},\widehat{q}\right)\end{aligned}$$

According to (1.20), we have that $\widehat{a}_F\left(u^{k_l},\widehat{v}^{k_l},\widehat{w}\right)$ is a sum of terms like these:

$$i) \qquad \int_{\Omega_0^F}\frac{\partial\widehat{v}_i^{k_l}}{\partial\widehat{x}_j}\frac{\partial\widehat{w}_i}{\partial\widehat{x}_j}d\widehat{x},\quad j=1,2,3$$

$$ii) \qquad \int_{\Omega_0^F}\frac{\partial\widehat{v}_i^{k_l}}{\partial\widehat{x}_1}\frac{\partial\widehat{w}_i}{\partial\widehat{x}_j}\left(u_j^{k_l}\right)'d\widehat{x},\quad j=2,3$$

$$iii) \qquad \int_{\Omega_0^F}\frac{\partial\widehat{v}_i^{k_l}}{\partial\widehat{x}_j}\frac{\partial\widehat{w}_i}{\partial\widehat{x}_1}\left(u_j^{k_l}\right)'d\widehat{x},\quad j=2,3$$

$$iv) \qquad \int_{\Omega_0^F}\frac{\partial\widehat{v}_i^{k_l}}{\partial\widehat{x}_j}\frac{\partial\widehat{w}_i}{\partial\widehat{x}_p}\left(u_j^{k_l}\right)'\left(u_p^{k_l}\right)'d\widehat{x},\quad j,p=2,3$$

From the definition of the weak convergence, we have

$$\forall\widehat{w}\in\widehat{W},\quad \lim_{l\to\mathbb{N}}\int_{\Omega_0^F}\frac{\partial\widehat{v}_i^{k_l}}{\partial\widehat{x}_j}\frac{\partial\widehat{w}_i}{\partial\widehat{x}_j}d\widehat{x}=\int_{\Omega_0^F}\frac{\partial\widehat{v}_i^{**}}{\partial\widehat{x}_j}\frac{\partial\widehat{w}_i}{\partial\widehat{x}_j}d\widehat{x}$$

The terms $ii)$, $iii)$ and $iv)$ have the same form:

$$\int_{\Omega_0^F}\frac{\partial\widehat{v}_i^{k_l}}{\partial\widehat{x}_j}\frac{\partial\widehat{w}_i}{\partial\widehat{x}_p}a^{k_l}d\widehat{x},\quad j,p=2,3.$$

Since $u_j^{k_l}$ and $u_p^{k_l}$ are strongly convergent to u_j^* and u_p^* in $H_0^2\left(]0,L[\right)$ respectively, we obtain that $\left(u_j^{k_l}\right)'$ and $\left(u_p^{k_l}\right)'$ are strongly convergent to $\left(u_j^*\right)'$ and $\left(u_p^*\right)'$in $H_0^1\left(]0,L[\right)$ respectively. Easily, it follows that the product $\left(u_j^{k_l}\right)'\left(u_p^{k_l}\right)'$ is strongly convergent to $\left(u_j^*\right)'\left(u_p^*\right)'$ in $H_0^1\left(]0,L[\right)$.

Therefore, we have that the sequence $\left\{a^{k_l}\right\}_{k_l\in\mathbb{N}}$ is strongly convergent in the space $H_0^1\left([0,L]\right)$. We denote by a its limit.

In the following, it will be useful the well known below result:

Lemma 1.6 *Let X be a reflexive Banach space with dual X'. For all sequence $\left\{w^l\right\}_{l\in\mathbb{N}}$ weakly convergent to w in X and all sequence of linear operators $\{A_l\}_{l\in\mathbb{N}}$ strongly convergent to A in $\mathcal{L}\left(X,X'\right)$, then the sequence $\left\{A_lw^l\right\}_{l\in\mathbb{N}}$ is weakly convergent to Aw in X'.*

In order to apply this Lemma, let us consider the Hilbert space

$$X=\left\{\phi\in W^1\left(\Omega_0^F\right);\ \phi=0\text{ on }\overline{\Sigma}_1\cup\overline{\Sigma}_2\right\}$$

equipped with the scalar product

$$(\psi,\phi)_X=\sum_{j=1}^{3}\int_{\Omega_0^F}\frac{\partial\psi}{\partial\widehat{x}_j}\frac{\partial\phi}{\partial\widehat{x}_j}d\widehat{x}$$

and the induced norm $\|\phi\|_X=\sqrt{(\phi,\phi)_X}$.

Also, let us consider the operators $A_l, A\in\mathcal{L}(X,X')$ definited by

$$\langle A_l\phi,\psi\rangle_{X',X}=\int_{\Omega_0^F}\frac{\partial\psi}{\partial\widehat{x}_j}\frac{\partial\phi}{\partial\widehat{x}_p}a^{k_l}d\widehat{x},\quad\forall\phi,\psi\in X$$
$$\langle A\phi,\psi\rangle_{X',X}=\int_{\Omega_0^F}\frac{\partial\psi}{\partial\widehat{x}_j}\frac{\partial\phi}{\partial\widehat{x}_p}\,a\,d\widehat{x},\quad\forall\phi,\psi\in X.$$

We have

$$\|(A_l-A)\,\phi\|_X=\sup_{\|\psi\|_X\le1}\langle(A_l-A)\,\phi,\psi\rangle=\sup_{\|\psi\|_X\le1}\int_{\Omega_0^F}\frac{\partial\psi}{\partial\widehat{x}_j}\frac{\partial\phi}{\partial\widehat{x}_p}\left(a^{k_l}-a\right)d\widehat{x}$$
$$\le\left(\int_{\Omega_0^F}\left(\frac{\partial\phi}{\partial\widehat{x}_p}\right)^2\left(a^{k_l}-a\right)^2d\widehat{x}\right)^{1/2}\le\max_{\widehat{x}_1\in[0,L]}\left|\left(a^{k_l}-a\right)(\widehat{x}_1)\right|\left(\int_{\Omega_0^F}\left(\frac{\partial\phi}{\partial\widehat{x}_p}\right)^2d\widehat{x}\right)^{1/2}$$
$$\le\max_{\widehat{x}_1\in[0,L]}\left|\left(a^{k_l}-a\right)(\widehat{x}_1)\right|\|\phi\|_X,\qquad\forall\phi\in X$$

Therefore

$$\|(A_l-A)\|_{\mathcal{L}(X,X')}\le\max_{\widehat{x}_1\in[0,L]}\left|\left(a^{k_l}-a\right)(\widehat{x}_1)\right|$$

But

$$\left|\left(a^{k_l}-a\right)(\widehat{x}_1)\right|=\left|\int_0^{\widehat{x}_1}\left(a^{k_l}-a\right)'(s)\,ds\right|\le\int_0^{\widehat{x}_1}\left|\left(a^{k_l}-a\right)'(s)\right|ds$$
$$\le\int_0^L\left|\left(a^{k_l}-a\right)'(s)\right|ds\le\sqrt{L}\left(\int_0^L\left(\left(a^{k_l}-a\right)'(s)\right)^2ds\right)^{1/2}\le\sqrt{L}\left\|a^{k_l}-a\right\|_{1,]0,L[}$$

then A_l is strongly convergent to A in $\mathcal{L}(X,X')$.

Applying the Lemma 1.6, we obtain that

$$\lim_{l\to\infty}\left\langle A_l\widehat{v}_i^{k_l},\widehat{w}_i\right\rangle_{X',X}=\langle A,\widehat{v}_i^{**},\widehat{w}_i\rangle_{X',X}$$

and consequently

$$\forall\widehat{w}\in\widehat{W},\quad\lim_{l\to\infty}\widehat{a}_F\left(u^{k_l},\widehat{v}^{k_l},\widehat{w}\right)=\widehat{a}_F\left(u^*,\widehat{v}^{**},\widehat{w}\right)$$

Using the same technique, we obtain

$$\forall\widehat{w}\in\widehat{W},\quad\lim_{l\to\infty}\widehat{b}_F\left(u^{k_l},\widehat{w},\widehat{p}^{k_l}\right)=\widehat{b}_F\left(u^*,\widehat{w},\widehat{p}^{**}\right)$$
$$\forall\widehat{q}\in\widehat{Q},\quad\lim_{l\to\infty}\widehat{b}_F\left(u^{k_l},\widehat{v}^{k_l},\widehat{q}\right)=\widehat{b}_F\left(u^*,\widehat{v}^{**},\widehat{q}\right)$$

By passing to the limit in the system e', we obtain

$$\begin{cases} \widehat{a}_F\left(u^*, \widehat{v}^{**}, \widehat{w}\right) + \widehat{b}_F\left(u^*, \widehat{w}, \widehat{p}^{**}\right) = \sum_{i=1}^{3} \int_{\Gamma_0} \widehat{\lambda}_i^* \widehat{w}_i \, d\widehat{\sigma}, & \forall \widehat{w} \in \widehat{W} \\ \widehat{b}_F\left(u^*, \widehat{v}^{**}, \widehat{q}\right) = 0, & \forall \widehat{q} \in \widehat{Q} \end{cases}$$

From the Proposition 1.4, we know that the above system has a unique solution, so $\widehat{v}^{**} = \widehat{v}^*$ and $\widehat{p}^{**} = \widehat{p}^*$.

Classically (see [8, vol. 4, chap. VI, Prop. 7, p. 1114]), we obtain that the whole sequence $\left\{\widehat{v}^k\right\}_{k\in\mathbb{N}}$ is weakly convergent to $\widehat{v}^*$ in $\widehat{W}$ and the whole sequence $\left\{\widehat{p}^k\right\}_{k\in\mathbb{N}}$ is weakly convergent to $\widehat{p}^*$ in $\widehat{Q}$.

V) We have:
the application mapping $\widehat{W}$ onto $\left(L^2\left(\Gamma_0\right)\right)^3$

$$\widehat{w} \to \widehat{w}_{|\Gamma_0}$$

is linear and strong continuous,
the application mapping $\left(L^2\left(\Gamma_0\right)\right)^3$ onto $\mathbb{R}$

$$\mu \to \|\mu\|_{0,\Gamma_0}$$

is convex and strong continuous,
the application mapping $\mathbb{R}$ onto $\mathbb{R}$

$$t \to \frac{1}{2} t^2$$

is convex and continuous.

From the elementary properties of the composed functions, we obtain that the application mapping $\widehat{W}$ onto $\mathbb{R}$

$$\widehat{w} \to \frac{1}{2} \left\|\widehat{w}_{|\Gamma_0}\right\|_{0,\Gamma_0}^2$$

is convex and strong continuous. It follows classically that it is weak sequentially lower semi-continuous, so

$$\frac{1}{2} \left\|\widehat{v}_{|\Gamma_0}^*\right\|_{0,\Gamma_0}^2 \leq \liminf_{k\to\infty} \frac{1}{2} \left\|\widehat{v}_{|\Gamma_0}^k\right\|_{0,\Gamma_0}^2$$

According to (1.25) and (1.26), the control $\widehat{\lambda}^*$ is optimal and $\frac{1}{2} \left\|\widehat{v}_{|\Gamma_0}^*\right\|_{0,\Gamma_0}^2$ is the optimal value of the cost function. □

Remark 1.3 *The etaps of the above proof are standard. Related results, but not including the fluid-structure interaction problems, may be founded in [9], [10] and [14].*

Remark 1.4 *Coupling the fluid-structure equations using the Neumann boundary control and Dirichlet boundary observation on the contact surface was employed in [11].*

Remark 1.5 *An open problem is to find additional conditions for the control constraint $\widehat{\lambda} \in \widehat{K}$ in order to obtain zero for the optimal value of the cost function, i.e. $\widehat{v}_{|\Gamma_0}^* = 0$.*

1.7 Conclusions

The mathematical model used in this paper permits to solve the coupled fluid-cable interaction problem via partitioned procedures, i.e. we can use the well established theories and numerical procedures for solving separately the fluid and the cable equations.

The control $\widehat{\lambda}$ could be considered as the "mortar" which couples the fluid equations with the cable equations. The Mortar Method was introduced in [5].

Using the arbitrary lagrangian eulerian coordinates, we have transformed a free boundary problem in a optimal control problem. Consequently, we have studied our problem in Sobolev spaces which are more attractive than working with shape topologies.

Other positive consequence, from the numerical point of view this time, is the following: we can use a fixed mesh for solving the fluid equations by the Finite Element Method.

Acknowledgments

The CEMRACS 96 (Centre d'Été Méditerranéen de Recherches Avancées en Calcul Scientifique, Luminy, France) and the ASCI Laboratory, University Paris Sud are warmly acknowledged for the financial support of this work.

Bibliography

[1] R. Adams - *Sobolev spaces*, Academic Press, 1975

[2] J.M. Arnaudies & H. Fraysse - *Compléments d'analyse*, Dunod, 1989

[3] I. Babuska - *Error Bounds for Finite Elements Method*, Numer. Math., 16 (1971), pp. 322-333

[4] M. Bernardou - *Formulation variationnelle, approximation et implementation de problèmes de barres et de poutre bi- et tri-dimensionnelles. Partie A: barres et de poutre tri-dimensionnelles*, Rapport de Recherche INRIA, no. 731, 1987

[5] C. Bernardi, Y. Maday & A. Patera - *A new non-conforming approach to domain decomposition: the mortar element method*, in *Nonlinear Partial Differential Equations and Their Applications*, H. Brezis, J.L. Lions, eds., Pitman, 1989

[6] H. Brezis - *Analyse fontionnelle. Théorie et applications*, Masson, 1983

[7] F. Brezzi - *On the Existence, Uniqueness and Approximation of Saddle-Point Problems Arising from Lagrangian Multipliers*, RAIRO, 8 (1974), pp. 129-151

[8] R. Dautray & J.L. Lions - *Analyse mathématique et calcul numérique pour les sciences et les techniques*, vol. 3,4,5,6, Masson, 1988

[9] J. Haslinger & P. Neittaanmaki - *Finite element approximation of optimal shape design*, J. Willey and Sons, New York, 1988

[10] J. Haslinger, P. Neittaanmaki & D. Tiba - *A variational inequality approach in optimal design problems*, in "Optimal control of partial differential equations II", K.H. Hoffman and W. Krabs, eds., ISNM 78, Birkhauser Verlag, 1987

[11] C.M. Murea - *Modélisation mathématique et numérique d'un problème tridimensionnel d'interaction entre un f luide incompressible et une structure élastique*, PhD Thesis, University of Franche-Comté, France, 1995

[12] W. Rudin - *Real and Complex Analysis*, Mc Graw - Hill, 1970

[13] J. Sokolowski & J.P. Zolesio - *Introduction to Shape Optimization, Shape Sensitivity Analysis*, Springer Verlag, 1992

[14] D. Tiba - *Optimal control of nonsmooth distributed parameter systems*, LNM 1459, Springer Verlag, 1990

Chapter 2

Sensitivity and approximation of coupled fluid-structure equations by the Virtual Control Method

This chapter is based on the paper:

C.M. Murea, C. Vázquez, Sensitivity and approximation of coupled fluid-structure equations by the virtual control method, *Appl. Math. Optim.*, **52** (2005), no. 2, pp. 183–218.

Abstract. The formulation of a particular fluid-structure interaction as an optimal control problem is the departure point of this work. The control is the vertical component of the force acting on the interface and the observation is the vertical component of the velocity of the fluid on the interface. This approach permits to solve the coupled fluid-structure problem by partitioned procedures.

The analytic expression for the gradient of the cost function is obtained in order to devise accurate numerical methods for the minimization problem.

Numerical results arising from blood flow in arteries are presented. To solve numerically the optimal control problem, we use a quasi Newton method which employs the analytic gradient of the cost function and the approximation of the inverse Hessian is updated by the Broyden, Fletcher, Goldforb, Shano (BFGS) scheme.

2.1 Introduction

In this paper we consider a variable bounded domain which is occupied by a steady newtonian incompressible creeping fluid. The boundary can be decomposed into a rigid part and an elastic part.

The mathematical model which governs the fluid is based on a steady Stokes equation while the deformation of the elastic part of the boundary verifies a particular beam equation without shearing stress. Therefore the solution of the model consists of the determination of the elastic boundary displacement and the computation of the velocity and the pressure in the fluid domain.

In a first sense, the physical problem is related with those treated in fluid-structure interaction literature but the vibration approach is not considered here.[30] In other sense, the asymptotic limit when the fluid domain width tends to zero can be modeled by a one-dimensional approach of Stokes equation, i.e. Reynolds equation, widely used in lubrication theory.[3]

On the other hand, if we think about the elastic boundary as part of the boundary of a two-dimensional domain which is unknown a priori, then the problem can be framed as a free boundary like problem. The free boundary aspect of the model motivates the need of two coupling boundary conditions: continuity of the velocity and of the stresses across the interface fluid-structure.

This kind of problem is of considerable interest in biomechanics (the simulation of blood flow in large arteries, [29], [17], [33], [8], [18], [38]), in aeroelasticity (fluttering of wings, [13], [14], [35], [36]), in cars industry (design of hydraulic shock absorber, [26]).

The existence results for the fluid-structure interaction can be found in [21], [23], [2] for the steady case and in [22], [12], [4] for the unsteady case.

Sensitivity analysis of a coupled fluid-structure system was investigated in [15].

The most frequently, the fluid-structure interaction problems are solved numerically by partitioned procedures, i.e. the fluid and the structure equations are solved separately, which allows to use the existing solvers for each sub-problem.

There are different strategies to discretise in time the unsteady fluid-structure interaction problem. A family of explicit algorithms known also as staggered was successfully employed for the aeroelastic applications.[13] Their stability properties were studied in [35] and [36]. For the stability reason, a very small time step is necessary.

As it shown in [26] and [33], the staggered algorithms are unstable when the structure is light and its density is comparable to that of its fluid. In order to obtain unconditionally stable algorithms, at each time step we have to solve a non-linear fluid-structure coupled system. This can be done using fixed point strategies with eventually a relaxation parameter, but it has slow convergence rate [26], [33], [17]. The convergence can be accelerated using Aitken's method [18] or transpiration condition [11].

Other way to accelerate the convergence is to use methods which employ the derivative. In [40] a block Newton algorithm was used where the derivative of the operators are approached by finite differences. Good convergence rate was obtained in [18] where the derivative of the operator was replaced by a much simpler operator. The block Schur-Newton method is proposed in [16] where the derivatives of the fluid and structure operators with respect to the state variables were computed exactly, but this algorithm has not been implemented yet.

In a previous work, a three-dimensional fluid-structure interaction was formulated as an optimal control system, where the control is the force acting on the interface and the observation is the velocity of the fluid on the interface.[32] The fluid equations were solved taking into account a given surface force on the interface. The existence of an optimal control was proved. We have to precise that the fluid-structure interaction problem and its optimal control version are not equivalent.

In this work, a two-dimensional steady state fluid-structure coupled problem is approximated by an optimal control system, where the control is the vertical component of the force acting on the interface and the observation is the vertical component of the velocity of the fluid on the interface. The control approach permits to solve the coupled fluid-structure problem by partitioned procedures.

The analytic computation of the gradient for the cost function is one of the main goals of this work in order to apply accurate numerical methods. Moreover, from the theoretical viewpoint, the optimality conditions can be written in terms of this analytic expression of the gradient. In fact, although the analytic formula for the gradient involves the solution of several auxiliary problems, the alternative use of finite difference approximations for the derivatives introduces truncation errors and it is potentially much more sensitive to ill-conditioning of the state equations.[27]

The aims of this paper are: to analyse the behavior of the fluid and structure subproblems under the variation of the force acting on the interface, to prove the differentiability of the cost function and to present numerical results arising from blood flow in arteries. To solve numerically the optimal control problem, we use a quasi Newton method which employs the analytic gradient of the cost function and the approximation of the inverse Hessian is updated by the Broyden, Fletcher, Goldforb, Shano (BFGS) scheme. This algorithm is faster than fixed point with relaxation or block Newton methods.

In Section 2 the particular fluid-structure problem is presented, related notations are introduced and the associated optimal control problem is briefly posed. In Section 3 the weak formulation of the structure equations is analysed and we precise the set of admissible controls. For a given structure displacement, the mixed formulations governing the fluid velocity and pressure are posed in the eulerian and arbitrary lagrangian eulerian coordinates in Sections 4 and 5, respectively. In these arbitrary lagrangian eulerian coordinates the optimal control system is detailed in Section 6. Next, the continuity and the differentiability of the cost function are proved in the Section 7 and 8. Moreover, the exact expression of the cost function gradient is obtained. In Section 9 we present an interesting application to blood flow simulation in medium vessels. For this, particular methods to solve the structure and fluid equations as well as specific algorithms for the discrete optimization problem are proposed. Some numerical results for real data are presented and discussed. The last section is devoted to some concluding remarks.

2.2 Presentation of the problem

In order to pose the equations for the model let us introduce some mathematical notations. Let L and H be two positive constants. We introduce the classical Sobolev space $U = H_0^2(0,L)$ and the sets (see the Figure 2.1):

$$\Omega_0^F = (0,L)\times(0,H), \quad \Gamma_0 = (0,L)\times\{H\}, \quad \Sigma_1 = \{0\}\times(0,H),$$
$$\Sigma_2 = (0,L)\times\{0\}, \quad \Sigma_3 = \{L\}\times(0,H), \quad \Sigma = \Sigma_1\cup\overline{\Sigma}_2\cup\Sigma_3.$$

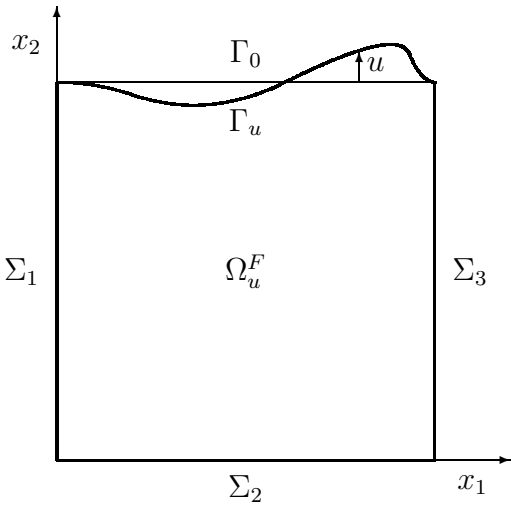

Figure 2.1: Sets appearing in the fluid-structure problem

As we have the continuous and compact inclusion of $H_0^2(0,L)\subset\mathcal{C}^1(0,L)$ then for each $u\in U$ we denote by u' its derivative (in fact it is a classical derivative) and by u'' its second (weak) derivative. For a given $e\in(0,H)$ we define the set

$$\begin{aligned}\mathcal{U}_{ad} &= \{u\in U;\, u(0)=u(L)=u'(0)=u'(L)=0,\\ &\quad \textstyle\int_0^L u(x_1)\,dx_1=0,\ H+u(x_1)\geq e,\ \forall x_1\in[0,L]\Big\}.\end{aligned}$$

Moreover, for each $u\in\mathcal{U}_{ad}$, we introduce the notations (see the Figure 2.1)

$$\begin{aligned}\Omega_u^F &= \left\{(x_1,x_2)\in\mathbb{R}^2;\, x_1\in(0,L),\, 0<x_2<H+u(x_1)\right\},\\ \Gamma_u &= \left\{(x_1,x_2)\in\mathbb{R}^2;\, x_1\in(0,L),\, x_2=H+u(x_1)\right\}.\end{aligned}$$

In view of the definition of the $\mathcal{U}_{ad}$, the two-dimensional domain occupied by the fluid is Ω_u^F, the elastic interface between fluid and structure is the free boundary Γ_u, while Σ represents the rigid boundary.

We suppose that the fluid is governed by the steady Stokes equations, while the deformation of the elastic part of the boundary verifies a particular beam equation without shearing stress.[5] We consider that the structure is a beam of axis parallel to Ox_1 with constant thickness h. We assume that the displacement of the beam is normal to its axis.

The problem is to find:

- $u : [0, L] \to \mathbb{R}$ the displacement of the structure,
- $v = (v_1, v_2)^T : \Omega_u^F \to \mathbb{R}^2$ the velocity of the fluid and
- $p : \Omega_u^F \to \mathbb{R}$ the pressure of the fluid,

such that

$$
\begin{aligned}
EI\, u''''(x_1) &= -\left(\sigma^F n \cdot e_2\right)_{(x_1, H+u(x_1))} \sqrt{1 + \left(u'(x_1)\right)^2} + f^S(x_1) && (2.1)\\
u\,(0) &= u\,(L) = u'\,(0) = u'\,(L) = 0 && (2.2)\\
\int_0^L u(x_1)\, dx_1 &= 0 && (2.3)\\
e &\leq \inf_{x_1 \in [0,L]} \{H + u\,(x_1)\} && (2.4)\\
-\mu \Delta v + \nabla p &= f^F, \quad in\ \Omega_u^F && (2.5)\\
\text{div } v &= 0, \quad in\ \Omega_u^F && (2.6)\\
v &= g, \quad on\ \Sigma && (2.7)\\
v &= 0, \quad on\ \Gamma_u && (2.8)
\end{aligned}
$$

where

- $EI = \frac{Eh^3}{12}$ is rigidity to bending modulus of the structure, E is the Young modulus, h is the thickness.
- $f^S : (0, L) \to \mathbb{R}$ are the averaged volume forces of the structure, in general the gravity forces and in this case we have $f^S(x_1) = -g_0 \rho^S h$, where g_0 is the gravity, ρ^S is the density of the structure,
- $\mu > 0$ is the viscosity of the fluid,
- $f^F = (f_1^F, f_2^F)^T : \Omega_u^F \to \mathbb{R}^2$ are the volume forces of the fluid, in general the gravity forces,
- $g = (g_1, g_2)^T : \Sigma \to \mathbb{R}^2$ is the imposed velocity profile of the fluid on the rigid boundary, such that

$$\int_\Sigma g \cdot n\, d\sigma = 0 \qquad (2.9)$$

- $\sigma^F = -p\,I + \mu\left(\nabla v + \nabla v^T\right)$ is the stress tensor of the fluid,
- $n = (n_1, n_2)^T$ the unit outward normal vector to $\partial\Omega_u^F$,
- $e_2 = (0,1)^T$ is the unit vector in the x_2 direction.

The incompressibility of the fluid (2.6) states that the volume of the fluid is conserved or equivalently $\int_0^L u(x_1)\,dx_1$ is constant. Without loss of generality, we assume that this constant is zero and we obtain the condition (2.3).

The inequality (2.4) implies that the fluid domain is connected. The constant e has not a physical meaning.

The system (2.1)-(2.8) is a coupled fluid-structure problem.

The displacement of the structure depends on the vertical component of the stresses exerced by the fluid on the interface (equation 2.1). This cames from the continuity of the stresses across the interface.

The movement of the structure changes the domain where the fluid equations must be solved (equations 2.5,2.6). Also, on the interface we have to impose the equality between the fluid and structure velocity (equation 2.8).

We shall introduce the control approach.

Let $\widehat{\lambda} : (0, L) \to \mathbb{R}$ be the control function.

The displacement of the structure is computed by

$$EI\,u''''(x_1) = -\widehat{\lambda}(x_1) + f^S(x_1), \quad \forall x_1 \in (0, L)$$

with boundary conditions (2.2), such that (2.3) and (2.4) hold.

We can compute the velocity and the pressure of the fluid as the solution of the equations (2.5), (2.6) with boundary conditions on the rigid boundary (2.7) together with boundary conditions on the interface: $v_1 = 0$ and

$$\left(\sigma^F n \cdot e_2\right)_{(x_1, H+u(x_1))} = \frac{\widehat{\lambda}(x_1)}{\sqrt{1 + \left(u'(x_1)\right)^2}}, \quad \forall x_1 \in (0, L).$$

The control problem is to find $\widehat{\lambda}$, such that $v_2 = 0$ on Γ_u.

As we use the value $-\widehat{\lambda}$ for the applied stresses in the equations of the structure and we take the value $\widehat{\lambda}$ in the equations of the fluid, the continuity of the stresses across the interface is strongly accomplished.

In the following, the boundary condition $v_{2|\Gamma_u} = 0$ is treated by the Least Square Method and we obtain the optimal control problem

$$\inf_{\widehat{\lambda}} \frac{1}{2} \left\| v_{2|\Gamma_u} \right\|^2.$$

The control $\widehat{\lambda}$ and the cost function are "virtual". The idea of Virtual Control which leads to Domain Decomposition Methods was presented in [28] and in the references given there.

Next, we shall precise the regularity of the control which is linked to the equivalence or not-equivalence between the fluid-structure equations (2.1)–(2.8) and its optimal control version.

If the system of fluid-structure equations (2.1)–(2.8) has a strong solution $u \in H^4(0,L)$, $v \in \left(H^2\left(\Omega_u^F\right)\right)^2$ and $p \in H^1\left(\Omega_u^F\right)$, then the control given by the relation

$$\widehat{\lambda}(x_1) = \left(\sigma^F n \cdot e_2\right)_{(x_1, H+u(x_1))} \sqrt{1 + \left(u'(x_1)\right)^2}$$

belongs to $L^2(0,L)$. In fact, the control is even smoother. In this case, the system (2.1)–(2.8) is equivalent to the control problem. So, there exists $\widehat{\lambda} \in L^2(0,L)$ such that $v_{2|\Gamma_u} = 0$. In [4] the existence of a strong solution was proved for a related problem.

If the system of fluid-structure equations (2.1)–(2.8) has only a week solution $u \in H^2(0,L)$, $v \in \left(H^1\left(\Omega_u^F\right)\right)^2$ and $p \in L^2\left(\Omega_u^F\right)$, then $\widehat{\lambda}$ is well defined in a space like the dual of $H_{00}^{1/2}(0,L)$, which is larger than $L^2(0,L)$. In this case, the optimal control problem

$$\inf_{\widehat{\lambda} \in L^2(0,L)} \frac{1}{2} \left\| v_{2|\Gamma_u} \right\|^2$$

has not solution, so it is not equivalent to the fluid-structure equations (2.1)–(2.8). Using the density of $L^2(0,L)$ in the dual of $H_{00}^{1/2}(0,L)$, we could prove that $\inf \frac{1}{2} \left\| v_{2|\Gamma_u} \right\|^2 = 0$ for $\widehat{\lambda} \in L^2(0,L)$, but this aspect will not study here.

The existence of a weak solution was proved in [21] and [2] for a two-dimensional steady state fluid-structure interaction problem, in [23] for a three-dimensional steady state, in [22] and [12] for an unsteady state.

In the following, we shall take $\widehat{\lambda}$ in $L^2(0,L)$ because it is simpler to approximate than the dual of $H_{00}^{1/2}(0,L)$.

2.3 Weak formulation for the structure equations

In this paragraph we present the weak formulation for the structure equations. We have assumed that the structure is governed by a classical beam equations without shearing stress.[5]

So, for a given $EI \in \mathbb{R}_+^*$ which is the rigidity to bending modulus of the structure, we define the bilinear form

$$\left\{ \begin{array}{rcl} a_S : U \times U & \rightarrow & \mathbb{R} \\ (\phi, \psi) & \mapsto & a_S(\phi, \psi) = EI \displaystyle\int_0^L \phi''(x_1)\, \psi''(x_1)\, dx_1 \,. \end{array} \right. \tag{2.10}$$

The bilinear form a_S is evidently symmetric and continuous. In addition, applying the Poincaré inequality (see [10] vol. 3, chap. IV, p. 920), we obtain that a_S is U-elliptic. Moreover, let U' be the dual of U. We denote by $\langle \cdot, \cdot \rangle_{U',U}$ the duality pairing between U' and U. A simple consequence of the Lax-Milgram Theorem (see [10] vol. 4, chap. VII, p. 1217) leads to the following result:

Proposition 2.1 *Let $f^S \in U'$ and $\eta \in L^2(0,L)$. Then, the problem:*
Find $u \in U$ such that

$$a_S(u,\psi) = \int_0^L \eta(x_1)\,\psi(x_1)\,dx_1 + \left\langle f^S, \psi \right\rangle_{U',U} \quad \forall \psi \in U \tag{2.11}$$

has a unique solution. Moreover the solution $u \in \mathcal{C}^1([0,L])$ and we have the $L^\infty(0,L)$ estimate:

$$\|u\|_{L^\infty(0,L)} \leq C_1 \|\eta\|_{L^2(0,L)} + C_2 \left\|f^S\right\|_{U'}$$

where C_1 and C_2 are constants.

When the data and the solution are smooth enough the solution u verifies the strong formulation given by:

$$\begin{aligned} EI\,u''''(x_1) &= \eta(x_1) + f^S(x_1),\ \forall x_1 \in (0,L) \\ u(0) &= u'(0) = 0, \\ u(L) &= u'(L) = 0. \end{aligned}$$

Remark 2.1 *The physical meaning of f^S is that of an external force applied to the elastic structure. For example, the consideration of an harmonic expression for f^S would lead to an harmonic response of the fluid-structure device. Also, the gravity forces are included in f^S. In the coupled model, η is associated to the fluid forces acting on the structure.*

In order to obtain a fluid domain with constant volume, we have to impose some condition to η. We denote by $L^2_0(0,L) = \left\{\eta \in L^2(0,L); \int_0^L \eta(x_1)\,dx_1 = 0\right\}$.

Proposition 2.2 *Let $f^S \in U'$ and $\eta \in L^2_0(0,L)$.*

i) Then there exist an unique $u \in U$, such that $\int_0^L u(x_1)\,dx_1 = 0$ and an unique constant $c \in \mathbb{R}$ solutions of

$$a_S(u,\psi) = \int_0^L (\eta(x_1) + c)\,\psi(x_1)\,dx_1 + \left\langle f^S, \psi \right\rangle_{U',U} \quad \forall \psi \in U \tag{2.12}$$

ii) Let $u_0 \in U$, such that $\int_0^L u_0\,dx_1 = 0$ and $c_0 \in \mathbb{R}$ are the solution of

$$a_S(u_0,\psi) = c_0 \int_0^L \psi(x_1)\,dx_1 + \left\langle f^S, \psi \right\rangle_{U',U} \quad \forall \psi \in U \tag{2.13}$$

and $u_\eta \in U$*, such that* $\int_0^L u_\eta \, dx_1 = 0$ *and* $\ell(\eta) \in \mathbb{R}$ *are the solution of*

$$a_S(u_\eta, \psi) = \int_0^L (\eta(x_1) + \ell(\eta)) \, \psi(x_1) \, dx_1 \quad \forall \psi \in U. \tag{2.14}$$

Then, $u = u_0 + u_\eta$*,* $c = c_0 + \ell(\eta)$ *and the applications*

$$\eta \in L_0^2(0, L) \mapsto u_\eta \in U, \qquad \eta \in L_0^2(0, L) \mapsto \ell(\eta) \in \mathbb{R}$$

are linear and continuous.

Proof. i) *Existence.* From the Proposition 2.1, there exist $u_1, u_2, u_3 \in U$ solutions of

$$\begin{array}{lcll} a_S(u_1, \psi) & = & \left\langle f^S, \psi \right\rangle_{U',U} & \forall \psi \in U \\ a_S(u_2, \psi) & = & \int_0^L \eta(x_1) \, \psi(x_1) \, dx_1 & \forall \psi \in U \\ a_S(u_3, \psi) & = & \int_0^L \psi(x_1) \, dx_1 & \forall \psi \in U \end{array}$$

From the third equation and using that a_S is elliptic, we obtain

$$0 < a_S(u_3, u_3) = \int_0^L u_3(x_1) \, dx_1.$$

We search $c \in \mathbb{R}$ and $u = u_1 + u_2 + c \cdot u_3$ such that $\int_0^L u(x_1) \, dx_1 = 0$ or equivalently

$$c = -\frac{\int_0^L (u_1 + u_2) dx_1}{\int_0^L u_3 dx_1}.$$

Uniqueness. Let u_i, c_i, $i = 1, 2$ be two solutions of (2.12), such that $\int_0^L u_i \, dx_1 = 0$. By subtracting, we obtain

$$a_S(u_1 - u_2, \psi) = (c_1 - c_2) \int_0^L \psi(x_1) \, dx_1, \quad \forall \psi \in U$$

and after the substitution $\psi = u_1 - u_2$ it follows

$$a_S(u_1 - u_2, u_1 - u_2) = (c_1 - c_2) \int_0^L (u_1 - u_2) dx_1.$$

But $\int_0^L (u_1 - u_2) dx_1 = 0$, then $a_S(u_1 - u_2, u_1 - u_2) = 0$ and consequently $u_1 = u_2$.
It follows that

$$0 = (c_1 - c_2) \int_0^L \psi(x_1) \, dx_1, \quad \forall \psi \in U$$

then $c_1 = c_2$.

ii) From (2.13) and (2.14), we obtain that $u_0+u_\eta \in U$ such that $\int_0^L u_0+u_\eta\, dx_1=0$ and $c_0+\ell(\eta)\in\mathbb{R}$ are solutions of

$$a_S\left(u_0+u_\eta,\psi\right)=\int_0^L\left(\eta\left(x_1\right)+c_0+\ell(\eta)\right)\psi\left(x_1\right)dx_1+\left\langle f^S,\psi\right\rangle_{U',U}\quad\forall\psi\in U.$$

From the uniqueness proved at the point i), it follows that $u=u_0+u_\eta$ and $c=c_0+\ell(\eta)$.

It is easy to see that the applications $\eta\mapsto u_\eta$ and $\eta\mapsto\ell(\eta)$ are linear. It remains to prove the continuity.

We replace $\psi=u_\eta$ in (2.14) and using $\int_0^L u_\eta dx_1=0$, we obtain

$$a_S\left(u_\eta,u_\eta\right)=\int_0^L\left(\eta\left(x_1\right)+\ell(\eta)\right)u_\eta\left(x_1\right)dx_1=\int_0^L\eta\left(x_1\right)u_\eta\left(x_1\right)dx_1.$$

But a_S is elliptic and using the Cauchy-Schwartz inequality, we have

$$\left\|u_\eta\right\|_U^2\le C\left\|\eta\right\|_{L^2(0,L)}\left\|u_\eta\right\|_{L^2(0,L)}\le C\left\|\eta\right\|_{L^2(0,L)}\left\|u_\eta\right\|_U$$

which proves the continuity of $\eta\mapsto u_\eta$.

From (2.14), we have

$$\ell(\eta)\int_0^L\psi\, dx_1=a_S\left(u_\eta,\psi\right)-\int_0^L\eta\psi\, dx_1,\quad\forall\psi\in U.$$

We take $\psi_0\in U$ such that $\int_0^L\psi_0 dx_1>0$ in the above equality. From the continuity of a_S, $\eta\mapsto u_\eta$ and using the Cauchy-Schwartz inequality, we obtain that $\eta\mapsto\ell(\eta)$ is continuous. □

Remark 2.2 *We obtain a displacement u such that $\int_0^L u\, dx_1=0$ if and only if the forces acting on the interface have the form $\eta+c_0+\ell(\eta)$, where $\eta\in L_0^2(0,L)$.*

In order to obtain a connected fluid domain, we must impose some condition on f^S and η.

Let us denote by $\mathcal{S}:L^2\left(0,L\right)\to U$ the map

$$\mathcal{S}(\eta)=u,\tag{2.15}$$

where u is the unique solution of (2.11).

We define the admissible set for the forces induced by the fluid

$$\mathcal{F}_{ad}=\mathcal{S}^{-1}\left(\mathcal{U}_{ad}\right).$$

Let $u_0\in U$, such that $\int_0^L u_0\, dx_1=0$ and $c_0\in\mathbb{R}$ solutions of (2.13). We assume that

$$C_1\left\|c_0\right\|_{L^2(0,L)}+C_2\left\|f^S\right\|_{U'}<H-e$$

consequently $\left\|u_0\right\|_{L^\infty(0,L)}<H-e$.

Proposition 2.3 *i) The set $\mathcal{F}_{ad}$ is convex and closed in $L^2(0,L)$.*
ii) If $\|u_0\|_{L^\infty(0,L)} < H - e$, then $\mathcal{F}_{ad}$ is non empty.

Proof. i) The set $\mathcal{U}_{ad}$ is convex and closed in U. The application $\mathcal{S}$ is continuous and affine. Consequently, $\mathcal{F}_{ad}$ is convex and closed.

ii) We use the same notations as in the Proposition 2.2 part *ii*). From the continuity at $\eta = 0$ of the linear function $\eta \mapsto \ell(\eta)$, for small $\|\eta\|_{L^2(0,L)}$ we obtain $\|u_\eta\|_{L^\infty(0,L)} < H - e - \|u_0\|_{L^\infty(0,L)}$. So, if we set $u = u_0 + u_\eta$, we have

$$\begin{aligned} \|u\|_{L^\infty(0,L)} &\leq \|u_0\|_{L^\infty(0,L)} + \|u_\eta\|_{L^\infty(0,L)} \\ &< \|u_0\|_{L^\infty(0,L)} + H - e - \|u_0\|_{L^\infty(0,L)} = H - e, \end{aligned}$$

which implies that $H + u(x_1) \geq e$, $\forall x_1 \in [0,L]$. From the Proposition 2.2 we have that $u = \mathcal{S}(\eta + c_0 + \ell(\eta))$ verifies $\int_0^L u(x_1)\, dx_1 = 0$. Consequently, for small $\|\eta\|_{L^2(0,L)}$, we have $\eta + c_0 + \ell(\eta) \in \mathcal{F}_{ad}$. □

2.4 Mixed formulation in variable fluid domain

For each $\eta \in F_{ad}$, let u be the solution of the equation (2.11) and let Ω_u^F be the domain occupied by the fluid.

In view of the properties of the inclusion $H_0^2(0,L)$ in $\mathcal{C}^1(0,L)$ then the elastic boundary Γ_u is Lipschitz, so we can define the trace space $H^{1/2}(\Gamma_u)$. Moreover, from a classical result Theorem 2 in Vol. 6, p. 652 [10], the trace function mapping $H^1\left(\Omega_u^F\right)$ into $H^{1/2}(\Gamma_u)$ is continuous and onto.

In order to establish the variational formulation and the model for the u-dependent problem in the u-dependent fluid domain let us consider the following Hilbert spaces:

$$\begin{aligned} W_u &= \left\{ w \in \left(H^1\left(\Omega_u^F\right)\right)^2;\ w_1 = 0 \text{ on } \partial\Omega_u^F, w_2 = 0 \text{ on } \overline{\Sigma} \right\}, \\ Q_u &= L^2\left(\Omega_u^F\right). \end{aligned}$$

We introduce in $\left(H^1\left(\Omega_u^F\right)\right)^2$ the divergence operator

$$\text{div } w = \frac{\partial w_1}{\partial x_1} + \frac{\partial w_2}{\partial x_2}, \quad w = (w_1, w_2) \in \left(H^1\left(\Omega_u^F\right)\right)^2.$$

Next straightforward lemma states an important property of this operator.

Lemma 2.1 *For all u in $\mathcal{U}_{ad}$, the operator* div *mapping W_u into Q_u is onto.*

This result is standard for the homogenous Dirichlet boundary condition on the $\partial\Omega_u^F$.[19]

For the mixed boundary condition (Dirichlet on Σ and Neumann on Γ_u) and for an exterior domain (the complement of a compact set), the proof of this kind of result could be found in [32]. The proof remains valid in our case when the domain is bounded.

We denote by $\mu > 0$ the viscosity of the fluid and by $\epsilon(v) = (\epsilon_{ij}(v))_{1\leq i,j\leq 2}$ the symmetric part of the deformation rate tensor, where $\epsilon_{ij}(v) = \frac{1}{2}\left(\frac{\partial v_i}{\partial x_j} + \frac{\partial v_j}{\partial x_i}\right)$. Next, let us consider the maps

$$\left\{\begin{array}{rcl} a_F : U \times W_u \times W_u & \rightarrow & \mathbb{R} \\ (u,v,w) & \mapsto & a_F(u,v,w) = 2\mu \displaystyle\sum_{i,j=1}^{2} \int_{\Omega_u^F} \epsilon_{ij}(v)\epsilon_{ij}(w)\, dx \end{array}\right. \tag{2.16}$$

and

$$\left\{\begin{array}{rcl} b_F : U \times W_u \times Q_u & \rightarrow & \mathbb{R} \\ (u,w,q) & \mapsto & b_F(u,w,q) = -\displaystyle\int_{\Omega_u^F} (\text{div } w)\, q\, dx. \end{array}\right. \tag{2.17}$$

The properties of the previous maps lead to the existence and uniqueness result [19]:

Proposition 2.4 *For all u in $\mathcal{U}_{ad}$ and λ in $L^2(\Gamma_u)$, the problem:*
Find $(v,\ p) \in W_u \times Q_u$ such that

$$\left\{\begin{array}{rcl} a_F(u,v,w) + b_F(u,w,p) & = & \displaystyle\sum_{i=1}^{2} \int_{\Omega_u^F} f_i^F w_i\, dx + \int_{\Gamma_u} \lambda w_2\, d\sigma,\ \forall w \in W_u \\ b_F(u,v,q) & = & 0,\ \forall q \in Q_u \end{array}\right. \tag{2.18}$$

has a unique solution.

Remark 2.3 *The system (2.18) represents a mixed formulation for the Stokes equations:*

$$\left\{\begin{array}{rcccl} -\mu\Delta v + \nabla p & = & f^F & in & \Omega_u^F \\ \text{div } v & = & 0 & in & \Omega_u^F \\ v & = & 0 & on & \Sigma \\ \left(\sigma^F n\right)\cdot e_2 & = & \lambda & on & \Gamma_u \\ v_1 & = & 0 & on & \Gamma_u \end{array}\right.$$

where μ is the viscosity of the fluid, v and p represent the velocity and the pressure of the fluid, $f^F = \left(f_1^F, f_2^F\right)^T \in \mathbb{R}^2$ are the gravity forces, $\sigma^F = -pI + 2\mu\epsilon(v)$ is the stress tensor of the fluid, n is the unit outward normal vector to Γ_u, $e_2 = (0,1)^T$ is the unit vector in the x_2 direction, λ is the vertical component of the surface forces on the elastic boundary Γ_u. We have a Dirichlet homogeneous boundary condition on the rigid boundary Σ and on the elastic boundary Γ_u we have a Neumann and a Dirichlet boundary conditions.

The equilibrium of the physical situation, corresponding to a fluid which occupies a two-dimensional region whose boundary contains an elastic part, is based on the balance of velocity and normal forces in that boundary. In our approach to this particular fluid-structure model both balances are obtained in an optimal control problem setting. One of the first difficulties of this formulation is the u-dependence of the fluid domain. To overcome this problem in next section we propose an equivalent mixed formulation problem in a fixed domain but with u-dependent coefficients.

2.5 Mixed formulation for the fluid equations in a fixed domain

In order to obtain the mixed formulation for the fluid equations in a fixed domain, the arbitrary lagrangian eulerian coordinates have been used. For this formulation in a fixed domain we obtain the existence of the solution.

For each $u \in U$ be given, let us consider the following one-to-one continuous differentiable transformation:

$$T_u : \overline{\Omega_0^F} \to \overline{\Omega_u^F}, \quad (\widehat{x}_1, \widehat{x}_2) \mapsto T_u(\widehat{x}_1, \widehat{x}_2) = \left(\widehat{x}_1, \frac{H + u(\widehat{x}_1)}{H} \widehat{x}_2 \right) \tag{2.19}$$

which admits the continuous differentiable inverse mapping

$$T_u^{-1} : \overline{\Omega_u^F} \to \overline{\Omega_0^F}, \quad (x_1, x_2) \mapsto T_u^{-1}(x_1, x_2) = \left(x_1, \frac{H x_2}{H + u(x_1)} \right) \tag{2.20}$$

and verifies that $T_u\left(\Omega_0^F\right) = \Omega_u^F$, $T_u(\Gamma_0) = \Gamma_u$ and $T_u(\widehat{x}) = \widehat{x}$, $\forall \widehat{x} \in \Sigma$. We set $x = T_u(\widehat{x})$ for each $x = (x_1, x_2) \in \Omega_u^F$ and $\widehat{x} = (\widehat{x}_1, \widehat{x}_2) \in \Omega_0^F$. We note $\sigma = T_u(\widehat{\sigma})$ for each $\sigma \in \Gamma_u$ and $\widehat{\sigma} \in \Gamma_0$.

Moreover, we denote by

$$\begin{aligned} \nabla T_u(\widehat{x}) &= \begin{pmatrix} 1 & 0 \\ \frac{u'(\widehat{x}_1)}{H}\widehat{x}_2 & \frac{H+u(\widehat{x}_1)}{H} \end{pmatrix} \\ \nabla\left(T_u^{-1}\right)(x) &= \begin{pmatrix} 1 & 0 \\ \frac{-u'(x_1)Hx_2}{(H+u(x_1))^2} & \frac{H}{H+u(x_1)} \end{pmatrix} \end{aligned}$$

the jacobian matrices of the transformations T_u and T_u^{-1} respectively. As usual for a given square matrix A, we denote by $\det(A)$, A^{-1}, A^T, $\operatorname{cof}(A)$ the determinant, the inverse, the transpose and the cofactor matrix, respectively. We have

$$(\nabla T_u)^{-1}(\widehat{x}) = \nabla\left(T_u^{-1}\right)(x) = \nabla\left(T_u^{-1}\right)(T_u(\widehat{x}))$$

and

$$\operatorname{cof}(\nabla T_u(\widehat{x})) = \det(\nabla T_u(\widehat{x}))\left((\nabla T_u(\widehat{x}))^{-1}\right)^T.$$

Associated with the transformation T_u we state the following useful lemma.

Lemma 2.2 *We have:*

1. *A function ϕ belongs to $L^1\left(\Omega_u^F\right)$ if and only if the function $\widehat{\phi}=\phi\circ T_u$ belongs to $L^1\left(\Omega_0^F\right)$. Moreover, in this case we have*

$$\int_{\Omega_u^F}\phi\left(x\right)dx=\int_{\Omega_0^F}\widehat{\phi}\left(\widehat{x}\right)\det\left(\nabla T_u\left(\widehat{x}\right)\right)d\widehat{x}. \tag{2.21}$$

2. *A function ϕ belongs to $L^1\left(\Gamma_u\right)$ if and only if the function $\widehat{\phi}=\phi\circ T_u$ belongs to $L^1\left(\Gamma_0\right)$. Moreover, in this case we have*

$$\int_{\Gamma_u}\phi\left(\sigma\right)d\sigma=\int_{\Gamma_0}\widehat{\phi}\left(\widehat{\sigma}\right)\widehat{\omega}_u\left(\widehat{\sigma}\right)d\widehat{\sigma} \tag{2.22}$$

where $\widehat{\omega}_u\left(\widehat{\sigma}\right)$ is given by

$$\widehat{\omega}_u\left(\widehat{\sigma}\right)=\left\|\mathrm{cof}\left(\nabla T_u\left(\widehat{\sigma}\right)\right)\widehat{n}\left(\widehat{\sigma}\right)\right\|_{\mathbb{R}^2} \tag{2.23}$$

with $\widehat{n}\left(\widehat{\sigma}\right)$ being the unit outward normal vector to Γ_0 in $\widehat{\sigma}$.

3. *A function ϕ belongs to $H^1\left(\Omega_u^F\right)$ if and only if the function $\widehat{\phi}=\phi\circ T_u$ belongs to $H^1\left(\Omega_0^F\right)$. Moreover, we have*

$$\begin{pmatrix}\frac{\partial\phi}{\partial x_1}\left(x\right)\\ \frac{\partial\phi}{\partial x_2}\left(x\right)\end{pmatrix}=\left(\left(\nabla T_u\right)^{-1}\left(\widehat{x}\right)\right)^T\begin{pmatrix}\frac{\partial\widehat{\phi}}{\partial\widehat{x}_1}\left(\widehat{x}\right)\\ \frac{\partial\widehat{\phi}}{\partial\widehat{x}_2}\left(\widehat{x}\right)\end{pmatrix}. \tag{2.24}$$

The first and second assertions of the above lemma follow from the well-known transport theorems in continuum mechanics.[20] The third part of the lemma is a consequence of basic results for Sobolev spaces [1] and the chain rule.

In our case, we have

$$\det\left(\nabla T_u\left(\widehat{x}\right)\right)=\frac{H+u(\widehat{x}_1)}{H},\quad \widehat{\omega}_u\left(\widehat{x}_1,H\right)=\sqrt{1+\left(u'(\widehat{x}_1)\right)^2}.$$

We denote by

$$\left(\nabla T_u\right)^{-1}\left(\widehat{x}\right)=\begin{pmatrix}1 & 0\\ \frac{-u'(\widehat{x}_1)\widehat{x}_2}{H+u(\widehat{x}_1)} & \frac{H}{H+u(\widehat{x}_1)}\end{pmatrix}=\begin{pmatrix}s_{11}(\widehat{x}) & s_{12}(\widehat{x})\\ s_{21}(\widehat{x}) & s_{22}(\widehat{x})\end{pmatrix}$$

and as a consequence of the above Lemma, we have

$$\begin{pmatrix}\frac{\partial v_1}{\partial x_1}(x) & \frac{\partial v_1}{\partial x_2}(x)\\ \frac{\partial v_2}{\partial x_1}(x) & \frac{\partial v_2}{\partial x_2}(x)\end{pmatrix}=\begin{pmatrix}\frac{\partial\widehat{v}_1}{\partial\widehat{x}_1}(\widehat{x}) & \frac{\partial\widehat{v}_1}{\partial\widehat{x}_2}(\widehat{x})\\ \frac{\partial\widehat{v}_2}{\partial\widehat{x}_1}(\widehat{x}) & \frac{\partial\widehat{v}_2}{\partial\widehat{x}_2}(\widehat{x})\end{pmatrix}\begin{pmatrix}s_{11}(\widehat{x}) & s_{12}(\widehat{x})\\ s_{21}(\widehat{x}) & s_{22}(\widehat{x})\end{pmatrix}.$$

In order to pose the variational formulation in the reference configuration let us consider the following Hilbert spaces:

$$\begin{aligned}\widehat{W} &= \left\{\widehat{w} \in \left(H^1\left(\Omega_0^F\right)\right)^2;\ \ \widehat{w}_1 = 0 \text{ on } \partial\Omega_0^F, \widehat{w}_2 = 0 \text{ on } \overline{\Sigma}\right\}\\ \widehat{Q} &= L^2\left(\Omega_0^F\right)\end{aligned}$$

equipped with their usual inner products.

We introduce the forms

$$\widehat{a}_F : \mathcal{U}_{ad} \times \widehat{W} \times \widehat{W} \to \mathbb{R} \qquad \widehat{b}_F : \mathcal{U}_{ad} \times \widehat{W} \times \widehat{Q} \to \mathbb{R}$$

defined by

$$\begin{aligned}&\widehat{a}_F(u,\widehat{v},\widehat{w}) = 2\mu \int_{\Omega_0^F} \left[\left(\tfrac{\partial\widehat{v}_1}{\partial\widehat{x}_1}s_{11} + \tfrac{\partial\widehat{v}_1}{\partial\widehat{x}_2}s_{21}\right)\left(\tfrac{\partial\widehat{w}_1}{\partial\widehat{x}_1}s_{11} + \tfrac{\partial\widehat{w}_1}{\partial\widehat{x}_2}s_{21}\right)\right.\\ &+\tfrac{1}{2}\left(\tfrac{\partial\widehat{v}_1}{\partial\widehat{x}_1}s_{12} + \tfrac{\partial\widehat{v}_1}{\partial\widehat{x}_2}s_{22} + \tfrac{\partial\widehat{v}_2}{\partial\widehat{x}_1}s_{11} + \tfrac{\partial\widehat{v}_2}{\partial\widehat{x}_2}s_{21}\right)\left(\tfrac{\partial\widehat{w}_1}{\partial\widehat{x}_1}s_{12} + \tfrac{\partial\widehat{w}_1}{\partial\widehat{x}_2}s_{22} + \tfrac{\partial\widehat{w}_2}{\partial\widehat{x}_1}s_{11} + \tfrac{\partial\widehat{w}_2}{\partial\widehat{x}_2}s_{21}\right)\\ &\left.+\left(\tfrac{\partial\widehat{v}_2}{\partial\widehat{x}_1}s_{12} + \tfrac{\partial\widehat{v}_2}{\partial\widehat{x}_2}s_{22}\right)\left(\tfrac{\partial\widehat{w}_2}{\partial\widehat{x}_1}s_{12} + \tfrac{\partial\widehat{w}_2}{\partial\widehat{x}_2}s_{22}\right)\right]\det\left(\nabla T_u(\widehat{x})\right)d\widehat{x}\\ &= 2\mu\sum_{i,j,k,\ell=1}^{2}\int_{\Omega_0^F} a_{k,\ell}^{i,j}(u,\widehat{x})\,\frac{\partial\widehat{v}_i}{\partial\widehat{x}_k}\frac{\partial\widehat{w}_j}{\partial\widehat{x}_\ell}\,d\widehat{x}.\end{aligned} \tag{2.25}$$

$$\begin{aligned}\widehat{b}_F(u,\widehat{w},\widehat{q}) &= -\int_{\Omega_0^F}\left(\tfrac{\partial\widehat{v}_1}{\partial\widehat{x}_1}s_{11} + \tfrac{\partial\widehat{v}_1}{\partial\widehat{x}_2}s_{21} + \tfrac{\partial\widehat{v}_2}{\partial\widehat{x}_1}s_{12} + \tfrac{\partial\widehat{v}_2}{\partial\widehat{x}_2}s_{22}\right)\widehat{q}\,\det\left(\nabla T_u(\widehat{x})\right)d\widehat{x}\\ &= -\int_{\Omega_0^F}\left(\tfrac{\partial\widehat{v}_1}{\partial\widehat{x}_1}\tfrac{H+u(\widehat{x}_1)}{H} - \tfrac{\partial\widehat{v}_1}{\partial\widehat{x}_2}\tfrac{u'(\widehat{x}_1)\widehat{x}_2}{H} + \tfrac{\partial\widehat{v}_2}{\partial\widehat{x}_2}\right)\widehat{q}\,d\widehat{x}.\end{aligned} \tag{2.26}$$

Let us consider $\widehat{f^F}(u) \in \widehat{W}'$ defined for all $\widehat{w}$ in $\widehat{W}$ by

$$\begin{aligned}\left\langle \widehat{f^F}(u), \widehat{w}\right\rangle_{\widehat{W}',\widehat{W}} &= \sum_{i=1}^{2}\int_{\Omega_0^F} f_i^F\widehat{w}_i\det\left(\nabla T_u(\widehat{x})\right)\,d\widehat{x}\\ &= \sum_{i=1}^{2}\int_{\Omega_0^F} f_i^F\widehat{w}_i\frac{H+u(\widehat{x}_1)}{H}\,d\widehat{x}.\end{aligned}$$

Proposition 2.5 *For all u in $\mathcal{U}_{ad}$ and $\widehat{\lambda}$ in $L^2(\Gamma_0)$, the problem:*
Find $(\widehat{v},\ \widehat{p}) \in \widehat{W} \times \widehat{Q}$ such that

$$\begin{cases}\widehat{a}_F(u,\widehat{v},\widehat{w}) + \widehat{b}_F(u,\widehat{w},\widehat{p}) &= \left\langle \widehat{f^F}(u), \widehat{w}\right\rangle + \displaystyle\int_{\Gamma_0}\widehat{\lambda}\widehat{w}_2\,d\widehat{\sigma}, \forall\widehat{w} \in \widehat{W}\\ \widehat{b}_F(u,\widehat{v},\widehat{q}) &= 0, \forall\widehat{q} \in \widehat{Q}\end{cases} \tag{2.27}$$

has a unique solution.

The problem (2.27) is obtained from (2.18) and reversely by using the one-to-one transformations T_u and T_u^{-1}. We have $\widehat{v} = v \circ T_u$, $\widehat{p} = p \circ T_u$ and $\widehat{\lambda} = \widehat{\omega}_u(\lambda \circ T_u)$, where $\widehat{\omega}_u$ is given by the formula (2.23). Therefore, the Proposition 2.5 is a consequence of the Proposition 2.4.

2.6 Optimal control setting

Let us consider the space $\widehat{M} = L^2(\Gamma_0)$. Next, we introduce the two linear and bounded operators

$$A_S : U \to U' \qquad C_S : \widehat{M} \to U'$$

defined by

$$\begin{aligned} \langle A_S\phi, \psi\rangle_{U',U} &= a_S(\phi,\psi) \qquad \forall \phi, \psi \in U \\ \left\langle C_S\widehat{\lambda}, \psi \right\rangle_{U',U} &= \int_0^L \widehat{\lambda}\ (x_1, H)\, \psi\ dx_1 \qquad \forall \widehat{\lambda} \in \widehat{M},\ \forall \psi \in U \end{aligned} \tag{2.28}$$

where a_S is defined by (2.10).

In terms of the operators defined by (2.28), equation (2.11) is posed in the form

$$A_S\, u\left(\widehat{\lambda}\right) = -C_S\, \widehat{\lambda} + f^S$$

which points out that the displacement of the structure $u\left(\widehat{\lambda}\right)$ depends on the forces $\widehat{\lambda}$.

For each u in $\mathcal{U}_{ad}$, there exist three linear bounded operators

$$A_F(u) : \widehat{W} \to \widehat{W}', \qquad B_F(u) : \widehat{W} \to \widehat{Q}', \qquad C_F : \widehat{M} \to \widehat{W}'$$

given by

$$\begin{aligned} \langle A_F(u)\,\widehat{v}, \widehat{w}\rangle_{\widehat{W}',\widehat{W}} &= \widehat{a}_F(u, \widehat{v}, \widehat{w}), \quad \forall \widehat{v}, \widehat{w} \in \widehat{W} \\ \langle B_F(u)\,\widehat{w}, \widehat{q}\rangle_{\widehat{Q}',\widehat{Q}} &= \widehat{b}_F(u, \widehat{w}, \widehat{q}), \quad \forall \widehat{w} \in \widehat{W}, \forall \widehat{q} \in \widehat{Q} \\ \left\langle C_F\widehat{\lambda}, w \right\rangle_{\widehat{W}',\widehat{W}} &= \int_{\Gamma_0} \widehat{\lambda}\widehat{w}_2\, d\widehat{\sigma}, \quad \forall \widehat{\lambda} \in \widehat{M}, \forall \widehat{w} \in \widehat{W}. \end{aligned} \tag{2.29}$$

So, the system (2.27) can be rewritten with operator notation in the form:

For $u \in \mathcal{U}_{ad}$ and $\widehat{\lambda} \in \widehat{M}$ given, find $\widehat{v}\left(u, \widehat{\lambda}\right) \in \widehat{W}$ and $\widehat{p}\left(u, \widehat{\lambda}\right) \in \widehat{Q}$ such that

$$\begin{cases} A_F(u)\,\widehat{v}\left(u, \widehat{\lambda}\right) + B_F^*(u)\,\widehat{p}\left(u, \widehat{\lambda}\right) = \widehat{f}^F(u) + C_F\widehat{\lambda} & \text{in } \widehat{W}' \\ B_F(u)\,\widehat{v}\left(u, \widehat{\lambda}\right) = 0 & \text{in } \widehat{Q}' \end{cases} \tag{2.30}$$

or in an equivalent matrix notation as

$$\begin{pmatrix} A_F(u) & B_F^*(u) \\ B_F(u) & 0 \end{pmatrix} \begin{pmatrix} \widehat{v}\left(u, \widehat{\lambda}\right) \\ \widehat{p}\left(u, \widehat{\lambda}\right) \end{pmatrix} = \begin{pmatrix} \widehat{f}^F(u) + C_F\widehat{\lambda} \\ 0 \end{pmatrix} \tag{2.31}$$

where $B_F^*(u)$ is the adjoint operator of $B_F(u)$.

In the next paragraph the fluid-structure coupled problem will be modeled by an optimal control system.

For each $\widehat{v} \in \widehat{W}$ we denote by $\widehat{v}_{|\Gamma_0}$ the trace on Γ_0 of $\widehat{v}$ and we denote by $\|\cdot\|_{0,\Gamma_0}$ the usual norm in $L^2(\Gamma_0)$. We denote by $J : \widehat{W} \to \mathbb{R}$, the function defined by

$$J(\widehat{w}) = \frac{1}{2} \left\| \widehat{w}_{2|\Gamma_0} \right\|_{0,\Gamma_0}^2 .$$

Moreover, let $j : \mathcal{F}_{ad} \to \mathbb{R}$ be the function defined by

$$j\left(\widehat{\lambda}\right) = J\left(\widehat{v}\left(u\left(\widehat{\lambda}\right), \widehat{\lambda}\right)\right). \tag{2.32}$$

We pose the following optimal control problem $(\mathcal{P})$:

$$\inf j\left(\widehat{\lambda}\right)$$

subject to the conditions:

1. $\widehat{\lambda} \in \mathcal{F}_{ad}$
2. $u\left(\widehat{\lambda}\right) \in \mathcal{U}_{ad}$ such that

$$A_S\, u\left(\widehat{\lambda}\right) = -C_S\, \widehat{\lambda} + f^S \tag{2.33}$$

3. $\widehat{v}\left(u\left(\widehat{\lambda}\right), \widehat{\lambda}\right) \in \widehat{W}, \quad \widehat{p}\left(u\left(\widehat{\lambda}\right), \widehat{\lambda}\right) \in \widehat{Q}$ such that

$$\begin{pmatrix} A_F\left(u\left(\widehat{\lambda}\right)\right) & B_F^*\left(u\left(\widehat{\lambda}\right)\right) \\ B_F\left(u\left(\widehat{\lambda}\right)\right) & 0 \end{pmatrix} \begin{pmatrix} \widehat{v}\left(u\left(\widehat{\lambda}\right), \widehat{\lambda}\right) \\ \widehat{p}\left(u\left(\widehat{\lambda}\right), \widehat{\lambda}\right) \end{pmatrix} = \begin{pmatrix} \widehat{f}^F(u) + C_F \widehat{\lambda} \\ 0 \end{pmatrix}. \tag{2.34}$$

Therefore, the previous formulation corresponds to an optimal control problem with Neumann like boundary control $(\widehat{\lambda})$ and Dirichlet like boundary observation $(\widehat{v}_{2|\Gamma_0})$. Moreover, the control appears also in the coefficients of the fluid equations (2.34) as it happens in some optimal design problems.[37], [41] The condition $\widehat{\lambda} \in \mathcal{F}_{ad}$ represents the control constraint, while the state constraint is given by the fact that $u\left(\widehat{\lambda}\right) \in \mathcal{U}_{ad}$.

This mathematical formulation provides an interesting tool for the numerical approximation of the *a priori* fluid-structure coupled problem in an uncoupled way. That is, the structure equations represented by the first two conditions and the fluid equations (2.34) can be solved separately in an iterative process.

As we mentioned in the second section, on the interface we have two boundary conditions: equality of the fluid and structure velocities (which is a Dirichlet like boundary condition) and equality of the stresses (which is a Neumann like boundary condition). In our approach we pursue both coupling conditions in the iterative algorithm:

- Step 1: We start with a guess for the forces $\widehat{\lambda}$ on the interface.
- Step 2: The displacement $u\left(\widehat{\lambda}\right)$ of the structure can be computed by (2.33).
- Step 3: Once the coefficients of the equations (2.34) have been obtained, we can compute the velocity and the pressure of the fluid as the solution of the weak mixed formulation on the fixed domain (2.34).
- Step 4: Update $\widehat{\lambda}$ in order to minimize the cost function j.

Remark 2.4 *As we use the value $-\widehat{\lambda}$ for the forces on Γ_0 in the equations of the structure and we take the value $\widehat{\lambda}$ in the equations of the fluid, the Neumann like boundary condition is strongly accomplished. The Dirichlet like boundary condition $\widehat{v}_{2|\Gamma_0}=0$ is approached by a Least Square formulation posed in terms of the minimization problem*

$$\inf \frac{1}{2}\left\|\widehat{v}_{2|\Gamma_0}\right\|_{0,\Gamma_0}^2.$$

2.7 Continuity of the cost function

In this subsection, we shall prove that the cost function j is continuous.

The cost function is the composition of the following functions:

$$\begin{aligned}\widehat{\lambda}\in\mathcal{F}_{ad} &\longmapsto u\left(\widehat{\lambda}\right)\in\mathcal{U}_{ad},\\ \left(u,\widehat{\lambda}\right)\in\mathcal{U}_{ad}\times\widehat{M} &\longmapsto \widehat{v}\left(u,\widehat{\lambda}\right)\in\widehat{W},\\ \widehat{w}\in\widehat{W} &\longmapsto J\left(\widehat{w}\right)\in\mathbb{R}.\end{aligned}$$

The first and the third are continuous, evidently. Next, by using the Implicit Function Theorem (see the Appendix), we shall prove that the second one is continuous too.

We define

$$\begin{aligned}\mathcal{U} = \{&u\in U;\, u(0)=u(L)=u'(0)=u'(L)=0,\\ &H+u(x_1)>0,\,\forall x_1\in[0,L]\},\end{aligned}\tag{2.35}$$

so that $\mathcal{U}_{ad}\subset\mathcal{U}\subset U$ and $\mathcal{U}$ is an open set of U.

Let us consider the function $h:\left(\widehat{M}\times\mathcal{U}\right)\times\left(\widehat{W}\times\widehat{Q}\right)\to\widehat{W}'\times\widehat{Q}'$ defined by

$$h\left((\widehat{\mu},u),(\widehat{w},\widehat{q})\right)=\left(A_F(u)\,\widehat{w}+B_F^*(u)\,\widehat{q}-\widehat{f}^F(u)-C_F\widehat{\mu},B_F(u)\,\widehat{w}\right).$$

Next we apply Theorem 2.4 (see the Appendix) for the case

$$X = \widehat{M} \times U,\ Y = Z = \widehat{W} \times \widehat{Q},\ G = \widehat{M} \times \mathcal{U} \times \widehat{W} \times \widehat{Q},$$
$$x_0 = \left(\widehat{\lambda}, u\left(\widehat{\lambda}\right)\right),\ y_0 = \left(\widehat{v}\left(u\left(\widehat{\lambda}\right), \widehat{\lambda}\right), \widehat{p}\left(u\left(\widehat{\lambda}\right), \widehat{\lambda}\right)\right),$$
$$x = (\widehat{\mu}, u),\ y = (\widehat{w}, \widehat{q}).$$

We have that $h(x_0, y_0) = 0$. According to the Proposition 2.5 and in view of the identities (2.30) and (2.31), we have that

$$\frac{\partial h}{\partial y}((\widehat{\mu}, u), (\widehat{w}, \widehat{q})) = \begin{pmatrix} A_F(u) & B_F^*(u) \\ B_F(u) & 0 \end{pmatrix} \in \mathcal{L}\left(\widehat{W} \times \widehat{Q}, \widehat{W}' \times \widehat{Q}'\right)$$

is invertible.

In view of the Remark 2.6 (see the Appendix), it remains to verify that h and $\frac{\partial h}{\partial y}$ are continuous in (x_0, y_0).

Proposition 2.6 *Let $\overline{u}$ be in $\mathcal{U}_{ad}$. We have*

$$\lim_{\|u-\overline{u}\|_U \to 0} \|A_F(u) - A_F(\overline{u})\|_{L(\widehat{W}, \widehat{W}')} = 0, \tag{2.36}$$

$$\lim_{\|u-\overline{u}\|_U \to 0} \|B_F(u) - B_F(\overline{u})\|_{L(\widehat{W}, \widehat{Q}')} = 0, \tag{2.37}$$

$$\lim_{\|u-\overline{u}\|_U \to 0} \|B_F^*(u) - B_F^*(\overline{u})\|_{L(\widehat{Q}, \widehat{W}')} = 0 \tag{2.38}$$

where $\|\cdot\|_U$ is the norm of the Sobolev space $U = H_0^2(0, L)$.

Proof. We have that

$$\langle A_F(u)\,\widehat{v}, \widehat{w}\rangle = \widehat{a}_F(u, \widehat{v}, \widehat{w})$$

where $\widehat{a}_F$ is defined by (2.25).

Next, by using the elementary integral calculus results, we obtain

$$\begin{aligned} |u(\widehat{x}_1)| &= \left|\int_0^{\widehat{x}_1} u'(s)\,ds\right| \le \int_0^{\widehat{x}_1} |u'(s)|\,ds \\ &\le \int_0^L |u'(s)|\,ds \le \left(\int_0^L |u'(s)|^2\,ds\right)^{1/2} \le \|u\|_U \end{aligned} \tag{2.39}$$

and analogously

$$\begin{aligned} |u'(\widehat{x}_1)| &= \left|\int_0^{\widehat{x}_1} u''(s)\,ds\right| \le \int_0^{\widehat{x}_1} |u''(s)|\,ds \\ &\le \int_0^L |u''(s)|\,ds \le \left(\int_0^L |u''(s)|^2\,ds\right)^{1/2} \le \|u\|_U. \end{aligned} \tag{2.40}$$

Since the coefficients of the bilinear form $\widehat{a}_F(u,\cdot,\cdot)$ are continuous with respect to u, u' and thanks to above inequalities, we obtain that there exists a constant $C_1\left(\Omega_0^F\right)$ depending only upon the shape of the domain Ω_0^F, such that for all $\widehat{v}$ and $\widehat{w}$ in $\widehat{W}$, we have

$$\widehat{a}_F(u-\overline{u},\widehat{v},\widehat{w}) \leq C_1\left(\Omega_0^F\right)\|u-\overline{u}\|_U \|\widehat{v}\|_{\widehat{W}} \|\widehat{w}\|_{\widehat{W}}.$$

It was essential for obtaining the above estimation the fact that the domain Ω_0^F is bounded!

It follows that

$$\|A_F(u)-A_F(\overline{u})\|_{L\left(\widehat{W},\widehat{W}'\right)} \stackrel{def}{=} \sup_{\|\widehat{v}\|_{\widehat{W}}\leq 1,\|\widehat{w}\|_{\widehat{W}}\leq 1} \langle (A_F(u)-A_F(\overline{u}))\,\widehat{v},\widehat{w}\rangle$$
$$= \sup_{\|\widehat{v}\|_{\widehat{W}}\leq 1,\|\widehat{w}\|_{\widehat{W}}\leq 1} \widehat{a}_F(u-\overline{u},\widehat{v},\widehat{w}) \leq C_1\left(\Omega_0^F\right)\|u-\overline{u}\|_U.$$

which proves the relation (2.36).

Analogously, we obtain the two other relations which complete the proof. □

Proposition 2.7 *The function*

$$u \in \mathcal{U}_{ad} \mapsto \widehat{f}^F(u) \in \widehat{W}'$$

is continuous.

Proof. We have

$$\begin{aligned}\left\|\widehat{f}^F(u)-\widehat{f}^F(\overline{u})\right\| &= \sup_{\|\widehat{w}\|\leq 1}\left|\sum_{i=1}^{2}\int_{\Omega_0^F}\widehat{f}_i^F(u-\overline{u})(\widehat{x}_1)\,\widehat{w}_i\,d\widehat{x}\right| \\ &\leq \|u-\overline{u}\|_U \sup_{\|\widehat{w}\|\leq 1}\left(\sum_{i=1}^{2}\int_{\Omega_0^F}\left|\widehat{f}_i^F\right||\widehat{w}_i|\,d\widehat{x}\right) \\ &\leq \|u-\overline{u}\|_U \sqrt{\sum_{i=1}^{2}\int_{\Omega_0^F}\left|\widehat{f}_i^F\right|^2 d\widehat{x}}\end{aligned}$$

and the conclusion holds. □

Corollary 2.1 *The function* $\frac{\partial h}{\partial y}$ *from* G *to* $\mathcal{L}\left(\widehat{W}\times\widehat{Q},\widehat{W}'\times\widehat{Q}'\right)$ *is continuous on* G.

Corollary 2.2 *The functions*

$$(u,\widehat{w}) \in \mathcal{U}_{ad}\times\widehat{W} \longmapsto A_F(u)\,\widehat{w} \in \widehat{W}'$$
$$(u,\widehat{w}) \in \mathcal{U}_{ad}\times\widehat{W} \longmapsto B_F(u)\,\widehat{w} \in \widehat{Q}'$$
$$(u,\widehat{q}) \in \mathcal{U}_{ad}\times\widehat{Q} \longmapsto B_F^*(u)\,\widehat{q} \in \widehat{W}'$$

are continuous.

Proof. Let $\overline{u}$ and $\widehat{v}$ be given in $\mathcal{U}_{ad}$ and $\widehat{W}$ respectively. We have

$$\begin{array}{rl} \|A_F(u)\,\widehat{w} - A_F(\overline{u})\,\widehat{v}\|_{\widehat{W}'} & \leq \\ \|A_F(u)\,\widehat{w} - A_F(\overline{u})\,\widehat{w} + A_F(\overline{u})\,\widehat{w} - A_F(\overline{u})\,\widehat{v}\|_{\widehat{W}'} & \leq \\ \|A_F(u) - A_F(\overline{u})\|_{L\left(\widehat{W},\widehat{W}'\right)}\,\|\widehat{w}\|_{\widehat{W}} + \|A_F(\overline{u})\|_{L\left(\widehat{W},\widehat{W}'\right)}\,\|\widehat{w} - \widehat{v}\|_{\widehat{W}}\,. & \end{array}$$

From Proposition 2.6, we have

$$\lim_{\|u-\overline{u}\|_U \to 0} \|A_F(u) - A_F(\overline{u})\|_{L\left(\widehat{W},\widehat{W}'\right)} = 0.$$

Next, since $\|\widehat{w} - \widehat{v}\|_{\widehat{W}} \to 0$, we get that $\|\widehat{w}\|_{\widehat{W}}$ is bounded and the proof is complete. □

Corollary 2.3 *The function h from G to $\widehat{W}' \times \widehat{Q}'$ is continuous on G.*

All the hypotheses of the Theorem 2.4 (see the Appendix) hold, so the implicit function $\theta : \widehat{M} \times \mathcal{U} \to \widehat{W} \times \widehat{Q}$ given by

$$\theta(\widehat{\mu}, u) = (\widehat{v}(u, \widehat{\mu}), \widehat{p}(u, \widehat{\mu}))$$

is continuous in $\left(\widehat{\lambda}, u\left(\widehat{\lambda}\right)\right)$. Moreover, this result holds for each $\widehat{\lambda} \in \widehat{M}$, such that $u\left(\widehat{\lambda}\right) \in \mathcal{U}$.

Therefore, we obtain that the cost function j defined in (2.32) is continuous on $\mathcal{F}_{ad}$, since it is the composition of three continuous functions.

2.8 Differentiability of the cost function

In this section we analyze the differentiability of the cost function as well as the expression of its gradient. We use the method of deformation of domains.[31], [7], [9]

In the four following lemmas, the differentiability of intermediate functions is established. Moreover, the analytic formula for their derivatives is obtained.

We follow the notations introduced in the previous sections.

Lemma 2.3 *The function $J : \widehat{W} \to \mathbb{R}$ defined by*

$$J(\widehat{w}) = \frac{1}{2}\,\|\widehat{w}_2\|^2_{0,\Gamma_0}$$

is Fréchet differentiable and

$$J'(\widehat{v})\,\widehat{w} = \int_{\Gamma_0} \widehat{v}_2 \widehat{w}_2\, d\widehat{\sigma}.$$

Proof. The function $\widehat{w} \longmapsto \int_{\Gamma_0} \widehat{v}_2 \widehat{w}_2 \, d\widehat{\sigma}$ is linear and continuous, evidently. We shall use the definition of the Fréchet differentiability detailed in the Appendix.

$$\lim_{\widehat{w}\to 0} \frac{\left| \frac{1}{2}\|\widehat{v}_2+\widehat{w}_2\|^2_{0,\Gamma_0} - \frac{1}{2}\|\widehat{v}_2\|^2_{0,\Gamma_0} - \int_{\Gamma_0} \widehat{v}_2\widehat{w}_2 \, d\widehat{\sigma} \right|}{\|\widehat{w}\|_{1,\Omega_0^F}}$$
$$= \lim_{\widehat{w}\to 0} \frac{\|\widehat{w}_2\|^2_{0,\Gamma_0}}{2\|\widehat{w}\|_{1,\Omega_0^F}} = \lim_{\widehat{w}\to 0} \frac{\|\widehat{w}_2\|_{0,\Gamma_0}}{\|\widehat{w}\|_{1,\Omega_0^F}} \frac{\|\widehat{w}_2\|_{0,\Gamma_0}}{2}.$$

Since $\|\widehat{w}_2\|_{0,\Gamma_0} \leq \|\widehat{w}\|_{0,\Gamma_0}$ and from the continuity of the trace operator defined on $H^1\left(\Omega_0^F\right)$, we have

$$\frac{\|\widehat{w}_2\|_{0,\Gamma_0}}{\|\widehat{w}\|_{1,\Omega_0^F}} \leq \frac{\|\widehat{w}\|_{0,\Gamma_0}}{\|\widehat{w}\|_{1,\Omega_0^F}} \leq const.$$

so the above limit is 0. □

Lemma 2.4 *Let $\widehat{v}$, $\widehat{w}$ be given in $\widehat{W}$ and $\widehat{q}$ in $\widehat{Q}$. Then the functions from $\mathcal{U}_{ad}$ to $\mathbb{R}$ defined by*

$$u \longmapsto \widehat{a}_F\left(u, \widehat{v}, \widehat{w}\right)$$
$$u \longmapsto \widehat{b}_F\left(u, \widehat{w}, \widehat{q}\right)$$

are Fréchet differentiable on $\mathcal{U}_{ad}$ and the derivatives have the forms:

$$\frac{\partial \widehat{a}_F}{\partial u}\left(u, \widehat{v}, \widehat{w}\right)\psi = 2\mu \sum_{i,j,k,\ell=1}^{2} \int_{\Omega_0^F} \frac{\partial a^{i,j}_{k,\ell}}{\partial u}\left(u, \widehat{x}\right)\psi \frac{\partial \widehat{v}_i}{\partial \widehat{x}_k}\frac{\partial \widehat{w}_j}{\partial \widehat{x}_\ell}\, d\widehat{x} \tag{2.41}$$

$$\frac{\partial \widehat{b}_F}{\partial u}\left(u, \widehat{w}, \widehat{q}\right)\psi = -\int_{\Omega_0^F} \frac{\psi\left(\widehat{x}_1\right)}{H}\frac{\partial \widehat{w}_1}{\partial \widehat{x}_1}\widehat{q}\, d\widehat{x} + \int_{\Omega_0^F} \frac{\psi'\left(\widehat{x}_1\right)\widehat{x}_2}{H}\frac{\partial \widehat{w}_1}{\partial \widehat{x}_2}\widehat{q}\, d\widehat{x}. \tag{2.42}$$

Proof. In view of the identity (2.26), the function

$$u \mapsto \widehat{b}_F\left(u, \widehat{w}, \widehat{q}\right)$$

is affine. Using the inequalities (2.39) and (2.40), we get the continuity of this function. Consequently, it is Fréchet differentiable.

But, for a linear and continuous function

$$u \in U \mapsto f\left(u\right) \in \mathbb{R}$$

the Fréchet derivative has the form

$$f'\left(u\right)\psi = f\left(\psi\right), \qquad \forall \psi \in U.$$

The above identity gives (2.42).

Using the same method, we can get the Fréchet differentiability and derivatives for all the terms of $\widehat{a}_F(u,\widehat{v},\widehat{w})$ which are affine with respect to u.

The only remaining point concerns the differentiability of the function

$$u \longmapsto \int_{\Omega_0^F} a_{k,\ell}^{i,j}(u,\widehat{x})\,\frac{\partial \widehat{v}_i}{\partial \widehat{x}_k}\frac{\partial \widehat{w}_j}{\partial \widehat{x}_\ell}\,d\widehat{x}.$$

where $u \in U \mapsto a_{k,\ell}^{i,j}(u,\cdot) \in L^\infty\left(\Omega_0^F\right)$ is nonlinear.

We apply the Theorem 2.7 concerning the differentiability of integrals with parameter (see the Appendix) in the case $\widehat{\Omega} \equiv \overline{\Omega}_0^F$ and

$$f(u,\widehat{x}) = a_{k,\ell}^{i,j}(u,\widehat{x})\,\frac{\partial \widehat{v}_i}{\partial \widehat{x}_k}\frac{\partial \widehat{w}_j}{\partial \widehat{x}_\ell}\,d\widehat{x}.$$

The uniform convergence is ensured due to the inequalities (2.39) and (2.40) and to the compactness of the domain $\overline{\Omega}_0^F$.

The elementary rules for computing Fréchet derivative establish the identity (2.41), which completes the proof. □

Lemma 2.5 *The function*

$$u \in \mathcal{U}_{ad} \;\mapsto \widehat{f}^F(u) \in \widehat{W}'$$

is Fréchet differentiable and the derivative $D\widehat{f}^F(u) \in \mathcal{L}\left(U,\widehat{W}'\right)$ *has the form*

$$\left\langle D\widehat{f}^F(u)\,\psi,\widehat{w}\right\rangle = \sum_{i=1}^{2}\int_{\Omega_0^F}\frac{\psi(\widehat{x}_1)}{H}f_i^F\widehat{w}_i\,d\widehat{x}, \quad \forall \widehat{w} \in \widehat{W}$$

Proof. The above function is affine and from the Proposition 2.7, it is continuous, then it is Fréchet differentiable. □

Lemma 2.6 *We have*

a) *the function from* $\mathcal{U}_{ad} \times \widehat{M}$ *into* $\widehat{W} \times \widehat{Q}$ *defined by*

$$\left(u,\widehat{\lambda}\right) \longmapsto \left(\widehat{v}\left(u,\widehat{\lambda}\right),\widehat{p}\left(u,\widehat{\lambda}\right)\right)$$

is Fréchet differentiable on $\mathcal{U}_{ad} \times \widehat{M}$,

b) *the derivative of the function*

$$\widehat{\lambda} \in \widehat{K} \longmapsto \widehat{v}\left(u\left(\widehat{\lambda}\right),\widehat{\lambda}\right) \in \widehat{W}$$

has the form

$$-\frac{\partial \widehat{v}}{\partial u}\left(u\left(\widehat{\lambda}\right),\widehat{\lambda}\right)A_S^{-1}C_S + \frac{\partial \widehat{v}}{\partial \widehat{\lambda}}\left(u\left(\widehat{\lambda}\right),\widehat{\lambda}\right).$$

Proof. a) Let $\widehat{\lambda}$ be in $\mathcal{F}_{ad}$. We have that $u\left(\widehat{\lambda}\right)$ computed from (2.43) belongs to $\mathcal{U}_{ad}$.

Let $\widehat{v}\left(u\left(\widehat{\lambda}\right),\widehat{\lambda}\right)$ and $\widehat{p}\left(u\left(\widehat{\lambda}\right),\widehat{\lambda}\right)$ be computed from (2.44).

We recall that $\mathcal{U}$ defined by (2.35) is an open set in U.

We apply the result concerning the differentiability of the implicit function (see the Theorem 2.7 in the Appendix) in the case

$$X=\widehat{M}\times U,\ Y=Z=\widehat{W}\times\widehat{Q},\ G=\widehat{M}\times\mathcal{U}\times\widehat{W}\times\widehat{Q},$$
$$x_0=\left(\widehat{\lambda},u\left(\widehat{\lambda}\right)\right),\ y_0=\left(\widehat{v}\left(u\left(\widehat{\lambda}\right),\widehat{\lambda}\right),\widehat{p}\left(u\left(\widehat{\lambda}\right),\widehat{\lambda}\right)\right),$$
$$x=(\widehat{\mu},u),\ y=(\widehat{w},\widehat{q})$$

for the function $h:\left(\widehat{M}\times\mathcal{U}\right)\times\left(\widehat{W}\times\widehat{Q}\right)\to\widehat{W}'\times\widehat{Q}'$ defined by

$$h\left((\widehat{\mu},u),(\widehat{w},\widehat{q})\right)=\left(A_F(u)\,\widehat{w}+B_F^*(u)\,\widehat{q}-\widehat{f}^F(u)-C_F\widehat{\mu},\ B_F(u)\,\widehat{w}\right).$$

In Section 2.7, we have proved that all the hypotheses of the Theorem 2.4 hold for the previous choice. It remains to show that $\frac{\partial h}{\partial x}$ exists on G and it is continuous in (x_0,y_0).

In order to prove that, we apply the Theorem 2.2 (see the Appendix). We have to prove that the functions $\frac{\partial h}{\partial\widehat{\mu}}$ and $\frac{\partial h}{\partial u}$ exist on G and they are continuous in (x_0,y_0).

But the function

$$\widehat{\mu}\in\widehat{M}\longmapsto h\left((\widehat{\mu},u),(\widehat{w},\widehat{q})\right)$$

is linear and continuous. Its Fréchet derivative is

$$\frac{\partial h}{\partial\widehat{\mu}}\left((\widehat{\mu},u),(\widehat{w},\widehat{q})\right)=(-C_F,0),$$

which is evidently continuous on G (because it is constant).

Next, we prove the similar result for $\frac{\partial h}{\partial u}$.

We obtain from the identities (2.41) and (2.42) that there exist three operators

$$\begin{aligned}
DA_F(u) &\in \mathcal{L}\left(\widehat{W},\mathcal{L}\left(U,\widehat{W}'\right)\right)\\
DB_F^*(u) &\in \mathcal{L}\left(\widehat{Q},\mathcal{L}\left(U,\widehat{W}'\right)\right)\\
DB_F(u) &\in \mathcal{L}\left(\widehat{W},\mathcal{L}\left(U,\widehat{Q}'\right)\right)
\end{aligned}$$

such that

$$\begin{aligned}
\left(\left(DA_F(u)\,\widehat{v}\right)\psi\right)\widehat{w} &= \frac{\partial\widehat{a}_F}{\partial u}(u,\widehat{v},\widehat{w})\,\psi\\
\left(\left(DB_F^*(u)\,\widehat{q}\right)\psi\right)\widehat{w} &= \frac{\partial\widehat{b}_F}{\partial u}(u,\widehat{w},\widehat{q})\,\psi\\
\left(\left(DB_F(u)\,\widehat{w}\right)\psi\right)\widehat{q} &= \frac{\partial\widehat{b}_F}{\partial u}(u,\widehat{w},\widehat{q})\,\psi
\end{aligned}$$

for all $u \in \mathcal{U}$, $\widehat{v}, \widehat{w} \in \widehat{W}$, $\widehat{q} \in \widehat{Q}$ and $\psi \in U$.

From the Lemma 2.4, we get that there exists a function ω, such that

$$\widehat{a}_F(\overline{u}+\psi,\widehat{v},\widehat{w}) - \widehat{a}_F(\overline{u},\widehat{v},\widehat{w}) - \frac{\partial \widehat{a}_F}{\partial u}(\overline{u},\widehat{v},\widehat{w})\,\psi = \|\psi\|_U\,\omega(\overline{u},\widehat{v},\widehat{w},\psi)$$

or equivalently

$$\begin{aligned}\langle A_F(\overline{u}+\psi)\,\widehat{v},\widehat{w}\rangle_{\widehat{W}',\widehat{W}} - \langle A_F(\overline{u})\,\widehat{v},\widehat{w}\rangle_{\widehat{W}',\widehat{W}} - \langle (DA_F(\overline{u})\,\widehat{v})\,\psi,\widehat{w}\rangle_{\widehat{W}',\widehat{W}} \\ = \|\psi\|_U\,\omega(\overline{u},\widehat{v},\widehat{w},\psi)\end{aligned}$$

and

$$\lim_{\psi\to 0}\omega(\overline{u},\widehat{v},\widehat{w},\psi) = 0.$$

In fact, we have that ω converges to 0 uniformly with respect to $\|\widehat{w}\|_{\widehat{W}} \leq 1$. More precisely, we have: $\forall \varepsilon > 0, \exists \delta_\varepsilon > 0, \forall \|\widehat{w}\|_{\widehat{W}} \leq 1, \forall \|u-\overline{u}\|_U \leq \delta_\varepsilon$,

$$|\omega(u,\widehat{v},\widehat{w},\psi) - \omega(\overline{u},\widehat{v},\widehat{w},\psi)| \leq \varepsilon.$$

Then the function

$$u \longmapsto A_F(u)\,\widehat{v} \in \widehat{W}'$$

is Fréchet differentiable and its derivative is

$$DA_F(u)\,\widehat{v} \in \mathcal{L}\left(U,\widehat{W}'\right).$$

In a similar way, we obtain that the function

$$u \longmapsto h((\widehat{\mu},u),(\widehat{w},\widehat{q})) \in \widehat{W}' \times \widehat{Q}'$$

is Fréchet differentiable and its derivative is

$$\frac{\partial h}{\partial u}((\widehat{\mu},u),(\widehat{w},\widehat{q})) = \left(DA_F(u)\,\widehat{w} + DB_F^*(u)\,\widehat{q} - D\widehat{f}^F(u),\ DB_F(u)\,\widehat{w}\right).$$

Following an analogous argument as in the Proposition 2.6 and Corollary 2.2, we get that the function $\frac{\partial h}{\partial u}$ is continuous on G.

Now, we can apply the Theorem 2.7 (see the Appendix) and we obtain that the implicit function $\theta : \widehat{M} \times \mathcal{U} \longrightarrow \widehat{W} \times \widehat{Q}$, given by

$$\theta(\widehat{\mu},u) = (\widehat{v}(u,\widehat{\mu}),\widehat{p}(u,\widehat{\mu})),$$

is Fréchet differentiable, which states the first part of this Lemma.

b) Next, from the identity $A_S\,u\left(\widehat{\lambda}\right) = -C_S\,\widehat{\lambda} + f^S$, we have that the function $\widehat{\lambda} \mapsto u\left(\widehat{\lambda}\right)$ is differentiable and $u'\left(\widehat{\lambda}\right) = -A_S^{-1}\,C_S$.

By using the chain rule, the derivative of the function

$$\widehat{\lambda} \mapsto \widehat{v}\left(u\left(\widehat{\lambda}\right), \widehat{\lambda}\right)$$

has the form

$$\frac{\partial \widehat{v}}{\partial u}\left(u\left(\widehat{\lambda}\right), \widehat{\lambda}\right) u'\left(\widehat{\lambda}\right) + \frac{\partial \widehat{v}}{\partial \widehat{\lambda}}\left(u\left(\widehat{\lambda}\right), \widehat{\lambda}\right) = -\frac{\partial \widehat{v}}{\partial u}\left(u\left(\widehat{\lambda}\right), \widehat{\lambda}\right) A_S^{-1} C_S + \frac{\partial \widehat{v}}{\partial \widehat{\lambda}}\left(u\left(\widehat{\lambda}\right), \widehat{\lambda}\right)$$

and the proof is complete. □

Now, we present the main result concerning the computation of the gradient for the fluid-structure interaction problem.

Theorem 2.1 *The cost function j defined by (2.32) is Fréchet differentiable. Moreover, we have forall $\widehat{\lambda}$ in $\mathcal{F}_{ad}$ and forall $\widehat{\mu}$ in $\widehat{M}$:*

$$\begin{aligned} j'\left(\widehat{\lambda}\right)\widehat{\mu} &= \left(\frac{\partial \widehat{a}_F}{\partial u}(u, \widehat{v}, \widehat{z}) + \frac{\partial \widehat{b}_F}{\partial u}(u, \widehat{z}, \widehat{p}) + \frac{\partial \widehat{b}_F}{\partial u}(u, \widehat{v}, \widehat{r})\right) A_S^{-1} C_S \widehat{\mu} \\ &\quad - \int_{\Omega_0^F} \frac{\left(A_S^{-1} C_S \widehat{\mu}\right)(\widehat{x}_1)}{H} f^F \cdot \widehat{z}\, d\widehat{x} + \int_{\Gamma_0} \widehat{v}_2 \frac{\partial \widehat{v}_2}{\partial \widehat{\lambda}}\left(u, \widehat{\lambda}\right) \widehat{\mu}\, d\widehat{\sigma}, \end{aligned}$$

where the displacement u is computed from

$$A_S\, u = -C_S\, \widehat{\lambda} + f^S, \tag{2.43}$$

the velocity $\widehat{v}$ and the pressure $\widehat{p}$ of the fluid are computed as solution of

$$\begin{cases} \widehat{a}_F(u, \widehat{v}, \widehat{w}) + \widehat{b}_F(u, \widehat{w}, \widehat{p}) &= \left\langle \widehat{f}^F(u), \widehat{w} \right\rangle + \displaystyle\int_{\Gamma_0} \widehat{\lambda} \widehat{w}_2\, d\widehat{\sigma},\ \forall \widehat{w} \in \widehat{W} \\ \widehat{b}_F(u, \widehat{v}, \widehat{q}) &= 0, \quad \forall \widehat{q} \in \widehat{Q}, \end{cases} \tag{2.44}$$

the adjoint state $\widehat{z}$ and $\widehat{r}$ are computed as solution of

$$\begin{cases} \widehat{a}_F(u, \widehat{w}, \widehat{z}) + \widehat{b}_F(u, \widehat{w}, \widehat{r}) &= \displaystyle\int_{\Gamma_0} \widehat{v}_2 \widehat{w}_2\, d\widehat{\sigma}, \quad \forall \widehat{w} \in \widehat{W} \\ \widehat{b}_F(u, \widehat{z}, \widehat{q}) &= 0, \quad \forall \widehat{q} \in \widehat{Q} \end{cases} \tag{2.45}$$

and $\frac{\partial \widehat{v}_2}{\partial \widehat{\lambda}}\left(u, \widehat{\lambda}\right)\widehat{\mu}$ is computed from

$$\begin{cases} \widehat{a}_F\left(u, \dfrac{\partial \widehat{v}}{\partial \widehat{\lambda}}\left(u, \widehat{\lambda}\right)\widehat{\mu}, \widehat{w}\right) + \widehat{b}_F\left(u, \widehat{w}, \dfrac{\partial \widehat{p}}{\partial \widehat{\lambda}}\left(u, \widehat{\lambda}\right)\widehat{\mu}\right) &= \displaystyle\int_{\Gamma_0} \widehat{\mu} \widehat{w}_2\, d\widehat{\sigma}, \forall \widehat{w} \in \widehat{W} \\ \widehat{b}_F\left(u, \dfrac{\partial \widehat{v}}{\partial \widehat{\lambda}}\left(u, \widehat{\lambda}\right)\widehat{\mu}, \widehat{q}\right) &= 0, \forall \widehat{q} \in \widehat{Q}. \end{cases} \tag{2.46}$$

Proof. According to the Lemma 2.3, Lemma 2.6 and the chain rule, we obtain that j is differentiable and

$$\begin{aligned} j'\left(\widehat{\lambda}\right)\widehat{\mu} &= J'\left(\widehat{v}\left(u\left(\widehat{\lambda}\right),\widehat{\lambda}\right)\right)\frac{\partial\widehat{v}}{\partial u}\left(u\left(\widehat{\lambda}\right),\widehat{\lambda}\right)u'\left(\widehat{\lambda}\right)\widehat{\mu} \\ &\quad + J'\left(\widehat{v}\left(u\left(\widehat{\lambda}\right),\widehat{\lambda}\right)\right)\frac{\partial\widehat{v}}{\partial\widehat{\lambda}}\left(u\left(\widehat{\lambda}\right),\widehat{\lambda}\right)\widehat{\mu} \\ &= \int_{\Gamma_0}\widehat{v}_2\left(u\left(\widehat{\lambda}\right),\widehat{\lambda}\right)\frac{\partial\widehat{v}_2}{\partial u}\left(u\left(\widehat{\lambda}\right),\widehat{\lambda}\right)u'\left(\widehat{\lambda}\right)\widehat{\mu}\,d\widehat{\sigma} \\ &\quad + \int_{\Gamma_0}\widehat{v}_2\left(u\left(\widehat{\lambda}\right),\widehat{\lambda}\right)\frac{\partial\widehat{v}_2}{\partial\widehat{\lambda}}\left(u\left(\widehat{\lambda}\right),\widehat{\lambda}\right)\widehat{\mu}\,d\widehat{\sigma}. \end{aligned}$$

Our next objective is to evaluate the first term of the above sum.

For this, let $(\widehat{z},\widehat{r})$ be the solution of the adjoint system (2.45). Next, replacing $\widehat{w}$ by $\frac{\partial\widehat{v}}{\partial u}\left(u\left(\widehat{\lambda}\right),\widehat{\lambda}\right)u'\left(\widehat{\lambda}\right)\widehat{\mu}$ in (2.45), we obtain:

$$\begin{aligned} &\int_{\Gamma_0}\widehat{v}_2\left(u\left(\widehat{\lambda}\right),\widehat{\lambda}\right)\frac{\partial\widehat{v}_2}{\partial u}\left(u\left(\widehat{\lambda}\right),\widehat{\lambda}\right)u'\left(\widehat{\lambda}\right)\widehat{\mu}\,d\widehat{\sigma} \\ &= \widehat{a}_F\left(u,\frac{\partial\widehat{v}}{\partial u}\left(u\left(\widehat{\lambda}\right),\widehat{\lambda}\right)u'\left(\widehat{\lambda}\right)\widehat{\mu},\widehat{z}\right)+\widehat{b}_F\left(u,\frac{\partial\widehat{v}}{\partial u}\left(u\left(\widehat{\lambda}\right),\widehat{\lambda}\right)u'\left(\widehat{\lambda}\right)\widehat{\mu},\widehat{r}\right). \end{aligned}$$

Next, if we derive the equations (2.27) with respect to u, we obtain

$$\begin{aligned} &\frac{\partial\widehat{a}_F}{\partial u}\left(u,\widehat{v}\left(u,\widehat{\lambda}\right),\widehat{w}\right)\psi+\frac{\partial\widehat{a}_F}{\partial\widehat{v}}\left(u,\widehat{v}\left(u,\widehat{\lambda}\right),\widehat{w}\right)\frac{\partial\widehat{v}}{\partial u}\left(u,\widehat{\lambda}\right)\psi \\ &+\frac{\partial\widehat{b}_F}{\partial u}\left(u,\widehat{w},\widehat{p}\left(u,\widehat{\lambda}\right)\right)\psi+\frac{\partial\widehat{b}_F}{\partial\widehat{q}}\left(u,\widehat{w},\widehat{p}\left(u,\widehat{\lambda}\right)\right)\frac{\partial\widehat{p}}{\partial u}\left(u,\widehat{\lambda}\right)\psi \\ &=\int_{\Omega_0^F}\frac{\psi\left(\widehat{x}_1\right)}{H}f^F\cdot\widehat{w}\,d\widehat{x},\quad\forall\widehat{w}\in\widehat{W},\ \forall\psi\in U \end{aligned} \tag{2.47}$$

and $\forall\widehat{q}\in\widehat{Q}$, $\forall\psi\in U$ we have

$$\frac{\partial\widehat{b}_F}{\partial u}\left(u,\widehat{v}\left(u,\widehat{\lambda}\right),\widehat{q}\right)\psi+\frac{\partial\widehat{b}_F}{\partial\widehat{w}}\left(u,\widehat{v}\left(u,\widehat{\lambda}\right),\widehat{q}\right)\frac{\partial\widehat{v}}{\partial u}\left(u,\widehat{\lambda}\right)\psi=0. \tag{2.48}$$

Now, replacing $\widehat{w}$ by $\widehat{z}$ in (2.47), $\widehat{q}$ by $\widehat{r}$ in (2.48) and ψ by $A_S^{-1}C_S\widehat{\mu}$ in (2.47) and (2.48), we obtain

$$\begin{aligned} &\frac{\partial\widehat{a}_F}{\partial u}\left(u,\widehat{v}\left(u,\widehat{\lambda}\right),\widehat{z}\right)A_S^{-1}C_S\widehat{\mu}+\frac{\partial\widehat{a}_F}{\partial\widehat{v}}\left(u,\widehat{v}\left(u,\widehat{\lambda}\right),\widehat{z}\right)\frac{\partial\widehat{v}}{\partial u}\left(u,\widehat{\lambda}\right)A_S^{-1}C_S\widehat{\mu} \\ &+\frac{\partial\widehat{b}_F}{\partial u}\left(u,\widehat{z},\widehat{p}\left(u,\widehat{\lambda}\right)\right)A_S^{-1}C_S\widehat{\mu}+\frac{\partial\widehat{b}_F}{\partial\widehat{q}}\left(u,\widehat{z},\widehat{p}\left(u,\widehat{\lambda}\right)\right)\frac{\partial\widehat{p}}{\partial u}\left(u,\widehat{\lambda}\right)A_S^{-1}C_S\widehat{\mu} \\ &=\int_{\Omega_0^F}\frac{\left(A_S^{-1}C_S\widehat{\mu}\right)\left(\widehat{x}_1\right)}{H}f^F\cdot\widehat{z}\,d\widehat{x} \end{aligned} \tag{2.49}$$

and

$$\frac{\partial \widehat{b}_F}{\partial u}\left(u,\widehat{v}\left(u,\widehat{\lambda}\right),\widehat{r}\right)A_S^{-1}C_S\widehat{\mu}+\frac{\partial \widehat{b}_F}{\partial \widehat{w}}\left(u,\widehat{v}\left(u,\widehat{\lambda}\right),\widehat{r}\right)\frac{\partial \widehat{v}}{\partial u}\left(u,\widehat{\lambda}\right)A_S^{-1}C_S\widehat{\mu}=0. \tag{2.50}$$

But the following functions

$$\widehat{v}\mapsto \widehat{a}_F\left(u,\widehat{v},\widehat{z}\right),\quad \widehat{q}\mapsto \widehat{b}_F\left(u,\widehat{v},\widehat{q}\right),\quad \widehat{w}\mapsto \widehat{b}_F\left(u,\widehat{w},\widehat{r}\right)$$

are linear and continuous. Consequently, they are differentiable and we have

$$\begin{aligned}
&\frac{\partial \widehat{a}_F}{\partial \widehat{v}}\left(u,\widehat{v}\left(u,\widehat{\lambda}\right),\widehat{z}\right)\frac{\partial \widehat{v}}{\partial u}\left(u,\widehat{\lambda}\right)A_S^{-1}C_S\widehat{\mu}=\widehat{a}_F\left(u,\frac{\partial \widehat{v}}{\partial u}\left(u,\widehat{\lambda}\right)A_S^{-1}C_S\widehat{\mu},\widehat{z}\right)\\
&\frac{\partial \widehat{b}_F}{\partial \widehat{q}}\left(u,\widehat{v}\left(u,\widehat{\lambda}\right),\widehat{z}\right)\frac{\partial \widehat{p}}{\partial u}\left(u,\widehat{\lambda}\right)A_S^{-1}C_S\widehat{\mu}=\widehat{b}_F\left(u,\widehat{v}\left(u,\widehat{\lambda}\right),\frac{\partial \widehat{p}}{\partial u}\left(u,\widehat{\lambda}\right)A_S^{-1}C_S\widehat{\mu}\right)\\
&\frac{\partial \widehat{b}_F}{\partial \widehat{w}}\left(u,\widehat{v}\left(u,\widehat{\lambda}\right),\widehat{r}\right)\frac{\partial \widehat{v}}{\partial u}\left(u,\widehat{\lambda}\right)A_S^{-1}C_S\widehat{\mu}=\widehat{b}_F\left(u,\frac{\partial \widehat{v}}{\partial u}\left(u,\widehat{\lambda}\right)A_S^{-1}C_S\widehat{\mu},\widehat{r}\right).
\end{aligned} \tag{2.51}$$

So, the identity (2.49) could be rewritten as follows

$$\begin{aligned}
&\frac{\partial \widehat{a}_F}{\partial u}\left(u,\widehat{v}\left(u,\widehat{\lambda}\right),\widehat{z}\right)A_S^{-1}C_S\widehat{\mu}+\widehat{a}_F\left(u,\frac{\partial \widehat{v}}{\partial u}\left(u,\widehat{\lambda}\right)A_S^{-1}C_S\widehat{\mu},\widehat{z}\right)\\
&+\frac{\partial \widehat{b}_F}{\partial u}\left(u,\widehat{z},\widehat{p}\left(u,\widehat{\lambda}\right)\right)A_S^{-1}C_S\widehat{\mu}+\widehat{b}_F\left(u,\widehat{v}\left(u,\widehat{\lambda}\right),\frac{\partial \widehat{p}}{\partial u}\left(u,\widehat{\lambda}\right)A_S^{-1}C_S\widehat{\mu}\right)\\
&=\int_{\Omega_0^F}\frac{\left(A_S^{-1}C_S\widehat{\mu}\right)\left(\widehat{x}_1\right)}{H}f^F\cdot\widehat{z}\,d\widehat{x}.
\end{aligned}$$

Since $\widehat{b}_F\left(u,\widehat{v}\left(u,\widehat{\lambda}\right),\widehat{q}\right)=0$ for all $\widehat{q}$, it follows that

$$\begin{aligned}
&\frac{\partial \widehat{a}_F}{\partial u}\left(u,\widehat{v}\left(u,\widehat{\lambda}\right),\widehat{z}\right)A_S^{-1}C_S\widehat{\mu}+\frac{\partial \widehat{b}_F}{\partial u}\left(u,\widehat{z},\widehat{p}\left(u,\widehat{\lambda}\right)\right)A_S^{-1}C_S\widehat{\mu}\\
&-\int_{\Omega_0^F}\frac{\left(A_S^{-1}C_S\widehat{\mu}\right)(\widehat{x}_1)}{H}f^F\cdot\widehat{z}\,d\widehat{x}=-\widehat{a}_F\left(u,\frac{\partial \widehat{v}}{\partial u}\left(u,\widehat{\lambda}\right)A_S^{-1}C_S\widehat{\mu},\widehat{z}\right)\\
&=\widehat{a}_F\left(u,\frac{\partial \widehat{v}}{\partial u}\left(u,\widehat{\lambda}\right)u'\left(\widehat{\lambda}\right)\widehat{\mu},\widehat{z}\right).
\end{aligned}$$

Now, replacing the third equality of (2.51) in (2.50), we get

$$\begin{aligned}
\frac{\partial \widehat{b}_F}{\partial u}\left(u,\widehat{v}\left(u,\widehat{\lambda}\right),\widehat{r}\right)A_S^{-1}C_S\widehat{\mu} &= -\widehat{b}_F\left(u,\frac{\partial \widehat{v}}{\partial u}\left(u,\widehat{\lambda}\right)A_S^{-1}C_S\widehat{\mu},\widehat{r}\right)\\
&= \widehat{b}_F\left(u,\frac{\partial \widehat{v}}{\partial u}\left(u,\widehat{\lambda}\right)u'\left(\widehat{\lambda}\right)\widehat{\mu},\widehat{r}\right)
\end{aligned}$$

which completes the computation of the first term of the gradient, i.e.

$$\begin{aligned}
&\int_{\Gamma_0}\widehat{v}_2\left(u\left(\widehat{\lambda}\right),\widehat{\lambda}\right)\frac{\partial \widehat{v}_2}{\partial u}\left(u\left(\widehat{\lambda}\right),\widehat{\lambda}\right)u'\left(\widehat{\lambda}\right)\widehat{\mu}\,d\widehat{\sigma}\\
&=\left(\frac{\partial \widehat{a}_F}{\partial u}\left(u,\widehat{v},\widehat{z}\right)+\frac{\partial \widehat{b}_F}{\partial u}\left(u,\widehat{z},\widehat{p}\right)+\frac{\partial \widehat{b}_F}{\partial u}\left(u,\widehat{v},\widehat{r}\right)\right)A_S^{-1}C_S\widehat{\mu}\\
&-\int_{\Omega_0^F}\frac{\left(A_S^{-1}C_S\widehat{\mu}\right)(\widehat{x}_1)}{H}f^F\cdot\widehat{z}\,d\widehat{x}.
\end{aligned}$$

Our next goal is to compute the second term of the gradient.

The function

$$\widehat{\lambda} \mapsto \begin{pmatrix} \widehat{v}\left(u,\widehat{\lambda}\right) \\ \widehat{p}\left(u,\widehat{\lambda}\right) \end{pmatrix} = \begin{pmatrix} A_F(u) & B_F^*(u) \\ B_F(u) & 0 \end{pmatrix}^{-1} \begin{pmatrix} C_F\widehat{\lambda} \\ 0 \end{pmatrix}$$

is linear and continuous, therefore it is differentiable. Moreover, we have

$$\begin{pmatrix} \frac{\partial \widehat{v}}{\partial \widehat{\lambda}}\left(u,\widehat{\lambda}\right)\widehat{\mu} \\ \frac{\partial \widehat{p}}{\partial \widehat{\lambda}}\left(u,\widehat{\lambda}\right)\widehat{\mu} \end{pmatrix} = \begin{pmatrix} A_F(u) & B_F^*(u) \\ B_F(u) & 0 \end{pmatrix}^{-1} \begin{pmatrix} C_F\widehat{\mu} \\ 0 \end{pmatrix}.$$

So, we can compute $\frac{\partial \widehat{v}_2}{\partial \widehat{\lambda}}\left(u,\widehat{\lambda}\right)\widehat{\mu}$ by solving a Stokes problem which permits to compute numerically the second term of the gradient and the proof is complete. □

2.9 Approximation and numerical results

In this Section we present a practical application of the optimal control algorithm presented in Section 2.6, having in view the computation of cost function gradient. For this, we propose particular numerical approximation methods.

Let $\phi_i \in L^2(0,L)$ be some particular given functions and let $\alpha_i \in \mathbb{R}$ be the discret controls to be identified, $1 \leq i \leq m$.

From the Proposition 2.2, *ii*) there exist $u_0 \in U$ such that $\int_0^L u_0\, dx_1 = 0$ and $c_0 \in \mathbb{R}$ solutions of (2.13) and $u_i \in U$ such that $\int_0^L u_i\, dx_1 = 0$ and $c_i \in \mathbb{R}$ solutions of

$$a_S(u_i,\psi) = \int_0^L (\phi_i(x_1) + c_i)\,\psi(x_1)\, dx_1 \quad \forall \psi \in U. \tag{2.52}$$

It was not necessary to have $\int_0^L \phi_i(x_1)\, dx_1 = 0$.

We take $\widehat{\lambda}(x_1,H) = -c_0 + \sum_{i=1}^m \alpha_i(-\phi_i(x_1) - c_i)$ in the equation (2.43) and we obtain the displacement $u = u_0 + \sum_{i=1}^m \alpha_i u_i$ such that $\int_0^L u\, dx_1 = 0$. In other words, $\widehat{\lambda}(x_1,H) = -c_0 + \sum_{i=1}^m \alpha_i(-\phi_i(x_1) - c_i)$ is an admissible control if and only if the displacement $u = u_0 + \sum_{i=1}^m \alpha_i u_i$ verifies the condition (2.4).

With the notation

$$\mathcal{J}(\alpha_1,\ldots,\alpha_m) = j\left(-c_0 + \sum_{i=1}^m \alpha_i(-\phi_i(x_1) - c_i)\right)$$

we have

$$\frac{\partial \mathcal{J}}{\partial \alpha_k}(\alpha_1,\ldots,\alpha_m) = j'\left(\widehat{\lambda} = -c_0 + \sum_{i=1}^{m}\alpha_i\left(-\phi_i\left(\widehat{x}_1\right) - c_i\right)\right)\left(-\phi_k - c_k\right)$$

$$= -\frac{\partial \widehat{a}_F}{\partial u}\left(u,\widehat{v},\widehat{z}\right)u_k - \frac{\partial \widehat{b}_F}{\partial u}\left(u,\widehat{z},\widehat{p}\right)u_k - \frac{\partial \widehat{b}_F}{\partial u}\left(u,\widehat{v},\widehat{r}\right)u_k$$
$$+\int_{\Omega_0^F}\frac{u_k\left(\widehat{x}_1\right)}{H}f^F\cdot\widehat{z}\,d\widehat{x} + \int_{\Gamma_0}\widehat{v}_2\frac{\partial \widehat{v}_2}{\partial \widehat{\lambda}}\left(u,\widehat{\lambda}\right)\left(-\phi_k - c_k\right)\,d\widehat{\sigma},$$

where $\widehat{v}$ and $\widehat{p}$ is the solution of (2.44), $\widehat{z}$ and $\widehat{r}$ is the solution of (2.45) and $\frac{\partial \widehat{v}_2}{\partial \widehat{\lambda}}\left(u,\widehat{\lambda}\right)\left(-\phi_k - c_k\right)$ is the solution of (2.46) for $\widehat{\mu} = -\phi_k - c_k$.

The problems (2.44), (2.45) and (2.46) represent weak forms of different Stokes equations written in the reference domain Ω_0^F. We know that (2.44), for example, is equivalent to (2.18) which represents a weak form of a Stokes equation written in the real domain Ω_u^F. For the approximation by Finite Elements Method, it is better to use (2.18) instead of (2.44), because there exists a large literature concerning mixed form of Stokes equations, see for example the standard works [19] and [6].

The function $\mathcal{J}$ is not defined in whole $\mathbb{R}^m$, but only for $\alpha = (\alpha_1,\ldots,\alpha_m)$ such that the displacement $u = u_0 + \sum_{i=1}^{m}\alpha_i u_i$ verifies the condition (2.4). If we ignore for the moment this constraint, so that we can use quasi-Newton methods like Broyden, Fletcher, Goldfarb, Shanno (BFGS) or Davidon, Fletcher, Powell (DFP) algorithms for the minimization problem without constraints

$$\inf \mathcal{J}(\alpha_1,\ldots,\alpha_m).$$

Constrained minimization algorithms like projected or penalization techniques can also be used.

Among the wide variety of possible applications of the here presented control approach of fluid-structure problems, we are interested in simulating the blood flow through medium vessels (arteries). The computation has been made in a domain of length $L = 3\ cm$ and height $H = 0.5\ cm$ which represents a half width of the vessel. In this case, the fluid is the blood and the structure is the wall of the vessel.

The numerical values of the following physical parameters have been taken from [17]. The viscosity of the blood was taken to be $\mu = 0.035\ \frac{g}{cm\cdot s}$, its density $\rho^F = 1\ \frac{g}{cm^3}$. The thickness of the vessel is $h = 0.1\ cm$, the Young modulus $E = 0.75\cdot 10^6\ \frac{g}{cm\cdot s^2}$, the density $\rho^S = 1.1\ \frac{g}{cm^3}$.

The gravitational acceleration is $g_0 = 981\ \frac{cm}{s^2}$ and the averaged volume force of the structure is $f^S(x_1) = -g_0\rho^S h$.

On the rigid boundary, we impose the following boundary conditions:

$$\begin{aligned} v_1(x_1,x_2) &= \begin{cases} \left(1-\frac{x_2^2}{H^2}\right)V_0, & (x_1,x_2)\in\Sigma_1\cup\Sigma_3 \\ V_0, & (x_1,x_2)\in\Sigma_2 \end{cases} \\ v_2(x_1,x_2) &= 0, \quad (x_1,x_2)\in\Sigma \end{aligned}$$

where $V_0 = 30\ \frac{cm}{s}$.[39] The volume force in fluid is $\mathbf{f}^F = (0, -g_0\rho^F)^T$. Imposing non-homogeneous Dirichlet boundary conditions for the velocity on the rigid boundary do not change the formula to compute the gradient of the cost function, excepting the space where we search the velocity $\widehat{v}$ in the problem (2.44).

Using the notations from the beginning of this section, we have $c_0 = g_0\rho^S h$ and $u_0 = 0$.

We take $m = 4$. Let $\xi_i = (i-1)L/(m-1)$ for $1 \leq i \leq m$. There exist ϕ_i polynomial functions of degree 3, such that $\phi_i(\xi_j) = \delta_{ij}$, where δ_{ij} is the Kronecker's symbol.

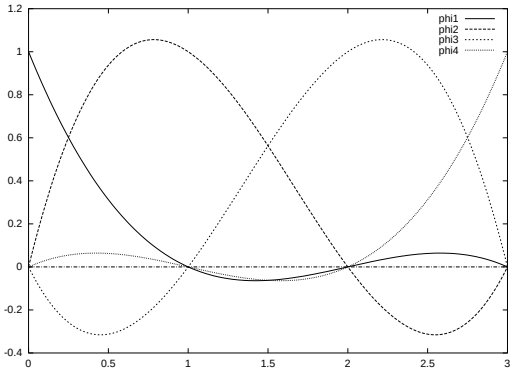

Figure 2.2: The shape functions ϕ_i for the approximation of the control

Let u_i, c_i be the solutions of (2.52). From the regularity of ϕ_i, we can use the following strong formulation in order to compute u_i, c_i:

$$\begin{aligned} EI\, u_i''''(x_1) &= \phi_i(x_1) + c_i,\ \forall x_1 \in (0, L) \\ u_i(0) &= u_i'(0) = 0, \\ u_i(L) &= u_i'(L) = 0 \\ \int_0^L u_i(x_1)\, dx_1 &= 0. \end{aligned}$$

We have computed u_i, c_i exactly, using the software *Mathematica*. The displacements u_i are polynomial functions of degree 7. We could use alternatively finite elements shape functions for ϕ_i, but in this case we should handle the weak formulation in order to compute u_i and c_i.

For the fluid we have used a Mixed Finite Elements Method, $P2$ Lagrange triangles for the velocity and $P1$ for the pressure [19], [6].

The numerical tests have been produced using *freefem++ v1.27*.[24] We have used the BFGS algorithm for the minimization problem with the starting point $\alpha = 0$ so that in the first five iterations the cost function takes the values presented in Table 1.

After 5 iterations we have obtained

$$(\alpha_1, \alpha_2, \alpha_3, \alpha_4) = (13.81347223,\ 2.81316723,\ -2.64008687,\ -13.98655258)$$

Iterations	$\mathcal{J}$
0	8.369704278
1	7.705856075
2	0.152977642
3	0.147957298
4	0.145206068
5	0.144683623

Table 2.1: The cost function history

and the gradient of the cost function was

$$\nabla\mathcal{J} = (0.000255,\ 0.004768,\ -0.020800,\ 0.009256)^T.$$

More iterations do not quantitatively change the values of α, the cost function and the solution. The relative change in successive values of α evaluated in the norm $\|\cdot\|_\infty$ is less than 0.02. The first four digits to the right of the decimal point of the cost function don't change after the fifth iteration. Ten iterations are required to achieve $\|\nabla\mathcal{J}\|_\infty \leq 10^{-6}$.

Notice that the condition (2.4) was not violated.

In order to compute $\nabla\mathcal{J}(\alpha)$, we have to solve the adjoint state problem (2.45) and m linear systems (2.46) which have the same matrix. The linear systems were solved by LU decomposition. We observe that (2.44) and (2.45) have the same left side, so when we compute $\nabla\mathcal{J}(\alpha)$ we can use the same LU decomposition obtained computing $\mathcal{J}(\alpha)$. If we compute $\nabla\mathcal{J}(\alpha)$ by the Finite Differences Method, we have to solve m linear systems, but the matrices are different because u changes, so using the analytic formula of the gradient is more advantageous.

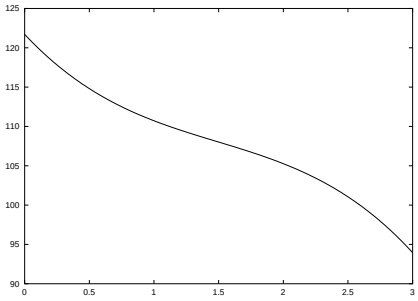

Figure 2.3: The applied stresses $-\widehat{\lambda} = c_0 + \sum_{i=1}^m \alpha_i\,(\phi_i + c_i)$ $[dyn/cm^2]$ on the interface

We have obtained $\left\|\widehat{\lambda} + \widehat{p}\right\|^2_{0,\Gamma_0} = 0.002878$, in other words, the vertical component of the stresses exerced by the fluid on the interface depends on the pressure only, $-\widehat{\lambda} \approx$

$\widehat{p}_{|\Gamma_0}$. This is justified by the following result [34]: if $\mathbf{v} \in \left(H^2\left(\Omega_u^F\right)\right)^2$, $p \in H^1\left(\Omega_u^F\right)$, $\mathbf{v}$ is constant on Γ_u, div $\mathbf{v} = 0$ in Ω_u^F, then $-\left(\sigma^F \mathbf{n}\right) \cdot \mathbf{n} = p$ on Γ_u. In our case $-\left(\sigma^F \mathbf{n}\right) \cdot e_2 = -\lambda$ and $\mathbf{n} \approx e_2$.

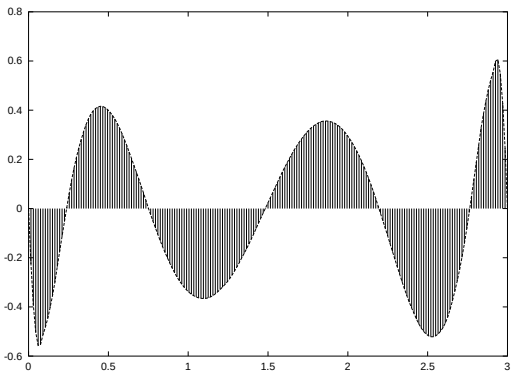

Figure 2.4: The velocity $[cm/s]$ on the boundary Γ_0

As we see in Figure 2.4, the velocity on the boundary Γ_0 is not null, but the maximum of the absolute value is less than 0.6 cm/s.

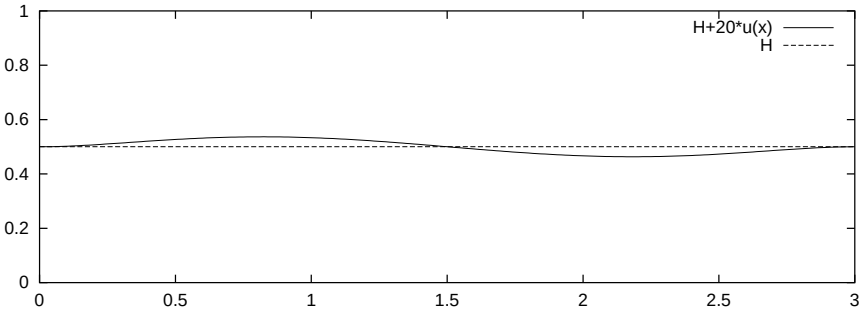

Figure 2.5: The displacement $[cm]$ of the vessel magnified by a factor 20

The displacement of the vessel is very small, it is less than 0.04 cm (see Figure 2.5). The pressure on the interface $\widehat{p}$ is almost the same as $-\widehat{\lambda}$, so it decreases from the inflow (left) to the outflow (right). The displacement of the interface is consequent with the pressure: the displacement of the vessel wall is outwards at the left and inwards at the right.

The computed velocity distribution is similar to a Poiseuille flow (see Figure 2.6).

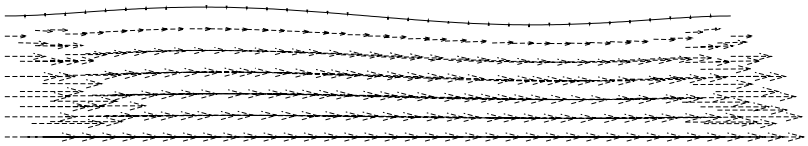

Figure 2.6: The velocity $[cm/s]$ reduced by a factor 100

2.10 Conclusions

In this work, a particular fluid-structure interaction model is formulated as an optimal control problem.

The optimal control setting allows to solve numerically the fluid-structure interaction problem (which is *a priori* a coupled problem) by an iterative algorithm such that the fluid and the structure equations are solved separately at each iteration. Thus, existing software packages could be adapted to approximate the solution of all the intermediate problems appearing in the algorithm.

The differentiability of the cost function and the analytical expression for its gradient are obtained.

In order to perform a numerical method, the analytic expression for the gradient reveals very useful and accurate to apply classical descent methods. To solve numerically a problem arising from blood flow in arteries, we have used a quasi Newton method which employs the analytic gradient of the cost function and the approximation of the inverse Hessian is updated by the Broyden, Fletcher, Goldforb, Shano (BFGS) scheme. This algorithm is faster than fixed point with relaxation or block Newton methods.

We can adapt this technique to the unsteady coupled fluid-structure problems.

2.11 Appendices

2.11.1 Fréchet differentiability

Let $(X, \|\cdot\|_X)$, $(Y, \|\cdot\|_Y)$ and $(Z, \|\cdot\|_Z)$ be three normed spaces.

Definition 2.1 *We say that the function $f : X \to Y$ is **Fréchet differentiable at** $x \in X$, if there exists $f'(x) \in \mathcal{L}(X, Y)$ such that*

$$\lim_{h \to 0} \frac{\|f(x+h) - f(x) - f'(x)\, h\|_Y}{\|h\|_X} = 0$$

*The linear operator $f'(x)$ is called the **Fréchet derivative of** f **at** x.*

In the case when $X = \prod_{i=1}^{n} X_i$, we denote by $\frac{\partial f}{\partial x_i}(x) \in \mathcal{L}(X_i, Y)$ the **Fréchet partial derivative of f with respect to x_i at $x \in X$.**

Theorem 2.2 *Let $f : X = \prod_{i=1}^{n} X_i \to Y$ be a function and let x^0 be an element of X. We assume that there exists V a neighborhood of x^0, such that $\frac{\partial f}{\partial x_i}$ exists on V and its are continuous in x^0.*

Then f is Fréchet differentiable in x^0 and

$$f'\left(x^0\right) h = \sum_{i=1}^{n} \frac{\partial f}{\partial x_i}\left(x^0\right) h_i$$

for all $h = (h_1, \ldots, h_n) \in X$.

Theorem 2.3 *Let $h : X \to Z$ be the composition of two mappings $f : X \to Y$ and $g : Y \to Z$*

$$h = g \circ f$$

Assume that f is Fréchet Differentiable in x and g in $f(x)$, then h is Fréchet differentiable in x and

$$h'(x) = g'(f(x)) \circ f'(x).$$

2.11.2 Implicit Function Theorem

We begin by recalling the Implicit Function Theorem. The proof of this result could be found in [25] for example.

Theorem 2.4 (The Implicit Function Theorem) *Let $(X, \|\cdot\|_X)$, $(Y, \|\cdot\|_Y)$ and $(Z, \|\cdot\|_Z)$ be normed spaces. We suppose that h is a mapping from an open subset G of $X \times Y$ into Z.*

Suppose (x_0, y_0) is a point in G and h is continuous in (x_0, y_0) such that:

i) $h(x_0, y_0) = 0$,

ii) *$\frac{\partial h}{\partial y}$ exists on G and it is continuous in (x_0, y_0),*

iii) *$\frac{\partial h}{\partial y}(x_0, y_0)$ is invertible and $\left(\frac{\partial h}{\partial y}(x_0, y_0)\right)^{-1}$ is continuous.*

Then there exists a neighborhood V of x_0 and a function $\theta : V \to Z$ such that:

iv) $\theta(x_0) = y_0$,

v) $h(x, \theta(x)) = 0$ *for all x in V,*

vi) *θ is continuous in x_0.*

Remark 2.5 *If h is continuous on G, then θ is continuous in a neighborhood of x_0.*

Remark 2.6 *In the case when X, Y and Z are Banach spaces, if $\frac{\partial h}{\partial y}(x_0, y_0) \in \mathcal{L}(Y, Z)$ is invertible, from the Open Mapping Theorem we have that $\left(\frac{\partial h}{\partial y}(x_0, y_0)\right)^{-1}$ is continuous.*

Theorem 2.5 (The differentiability of the implicit funtion) *Moreover, if there exists $\frac{\partial h}{\partial x}$ on G continuous in (x_0, y_0), then the implicit function θ is Fréchet differentiable in x_0 and*

$$\theta'(x_0) = -\left(\frac{\partial h}{\partial y}(x_0, y_0)\right)^{-1} \frac{\partial h}{\partial x}(x_0, y_0).$$

2.11.3 Integrals with parameter

Let U be a Hilbert space and let $\widehat{\Omega}$ be a compact set of $\mathbb{R}^2$.

Theorem 2.6 (continuity of integrals with parameter) *Let f be a function from $U \times \widehat{\Omega}$ to $\mathbb{R}$ such that for all $u \in U$ the function*

$$\widehat{x} \in \widehat{\Omega} \longmapsto f(u, \widehat{x})$$

is Lebesgue integrable.

Let $\overline{u}$ be an element of U such that $f(u, \widehat{x})$ converges to $f(\overline{u}, \widehat{x})$ uniformly with respect to $\widehat{x}$, when u converges to $\overline{u}$.

Then

$$\lim_{u \to \overline{u}} \int_{\widehat{\Omega}} f(u, \widehat{x})\, d\widehat{x} = \int_{\widehat{\Omega}} f(\overline{u}, \widehat{x})\, d\widehat{x}.$$

Theorem 2.7 (differentiability of integrals with parameter) *Moreover, we assume that:*

a) *for all $u \in U$ and for all $\widehat{x} \in \widehat{\Omega}$, the Fréchet derivative*

$$\frac{\partial f}{\partial u}(u, \widehat{x}) \in U'$$

exists,

b) *the functions*

$$\widehat{x} \in \widehat{\Omega} \longmapsto \frac{\partial f}{\partial u}(u, \widehat{x})\, \psi \in \mathbb{R}$$

are Lebesgue integrable for all $\psi \in U$,

c) $\frac{\partial f}{\partial u}(u, \widehat{x})$ *converges in* U' *to* $\frac{\partial f}{\partial u}(\overline{u}, \widehat{x})$ *uniformly with respect to* $\widehat{x}$*, when* u *converges to* $\overline{u}$*.*

Then, the function F *from* U *to* $\mathbb{R}$*, defined by*

$$F(u) = \int_{\widehat{\Omega}} f(u, \widehat{x})\, d\widehat{x}$$

is Fréchet differentiable in $\overline{u}$ *and*

$$F'(\overline{u})\,\psi = \int_{\widehat{\Omega}} \frac{\partial f}{\partial u}(\overline{u}, \widehat{x})\,\psi d\widehat{x}$$

for all $\psi \in U$*.*

Acknowledgments

This work has been partially supported by the Research Projects of Xunta de Galicia (PGIDIT-02-PXIC-10503-PN) and D.G.E.S. (BFM2001-3261-CO2-02). Moreover the author C.M. Murea has been granted by Xunta de Galicia to have a post of "Profesor Visitante" at the University of La Coruna. The authors are very gratefull to the anonymous referee whose questions and comments have contributed to improve the contents of this paper.

Bibliography

[1] Adams R. (1975) Sobolev spaces, Academic Press

[2] Bayada G., Chambat M., Cid B., Vazquez C. (2004) On the existence of solution for a non-homogeneus Stokes-rod coupled problem, Nonlinear Analysis: Theory, Methods and Applications, 59:1-19

[3] Bayada G., Durany J., Vázquez C. (1995) Existence of a Solution for a Lubrication Problem in Elastic Journal Bearings with Thin Bearing, Math. Meth. Appl. Sci. 18:455–466

[4] Beirao da Veiga H. (2004) On the existence of strong solution to a coupled fluid-structure evolution problem, J. Math. Fluid Mech. 6:21–52

[5] Bernardou M. (1987) Formulation variationnelle, approximation et implementation de problèmes de barres et de poutre bi-et tri-dimensionnelles., Partie A: barres et de poutre tri-dimensionnelles, Rapport de Recherche INRIA, no. 731

[6] Brezzi F., Fortin M. (1991) Mixed and Hybrid Finite Element Methods, Springer Verlag

[7] Céa J. (1986) Conception optimale ou identification de formes: calcul rapide de la dérivée directionnelle de la fonction coût, RAIRO Model. Math. Anal. Numer. 20(3):371–402

[8] Chen H., Sheu T. (2003) Finite-element simulation of incompressible fluid flow in an elastic vessel, Int. J. Numer. Meth. Fluids 42:131–146

[9] Chenais D., Monnier J., Vila J.P. (2001) Shape optimal design problem with convective and radiative heat transfer: analysis and implementation, J. Optim. Theory Appl. 110(1):75–117

[10] Dautray R., Lions J.L. (1988) Analyse mathématique et calcul numérique pour les sciences et les techniques, vol. 3,4, Masson

[11] Deparis S., Fernandez M.A., Formaggia L. (2003) Acceleration of a fixed point algorithm for fluid-structure interaction using transpiration conditions, M2AN Math. Model. Numer. Anal. 37(4):601–616

[12] Desjardins B., Esteban M. , Grandmont C., Le Tallec P. (2001) Weak solutions for a fluid-elastic structure interaction model, Rev. Mat. Complut. 14(2):523–538

[13] Farhat C., Lesoinne M. (2000) Two efficient staggered algorithms for the serial and parallel solution of three-dimensional nonlinear transient aeroelastic problems, Comput. Methods Appl. Mech. Engrg. 182(3-4):499–515

[14] Farhat C., Geuzaine Ph., Grandmont C. (2001) The discrete geometric conservation law and the nonlinear stability of ALE schemes for the solution of flow problems on moving grids, J. Comput. Phys. 174(2):669–694

[15] Fernandez M. A., Moubachir M. (2002) Sensitivity analysis for an incompressible aeroelastic system, Math. Models Methods Appl. Sci. 12(8):1109–1130

[16] Fernandez M. A., Moubachir M. (2003) An exact block-Newton algorithm for solving fluid-structure interaction problems, C. R. Math. Acad. Sci. Paris 336(8):681–686

[17] Formaggia L., Gerbeau J. F., Nobile F., Quarteroni A. (2001) On the coupling of 3D and 1D Navier-Stokes equations for flow problems in compliant vessels, Comput. Methods Appl. Mech. Engrg. 191(6-7):561–582

[18] Gerbeau J. F., Vidrascu M. (2003) A quasi-Newton algorithm on a reduced model for fluid - structure interaction problems in blood flows, M2AN Math. Model. Numer. Anal. 37(4):631–647

[19] Girault V., Raviart P.A. (1986) Finite Element Methods for Navier-Stokes Equations. Theory and Algorithms, Springer Verlag

[20] Gurtin M. E. (1981) An Introduction to Continuum Mechanics, Academic Press

[21] Grandmont C. (1998) Existence et unicité de solutions d'un problm̀e de couplage fluide-structure bidimensionnel stationnaire, C. R. Acad. Sci. Paris Sér. I Math. 326(5):651–656

[22] Grandmont C., Maday Y. (2000) Existence for an unsteady fluid-structure interaction problem, M2AN Math. Model. Numer. Anal. 34(3):609–636

[23] Grandmont C. (2002) Existence for a three-dimensional steady state fluid-structure interaction problem, J. Math. Fluid Mech. 4(1):76–94

[24] Hecht F., Pironneau O. (May 2003) A finite element software for PDE: freefem++, `http://www-rocq.inria.fr/Frederic.Hecht`

[25] Kantarovich C.V., Akilov G.P. (1964) Functional Analysis in Normed Spaces, McMillan

[26] Le Tallec P., Mouro J. (2001) Fluid-structure interaction with large structural displacements, Comput. Methods Appl. Mech. Engrg. 190(24-25):3039–3067

[27] Lewis R.M. (1997) A nonlinear programming perspective on sensitivity calculations for systems governed by state equations, NASA-ICASE Report no. 12

[28] Lions J.-L., Pironneau O. (2000) Virtual control, replicas and decomposition of operators, C. R. Acad. Sci. Paris Sér. I Math. 330(1):47–54

[29] Maday Y., Maury B., Metier P. (1999) Interaction de fluides potentiels avec une membrane élastique, in ESAIM Proc. 10, Soc. Math. Appl. Indust., Paris, pp. 23–33

[30] Morand H.J.-P., Ohayon R. (1995) Fluid-Structure Interaction, John Wiley

[31] Murat F., Simon J. (1976) Sur le contrôle par un domaine géométrique, Prépublication du Laboratoire d'Analyse Numérique, no. 74015, Université de Paris 6

[32] Murea C.M., Maday Y. (1996) Existence of an Optimal Control for a Nonlinear Fluid-Cable Interaction Problem, Rapport of research CEMRACS 96, C.I.R.M. Luminy, France

[33] Nobile F. (2001) Numerical approximation of fluid-structure interaction problems with application to haemodynamics, PhD, Ecole Polytechnique Féderale de Lausanne, Switzerland

[34] Osses A. (2001) A rotated multiplier applied to the controllability of waves, elasticity and tangential Stokes control, SIAM J. Control Optim. 40(3):777–800

[35] Piperno S., Farhat C., Larrouturou B. (1995) Partitioned procedures for the transient solution of coupled aeroelastic problems. I. Model problem, theory and two-dimensional application, Comput. Methods Appl. Mech. Engrg. 124:79–112

[36] Piperno S., Farhat C., Larrouturou B. (2001) Partitioned procedures for the transient solution of coupled aeroelastic problems. II. Energy transfer analysis and three-dimensional application, Comput. Methods Appl. Mech. Engrg. 190:3147–3170

[37] Pironneau O. (1984) Optimal Shape Design for Elliptic Problems, Springer Verlag

[38] Quarteroni A., Formaggia L. (2003) Mathematical Modelling and Numerical Simulation of the Cardiovascular System, in Modelling of Living Systems, ed. N. Ayache, Handbook of Numerical Analysis Series, eds. P.G. Ciarlet and J.L. Lions, Elsevier

[39] Schmidt-Nielsen K. (1998) Physiologie animale. Adaptation et milieux de vie, Dunod

[40] Steindorf J., Matthies H.G. (2002) Partioned but strongly coupled iteration schemes for nonlinear fluid-structure interaction, Comput. & Structures, 80:1991–1999

[41] Tiba D. (1995) Lectures on Optimal Control of Elliptic Equations, University of Jyvaskyla

Chapter 3

The BFGS algorithm for a nonlinear least squares problem arising from blood flow in arteries

This chapter is based on the paper:

C.M. Murea, The BFGS algorithm for a nonlinear least squares problem arising from blood flow in arteries, *Comput. Math. Appl.*, **49** (2005), 171–186.

Abstract. Using the Arbitrary Lagrangian Eulerian coordinates and the Least Squares Method, a two dimensional steady fluid structure interaction problem is transformed in an optimal control problem. Sensitivity analysis is presented. The BFGS algorithm gives satisfactory numerical results even when we use a reduced number of discrete controls.

3.1 Introduction

In this paper we consider a two dimensional fluid structure interaction. The mathematical model which governs the fluid is the steady Stokes equations, while the structure verifies the beam equation which does not involve shearing stress. The solution of the model is given by the displacement of the structure, the velocity and the pressure of the fluid. The boundary of the fluid admits the following decomposition: a moving part, which represents the interface between the fluid and the structure, and a rigid part. This kind of problem is of considerable interest in the simulation of blood flow in large arteries (see [1], [2], [3]) or in aeroelasticity (see [4]).

The existence results for the fluid structure interaction can be found in [5], [6] for the steady case and in [7], [8], [9] for the unsteady case.

Sensitivity analysis of a coupled fluid structure system was investigated in [10].

The asymptotic limit when the fluid domain width approaches to zero can be modeled by a one dimensional model of Stokes equation, widely used in lubrication theory (see [11]).

In a previous work ([12]), a three dimensional fluid structure interaction was formulated as an optimal control system, where the control is the force acting on the interface and the observation is the velocity of the fluid on the interface. The fluid equations were solved taking into account a given surface force on the interface.

A similar approach was used in [13], where it was proved that the cost function is differentiable. The analytic computation of the gradient for the cost function is important because it enables us to apply accurate numerical methods (see [14]). The exact gradient of the cost function is computed in [13].

Numerical results for a two dimensional fluid structure interaction using the optimal control method are presented in [15]. The fluid equations are solved subject to the conditions of zero normal velocity and a given value of pressure on the interface. The control is the value of the pressure at the interface and the observation is the tangential velocity on the interface.

The most frequently, the fluid-structure interaction problems are solved numerically by partitioned procedures, i.e. the fluid and the structure equations are solved separately, which enables us to use the existing solvers for each sub-problem.

This can be done using fixed point strategies with eventually a relaxation parameter, but these methods do not always converge or they have slow convergence rate [16], [17], [1]. The convergence can be accelerated using Aitken's method [2] or transpiration condition [18].

Other way to accelerate the convergence is to use methods which employ the derivative. In [19] a block Newton algorithm was used where the derivative of the operators are approached by finite differences. Good convergence rate was obtained in [2] where the derivative of the operator was replaced by a simpler operator. At each time step, a quasi-Newton algorithm was used to solve a fluid-structure interaction problem. The mean number of iterations of the quasi-Newton algorithm is 6.1. With the Aitken acceleration method this number is 24.1. At each iteration, a Stokes and a Laplacian problems were solved in the current fluid domain.

In the present work, a fluid structure interaction problem was formulated as an optimal control system, where the control is the force acting on the interface and the observation is the pressure on the interface. The boundary condition to be imposed on the fluid is that all components of the velocity are zero at the interface.

To solve numerically the optimal control problem, we use a quasi Newton method which employs the analytic gradient of the cost function and the approximation of the inverse Hessian is updated by the Broyden, Fletcher, Goldforb, Shano (BFGS) scheme. This algorithm is faster than fixed point with relaxation or block Newton methods which represents the main advantage of using the optimal control approach for fluid-structure interaction problem. The finite element functions of the normal stresses at the interface

are not necessary the same as the trace on the interface of the pressure finite element functions. This is another advantage by comparison with the fixed point approach.

An outline of the paper is as follows. First, we prove that the normal force acting on the structure depends only on the pressure. Then, an exact solution for a particular fluid structure interaction is given. Using the Least Square Method, the fluid structure interaction will be reformulated as an optimal control problem. We will analyse the dependence of the displacement of the interface, the velocity, the pressure of the fluid and the cost function on variations of the discrete control. Finally, numerical results are presented.

3.2 Notations

Let L and H be two positive constants. We define the set

$$\begin{aligned}\mathcal{U}_{ad} &= \{u \in \mathcal{C}^1([0,L]);\, u(0) = u(L) = u'(0) = u'(L) = 0,\\ &\quad \int_0^L u(x_1)\,dx_1 = 0,\ \inf_{x_1\in[0,L]}\{H + u(x_1)\} > 0\Big\}\end{aligned}$$

where u' is the first derivative of u.

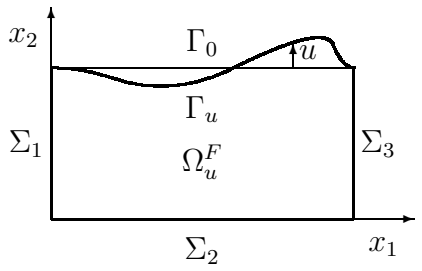

Figure 3.1: Sets appearing in the fluid-structure problem

For each $u \in \mathcal{U}_{ad}$, we introduce the notations (see Figure 3.1)

$$\begin{aligned}\Omega_u^F &= \{(x_1,x_2) \in \mathbb{R}^2;\, x_1 \in (0,L),\, 0 < x_2 < H + u(x_1)\},\\ \Gamma_u &= \{(x_1,x_2) \in \mathbb{R}^2;\, x_1 \in (0,L),\, x_2 = H + u(x_1)\}.\end{aligned}$$

Also, we denote

$$\begin{aligned}\Sigma_1 &= \big\{(0,x_2) \in \mathbb{R}^2;\, x_2 \in (0,H)\big\}\\ \Sigma_2 &= \big\{(x_1,0) \in \mathbb{R}^2;\, x_1 \in (0,L)\big\}\\ \Sigma_3 &= \big\{(L,x_2) \in \mathbb{R}^2;\, x_2 \in (0,H)\big\}.\end{aligned}$$

The two-dimensional domain occupied by the fluid is Ω_u^F, the interface between the fluid and the structure is Γ_u, while $\Sigma = \Sigma_1 \cup \overline{\Sigma}_2 \cup \Sigma_3$ represents the rigid boundary of the fluid.

In the following, we denote by $\mathbf{n} = (n_1, n_2)^T$ the unit outward normal vector and by $\tau = (\tau_1, \tau_2)^T = (-n_2, n_1)^T$ the unit tangential vector to $\partial\Omega_u^F$.

3.3 Position of the problem

We suppose that the fluid is governed by the steady Stokes equations, while the deformation of the elastic part of the boundary verifies a particular beam equation which does not involve shearing stress (see [20]). We consider that the structure is a beam of axis parallel to Ox_1 with constant thickness h. We assume that the displacement of the beam is normal to its axis.

The problem is to find:

- $u : [0, L] \to \mathbb{R}$ the displacement of the structure,
- $\mathbf{v} = (v_1, v_2)^T : \Omega_u^F \to \mathbb{R}^2$ the velocity of the fluid and
- $p : \Omega_u^F \to \mathbb{R}$ the pressure of the fluid,

such that

$$u''''(x_1) = \frac{1}{D}\left(f^S(x_1) + p\left(x_1, H + u(x_1)\right)\right), \quad \forall x_1 \in (0, L) \tag{3.1}$$

$$u(0) = u(L) = u'(0) = u'(L) = 0 \tag{3.2}$$

$$\int_0^L u(x_1)\, dx_1 = 0 \tag{3.3}$$

$$0 < \inf_{x_1 \in [0,L]} \{H + u(x_1)\} \tag{3.4}$$

$$-\mu\Delta\mathbf{v} + \nabla p = \mathbf{f}^F, \quad in\ \Omega_u^F \tag{3.5}$$

$$\text{div}\ \mathbf{v} = 0, \quad in\ \Omega_u^F \tag{3.6}$$

$$\mathbf{v} = \mathbf{g}, \quad on\ \Sigma \tag{3.7}$$

$$\mathbf{v} = 0, \quad on\ \Gamma_u \tag{3.8}$$

where

- $D = \frac{Eh^3}{12}$ is a structure constant, E is the Young modulus, h is the thickness.
- $f^S : (0, L) \to \mathbb{R}$ are the averaged volume forces of the structure, in general the gravity forces and in this case we have $f^S(x_1) = -g_0\rho^S h$, where g_0 is the gravity, ρ^S is the density of the structure,

- $\mu > 0$ is the viscosity of the fluid,
- $\mathbf{f}^F = (f_1^F, f_2^F)^T : \Omega_u^F \to \mathbb{R}^2$ are the volume forces of the fluid, in general the gravity forces,
- $\mathbf{g} = (g_1, g_2)^T : \Sigma \to \mathbb{R}^2$ is the imposed velocity profile of the fluid on the rigid boundary, such that

$$\int_\Sigma \mathbf{g} \cdot \mathbf{n} \, d\sigma = 0. \tag{3.9}$$

The incompressibility of the fluid (3.6) together with the boundary conditions (3.7), (3.8) and the relation (3.9) imply that the volume of the fluid is conserved or equivalently $\int_0^L u(x_1)\, dx_1$ is constant. Without loss of generality, we assume that this constant is zero and we obtain the condition (3.3).

The inequality (3.4) states that the fluid domain is connected.

For the Newtonian fluids, the stress tensor σ has the form

$$\sigma = -p\, I + \mu \left(\nabla \mathbf{v} + \nabla \mathbf{v}^T \right),$$

consequently, the fluid forces acting on the structure are $-\sigma \mathbf{n}$.

Proposition 3.1 *If* $\mathbf{v} \in \left(H^2\left(\Omega_u^F\right)\right)^2$, $p \in H^1\left(\Omega_u^F\right)$, $\mathbf{v}$ *is constant on* Γ_u, div $\mathbf{v} = 0$ *in* Ω_u^F, *then* $-(\sigma \mathbf{n}) \cdot \mathbf{n} = p$ *on* Γ_u.

Proof. This result is a corollary of the Proposition 3.1 from [21] and it is similar to the Proposition 4.5 from the same paper. We have that

$$-(\sigma \mathbf{n}) \cdot \mathbf{n} = p - \mu \left(\left(\nabla \mathbf{v} + \nabla \mathbf{v}^T \right) \mathbf{n} \right) \cdot \mathbf{n}$$

and

$$\nabla \mathbf{v} + \nabla \mathbf{v}^T = \begin{pmatrix} 2\frac{\partial v_1}{\partial x_1} & \frac{\partial v_1}{\partial x_2} + \frac{\partial v_2}{\partial x_1} \\ \frac{\partial v_1}{\partial x_2} + \frac{\partial v_2}{\partial x_1} & 2\frac{\partial v_2}{\partial x_2} \end{pmatrix}.$$

It is follows that

$$\left(\left(\nabla \mathbf{v} + \nabla \mathbf{v}^T \right) \mathbf{n} \right) \cdot \mathbf{n} = 2\frac{\partial v_1}{\partial x_1} n_1^2 + 2\left(\frac{\partial v_1}{\partial x_2} + \frac{\partial v_2}{\partial x_1} \right) n_1 n_2 + 2\frac{\partial v_2}{\partial x_2} n_2^2.$$

In Proposition 3.1 from [21], it is proved that $\frac{\partial v_i}{\partial x_j} n_k = \frac{\partial v_i}{\partial x_k} n_j$, $\forall i, j, k \in \{1, 2\}$, so $\left(\frac{\partial v_1}{\partial x_2} + \frac{\partial v_2}{\partial x_1} \right) n_1 n_2 = \frac{\partial v_1}{\partial x_1} n_2^2 + \frac{\partial v_2}{\partial x_2} n_1^2$ and this implies that

$$\left(\left(\nabla \mathbf{v} + \nabla \mathbf{v}^T \right) \mathbf{n} \right) \cdot \mathbf{n} = 2\frac{\partial v_1}{\partial x_1} \left(n_1^2 + n_2^2 \right) + 2\frac{\partial v_2}{\partial x_2} \left(n_1^2 + n_2^2 \right) = 2 \,\text{div}\, \mathbf{v} = 0$$

which ends the proof. □

Under the assumption of small displacement of the beam, it follows that $\mathbf{n} \approx (0, 1)^T$. Then, it is reasonable to solve the beam equation (3.1) under the fluid forces given by $p\left(x_1, H + u(x_1)\right)$, $x_1 \in (0, L)$.

3.4 Exact solution for a particular case

We assume that the density of the fluid is constant ρ^F and the volume forces in the fluid have the form $\mathbf{f}^F = (0, -\rho^F g_0)^T$, where g_0 is the gravitational acceleration. The velocity profile of the fluid on the rigid boundary is given by:

$$\begin{array}{rcl} g_1(x_1,x_2) & = & \begin{cases} \left(1-\frac{x_2^2}{H^2}\right)V_0, & (x_1,x_2)\in\Sigma_1\cup\Sigma_3 \\ V_0, & (x_1,x_2)\in\Sigma_2 \end{cases} \\ g_2(x_1,x_2) & = & 0, \quad (x_1,x_2)\in\Sigma. \end{array}$$

We assume that the density of the structure ρ^S and its thickness h are constant. We assume that the averaged volume forces in the structure have the form

$$f^S(x_1) = -\rho^S g_0\, h + \frac{2\mu V_0}{H^2}x_1, \quad \forall x_1\in(0,L). \tag{3.10}$$

Then, we have the following solution for the system (3.1)–(3.8):

$$\begin{array}{rcl} u(x_1) & = & 0, \quad \forall x_1\in(0,L) \\ v_1(x_1,x_2) & = & \left(1-\frac{x_2^2}{H^2}\right)V_0, \quad \forall (x_1,x_2)\in\Omega_u^F \\ v_2(x_1,x_2) & = & 0, \quad \forall (x_1,x_2)\in\Omega_u^F \\ p(x_1,x_2) & = & \rho^S g_0\, h - \frac{2\mu V_0}{H^2}x_1 + \rho^F g_0\,(H-x_2), \quad \forall (x_1,x_2)\in\Omega_u^F. \end{array}$$

Remark 3.1 *The term $\frac{2\mu V_0}{H^2}x_1$ in (3.10) is artificial. It was added to obtain a solution where the displacement of the beam is null and the flow is Poiseuille.*

3.5 Fixed point approach

We start with a result concerning the equations of the interface.

Proposition 3.2 *For a given continuous function $\eta : [0,L]\to\mathbb{R}$ there exist a unique function $u : [0,L]\to\mathbb{R}$ of class $\mathcal{C}^4$ and a unique constant $c\in\mathbb{R}$ solutions of*

$$u''''(x_1) = \frac{1}{D}\left(\eta(x_1)+c\right), \quad \forall x_1\in(0,L) \tag{3.11}$$

with boundary conditions (3.2), such that the equality (3.3) holds.

Proof. *Existence.* Let $u_\eta : [0,L]\to\mathbb{R}$ be the unique solution of

$$u''''(x_1) = \frac{1}{D}\eta(x_1), \quad \forall x_1\in(0,L)$$

with boundary conditions (3.2). The unique solution of

$$u''''(x_1) = \frac{1}{D}, \quad \forall x_1 \in (0, L)$$

with boundary conditions (3.2) is $x_1 \in [0, L] \mapsto \frac{x_1^2(x_1-L)^2}{24D} \in \mathbb{R}$.

Then, the solutions of (3.11) and (3.2) have the form

$$u(x_1) = u_\eta(x_1) + c\frac{x_1^2(x_1 - L)^2}{24D}.$$

The equality (3.3) is equivalent to

$$\int_0^L u_\eta(x_1)\, dx_1 + c \int_0^L \frac{x_1^2(x_1 - L)^2}{24D}\, dx_1 = 0$$

consequently, if we set

$$c = -\frac{720D}{L^5} \int_0^L u_\eta(x_1)\, dx_1,$$

then the condition (3.3) holds.

Uniqueness. Let u_i, c_i, $i = 1, 2$ be two solutions of (3.11), such that $\int_0^L u_i\, dx_1 = 0$. By subtracting, we obtain that

$$(u_1 - u_2)''''(x_1) = \frac{1}{D}(c_1 - c_2), \quad \forall x_1 \in (0, L)$$

and $u_1 - u_2$ verifies the boundary conditions (3.2). Consequently we have $(u_1 - u_2)(x_1) = (c_1 - c_2)\frac{x_1^2(x_1-L)^2}{24D}$. Since $\int_0^L (u_1 - u_2) dx_1 = 0$, we obtain $c_1 - c_2 = 0$ and $u_1 - u_2 = 0$. □

From the above Proposition, it follows that for a given continuous function $\lambda_0 : (0, L) \to \mathbb{R}$, such that $\int_0^L \lambda_0(x_1)\, dx_1 = 0$, we can solve the beam equations

$$u''''(x_1) = \frac{1}{D}\left(f^S(x_1) + \lambda_0(x_1) + c\right), \quad \forall x_1 \in (0, L) \tag{3.12}$$

with boundary conditions (3.2) where c is the real constant such that the equality (3.3) holds.

Let $\mathcal{S}$ be defined by

$$\mathcal{S}(\lambda_0) = u. \tag{3.13}$$

If $0 < \inf_{x_1 \in [0,L]} \{H + u(x_1)\}$, we can solve the Stokes equations (3.5)–(3.8) and we obtain v and p. The pressure is determined up to an additive constant, i.e. it has the form $p = p_0 + C$, where p_0 is a particular solution and C is a real constant. We will take p_0 such that $\int_0^L p_0(x_1, H + u(x_1))\, dx_1 = 0$.

We denote by $\mathcal{F}(u)$ the function

$$x_1 \in (0,L) \mapsto p_0\left(x_1, H + u(x_1)\right). \tag{3.14}$$

The function $\mathcal{F}(u)$ is well defined, if the trace of the pressure p_0 on Γ_u exits. For this, we have to precise the regularity of the solution of Stokes equations.

Let $\overline{\mathbf{g}} : \partial\Omega_u^F \to \mathbb{R}$ be defined by $\overline{\mathbf{g}}(\mathbf{x}) = 0$ for $\mathbf{x} \in \Gamma_u$ and $\overline{\mathbf{g}}(\mathbf{x}) = \mathbf{g}(\mathbf{x})$ for $\mathbf{x} \in \Sigma$.

If $\partial\Omega_u^F$ is Lipschitz continuous, Ω_u^F is a connected domain, $\mathbf{f}^F \in \left(H^{-1}\left(\Omega_u^F\right)\right)^2$, $\overline{\mathbf{g}} \in \left(H^{1/2}\left(\partial\Omega_u^F\right)\right)^2$ such that $\int_{\partial\Omega_u^F} \overline{\mathbf{g}} \cdot \mathbf{n}\, d\sigma = 0$, then the problem :
find $\mathbf{v} \in \left(H^1\left(\Omega_u^F\right)\right)^2$, $\mathbf{v} = \overline{\mathbf{g}}$ on $\partial\Omega_u^F$ and $p \in L^2\left(\Omega_u^F\right)/\mathbb{R}$

$$\left\{\begin{array}{lcll} \displaystyle\int_{\Omega_u^F} \nabla\mathbf{v} \cdot \nabla\mathbf{w}\, d\mathbf{x} - \int_{\Omega_u^F} (\text{div } \mathbf{w})\, p\, d\mathbf{x} & = & \displaystyle\int_{\Omega_u^F} \mathbf{f}^F \cdot \mathbf{w}\, d\mathbf{x}, & \forall \mathbf{w} \in \left(H_0^1\left(\Omega_u^F\right)\right)^2 \\ -\displaystyle\int_{\Omega_u^F} (\text{div } \mathbf{v})\, q\, d\mathbf{x} & = & 0, & \forall q \in L^2\left(\Omega_u^F\right)/\mathbb{R} \end{array}\right. \tag{3.15}$$

has a unique solution.

Moreover, if $\partial\Omega_u^F$ is of class $\mathcal{C}^2$, $\mathbf{f}^F \in \left(L^2\left(\Omega_u^F\right)\right)^2$ and $\overline{\mathbf{g}} \in \left(H^{3/2}\left(\partial\Omega_u^F\right)\right)^2$, then $\mathbf{v} \in \left(H^2\left(\Omega_u^F\right)\right)^2$ and $p \in H^1\left(\Omega_u^F\right)/\mathbb{R}$.

These results could be found in [22, p. 88].

The fixed point approach is to find λ_0 such that $\mathcal{F} \circ \mathcal{S}(\lambda_0) = \lambda_0$, where $\mathcal{S}$ and $\mathcal{F}$ are defined by (3.13) and (3.14).

The existence of a fixed point will not be treated here. It is important to note that if we want to apply the Schauder's fixed point theorem, the regularity of λ_0 and $\mathcal{F} \circ \mathcal{S}(\lambda_0)$ must be the same. It is not the case in our framework: for $\lambda_0 \in \mathcal{C}^0(0,L)$, we have $\mathcal{S}(\lambda_0) = u \in \mathcal{C}^4(0,L)$ and consequently $\mathcal{F}(u) \in H^{1/2}(0,L)$. It is known that $H^{1/2}(0,L)$ is not included in $\mathcal{C}^0(0,L)$, but $H^{1/2+\epsilon}(0,L) \subset \mathcal{C}^0(0,L)$ for $\epsilon > 0$. Existence results for related steady fluid-structure interaction problems can be found in [5] and [6].

In the following, we relax the fixed point problem by the Least Squares Method and we obtain an optimization problem.

3.6 Least Squares approach

Let $\phi_i : [0,L] \to \mathbb{R}$ be some particular given functions and α_i are the scalar parameters to be identified, $1 \leq i \leq m$.

Let us comment the regularity and the shape of ϕ_i. We take $\phi_i \in \mathcal{C}^0(0,L)$, the condition $\int_0^L \phi_i(x_1)dx_1 = 0$ is not necessary needed. Also, the functions ϕ_i are not necessary the same that the trace on the interface of the pressure finite element functions. This is an advantage by comparison with the fixed point approach.

For given $\alpha = (\alpha_1, \ldots, \alpha_m)$, we find $u : [0, L] \to \mathbb{R}$ and $c(\alpha) \in \mathbb{R}$ solutions of

$$u''''(x_1) = \frac{1}{D}\left(f^S(x_1) + \sum_{i=1}^{m} \alpha_i \phi_i(x_1) + c(\alpha)\right), \quad \forall x_1 \in (0, L) \tag{3.16}$$

with boundary conditions (3.2), such that (3.3) holds.

The next step is to solve the Stokes equations in the domain Ω_u^F and we obtain $\mathbf{v}$ and p. We assume that $p \in H^1\left(\Omega_u^F\right)$ and we set $p_0 = p - \frac{1}{L}\int_0^L p\left(x_1, H + u(x_1)\right) dx_1$. It follows that

$$\int_0^L p_0\left(x_1, H + u(x_1)\right) dx_1 = 0. \tag{3.17}$$

Let $J : \mathbb{R}^m \to \mathbb{R}$ be defined by

$$J(\alpha) = \int_0^L \left(\sum_{i=1}^{m} \alpha_i \left(\phi_i(x_1) - \frac{1}{L}\int_0^L \phi_i(x_1) dx_1\right) - p_0\left(x_1, H + u(x_1)\right)\right)^2 dx_1.$$

Now, the problem is to find $\alpha \in \mathbb{R}^m$ solution of

$$\begin{cases} \inf J(\alpha) \\ u \textit{ solution of } (3.16),\ (3.2),\ (3.3), \\ u \textit{ verifies } (3.4), \\ \mathbf{v},\ p_0 \textit{ solution of } (3.5) - (3.8), \\ p_0 \textit{ verifies } (3.17). \end{cases} \tag{3.18}$$

In other words, we try to find a solution of the system (3.1)–(3.8) such that

$$p\left(x_1, H + u(x_1)\right) \approx \sum_{i=1}^{m} \alpha_i \phi_i(x_1) + c(\alpha), \quad \forall x_1 \in (0, L)$$

where $\alpha \in \mathbb{R}^m$ and $p(x_1, x_2) = p_0(x_1, x_2) + \sum_{i=1}^m \frac{\alpha_i}{L}\int_0^L \phi_i(x_1) dx_1 + c(\alpha)$, for $(x_1, x_2) \in \Omega_u^F$.

The discrete control is $\alpha \in \mathbb{R}^m$ and the observation is the trace of the pressure on the interface, more precisely

$$x_1 \in (0, L) \to p_0\left(x_1, H + u(x_1)\right).$$

3.7 Sensitivity analysis

We shall analyse the dependence of the displacement of the interface u, the velocity, the pressure of the fluid $\mathbf{v}$, p and the cost function J on variations of the discrete control α.

3.7.1 Sensitivity of the displacement of the interface

Proposition 3.3 *The applications $\alpha \to u$ and $\alpha \to c(\alpha)$ are affine, where u and $c(\alpha)$ are the solutions of the equation (3.16) with boundary conditions (3.2), such that (3.3) holds. More precisely,*

$$\begin{array}{rcl} u & = & u_0 + \sum_{i=1}^m \alpha_i u_i \\ c(\alpha) & = & c_0 + \sum_{i=1}^m \alpha_i c_i \end{array}$$

where u_0, c_0 verify

$$\left\{ \begin{array}{rcl} u_0''''(x_1) & = & \frac{1}{D}\left(f^S(x_1) + c_0\right), \quad \forall x_1 \in (0,L) \\ u_0(0) & = & u_0(L) = u_0'(0) = u_0'(L) = 0 \\ \int_0^L u_0(x_1)\,dx_1 & = & 0 \end{array} \right. \tag{3.19}$$

and u_i, c_i verify

$$\left\{ \begin{array}{rcl} u_i''''(x_1) & = & \frac{1}{D}\left(\phi_i(x_1) + c_i\right), \quad \forall x_1 \in (0,L) \\ u_i(0) & = & u_i(L) = u_i'(0) = u_i'(L) = 0 \\ \int_0^L u_i(x_1)\,dx_1 & = & 0. \end{array} \right. \tag{3.20}$$

Proof. According to Proposition 3.2, the systems (3.19) and (3.20) have unique solutions. By addition, we obtain

$$\left(u_0 + \sum_{i=1}^m \alpha_i u_i\right)''''(x_1) = \frac{1}{D}\left(f^S(x_1) + \sum_{i=1}^m \alpha_i \phi_i(x_1) + c_0 + \sum_{i=1}^m \alpha_i c_i\right).$$

Also, the application $x_1 \mapsto \left(u_0 + \sum_{i=1}^m \alpha_i u_i\right)(x_1)$ verifies the boundary conditions (3.2) and $\int_0^L \left(u_0 + \sum_{i=1}^m \alpha_i u_i\right)(x_1)\,dx_1 = 0$. From the Proposition 3.2 and the definition of u and $c(\alpha)$ by (3.16), (3.2), (3.3), we obtain the conclusion. □

3.7.2 Sensitivity of the velocity and the pressure of the fluid

In order to study the sensitivity of the velocity and the pressure of the fluid we follow [13] where the Arbitrary Lagrangian Eulerian (ALE) coordinates have been used.

We denote by $\Omega_0^F = (0,L)\times(0,H)$ the reference domain and by $\Gamma_0 = (0,L)\times\{H\}$ its top boundary. For each $u \in \mathcal{U}_{ad}$ we consider the following one-to-one continuous differentiable transformation $T_u : \overline{\Omega_0^F} \to \overline{\Omega_u^F}$ given by:

$$T_u(\widehat{x}_1, \widehat{x}_2) = \left(\widehat{x}_1, \frac{H + u(\widehat{x}_1)}{H}\widehat{x}_2\right)$$

which admits the continuous differentiable inverse mapping

$$T_u^{-1}(x_1, x_2) = \left(x_1, \frac{H x_2}{H + u(x_1)}\right)$$

and verifies that $T_u\left(\Omega_0^F\right)=\Omega_u^F$, $T_u\left(\Gamma_0\right)=\Gamma_u$ and $T_u\left(\widehat{x}\right)=\widehat{x}$, $\forall\widehat{x}\in\Sigma$.

We set $\mathbf{x}=T_u\left(\widehat{\mathbf{x}}\right)$ for each $\mathbf{x}=(x_1,x_2)\in\Omega_u^F$ and $\widehat{\mathbf{x}}=(\widehat{x}_1,\widehat{x}_2)\in\Omega_0^F$.

We denote by $\widehat{\mathbf{v}}(\widehat{\mathbf{x}})=\mathbf{v}\left(T_u(\widehat{\mathbf{x}})\right)$ and $\widehat{p}(\widehat{\mathbf{x}})=p\left(T_u(\widehat{\mathbf{x}})\right)$ the velocity and the pressure in the reference domain Ω_0^F.

In order to pose the variational formulation in the reference configuration let us consider the following Hilbert spaces:

$$\begin{aligned}\widehat{W} &= \left(H_0^1\left(\Omega_0^F\right)\right)^2\\ \widehat{Q} &= L^2\left(\Omega_0^F\right)/\mathbb{R}\end{aligned}$$

equipped with their usual inner products. We introduce the forms

$$\widehat{a}_F:\mathbb{R}^m\times\left(H^1\left(\Omega_0^F\right)\right)^2\times\left(H^1\left(\Omega_0^F\right)\right)^2\to\mathbb{R}\qquad \widehat{b}_F:\mathbb{R}^m\times\left(H^1\left(\Omega_0^F\right)\right)^2\times\widehat{Q}\to\mathbb{R}$$

defined by

$$\begin{aligned}\widehat{a}_F\left(\alpha,\widehat{\mathbf{v}},\widehat{\mathbf{w}}\right) &= \sum_{i=1}^{2}\int_{\Omega_0^F}\left(\frac{H+u\left(\widehat{x}_1\right)}{H}\frac{\partial\widehat{v}_i}{\partial\widehat{x}_1}\frac{\partial\widehat{w}_i}{\partial\widehat{x}_1}-\frac{u'\left(\widehat{x}_1\right)\widehat{x}_2}{H}\frac{\partial\widehat{v}_i}{\partial\widehat{x}_2}\frac{\partial\widehat{w}_i}{\partial\widehat{x}_1}\right)d\widehat{\mathbf{x}}\\ &+ \sum_{i=1}^{2}\int_{\Omega_0^F}\left(-\frac{u'\left(\widehat{x}_1\right)\widehat{x}_2}{H}\frac{\partial\widehat{v}_i}{\partial\widehat{x}_1}\frac{\partial\widehat{w}_i}{\partial\widehat{x}_2}+\frac{H^2+\left(u'\left(\widehat{x}_1\right)\widehat{x}_2\right)^2}{H\left(H+u\left(\widehat{x}_1\right)\right)}\frac{\partial\widehat{v}_i}{\partial\widehat{x}_2}\frac{\partial\widehat{w}_i}{\partial\widehat{x}_2}\right)d\widehat{\mathbf{x}},\\ \widehat{b}_F\left(\alpha,\widehat{\mathbf{w}},\widehat{q}\right) &= -\int_{\Omega_0^F}\left(\frac{H+u\left(\widehat{x}_1\right)}{H}\frac{\partial\widehat{w}_1}{\partial\widehat{x}_1}-\frac{u'\left(\widehat{x}_1\right)\widehat{x}_2}{H}\frac{\partial\widehat{w}_1}{\partial\widehat{x}_2}+\frac{\partial\widehat{w}_2}{\partial\widehat{x}_2}\right)\widehat{q}\,d\widehat{\mathbf{x}}.\end{aligned}$$

We assume that the volume forces in fluid are constant $\mathbf{f}^F=(f_1^F,f_2^F)^T\in\mathbb{R}^2$ and we consider $\widehat{\mathbf{f}}^F(\alpha)\in\widehat{W}'$ defined by

$$\left\langle\widehat{\mathbf{f}}^F(\alpha),\widehat{w}\right\rangle=\sum_{i=1}^{2}\int_{\Omega_0^F}\frac{H+u\left(\widehat{x}_1\right)}{H}f_i^F\widehat{w}_i\,d\widehat{\mathbf{x}},\quad\forall\widehat{\mathbf{w}}\in\widehat{W}.$$

We remark that the displacement u which appears in the coefficients depends on α.

The problem: find $\widehat{\mathbf{v}}\in\left(H^1\left(\Omega_0^F\right)\right)^2$, $\widehat{\mathbf{v}}|_\Sigma=\mathbf{g}$, $\widehat{\mathbf{v}}|_{\Gamma_0}=0$, $\widehat{p}\in\widehat{Q}$ *such that*

$$\left\{\begin{array}{lll}\widehat{a}_F\left(\alpha,\widehat{\mathbf{v}},\widehat{\mathbf{w}}\right)+\widehat{b}_F\left(\alpha,\widehat{\mathbf{w}},\widehat{p}\right) &= \left\langle\widehat{\mathbf{f}}^F(\alpha),\widehat{\mathbf{w}}\right\rangle, & \forall\widehat{\mathbf{w}}\in\widehat{W}\\ \widehat{b}_F\left(\alpha,\widehat{\mathbf{v}},\widehat{q}\right) &= 0, & \forall\widehat{q}\in\widehat{Q}\end{array}\right.\tag{3.21}$$

has a unique solution.

The problem (3.21) is obtained from (3.15) and conversely by using the one-to-one transformations T_u and T_u^{-1}. The equivalence of (3.21) and (3.15) follows from the transport theorems in continuum mechanics (see [23]), the chain rule and basic results

for Sobolev spaces (see [24]). The conclusion of this proposition is a consequence of the existence and uniqueness of (3.15).

Let $\widehat{\mathbf{v}}$, $\widehat{\mathbf{w}}$ be given in $\left(H^1\left(\Omega_0^F\right)\right)^2$ and $\widehat{q}$ in $\widehat{Q}$. Then functions from $\mathbb{R}^m$ to $\mathbb{R}$ defined by

$$\begin{aligned}\alpha &\longmapsto \widehat{a}_F\left(\alpha,\widehat{\mathbf{v}},\widehat{\mathbf{w}}\right)\\ \alpha &\longmapsto \widehat{b}_F\left(\alpha,\widehat{\mathbf{w}},\widehat{q}\right)\\ \alpha &\longmapsto \left\langle\widehat{\mathbf{f}}^F\left(\alpha\right),\widehat{\mathbf{w}}\right\rangle\end{aligned}$$

are differentiable and the partial derivatives have the forms:

$$\begin{aligned}\frac{\partial\widehat{a}_F}{\partial\alpha_k}\left(\alpha,\widehat{\mathbf{v}},\widehat{\mathbf{w}}\right) &= \sum_{i=1}^{2}\int_{\Omega_0^F}\left(\frac{u_k\left(\widehat{x}_1\right)}{H}\frac{\partial\widehat{v}_i}{\partial\widehat{x}_1}\frac{\partial\widehat{w}_i}{\partial\widehat{x}_1}-\frac{u_k'\left(\widehat{x}_1\right)\widehat{x}_2}{H}\frac{\partial\widehat{v}_i}{\partial\widehat{x}_2}\frac{\partial\widehat{w}_i}{\partial\widehat{x}_1}\right)d\widehat{\mathbf{x}}\\ &+ \sum_{i=1}^{2}\int_{\Omega_0^F}\left(-\frac{u_k'\left(\widehat{x}_1\right)\widehat{x}_2}{H}\frac{\partial\widehat{v}_i}{\partial\widehat{x}_1}\frac{\partial\widehat{w}_i}{\partial\widehat{x}_2}\right)d\widehat{\mathbf{x}}\\ &+ \sum_{i=1}^{2}\int_{\Omega_0^F}\left(\frac{2u_k'\left(\widehat{x}_1\right)u'\left(\widehat{x}_1\right)\left(\widehat{x}_2\right)^2}{H\left(H+u\left(\widehat{x}_1\right)\right)}\frac{\partial\widehat{v}_i}{\partial\widehat{x}_2}\frac{\partial\widehat{w}_i}{\partial\widehat{x}_2}\right)d\widehat{\mathbf{x}}\\ &+ \sum_{i=1}^{2}\int_{\Omega_0^F}\left(\frac{-u_k\left(\widehat{x}_1\right)\left(H^2+\left(u'\left(\widehat{x}_1\right)\widehat{x}_2\right)^2\right)}{H\left(H+u\left(\widehat{x}_1\right)\right)^2}\frac{\partial\widehat{v}_i}{\partial\widehat{x}_2}\frac{\partial\widehat{w}_i}{\partial\widehat{x}_2}\right)d\widehat{\mathbf{x}}\\ \frac{\partial\widehat{b}_F}{\partial\alpha_k}\left(\alpha,\widehat{\mathbf{w}},\widehat{q}\right) &= -\int_{\Omega_0^F}\left(\frac{u_k\left(\widehat{x}_1\right)}{H}\frac{\partial\widehat{w}_1}{\partial\widehat{x}_1}-\frac{u_k'\left(\widehat{x}_1\right)\widehat{x}_2}{H}\frac{\partial\widehat{w}_1}{\partial\widehat{x}_2}\right)\widehat{q}\,d\widehat{\mathbf{x}}\\ \frac{\partial}{\partial\alpha_k}\left\langle\widehat{\mathbf{f}}^F\left(\alpha\right),\widehat{\mathbf{w}}\right\rangle &= \sum_{i=1}^{2}\int_{\Omega_0^F}\frac{u_k\left(\widehat{x}_1\right)}{H}f_i^F\widehat{w}_i\,d\widehat{\mathbf{x}}.\end{aligned}$$

This above result is a consequence of the differentiability of integrals with respect to parameters. In our case the parameter is α. Applying the Implicit Function Theorem, we obtain the following result.

The applications $\alpha\in\mathbb{R}^m\mapsto\widehat{\mathbf{v}}\in\left(H^1\left(\Omega_0^F\right)\right)^2$ and $\alpha\in\mathbb{R}^m\mapsto\widehat{p}\in\widehat{Q}$ are differentiables and the partial derivatives $\frac{\partial\widehat{\mathbf{v}}}{\partial\alpha_k}\in\widehat{W}$ and $\frac{\partial\widehat{p}}{\partial\alpha_k}\in\widehat{Q}$ verify

$$\left\{\begin{array}{ll}\widehat{a}_F\left(\alpha,\frac{\partial\widehat{\mathbf{v}}}{\partial\alpha_k},\widehat{\mathbf{w}}\right)+\widehat{b}_F\left(\alpha,\widehat{\mathbf{w}},\frac{\partial\widehat{p}}{\partial\alpha_k}\right) = \frac{\partial}{\partial\alpha_k}\left\langle\widehat{\mathbf{f}}^F\left(\alpha\right),\widehat{\mathbf{w}}\right\rangle-\frac{\partial\widehat{a}_F}{\partial\alpha_k}\left(\alpha,\widehat{\mathbf{v}},\widehat{\mathbf{w}}\right)-\frac{\partial\widehat{b}_F}{\partial\alpha_k}\left(\alpha,\widehat{\mathbf{w}},\widehat{p}\right),\\ \widehat{b}_F\left(\alpha,\frac{\partial\widehat{\mathbf{v}}}{\partial\alpha_k},\widehat{q}\right) = -\frac{\partial\widehat{b}_F}{\partial\alpha_k}\left(\alpha,\widehat{\mathbf{v}},\widehat{q}\right)\end{array}\right. \tag{3.22}$$

for all $\widehat{\mathbf{w}}$ in $\widehat{W}$ and for all $\widehat{q}$ in $\widehat{Q}$.

3.7.3 Sensitivity of the cost function

If $p_0 \in H^1\left(\Omega_u^F\right)$ such that $\int_0^L p_0\left(x_1, H + u(x_1)\right)\, dx_1 = 0$, then $\int_0^L \widehat{p}_0\left(x_1, H\right)\, dx_1 = 0$, where $\widehat{p}_0 = p_0 \circ T_u$. Also, we have $\int_0^L \frac{\partial \widehat{p}_0}{\partial \alpha_k}\left(x_1, H\right)\, dx_1 = 0$.

The application $\alpha \in \mathbb{R}^m \mapsto J(\alpha)$ is differentiable and the partial derivatives $\frac{\partial J}{\partial \alpha_k}(\alpha)$ have the forms:

$$2\int_0^L \left(\phi_k(x_1) - \int_0^L \frac{\phi_k}{L} dx_1 - \frac{\partial \widehat{p}_0}{\partial \alpha_k}(x_1, H)\right)\left(\sum_{i=1}^m \alpha_i \left(\phi_i(x_1) - \int_0^L \frac{\phi_i}{L} dx_1\right) - \widehat{p}_0\left(x_1, H\right)\right) dx_1 \tag{3.23}$$

3.8 Numerical results

We are interested in simulating the blood flow through medium vessels (arteries). The computation has been made in a domain of length $L = 3\ cm$ and height $H = 0.5\ cm$ which represents a half width of the vessel. In this case, the fluid is the blood and the structure is the wall of the vessel.

The numerical values of the following physical parameters have been taken from [1]. The viscosity of the blood was taken to be $\mu = 0.035\ \frac{g}{cm \cdot s}$, its density $\rho^F = 1\ \frac{g}{cm^3}$. The thickness of the vessel is $h = 0.1\ cm$, the Young modulus $E = 0.75 \cdot 10^6\ \frac{g}{cm \cdot s^2}$, the density $\rho^S = 1.1\ \frac{g}{cm^3}$.

The gravitational acceleration is $g_0 = 981\ \frac{cm}{s^2}$ and the averaged volume force of the structure is $f^S(x_1) = -g_0 \rho^S h$.

On the rigid boundary, we impose the following boundary conditions:

$$\begin{array}{rcl} v_1(x_1, x_2) & = & \begin{cases} \left(1 - \frac{x_2^2}{H^2}\right) V_0, & (x_1, x_2) \in \Sigma_1 \cup \Sigma_3 \\ V_0, & (x_1, x_2) \in \Sigma_2 \end{cases} \\ v_2(x_1, x_2) & = & 0, \quad (x_1, x_2) \in \Sigma \end{array}$$

where $V_0 = 30\ \frac{cm}{s}$ (see [25]). The volume force in fluid is $\mathbf{f}^F = (0, -g_0 \rho^F)^T$.

The numerical tests have been produced using *freefem++ v1.27* (see [26]).

For the fluid we have used the Mixed Finite Element Method, $P2$ Lagrange triangles for the velocity and $P1$ for the pressure.

3.8.1 Optimization without using the derivative

Numerical test 1.

We use the same notations as in the previous sections, in particular m and ϕ_i refer to the equation (3.16). We set $m = 1$ and $\phi_1(x_1) = x_1 - L/2$. In this case $c_0 = g_0\rho^S h$, $u_0 = 0$, $c_1 = 0$ and

$$u_1(x_1) = \frac{x_1^2 \left(L - x_1\right)^2 (x_1 - L/2)}{240D}, \quad u(x_1) = \alpha_1 u_1(x_1).$$

We remark that the displacement of the interface is computed exactly.

We have evaluated the cost function for equidistant points of step length 0.5 in the interval $[-20,\ 5]$. For each α_1, we generate a mesh for Ω_u^F, where the displacement u depends on α_1. A typical mesh of 198 triangles and 128 vertices is shown below.

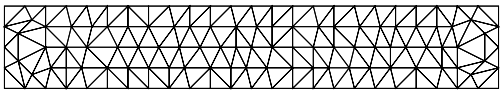

Figure 3.2: A typical mesh

The condition (3.4) was not violated. Then, we solve the Stokes equations (3.15) on this mesh.

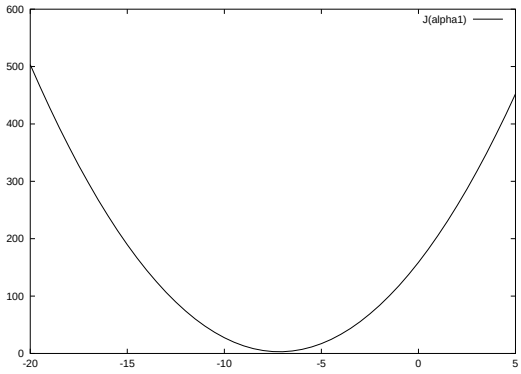

Figure 3.3: The cost function

The graph $\alpha_1 \to J(\alpha_1)$ seems to be strictly convex, consequently the optimal control is unique (see Figure 3.3). The cost function has the value $J = 158.76$ for $\alpha_1 = 0$. The minimal value of the cost function $J = 3.04$ was obtained for $\alpha_1 = -7$.

The displacement of the vessel is very small, so the behavior of the blood flow is like the Poiseuille flow.

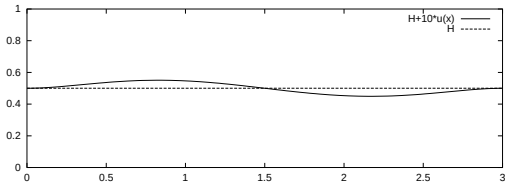

Figure 3.4: The displacement of the vessel magnified by 10

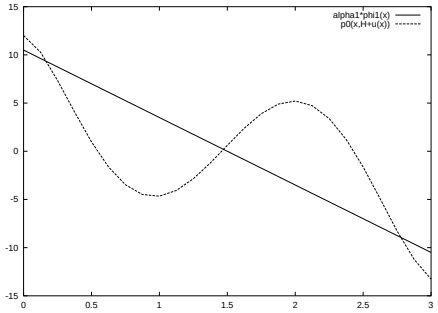

Figure 3.5: The optimal control $\alpha_1\phi_1(x_1)$ and the optimal observation $p_0(x_1, H+u(x_1))$

The optimal control is -7 and the pressure on the interface can be approached by $-7(x_1 - L/2) + g_0\rho^S h$. The pressure difference between the outflow (right) and inflow (left) is $-7L$.

If we take the averaged volume forces in the vessel of the form $f^S(x_1) = \frac{2\mu V_0}{H^2}x_1 - \rho^S g_0\, h$ we obtain the Poiseuille flow for the blood. The pressure on the interface in this case is $p(x_1, H) = -\frac{2\mu V_0}{H^2}x_1 + g_0\rho^S h$ where $-\frac{2\mu V_0}{H^2} = -8.4$ and the pressure difference between the outflow and inflow is $-8.4L$, so there is a lose of the pressure. The displacement of the interface is consequent: the shape of the vessel is inflow at the left and outflow at the right (see Figure 3.4). In Figure 3.5 we observe the difference between the optimal control and the optimal observation. In the fixed point approach, the two graphs must be identical.

If the condition (3.4) is violated, we have

$$\inf_{x_1\in[0,L]} \{H + u\,(x_1)\} = 0$$

and we say that the vessel is collapsed. Numerical results for this case are presented in [27].

3.8.2 The BFGS algorithm

The BFGS algorithm is a quasi-Newton iterative method for solving unconstrained optimization problem $\inf\{J(\alpha);\ \alpha \in \mathbb{R}^m\}$.

Step 0 Choose a starting point $\alpha^0 \in \mathbb{R}^m$, an $m \times m$ symmetric positive matrix H_0 and a positive scalar ϵ. Set $k = 0$.

Step 1 Compute $\nabla J(\alpha^k)$.

Step 2 If $\left\|\nabla J(\alpha^k)\right\| < \epsilon$ stop.

Step 3 Set $\mathbf{d}^k = -H_k \nabla J(\alpha^k)$.

Step 4 Determine $\alpha^{k+1} = \alpha^k + \theta_k \mathbf{d}^k$, $\theta_k > 0$ by means of an approximate minimization

$$J(\alpha^{k+1}) \approx \min_{\theta \geq 0} J(\alpha^k + \theta \mathbf{d}^k).$$

Step 5 Compute $\delta_k = \alpha^{k+1} - \alpha^k$.

Step 6 Compute $\nabla J(\alpha^{k+1})$ and $\gamma_k = \nabla J(\alpha^{k+1}) - \nabla J(\alpha^k)$.

Step 7 Compute

$$H_{k+1} = H_k + \left(1 + \frac{\gamma_k^T H_k \gamma_k}{\delta_k^T \gamma_k}\right) \frac{\delta_k \delta_k^T}{\delta_k^T \gamma_k} - \frac{\delta_k \gamma_k^T H_k + H_k \gamma_k \delta_k^T}{\delta_k^T \gamma_k}$$

Step 8 Update $k = k + 1$ and go to the **Step 2**.

For the inaccurate line search at the **Step 4**, the methods of Goldstein and Armijo were used. If we denote by $g : [0, \infty) \to \mathbb{R}$ the function $g(\theta) = J(\alpha^k + \theta \mathbf{d}^k)$, we determine $\theta_k > 0$ such that

$$g(0) + (1 - \lambda)\, \theta_k g'(0) \leq g(\theta_k) \leq g(0) + \lambda \theta_k g'(0) \tag{3.24}$$

where $\lambda \in (0, 1/2)$.

In the BGSF algorithm, we have used (3.21) which is the ALE version of the Stokes equations in the reference domain in order to compute the cost function and we have used (3.22) and (3.23) in order to compute $\nabla J(\alpha)$.

Remark 3.2 *In order to compute $\nabla J(\alpha)$ by (3.22) and (3.23), we have to solve m linear systems which have the same matrix. The linear systems were solved by LU decomposition. We observe that (3.21) and (3.22) have the same left-hand side, so when we compute $\nabla J(\alpha)$ we can use the same LU decomposition obtained computing $J(\alpha)$ by (3.21).*

We could compute $\nabla J(\alpha)$ by the Finite Differences Method

$$\frac{\partial J}{\partial \alpha_k}(\alpha) \approx \frac{J(\alpha + \Delta\alpha_k \mathbf{e_k}) - J(\alpha)}{\Delta \alpha_k} \tag{3.25}$$

where $\mathbf{e_k}$ *is the k-th vector of the canonical base of* $\mathbb{R}^m$ *and* $\Delta\alpha_k > 0$ *is the grid spacing. In this case, the cost function J need to be evaluated in each* $\alpha + \Delta\alpha_k \mathbf{e_k}$, $k = 1, \ldots, m$. *We have to solve m linear systems obtained from (3.21), but the matrices are different, so using the analytic formula of the gradient (3.22) is more advantageous.*

Numerical test 2.

We have performed the numerical test in the case $m = 1$ and $\phi_1(x_1) = x_1 - L/2$.

In the table below, we show the gradient of the cost function computed by (3.22) and (3.23), respectively by the Finite Differences Method (3.25) with $\Delta\alpha_1 = 0.5$, which proves the validity of the analytic formula.

α_1	$\nabla J(\alpha_1)$ using (3.22) and (3.23)	$\nabla J(\alpha_1)$ using Finite Differences (3.25)
-20	-77.88	-76.50
-15	-47.55	-46.09
-10	-17.22	-15.70
-5	13.13	14.63
0	43.49	45.03
5	73.87	72.40

The starting point for the BFGS algorithm is $\alpha_1 = 0$ and the stopping criteria is $\|\nabla \mathcal{J}\|_\infty \leq 10^{-6}$.

Iterations	α_1	$J(\alpha_1)$	$\|\nabla J(\alpha_1)\|_\infty$
0	0	158.70	43.49
1	-43.49	4003.66	-220.03
2	-7.17907	2.95985	-0.100582
3	-7.16247	2.95899	0.000232724
4	-7.1625	2.95899	-2.53259e-10

The condition (3.4) was not violated. The minimal value of the cost function $J = 2.95899$ was obtained for $\alpha_1 = -7.1625$, after 5 iterations. The line search algorithm for the approximate minimization at the Step 4 was not activated, we take $\theta_K = 1$. The computed displacements of the vessel are almost the same as in the Figure 3.4. If we activate the line search algorithm and we set to 3 the maximal number of evaluation of the cost function at the Step 4, we obtain $\alpha_1^0 = 0$, $\alpha_1^1 = -7.17207$, $\alpha_1^2 = -7.16251$, $\alpha_1^3 = -7.16249$, $\alpha_1^4 = -7.1625$.

Numerical test 3.

We take $m = 4$. Let $\xi_i = (i-1)L/(m-1)$ for $1 \leq i \leq m$ be an uniform grid of $[0, L]$. For each $i = 1, \ldots, m$, there exists a unique ϕ_i polynomial function of degree 3, such that $\phi_i(\xi_j) = \delta_{ij}$, where δ_{ij} is the Kronecker's symbol. The functions ϕ_i are not necessary the same as the trace on the interface of the pressure finite element functions. Other choice for ϕ_i could be the vibration modes of the beam equations.

Let u_i, c_i be the solutions of (3.20). We have computed u_i, c_i exactly, using the software *Mathematica*. The displacements u_i are polynomial functions of degree 7.

The fluid equations were solved in the reference mesh shown in Figure 3.2.

The starting point for the BFGS algorithm is $\alpha = 0$ and the stopping criteria is $\|\nabla \mathcal{J}\|_\infty \leq 10^{-6}$. The analytic formula of the gradient was employed.

Iterations	J	$\|\nabla J\|_\infty$
0	158.70	21.29
1	42.88	3.51
2	20.39	2.38
3	0.168155	0.30
4	0.165842	0.008
5	0.165653	2.5e-7

Five iterations are required to achieve $\|\nabla \mathcal{J}\|_\infty \leq 10^{-6}$ and the obtained discrete optimal control is

$$(\alpha_1, \alpha_2, \alpha_3, \alpha_4) = (13.2723413,\ 2.89419278,\ -2.704038443,\ -13.46249563).$$

The optimal value of the cost function for $m = 4$ is $J = 0.165653$ which is less than $J = 2.95899$ in the case $m = 1$.

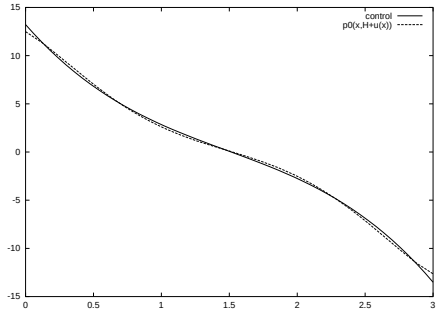

Figure 3.6: The optimal control function $\sum_{i=1}^{m} \alpha_i \left(\phi_i(x_1) - \frac{1}{L} \int_0^L \phi_i(x_1) dx_1 \right)$ and the optimal observation $p_0(x_1, H + u(x_1))$

The displacement of the vessel is very small, it is less than 0.04 cm. The computed velocity distribution is similar to a Poiseuille flow (see Figure 3.7).

3.9 Conclusions

Using the Least Squares Method and the Arbitrary Lagrangian Eulerian coordinates, a two dimensional steady fluid structure interaction problem was transformed into an optimal control problem.

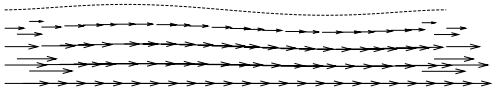

Figure 3.7: The displacement $[cm]$ of the vessel magnified by a factor 20 and the velocity $[cm/s]$ reduced by a factor 100

The BFGS algorithm has given satisfactory numerical results even when a reduced number of discrete controls were used. The analytic formula of the gradient was employed. Computational results reveal that the displacement of the interface is very small when the velocity profile is parabolic at the inflow and outflow.

We have obtained a smaller optimal value by increasing the number of the controls and by changing the shape of the control functions.

In a forthcoming paper, the techniques used here will be adapted to the unsteady fluid-structure interaction problems. The vibration modes of the structure will be the control shape functions.

Acknowledgments

The author is very grateful to the anonymous referees whose suggestions and comments have contributed to improve the content of this paper.

Bibliography

[1] L. Formaggia, J. F. Gerbeau, F. Nobile and A. Quarteroni, On the coupling of 3D and 1D Navier-Stokes equations for flow problems in compliant vessels, *Comput. Methods Appl. Mech. Engrg.* **191**(6-7) 561–582 (2001).

[2] J. F. Gerbeau and M. Vidrascu, A quasi-Newton algorithm on a reduced model for fluid - structure interaction problems in blood flows, *M2AN Math. Model. Numer. Anal.* **37**(4) 631–647 (2003).

[3] H. Chen and T. Sheu, Finite-element simulation of incompressible fluid flow in an elastic vessel, *Int. J. Numer. Meth. Fluids* **42** 131–146 (2003).

[4] C. Farhat, Ph. Geuzaine and C. Grandmont, The discrete geometric conservation law and the nonlinear stability of ALE schemes for the solution of flow problems on moving grids, *J. Comput. Phys.* **174**(2) 669–694 (2001).

[5] C. Grandmont, Existence for a three-dimensional steady state fluid-structure interaction problem, *J. Math. Fluid Mech.* **4**(1) 76–94 (2002).

[6] G. Bayada, M. Chambat, B. Cid and C. Vazquez, On the existence of solution for a non-homogeneus Stokes-rod coupled problem, *Nonlinear Analysis: Theory, Methods and Applications*, **59** 1-19 (2004).

[7] C. Grandmont and Y. Maday, Existence for an unsteady fluid-structure interaction problem, *M2AN Math. Model. Numer. Anal.* **34**(3) 609–636 (2000).

[8] B. Desjardins, M. Esteban, C. Grandmont and P. Le Tallec, Weak solutions for a fluid-elastic structure interaction model, *Rev. Mat. Complut.* **14**(2) 523–538 (2001).

[9] H. Beirao da Veiga, On the existence of strong solution to a coupled fluid structure evolution problem, *J. Math. Fluid Mech.* **6**, 21–52 (2004).

[10] M. A. Fernandez and M. Moubachir, Sensitivity analysis for an incompressible aeroelastic system, *Math. Models Methods Appl. Sci.* **12**(8) 1109–1130 (2002).

[11] G. Bayada, J. Durany and C. Vázquez, Existence of a Solution for a Lubrication Problem in Elastic Journal Bearings with Thin Bearing, *Math. Meth. Appl. Sci.*, **18** 455–466 (1995).

[12] C. Murea and Y. Maday, Existence of an Optimal Control for a Nonlinear Fluid-Cable Interaction Problem, Rapport de recherche CEMRACS 96, C.I.R.M. Luminy, France, (1996).

[13] C. Murea and C. Vázquez, Sensitivity and approximation of fluid-structure coupled by virtual control method, *Appl. Math. Optim.*, accepted

[14] R.M. Lewis, A nonlinear programming perspective on sensitivity calculations for systems governed by state equations, NASA-ICASE Report no. 12, (1997).

[15] C. Murea, Optimal control approach for the fluid-structure interaction problems, In *Proceedings of the Fourth European Conference on Elliptic and Parabolic Problems, Rolduc and Gaeta*, 2001, (Edited by J. Bemelmans et al), pp. 442–450, World Scientific Publishing Co. Pte. Ltd., (2002).

[16] P. Le Tallec and J. Mouro, Fluid-structure interaction with large structural displacements, *Comput. Methods Appl. Mech. Engrg.* **190**(24-25) 3039–3067 (2001).

[17] F. Nobile, Numerical approximation of fluid-structure interaction problems with application to haemodynamics, PhD, Ecole Polytechnique Féderale de Lausanne, Switzerland, (2001).

[18] S. Deparis, M.A. Fernandez and L. Formaggia, Acceleration of a fixed point algorithm for fluid-structure interaction using transpiration conditions, *M2AN Math. Model. Numer. Anal.* **37**(4) 601–616 (2003).

[19] J. Steindorf and H.G. Matthies, Partioned but strongly coupled iteration schemes for nonlinear fluid-structure interaction, *Comput. & Structures*, **80** 1991–1999 (2002).

[20] M. Bernadou, Formulation variationnelle, approximation et implementation de problemes de barres et de poutres bi- et tri-dimensionnelles. Partie B : barres et poutres bidimensionnelles, Rapport Techique no 86, INRIA, (1987).

[21] A. Osses, A rotated multiplier applied to the controllability of waves, elasticity and tangential Stokes control, *SIAM J. Control Optim.* **40**(3) 777–800 (2001).

[22] V. Girault and P.-A. Raviart, *Finite element methods for Navier-Stokes equations. Theory and algorithms*, Springer Series in Computational Mathematics, Springer-Verlag, Berlin, (1986).

[23] M. E. Gurtin, *An Introduction to Continuum Mechanics*, Academic Press, (1981).

[24] R. Adams, *Sobolev spaces*, Academic Press, (1975).

[25] K. Schmidt-Nielsen, *Physiologie animale. Adaptation et milieux de vie*, Dunod, (1998).

[26] F. Hecht and O. Pironneau, A finite element software for PDE: freefem++, `http://www-rocq.inria.fr/Frederic.Hecht` [May 2003]

[27] M. Thiriet, A Three dimensional Numerical Method of a Critical Flow in a Collapsed Tube, Rapport de Recherche no 3867, INRIA, (2000).

Chapter 4

Optimal control approach for the fluid-structure interaction problems

This chapter is based on the paper:

C.M. Murea, Optimal control approach for the fluid-structure interaction problems, *Proceedings of the Fourth European Conference on Elliptic and Parabolic Problems*, Rolduc and Gaeta, 2001, J. Bemelmans et al (eds.), World Scientific Publishing Co. Pte. Ltd., pp. 442–450, 2002

4.1 Introduction

A fluid-structure interaction problem is studied. We are interested by the displacement of the structure and by the velocity and the pressure of the fluid.

The contact surface between fluid and structure is unknown a priori, therefore it is a free boundary like problem.

In the classical approaches, the fluid and structure equations are coupled via two boundary conditions: the continuity of the velocity and of the constraint vector at the contact surface.

In our approach, the equality of the fluid and structure velocities at the contact surface will be relaxed and treated by the Least Squares Method.

We start with a guess for the contact forces. The displacement of the structure can be computed. We suppose that the fluid domain is completely determined by the displacement of the structure. Knowing the actual domain of the fluid and the contact forces, we can compute the velocity and the pressure of the fluid.

In this way, the equality of the fluid and structure forces at the contact surface is trivially accomplished.

The problem is to find the contact forces such that the equality of the fluid and structure velocities at the contact surface holds.

It's a exact controllability problem with Dirichlet boundary control and Dirichlet boundary observation.

In order to obtain some existence results, this exact controllability problem will be transformed in an optimal control problem using the Least Squares Method.

This mathematical model permits to solve numerically the coupled fluid-structure problem via partitioned procedures (i.e. in a decoupled way, more precisely the fluid and the structure equations are solved separately).

The aim of this paper is to present an optimal control approach for a fluid structure interaction problem and some numerical tests.

4.2 Notations

We study the flow in the two-dimensional canal of breadth L_2

$$\Omega = \left\{(x_1, x_2) \in \mathbb{R}^2;\ 0 < x_1 < L_2,\ -H < x_2 < +H\right\}.$$

In the interior of the canal there exists a deformable beam fixed at the one of the his extremities (see the Figure 4.1).

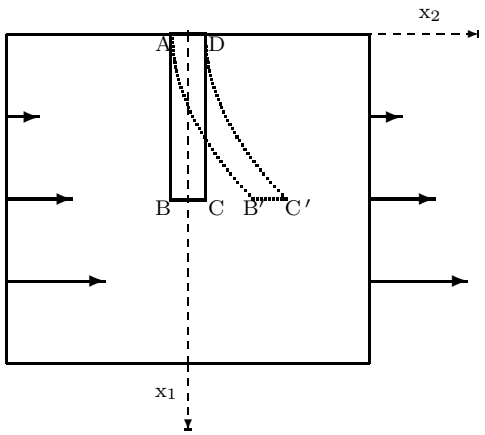

Figure 4.1: The flow around a deformable beam

In the absence of the fluid, the beam has the parallelepiped shape $[ABCD]$. The coordinates of the vertices are

$$A = (-r, 0)\,,\ B = (-r, L_1)\,,\ C = (r, L_1)\,,\ D = (r, 0)\,.$$

The beam is deformed under the action of the fluid and it will have the shape $[AB'C'D]$. The deformation of the beam is described using the displacement of the median thread

$$u = (u_1, u_2) : [0, L_1] \to \mathbb{R}^2.$$

which satisfy the compatibility condition $u_1(0) = 0, u_2(0) = 0$. For instant, we assume that $u_1 = 0$.

The domain occupied by the beam is

$$\Omega_u^S = \left\{(x_1, x_2) \in \mathbb{R}^2;\ x_1 \in]0, L_1[\,,\ |x_2 - u_2(x_1)| < r\right\}.$$

Consequently, the domain occupied by the fluid is

$$\Omega_u^F = \Omega \backslash \overline{\Omega_u^S}.$$

The contact surface between fluid and beam is $\Gamma_u =]AB'[\cup [B'C'] \cup]C'D[$ where

$$\begin{aligned}]AB'[&= \left\{(x_1, x_2) \in \mathbb{R}^2;\ x_1 \in]0, L_1[\,,\ x_2 = u_2(x_1) - r\right\}, \\ [B'C'] &= \left\{(x_1, x_2) \in \mathbb{R}^2;\ x_1 = L_1,\ x_2 \in [-r, r]\right\}, \\ ]C'D[&= \left\{(x_1, x_2) \in \mathbb{R}^2;\ x_1 \in]0, L_1[\,,\ x_2 = u_2(x_1) + r\right\}. \end{aligned}$$

The other boundary of the fluid domain is noted Γ_1.

4.3 Beam equations

The beam has one end clamped and the other is free. It is deformed under the flexion efforts and we suppose that the longitudinal traction compression forces are negligible. We don't take into account the effect of the transverse shear. We present the mathematical model, following [1].

In view of the Sobolev Embedding Theorem, we have

$$H^2(]0, L_1[) \hookrightarrow \mathcal{C}^1([0, L_1])$$

and we denote

$$U = \left\{\phi \in H^2(]0, L_1[);\ \phi(0) = \phi'(0) = 0\right\}.$$

Let $D_2 \in \mathbb{R}_+^*$ be given by the formula

$$D_2 = E \int_S x_2^2 \, dx_2 dx_3$$

where E is the Young's module and S is the cross section of the beam. We set

$$\left\{ \begin{array}{c} a_S : U \times U \to \mathbb{R} \\ a_S(\phi, \psi) = D_2 \displaystyle\int_{]0, L_1[} \frac{d^2\phi}{dx_1^2}(x_1) \frac{d^2\psi}{dx_1^2}(x_1)\, dx_1. \end{array} \right. \tag{4.1}$$

Remark 4.1 *As a consequence of the Lax-Milgram Theorem, we have the following result:*
Let $f_2^S \in L^2(]0,L_1[)$ and $\eta_2 \in L^2(]0,L_1[)$. Then the problem:
Find u_2 in U such that

$$a_S(u_2,\psi)=\int_{]0,L_1[}\eta_2(x_1)\,\psi(x_1)\,dx_1+\int_{]0,L_1[}f_2^S(x_1)\,\psi(x_1)\,dx_1,\quad \forall\psi\in U \tag{4.2}$$

has a unique solution.

The volume forces (the gravity forces) are included in f_2^S. We denote by η_2 the fluid forces acting on the beam.

When the data and the solution are smooth enough the solution u_2 verifies the strong formulation given by:

$$\begin{gathered}u_2''''(x_1)=\frac{1}{D_2}\left(\eta_2(x_1)+f_2^S(x_1)\right),\quad \forall x_1\in]0,L_1[\\ u_2(0)=u_2'(0)=u_2''(L_1)=u_2'''(L_1)=0.\end{gathered}$$

In the particular case $f_2^S=0$ and $\eta_2(x_1)=\alpha+\beta x_1+\gamma x_1^2$, we obtain

$$\begin{aligned}u_2(x_1) &= \frac{1}{360D_2}\left[15\left(x_1^2-4x_1L_1+6L_1^2\right)\alpha+3\left(x_1^3-10x_1L_1^2+20L_1^3\right)\beta\right.\\ &\left.+\left(x_1^4-20x_1L_1^3+45L_1^4\right)\gamma\right].\end{aligned}$$

4.4 Fluid equations in moving domain

We suppose that the fluid is governed by the two dimensional Stokes equations in the velocity-pressure-vorticity formulation:
Find the velocity $v:\overline{\Omega}_u^F\to\mathbb{R}^2$, the pressure $p:\overline{\Omega}_u^F\to\mathbb{R}$ and the vorticity $\omega:\overline{\Omega}_u^F\to\mathbb{R}$, such that

$$\left\{\begin{array}{rcll}\dfrac{\partial p}{\partial x_1}+\mu\dfrac{\partial\omega}{\partial x_2} &=& f_1^F & \text{in } \Omega_u^F\\ \dfrac{\partial p}{\partial x_2}-\mu\dfrac{\partial\omega}{\partial x_1} &=& f_2^F & \text{in } \Omega_u^F\\ \omega-\dfrac{\partial v_2}{\partial x_1}+\dfrac{\partial v_1}{\partial x_2} &=& 0 & \text{in } \Omega_u^F\\ \operatorname{div} v &=& 0 & \text{in } \Omega_u^F\\ v &=& g & \text{on } \Gamma_1\\ v\cdot n &=& 0 & \text{on } \Gamma_u\\ p &=& p_0 & \text{on } \Gamma_u\\ \omega &=& 0 & \text{on } \Gamma_1.\end{array}\right. \tag{4.3}$$

On Γ_u, we have the boundary conditions $v \cdot n = 0$ and $p = p_0$. The validity of these boundary conditions was proved using the least squares variational formulation. See ([3, Chap. 8]) for more details.

The boundary conditions $p = p_0$ and $v \cdot \tau = 0$ were studied in [10] and the slip boundary conditions $v \cdot n = 0$ and $(\sigma n) \cdot \tau = 0$, where σ is the stress tensor, were studied in [11] and [12], but these boundary conditions aren't appropriate for our approach of the fluid structure interaction.

Now, we will present the least squares variational formulation for the problem (4.3).

Let u_2 be the solution of the equation (4.2).

We have

$$H^2\left(]0, L_1[\right) \hookrightarrow \mathcal{C}^1\left([0, L_1]\right)$$

therefore the domain Ω_u^F has a Lipschitz boundary, so that we can define the spaces $H^1\left(\Omega_u^F\right)$, $H^{1/2}\left(\Gamma_1\right)$ and $H^{1/2}\left(\Gamma_u\right)$. We recall that $\partial\Omega_u^F = \overline{\Gamma}_u \cup \overline{\Gamma}_1$. We denote by $n = (n_1, n_2)$ the unit outward normal vector and by $\tau = (-n_2, n_1)$ an unit tangential vector to $\partial\Omega_u^F$.

We denote by $\cdot$ the scalar product.

Let us consider the following vectorial spaces

$$\begin{aligned} W &= \left\{ w = (w_1, w_2) \in H^1\left(\Omega_u^F\right)^2;\ w = 0 \text{ on } \Gamma_1 \text{ and } w \cdot n = 0 \text{ on } \Gamma_u \right\}, \\ Q &= \left\{ q \in H^1\left(\Omega_u^F\right);\ q = 0 \text{ on } \Gamma_u \right\}, \\ M &= \left\{ \omega \in H^1\left(\Omega_u^F\right);\ \omega = 0 \text{ on } \Gamma_1 \right\}. \end{aligned}$$

Let $g \in H_0^{1/2}\left(\Gamma_1\right)^2$ be given, such that $\int_{\Gamma_1} g \cdot n \, d\sigma = 0$. Then there exists $v_0 \in H^1\left(\Omega_u^F\right)^2$, such that $\operatorname{div} v_0 = 0$ in Ω_u^F, $v_0 = 0$ on Γ_u and $v_0 = g$ on Γ_1.

Let p_0 be given in $H^{1/2}\left(\Gamma_u\right)$. Then there exists a function in $H^1\left(\Omega_u^F\right)$, such that its trace is p_0. We denote this function by p_0, also.

Proposition 4.1 *For all u_2 in U, and f^F in $L^2\left(\Omega_u^F\right)^2$, the problem:*
Find $v - v_0 \in W$, $p - p_0 \in Q$, $\omega \in M$, such that

$$\begin{aligned} &\left(\frac{\partial p}{\partial x_1} + \mu \frac{\partial \omega}{\partial x_2}, \frac{\partial q}{\partial x_1} + \mu \frac{\partial \rho}{\partial x_2} \right) + \left(\frac{\partial p}{\partial x_2} - \mu \frac{\partial \omega}{\partial x_1}, \frac{\partial q}{\partial x_2} - \mu \frac{\partial \rho}{\partial x_1} \right) \\ &+ \left(\omega - \frac{\partial v_2}{\partial x_1} + \frac{\partial v_1}{\partial x_2}, \rho - \frac{\partial w_2}{\partial x_1} + \frac{\partial w_1}{\partial x_2} \right) + (\operatorname{div} v, \operatorname{div} w) \\ &= \left(f_1^F, \frac{\partial q}{\partial x_1} + \mu \frac{\partial \rho}{\partial x_2} \right) + \left(f_2^F, \frac{\partial q}{\partial x_2} - \mu \frac{\partial \rho}{\partial x_1} \right), \quad \forall w \in W, \forall q \in Q, \forall \rho \in M \end{aligned} \tag{4.4}$$

has a unique solution.

Here, $\mu > 0$ is the dynamic viscosity of the fluid, f^F is the external given force per unit volume and $(\cdot,\cdot)$ is the inner product of $L^2\left(\Omega_u^F\right)$.

Proof. We first prove that

$$\left\|\frac{\partial q}{\partial x_1}+\mu\frac{\partial \rho}{\partial x_2}\right\|_0^2+\left\|\frac{\partial q}{\partial x_2}-\mu\frac{\partial \rho}{\partial x_1}\right\|_0^2=\|\nabla q\|_0^2+\mu^2\|\nabla\rho\|_0^2$$

where $\|\cdot\|_0$ is the standard norm of $L^2\left(\Omega_u^F\right)$.

Le us consider that $q\in\mathcal{C}^1\left(\Omega_u^F\right)$, $q=0$ on Γ_u and $\rho\in\mathcal{C}^2\left(\Omega_u^F\right)$, $\rho=0$ on Γ_1. We have

$$\left\|\frac{\partial q}{\partial x_1}+\mu\frac{\partial \rho}{\partial x_2}\right\|_0^2+\left\|\frac{\partial q}{\partial x_2}-\mu\frac{\partial \rho}{\partial x_1}\right\|_0^2=\|\nabla q\|_0^2+\mu^2\|\nabla\rho\|_0^2+2\mu\left(\frac{\partial q}{\partial x_1},\frac{\partial \rho}{\partial x_2}\right)-2\mu\left(\frac{\partial q}{\partial x_2},\frac{\partial \rho}{\partial x_1}\right).$$

But using Green's formula, we have

$$\begin{aligned}&\left(\frac{\partial q}{\partial x_1},\frac{\partial \rho}{\partial x_2}\right)-\left(\frac{\partial q}{\partial x_2},\frac{\partial \rho}{\partial x_1}\right)\\ &=\int_{\partial\Omega_u^F}q\frac{\partial\rho}{\partial x_2}n_1\,d\sigma-\int_{\partial\Omega_u^F}q\frac{\partial\rho}{\partial x_1}n_2\,d\sigma-\left(q,\frac{\partial^2\rho}{\partial x_2\partial x_1}\right)+\left(q,\frac{\partial^2\rho}{\partial x_1\partial x_2}\right)\\ &=\int_{\Gamma_1}q\left(\nabla\rho\cdot\tau\right)\,d\sigma+\left(q,-\frac{\partial^2\rho}{\partial x_2\partial x_1}+\frac{\partial^2\rho}{\partial x_1\partial x_2}\right).\end{aligned}$$

By assumption of the regularity of ρ, we have $\frac{\partial^2\rho}{\partial x_2\partial x_1}=\frac{\partial^2\rho}{\partial x_1\partial x_2}$.

Since $\rho=0$ on Γ_1, we obtain that $\nabla\rho\cdot\tau=0$ on Γ_1 and then, by a density argument, the equality from the beginning of the proof holds.

The rest of the proof runs as in [3, Sect. 8.2.2]. □

4.5 Optimal control approach of the fluid-structure interaction problem

In the classical approaches, the fluid and structure equations are coupled via two boundary conditions: continuity of the velocities and continuity of the forces on the contact surface.

We denote by $\lambda=(\lambda_1,\lambda_2)$ the forces induced by the beam on the contact surface. Consequently, $-\lambda$ represent the forces induced by the fluid acting to the beam.

We denote by $S: M\to U$ the application which computes the displacement of the beam knowing the forces on the contact surface. This application is linear and continuous.

We denote by $F: U\times M\to W\times Q$ the application which computes the velocity and the pressure of the fluid knowing the displacement of the beam (therefore the domain of the fluid) and the forces on the contact surface. This application is non-linear on $U\times M$.

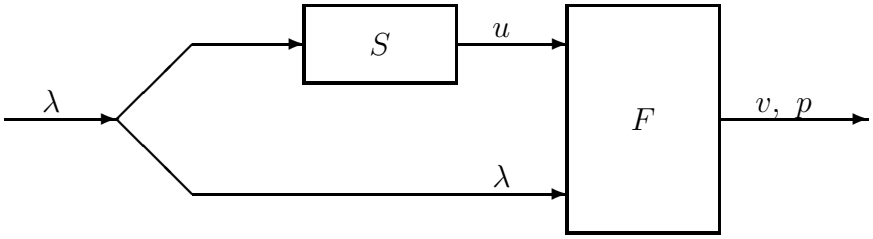

Figure 4.2: The computing scheme

We search to find out λ, such that $v_{|\Gamma_u} = 0$. This is a exact controllability problem. In our approach, the target condition will be relaxed. We assume that the forces on the contact surface have the form $\lambda = -p_0\, n$, where p_0 is the pressure of the fluid.

We consider the following optimal control problem:

$$\inf J\left(\alpha_1, \alpha_2, \beta_1, \beta_2, \gamma_1, \gamma_2\right) = \frac{1}{2}\left\|v \cdot \tau\right\|^2_{0,\Gamma_u} \tag{4.5}$$

subject to:

$$\left(\alpha_1, \alpha_2, \beta_1, \beta_2, \gamma_1, \gamma_2\right) \in K \subset \mathbb{R}^6 \tag{4.6}$$

$$\begin{array}{rcl} u_2(x_1) & = & \dfrac{1}{360 D_2}\left[15\left(x_1^2 - 4x_1L_1 + 6L_1^2\right)\left(\alpha_1 - \alpha_2\right)\right. \\ & & +3\left(x_1^3 - 10x_1L_1^2 + 20L_1^3\right)\left(\beta_1 - \beta_2\right) \\ & & \left. +\left(x_1^4 - 20x_1L_1^3 + 45L_1^4\right)\left(\gamma_1 - \gamma_2\right)\right] \end{array} \tag{4.7}$$

(v, p, ω) solution of the Stokes problem (4.4) with

$$p_0\left(x_1, x_2\right) = \begin{cases} \left(\alpha_1 + \beta_1 x_1 + \gamma_1 x_1^2\right), & \text{if } \left(x_1, x_2\right) \in \left]A, B'\right] \\ \left(\alpha_2 + \beta_2 x_1 + \gamma_2 x_1^2\right), & \text{if } \left(x_1, x_2\right) \in \left]D, C'\right] \\ \left(\frac{1}{2} - \frac{x_2}{2r}\right) p_0\left(B'\right) + \left(\frac{1}{2} + \frac{x_2}{2r}\right) p_0\left(C'\right), & \text{if } \left(x_1, x_2\right) \in \left]B', C'\right[\end{cases} \tag{4.8}$$

It's an optimal control problem with Dirichlet boundary control (p_0) and Dirichlet boundary observation ($v_{|\Gamma_u}$).

The relation (4.6) represents the control constraint.

The relation (4.7) represents the displacement of the beam under the cross forces $\lambda_2 = (\alpha_1 + \beta_1 x_1 + \gamma_1 x_1^2)$ on $]A, B'[$ and $\lambda_2 = (-\alpha_2 - \beta_2 x_1 - \gamma_2 x_1^2)$ on $]D, C'[$. We assume that the displacement of the beam under the longitudinal forces λ_1 is negligible.

This mathematical model permits to solve numerically the coupled fluid-cable problem via partitioned procedures (i.e. in a decupled way, more precisely the fluid and the cable equations are solved separately).

Remark 4.2 *The existence of an optimal control could be find in [5] for a related problem. In [7] it is proved the differentiability of the cost function and it is given the analytic formula for the gradient.*

Remark 4.3 *An open problem is to find additional conditions in order to obtain zero for the optimal value of the cost function. This is an approximate controllability problem. For a linear model (the domain of the fluid doesn't depend upon the displacement of the structure), we can find approximate controllability results in [4], [8] and [9].*

Remark 4.4 *If $v \cdot \tau$ is constant on Γ_u, then v is constant on Γ_u. Using [9, Prop. 3.1], we can prove that $(\sigma n) \cdot n = -p_0$, where σ is the stress tensor. Consequently, solving the beam equations under the action of the surface forces $-\lambda = p_0\, n$ on Γ_u is reasonable.*

4.6 Numerical tests

The parameters for the simulation are listed below:

the geometry $L_1 = 0.5$, $L_2 = 1$, $H = 2$, $r = 0.05$,

the beam $D_2 = 5$,

the fluid $\mu = 1$, $f^F = 0$, $g = (0, Vx_1)$ on the left and right parts of Γ_1, $g = (0, V)$ on the bottom of Γ_1, $g = (0, 0)$ on the top parts of Γ_1, $V = 0.5$.

The choice of these parameters induces small displacements of the beam. The fundamental hypothesis in linear elasticity of the beam is that the displacements remain small. The optimal control approach for fluid structure interaction presented in the present paper could be employed also for the large displacements of the structure, but in this case we have to use a well adapted model for the structure.

For a guest $(\alpha_1, \alpha_2, \beta_1, \beta_2, \gamma_1, \gamma_2)$, we compute the displacement of the beam using the formula (4.7).

Now, we know the moving boundary of the fluid and we generate a mesh consisting of triangular elements. Then, we solve the fluid equations (4.4) with boundary condition (4.8). We have used the P_1 finite element for the velocity, the pressure and the vorticity.

The target is to minimize the cost function (4.5).

The numerical tests have been produced using *freefem+* (see [2]).

The boundary condition $v \cdot n = 0$ on Γ_u was replaced by $v_2 = 0$.

The computed velocity isn't a divergence-free field. For a better approximation of the incompressibility condition, we can penalize the term $(\operatorname{div} v, \operatorname{div} w)$ in (4.4).

The optimal value of the cost function is J=2.36033e-04 and it was obtained for the penalizing factor 10^5. In this case $\|\operatorname{div} v\|_0^2$ is 4.80281e-04.

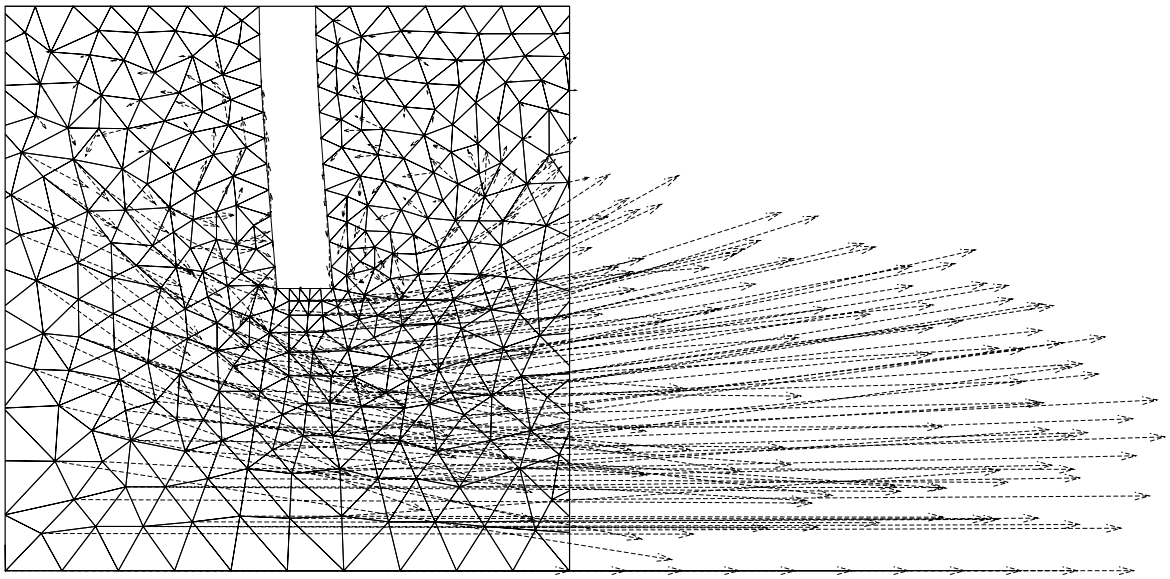

Figure 4.3: The computed velocity around the beam

In the Figure 4.3, we can see the corresponding displacement of the beam and the velocity of the fluid. The velocity of the fluid was multiplied by 2 for a better visualization.

We can avoid to generate a new mesh for each evaluation of the cost function by using the dynamic mesh like in [6].

Bibliography

[1] M. Bernadou, *Formulation variationnelle, approximation et implementation de problemes de barres et de poutres bi- et tri-dimensionnelles. Partie B : barres et poutres bidimensionnelles*, Rapport Techique no 86, INRIA, 1987

[2] D. Bernardi, F. Hecht, K. Ohtsuka, O. Pironneau, A finite element software for PDE: freefem+, `http://www-rocq.inria.fr/Frederic.Hecht`

[3] B.N. Jiang, *The least squares finite element method. Theory and applications in computational fluid dynamics and electromagnetism*, Springer, 1998

[4] J. L. Lions, E. Zuazua, Approximate controllability of a hydroelastic coupled system, *ESAIM: Contr. Optim. Calc. Var.*, **1** (1995) 1–15

[5] C.M. Murea, Y. Maday, *Existence of an optimal control for a nonlinear fluid-cable interaction problem*, Rapport de recherche CEMRACS 96, Luminy, France, 1996

[6] C.M. Murea, Dynamic meshes generation using the relaxation method with applications to fluid-structure interaction problems, *An. Univ. Bucuresti Mat.*, **47** (1998), No. 2, 177–186

[7] C.M. Murea, C. Vazquez, Computation of the gradient for a nonlinear fluid-structure interaction problem, in preparation

[8] A. Osses, J. P. Puel, Approximate controllability for a linear model of fluid structure interaction, *ESAIM: Contr. Optim. Calc. Var.*, **4** (1999) 497–513

[9] A. Osses, A rotated multiplier applied to the controllability of waves, elasticity and tangential Stokes control, to appear in *SIAM J. Control Optim.*

[10] O. Pironneau, Conditions aux limites sur la pression pour les équations de Stokes et Navier-Stokes, *C.R. Acad. Sc. Paris*, **303** (1986), Série I, No. 9, 403–406

[11] R. Verfurth, Finite element approximation of incompressible Navier-Stokes equations with slip boundary condition, *Numer. Math.*, **50** (1987) 697–721

[12] R. Verfurth, Finite element approximation of incompressible Navier-Stokes equations with slip boundary condition II, *Numer. Math.*, **59** (1991) 615–636

Part II

Unsteady fluid-structure interaction

Chapter 5

Numerical simulation of a pulsatile flow through a flexible channel

This chapter is based on the paper:

C.M. Murea, Numerical simulation of a pulsatile flow through a flexible channel, *ESAIM: Math. Model. Numer. Anal.* **40** (2006), no 6, 1101-1125

Abstract. An algorithm for approximation of an unsteady fluid-structure interaction problem is proposed. The fluid is governed by the Navier-Stokes equations with boundary conditions on pressure, while for the structure a particular plate model is used. The algorithm is based on the modal decomposition and the Newmark method for the structure and on the Arbitrary Lagrangian Eulerian coordinates and the Finite Element Method for the fluid. In this paper, the continuity of the stresses at the interface was treated by the Least Squares Method. At each time step we have to solve an optimization problem which permits us to use moderate time step. This is the main advantage of this approach. In order to solve the optimization problem, we have employed the Broyden, Fletcher, Goldforb, Shano method where the gradient of the cost function was approached by the Finite Difference Method. Numerical results are presented.

Introduction

We consider a pulsatile incompressible flow through a channel with elastic walls. Following [28], the therm pulsatility means the rapid increase and decrease of the flow rate in a first phase, followed by a longer phase where the flow rate is small. This kind of fluid-structure interaction arises in car industries, for example the dynamic behavior of a hydraulic shock absorber [22] or in the design of sensors subject to large acceleration

during impact [20] or in bio-mechanics, for example, the interaction between a bio-fluid and a living tissue [29].

The mathematical model which governs the fluid is the unsteady Navier-Stokes equations with boundary condition on the pressure. For the structure, a particular plate model is used.

The most frequently, the fluid-structure interaction problems are solved numerically by partitioned procedures, i.e. the fluid and the structure equations are solved separately.

There are different strategies to discretize in time the unsteady fluid-structure interaction problem. A family of explicit algorithms known also as staggered was successfully employed for the aeroelastic applications [11]. As it shown in [22] and [26], the staggered algorithms are unstable when the structure is light and its density is comparable to that of its fluid, such in the bio-mechanics applications. For a simplified fluid-structure problem, the unconditionally instability of the explicit algorithms is proved in [3].

In order to obtain unconditionally stable algorithms, at each time step we have to solve a non-linear fluid-structure coupled system. This can be done by using: fixed point strategies [22, 26, 13, 29], Newton method where the gradient is approached by Finite Differences [30], quasi-Newton method [14], Newton method with exact Jacobian [12]. The starting point for these iterative methods at the current time step is computed by extrapolating the solutions at the previous time steps.

We will see in the numerical tests presented in this paper that the solution at the previous time step, which is used as a starting point for the next time step, it is not close to the solution at the current time step. Such phenomena is amplified during the phase when the flow rate increase or decrease rapidly or if we increase the time step.

The fixed point and Newton like algorithms are not suitable in this case, since these methods diverge if the starting point is not sufficiently close to the solution.

In this paper, the continuity of the stresses at the interface will be treated by the Least Squares Method and at each time step we have to solve an optimization problem which is less sensitive to the choice of the starting point and it permits us to use moderate time step. This is the main advantage of this approach.

The outline of this paper is as follows. In Section 1 the approximation of the structure by the modal decomposition and Newmark scheme is presented. The Arbitrary Lagrangian Eulerian Method for Navier-Stokes equations in moving domain is detailed in Section 2. The coupled fluid-structure algorithm is introduced in Section 3. In order to solve the optimization problem at each time step, we have employed the Broyden, Fletcher, Goldforb, Shano method and the gradient of the cost function was approached by the Finite Difference Method. Numerical results are presented and discussed in Section 4. The last section is devoted to some concluding remarks.

5.1 Approximation of the structure

5.1.1 Strong equations of the structure

The following system was obtained from the equations of a linear elastic, homogeneous, isotropic plate (see [10]) which is parallel to the plane Ox_1x_3, under the hypothesis that the vertical displacement is independent of x_3.

Let $L > 0$ denote the length, $h^S > 0$ the thickness, $\rho^S > 0$ the mass density, $E > 0$ the Young modulus, $0 < \nu \leq 0.5$ the Poisson ratio, $T > 0$ the length of the time interval, $\eta : (0, L) \times (0, T) \to \mathbb{R}$ the applied transverse force per unit area, $u^0 : (0, L) \to \mathbb{R}$ the initial displacement, $\dot{u}^0 : (0, L) \to \mathbb{R}$ the initial velocity.

The problem is to find the transverse displacement $u : [0, L] \times [0, T] \to \mathbb{R}$ such that

$$\rho^S h^S \frac{\partial^2 u}{\partial t^2}(x_1, t) + \frac{E(h^S)^3}{12(1-\nu^2)} \frac{\partial^4 u}{\partial x_1^4}(x_1, t) = \eta(x_1, t), \quad (x_1, t) \in (0, L) \times (0, T) \tag{5.1}$$

$$u(0, t) = 0, \ \frac{\partial u}{\partial x_1}(0, t) = 0, \quad t \in (0, T) \tag{5.2}$$

$$u(L, t) = 0, \ \frac{\partial u}{\partial x_1}(L, t) = 0, \quad t \in (0, T) \tag{5.3}$$

$$u(x_1, 0) = u^0(x_1), \quad x_1 \in (0, L) \tag{5.4}$$

$$\frac{\partial u}{\partial t}(x_1, 0) = \dot{u}^0(x_1), \quad x_1 \in (0, L) \tag{5.5}$$

The above model is suitable for the flat thin structures. The time derivative of the angular momentum $\frac{\rho^S (h^S)^3}{12} \frac{\partial^4 u}{\partial t^2 \partial x_1^2}$ was neglected since the structure is thin and consequently $(h^S)^3$ is very small. On the contrary, the factor $\frac{E(h^S)^3}{12(1-\nu^2)}$ could not be neglected because the Young modulus E is in general a big number.

In [28, 29], for numerical simulations of the blood flow in arteries, the vascular wall was modeled as a axisymetric membrane

$$\rho^S h^S \frac{\partial^2 u}{\partial t^2}(x_1, t) - h^S G k \frac{\partial^2 u}{\partial x_1^2}(x_1, t) + \frac{E h^S}{12(1-\nu^2)R^2} u(x_1, t) = \eta(x_1, t).$$

Some authors add the visco-elastic term $\frac{\partial^3 u}{\partial x_1^2 \partial t}$ to the membrane model in order to obtain a priori estimation of an energy [23], or to regularize the solution [4], or to stabilize the numerical schemes [8].

5.1.2 Natural frequencies and normal mode shapes

This subsection follows the general reference [5] vol. 7, chap. XV and the particular example 5.3, p. 192 from the same reference. Another general reference in this topic is [21].

We denote by $0 < s_0 < \cdots < s_i < \ldots$ the solutions of the equation

$$\cos(s)\cosh(s) = 1, \quad s > 0.$$

We set $a_i = s_i/L$. For each $i \in \mathbb{N}$ there exists an unique normal mode shape $\phi_i \in \mathcal{C}^4([0,L])$ such that

$$\phi_i''''(x_1) = (a_i)^4\phi_i(x_1), \quad x_1 \in (0,L) \tag{5.6}$$

$$\phi_i(0) = \frac{\partial\phi_i}{\partial x_1}(0) = 0, \tag{5.7}$$

$$\phi_i(L) = \frac{\partial\phi_i}{\partial x_1}(L) = 0, \tag{5.8}$$

$$\int_0^L \phi_i^2(x_1)\,dx_1 = 1. \tag{5.9}$$

Let $\omega_i = \left(\frac{s_i}{L}\right)^2\sqrt{\frac{E(h^S)^3}{12(1-\nu^2)\rho^S h^S}}$ be the ith natural frequency associated with ϕ_i.

The normal mode shapes ϕ_i for $i \in \mathbb{N}$ form an orthonormal basis of $L^2(0,L)$. There exists an unique decomposition of η of the form

$$\eta(x_1,t) = \sum_{i\geq 0}\alpha_i(t)\phi_i(x_1).$$

The problem (5.1)–(5.5) has a solution of the form

$$u(x_1,t) = \sum_{i\geq 0} q_i(t)\phi_i(x_1)$$

where q_i is the solution of the second order differential equation

$$q_i''(t) + \omega_i^2 q_i(t) = \frac{1}{\rho^S h^S}\alpha_i(t), \quad t \in (0,T) \tag{5.10}$$

$$q_i(0) = \int_0^L u^0(x_1)\phi_i(x_1)\,dx_1 \tag{5.11}$$

$$q_i'(0) = \int_0^L \dot{u}^0(x_1)\phi_i(x_1)\,dx_1. \tag{5.12}$$

5.1.3 The Newmark method

We recall the Newmark method employed to approximate second order systems of ordinary differential equations.

Let $N \in \mathbb{N}^*$ be the number of time steps and $\Delta t = T/N$ the time step. We set $t_n = n\Delta t$ for $n = 0, 1, \ldots, N$. We denote $\alpha_i^n = \alpha_i(t_n)$ and let q_i^n, $\dot{q}_i^n$, $\ddot{q}_i^n$ be approximations of $q_i(t_n)$, $q_i'(t_n)$, $q_i''(t_n)$ respectively.

Knowing q_i^n, $\dot{q}_i^n$, $\ddot{q}_i^n$ and α_i^{n+1}, find q_i^{n+1}, $\dot{q}_i^{n+1}$, $\ddot{q}_i^{n+1}$ such that:

$$\ddot{q}_i^{n+1} + \omega_i^2 q_i^{n+1} = \frac{1}{\rho^S h^S}\alpha_i^{n+1}, \tag{5.13}$$

$$\dot{q}_i^{n+1} = \dot{q}_i^n + \Delta t\left[(1-\delta)\ddot{q}_i^n + \delta\ddot{q}_i^{n+1}\right], \tag{5.14}$$

$$q_i^{n+1} = q_i^n + \Delta t\dot{q}_i^n + (\Delta t)^2\left[\left(\frac{1}{2}-\theta\right)\ddot{q}_i^n + \theta\ddot{q}_i^{n+1}\right] \tag{5.15}$$

where δ and θ are two real parameters.

Substituting (5.15) into (5.13) results in an equation that may be solved for $\ddot{q}_i^{n+1}$:

$$\left(1+\omega_i^2(\Delta t)^2\theta\right)\ddot{q}_i^{n+1} = \frac{1}{\rho^S h^S}\alpha_i^{n+1} - \omega_i^2\left[q_i^n + \Delta t\dot{q}_i^n + (\Delta t)^2\left(\frac{1}{2}-\theta\right)\ddot{q}_i^n\right]. \tag{5.16}$$

Once $\ddot{q}_i^{n+1}$ is determined, (5.14) and (5.15) serve to define $\dot{q}_i^{n+1}$ and q_i^{n+1}, respectively.

Following [5], vol. 9, p. 922, this method is unconditional stable for $2\theta \geq \delta \geq 1/2$. It is first order accuracy if $\delta \neq 1/2$. If $\delta = 1/2$, it is second order accuracy in the case $\theta \neq 1/12$ and forth order accuracy is achieved if $\theta = 1/12$.

Only the first m modes will be considered. We denote by

$$u_m^n(x_1) = \sum_{i=0}^{m-1} q_i^n\phi_i(x_1), \quad \dot{u}_m^n(x_1) = \sum_{i=0}^{m-1}\dot{q}_i^n\phi_i(x_1), \quad \ddot{u}_m^n(x_1) = \sum_{i=0}^{m-1}\ddot{q}_i^n\phi_i(x_1)$$

the approximations of $u(x_1,t_n)$, $\frac{\partial u}{\partial t}(x_1,t_n)$, $\frac{\partial^2 u}{\partial t^2}(x_1,t_n)$ respectively.

5.2 Approximations of the unsteady Navier-Stokes equations in a moving domain

5.2.1 Strong form of the unsteady Navier-Stokes equations

Let $u : [0,L]\times[0,T] \to \mathbb{R}$ be the transverse displacement of a thin elastic wall. For each time instant $t \in [0,T]$, we assume that $u(\cdot,t) : [0,L] \to \mathbb{R}$ is at least of class $\mathcal{C}^1$. We suppose that an admissible displacement verifies:

$$u(0,t) = \tfrac{\partial u}{\partial x_1}(0,t) = 0,\ u(L,t) = \tfrac{\partial u}{\partial x_1}(L,t) = 0, \quad \forall t \in [0,T],$$
$$0 < H + u(x_1,t), \quad \forall (x_1,t) \in [0,L]\times[0,T]$$

where H is a positive constant.

For each $t \in [0,T]$, we introduce the notations (see Figure 5.1)

$$\begin{aligned}\Omega_t^F &= \left\{(x_1,x_2)\in\mathbb{R}^2;\ x_1\in(0,L),\ 0<x_2<H+u\left(x_1,t\right)\right\},\\ \Gamma_t &= \left\{(x_1,x_2)\in\mathbb{R}^2;\ x_1\in(0,L),\ x_2=H+u\left(x_1,t\right)\right\}.\end{aligned}$$

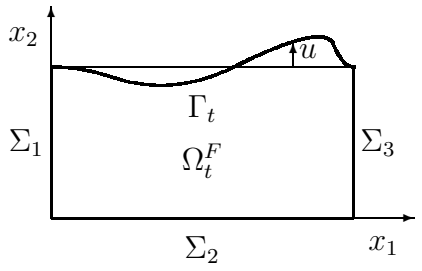

Figure 5.1: Example of an admissible domain

Also, we denote

$$\begin{aligned}\Sigma_1 &= \left\{(0,x_2)\in\mathbb{R}^2;\, x_2\in(0,H)\right\},\\ \Sigma_2 &= \left\{(x_1,0)\in\mathbb{R}^2;\, x_1\in(0,L)\right\},\\ \Sigma_3 &= \left\{(L,x_2)\in\mathbb{R}^2;\, x_2\in(0,H)\right\}.\end{aligned}$$

The two-dimensional domain occupied by the fluid is Ω_t^F, the elastic wall is Γ_t, the rigid one is Σ_2, while Σ_1 and Σ_3 represent the upstream and downstream sections, respectively. The boundaries Σ_1 and Σ_3 are artificial.

In the following, we denote by $\mathbf{n}=(n_1,n_2)^T$ the unit outward normal vector and by $\boldsymbol{\tau}=(\tau_1,\tau_2)^T=(-n_2,n_1)^T$ the unit tangential vector to $\partial\Omega_t^F$.

For all $t\in[0,T]$ and for all $\mathbf{x}=(x_1,x_2)^T\in\Omega_t^F$, find the velocity $\mathbf{v}(\mathbf{x},t)\in\mathbb{R}^2$ and the pressure $p(\mathbf{x},t)\in\mathbb{R}$ such that:

$$\rho^F\left(\frac{\partial\mathbf{v}}{\partial t}+(\mathbf{v}\cdot\nabla)\mathbf{v}\right)-\mu\Delta\mathbf{v}+\nabla p = \mathbf{f}^F,\quad \forall t\in(0,T),\forall\mathbf{x}\in\Omega_t^F \tag{5.17}$$

$$\nabla\cdot\mathbf{v} = 0,\quad \forall t\in(0,T),\forall\mathbf{x}\in\Omega_t^F \tag{5.18}$$

$$\mathbf{v}\times\mathbf{n} = 0,\quad \text{on } \Sigma_1\times(0,T) \tag{5.19}$$

$$p = P_{in},\quad \text{on } \Sigma_1\times(0,T) \tag{5.20}$$

$$\mathbf{v} = \mathbf{g},\quad \text{on } \Sigma_2\times(0,T) \tag{5.21}$$

$$\mathbf{v}\times\mathbf{n} = 0,\quad \text{on } \Sigma_3\times(0,T) \tag{5.22}$$

$$p = P_{out},\quad \text{on } \Sigma_3\times(0,T) \tag{5.23}$$

$$\mathbf{v}\left(x_1,H+u(x_1,t),t\right) = \left(0,\frac{\partial u}{\partial t}(x_1,t)\right)^T,\quad \forall(x_1,t)\in(0,L)\times(0,T) \tag{5.24}$$

$$\mathbf{v}(\mathbf{x},0) = \mathbf{v}^0(\mathbf{x}),\quad \forall\mathbf{x}\in\Omega_0^F \tag{5.25}$$

where

- $\rho^F>0$ and $\mu>0$ are the mass density and the viscosity of the fluid,

- $\mathbf{f}^F = (f_1^F, f_2^F)$ are the applied volume forces, in general the gravity forces,
- $\mathbf{g} = (g_1, g_2)^T : \Sigma_2 \times (0,T) \to \mathbb{R}^2$ is the imposed velocity profile on a part of the rigid boundary,
- $P_{in} : \Sigma_1 \times (0,T) \to \mathbb{R}$ and $P_{out} : \Sigma_3 \times (0,T) \to \mathbb{R}$ are prescribed boundary pressure,
- $\mathbf{v}^0 : \Omega_0^F \to \mathbb{R}^2$ is initial velocity and Ω_0^F is the initial domain.

We have supposed that the displacement u and the velocity $\frac{\partial u}{\partial t}$ of the moving wall are known, consequently the moving domain Ω_t^F which depends on u and the prescribed velocity on the elastic boundary Γ_t appearing in the boundary condition (5.24) are given.

The following notations have been used: $\mathbf{v} = (v_1, v_2)^T$, $\nabla \cdot \mathbf{v} = \frac{\partial v_1}{\partial x_1} + \frac{\partial v_2}{\partial x_2}$, $\mathbf{v} \times \mathbf{n} = v_1 n_2 - v_2 n_1$, $\Delta v_i = \frac{\partial^2 v_i}{\partial x_1^2} + \frac{\partial^2 v_i}{\partial x_2^2}$ for $i = 1, 2$,

$$\nabla p = \begin{pmatrix} \frac{\partial p}{\partial x_1} \\ \frac{\partial p}{\partial x_2} \end{pmatrix}, \quad \Delta \mathbf{v} = \begin{pmatrix} \Delta v_1 \\ \Delta v_2 \end{pmatrix}, \quad (\mathbf{v} \cdot \nabla)\mathbf{v} = \begin{pmatrix} v_1 \frac{\partial v_1}{\partial x_1} + v_2 \frac{\partial v_1}{\partial x_2} \\ v_1 \frac{\partial v_2}{\partial x_1} + v_2 \frac{\partial v_2}{\partial x_2} \end{pmatrix}.$$

The Navier-Stokes equations with boundary condition on pressure were firstly studied in [27].

5.2.2 The Arbitrary Lagrangian Eulerian coordinates and the time discretization

The Arbitrary Lagrangian Eulerian (ALE) framework was successfully used for the fluid structure interaction problems (see [29] and the references given there).

We denote by $\widehat{\Omega}^F = (0, L) \times (0, H)$ the reference domain and by $\widehat{\Gamma} = (0, L) \times \{H\}$ its top boundary. Since the moving boundary is a graph of a real function and the reference domain is a rectangle, we can construct explicitly so called the ALE map.

For each admissible displacement u, we consider following family of one-to-one continuous differentiable transformation $\mathcal{A}_t : \widehat{\Omega}^F \to \Omega_t^F$ given by:

$$\mathcal{A}_t(\widehat{x}_1, \widehat{x}_2) = \left(\widehat{x}_1, \frac{H + u(\widehat{x}_1, t)}{H} \widehat{x}_2 \right)^T$$

which admits the continuous differentiable inverse mapping

$$\mathcal{A}_t^{-1}(x_1, x_2) = \left(x_1, \frac{H x_2}{H + u(x_1, t)} \right)^T$$

and verifies that $\mathcal{A}_t\left(\widehat{\Omega}^F\right) = \Omega_t^F$, $\mathcal{A}_t\left(\widehat{\Gamma}\right) = \Gamma_t$ and $\mathcal{A}_t(\widehat{x}) = \widehat{x}$, $\forall \widehat{x} \in \Sigma$.

We set $\mathbf{x} = \mathcal{A}_t(\widehat{\mathbf{x}})$ for each $\mathbf{x} = (x_1, x_2) \in \Omega_t^F$ and $\widehat{\mathbf{x}} = (\widehat{x}_1, \widehat{x}_2) \in \widehat{\Omega}^F$.

We denote by $\widehat{\mathbf{v}}(\widehat{\mathbf{x}},t)=\mathbf{v}\left(\mathcal{A}_t(\widehat{\mathbf{x}}),t\right)$ and $\widehat{p}(\widehat{\mathbf{x}},t)=p\left(\mathcal{A}_t(\widehat{\mathbf{x}}),t\right)$ the velocity and the pressure using so-called Arbitrary Lagrangian Eulerian coordinates.

Let $\widehat{\mathbf{x}}$ be fixed. According to the chain rule, we have

$$\frac{\partial\widehat{\mathbf{v}}}{\partial t}(\widehat{\mathbf{x}},t)=\frac{d}{d\,t}\left[\mathbf{v}\left(\mathcal{A}_t(\widehat{\mathbf{x}}),t\right)\right]=\left(\frac{\partial\mathcal{A}_t}{\partial t}(\widehat{\mathbf{x}})\cdot\nabla\right)\mathbf{v}\left(\mathcal{A}_t(\widehat{\mathbf{x}}),t\right)+\frac{\partial\mathbf{v}}{\partial t}\left(\mathcal{A}_t(\widehat{\mathbf{x}}),t\right)$$

which implies

$$\frac{\partial\mathbf{v}}{\partial t}\left(\mathbf{x},t\right)=\frac{\partial\widehat{\mathbf{v}}}{\partial t}(\widehat{\mathbf{x}},t)-\left(\frac{\partial\mathcal{A}_t}{\partial t}(\widehat{\mathbf{x}})\cdot\nabla\right)\mathbf{v}\left(\mathbf{x},t\right). \tag{5.26}$$

Let $N\in\mathbb{N}^*$ be the number of time steps and $\Delta t=T/N$ the time step. We set $t_n=n\Delta t$ for $n=0,1,\ldots,N$. We will indicate $\mathbf{v}^{n+1}(\mathbf{x})$, $p^{n+1}(\mathbf{x})$ the approximations of $\mathbf{v}(\mathbf{x},t_{n+1})$, $p(\mathbf{x},t_{n+1})$ for $\mathbf{x}\in\Omega^F_{t_{n+1}}$.

We denote $\mathbf{x}=\mathcal{A}_{t_{n+1}}(\widehat{\mathbf{x}})$ and consequently $\widehat{\mathbf{x}}=\mathcal{A}^{-1}_{t_{n+1}}(\mathbf{x})$.

We can use the first order finite difference scheme

$$\begin{array}{l}\frac{\partial\widehat{\mathbf{v}}}{\partial t}(\widehat{\mathbf{x}},t_{n+1})\approx\frac{\widehat{\mathbf{v}}(\widehat{\mathbf{x}},t_{n+1})-\widehat{\mathbf{v}}(\widehat{\mathbf{x}},t_n)}{\Delta t}=\frac{\mathbf{v}\left(\mathcal{A}_{t_{n+1}}(\widehat{\mathbf{x}}),t_{n+1}\right)-\mathbf{v}(\mathcal{A}_{t_n}(\widehat{\mathbf{x}}),t_n)}{\Delta t}\\ =\frac{\mathbf{v}(\mathbf{x},t_{n+1})-\mathbf{v}\left(\mathcal{A}_{t_n}\circ\mathcal{A}^{-1}_{t_{n+1}}(\mathbf{x}),t_n\right)}{\Delta t}\approx\frac{\mathbf{v}^{n+1}(\mathbf{x})-\mathbf{v}^n\left(\mathcal{A}_{t_n}\circ\mathcal{A}^{-1}_{t_{n+1}}(\mathbf{x})\right)}{\Delta t}.\end{array}$$

Observe that the derivative $\frac{\partial\widehat{\mathbf{v}}}{\partial t}(\widehat{\mathbf{x}},t_{n+1})$ which depends on the ALE coordinates $\widehat{\mathbf{x}}$ can be approached by the expression $\frac{\mathbf{v}^{n+1}(\mathbf{x})-\mathbf{v}^n\left(\mathcal{A}_{t_n}\circ\mathcal{A}^{-1}_{t_{n+1}}(\mathbf{x})\right)}{\Delta t}$ written using the Eulerian coordinates $\mathbf{x}$.

By the definition, it follows

$$\frac{\partial\mathcal{A}_t}{\partial t}(\widehat{\mathbf{x}})=\left(0,\frac{\frac{\partial u}{\partial t}\left(\widehat{x}_1,t\right)}{H}\widehat{x}_2\right)^T$$

and by replacing $\widehat{\mathbf{x}}=\mathcal{A}^{-1}_{t_{n+1}}(\mathbf{x})$, we obtain

$$\boldsymbol{\vartheta}^{n+1}(\mathbf{x})\stackrel{def}{=}\frac{\partial\mathcal{A}_t}{\partial t}(\widehat{\mathbf{x}})|_{t=t_{n+1}}=\left(0,\frac{\partial u}{\partial t}\left(x_1,t_{n+1}\right)\frac{x_2}{H+u\left(x_1,t_{n+1}\right)}\right)^T.$$

Finally, from the equality (5.26), we can employ the approximation

$$\frac{\partial\mathbf{v}}{\partial t}(\mathbf{x},t_{n+1})\approx\frac{\mathbf{v}^{n+1}(\mathbf{x})-\mathbf{v}^n\left(\mathcal{A}_{t_n}\circ\mathcal{A}^{-1}_{t_{n+1}}(\mathbf{x})\right)}{\Delta t}-\left(\boldsymbol{\vartheta}^{n+1}(\mathbf{x})\cdot\nabla\right)\mathbf{v}^{n+1}(\mathbf{x}). \tag{5.27}$$

The time-advancing scheme is: knowing the velocity $\mathbf{v}^n:\Omega^F_{t_n}\to\mathbb{R}^2$ of the fluid at the previous time step and the displacement $u(\cdot,t_{n+1})$, the velocity $\frac{\partial u}{\partial t}(\cdot,t_{n+1})$ of the

moving boundary at the current time step, find the velocity $\mathbf{v}^{n+1} : \Omega^F_{t_{n+1}} \to \mathbb{R}^2$, the pressure $p^{n+1} : \Omega^F_{t_{n+1}} \to \mathbb{R}$ of the fluid, such that

$$\begin{aligned}
\rho^F \left(\frac{\mathbf{v}^{n+1}}{\Delta t} + \left((\mathbf{V}^n - \boldsymbol{\vartheta}^{n+1}) \cdot \nabla \right) \mathbf{v}^{n+1} \right) - \mu \Delta \mathbf{v}^{n+1} + \nabla p^{n+1} &= \rho^F \frac{\mathbf{V}^n}{\Delta t} + \mathbf{f}^F \\
&\quad \text{in } \Omega^F_{t_{n+1}} \qquad (5.28) \\
\nabla \cdot \mathbf{v}^{n+1} &= 0 \text{ in } \Omega^F_{t_{n+1}} \qquad (5.29) \\
\mathbf{v}^{n+1} \times \mathbf{n} &= 0 \text{ on } \Sigma_1 \qquad (5.30) \\
p^{n+1} &= P_{in}(\cdot, t_{n+1}) \\
&\quad \text{on } \Sigma_1 \qquad (5.31) \\
\mathbf{v}^{n+1} &= \mathbf{g}(\cdot, t_{n+1}) \text{ on } \Sigma_2 \qquad (5.32) \\
\mathbf{v}^{n+1} \times \mathbf{n} &= 0 \text{ on } \Sigma_3 \qquad (5.33) \\
p^{n+1} &= P_{out}(\cdot, t_{n+1}) \\
&\quad \text{on } \Sigma_3 \qquad (5.34) \\
\mathbf{v}^{n+1}\left(x_1, H + u(x_1, t_{n+1}), t\right) &= \left(0, \frac{\partial u}{\partial t}(x_1, t_{n+1})\right)^T, \\
&\quad 0 < x_1 < L. \qquad (5.35)
\end{aligned}$$

where $\mathbf{V}^n(\mathbf{x}) = \mathbf{v}^n\left(\mathcal{A}_{t_n} \circ \mathcal{A}^{-1}_{t_{n+1}}(\mathbf{x})\right)$ for all $\mathbf{x}$ in $\Omega^F_{t_{n+1}}$.

This is a first order time accurate scheme. The time derivative was approached by the backward Euler method. The nonlinear term $(\mathbf{v} \cdot \nabla)\mathbf{v}$ was treated semi-implicit, therefore we obtain a linear system whose associated matrix is not symmetric and it changes at each time step.

5.2.3 Mixed Finite Element approximation

We introduce the following Hilbert spaces:

$$\begin{aligned}
W^{n+1} &= \left\{ \mathbf{w} \in \left(H^1\left(\Omega^F_{t_{n+1}}\right)\right)^2;\ \mathbf{w} \times \mathbf{n} = 0 \text{ on } \Sigma_1 \cup \Sigma_3,\ \mathbf{w} = 0 \text{ on } \Sigma_2 \cup \Gamma_{t_{n+1}} \right\}, \\
Q^{n+1} &= L^2\left(\Omega^F_{t_{n+1}}\right).
\end{aligned}$$

Find the velocity $\mathbf{v}^{n+1} \in \left(H^1\left(\Omega^F_{t_{n+1}}\right)\right)^2$ satisfies the boundary conditions (5.30), (5.32), (5.33), (5.35) and the pressure $p^{n+1} \in L^2\left(\Omega^F_{t_{n+1}}\right)$ such that

$$\left\{ \begin{array}{lcll}
a^{n+1}_F\left(\mathbf{v}^{n+1}, \mathbf{w}\right) + d^{n+1}_F\left(\mathbf{v}^{n+1}, \mathbf{w}\right) + b^{n+1}_F\left(\mathbf{w}, p^{n+1}\right) &=& \ell^{n+1}(\mathbf{w}), & \forall \mathbf{w} \in W^{n+1} \\
b^{n+1}_F\left(\mathbf{v}^{n+1}, q\right) &=& 0, & \forall q \in Q^{n+1}
\end{array} \right. \qquad (5.36)$$

where

$$\begin{aligned} a_F^{n+1}\left(\mathbf{v}^{n+1},\mathbf{w}\right) &= \frac{\rho^F}{\Delta t}\left(\mathbf{v}^{n+1},\mathbf{w}\right) \\ &\quad +\mu\left(\nabla\times\mathbf{v}^{n+1},\nabla\times\mathbf{w}\right)+\mu\left(\nabla\cdot\mathbf{v}^{n+1},\nabla\cdot\mathbf{w}\right) \quad (5.37)\\ d_F^{n+1}\left(\mathbf{v}^{n+1},\mathbf{w}\right) &= \rho^F\left(\left(\left(\mathbf{V}^n-\boldsymbol{\vartheta}^{n+1}\right)\cdot\nabla\right)\mathbf{v}^{n+1},\mathbf{w}\right) \quad (5.38)\\ b_F^{n+1}\left(\mathbf{w},q\right) &= -\left(\nabla\cdot\mathbf{w},q\right) \quad (5.39)\\ \ell^{n+1}\left(\mathbf{w}\right) &= \frac{\rho^F}{\Delta t}\left(\mathbf{V}^n,\mathbf{w}\right)+\left(\mathbf{f}^F,\mathbf{w}\right) \\ &\quad -\int_{\Sigma_1}P_{in}(\cdot,t_{n+1})\mathbf{n}\cdot\mathbf{w}\,d\gamma-\int_{\Sigma_3}P_{out}(\cdot,t_{n+1})\mathbf{n}\cdot\mathbf{w}\,d\gamma \quad (5.40)\end{aligned}$$

and $(\cdot,\cdot)$ is the scalar product of $L^2\left(\Omega_{t_{n+1}}^F\right)$ or $\left(L^2\left(\Omega_{t_{n+1}}^F\right)\right)^2$.

Following [27, 17], the bilinear form $(\nabla\times\mathbf{y},\nabla\times\mathbf{w})+(\nabla\cdot\mathbf{y},\nabla\cdot\mathbf{w})$ is W^{n+1} elliptic and b_F^{n+1} satisfies *inf-sup* condition or Ladyzhenskaya-Babuska-Brezzi condition. If the bilinear form $a_F^{n+1}+d_F^{n+1}$ is elliptic on the subspace $\{\mathbf{w}\in W^{n+1};\ \nabla\cdot\mathbf{w}=0\}$, then the problem (5.36) has an unique solution.

For the approximation of the fluid velocity we have been used the finite elements $\mathbb{P}_1$ + *bubble* also refereed to as MINI elements introduced by Arnold, Brezzi and Fortin. For the fluid pressure the finite elements $\mathbb{P}_1$ have been employed.

5.3 Approximation of the coupled fluid-structure equations

5.3.1 Strong form of the coupled equations

In the previous sections, we have introduced separately the structure and the fluid equations.

The coupled fluid structure problem is: find the transverse displacement u satisfies (5.1)–(5.5), the velocity $\mathbf{v}$ and the pressure p satisfy (5.17)–(5.25) such that

$$\eta(x_1,t)=-\left(\sigma^F\mathbf{n}\cdot\mathbf{e}_2\right)_{(x_1,H+u(x_1,t))}\sqrt{1+\left(\frac{\partial u}{\partial x_1}(x_1,t)\right)^2} \quad (5.41)$$

where $\sigma^F=-p\,I+\mu\left(\nabla\mathbf{v}+\nabla\mathbf{v}^T\right)$ is the stress tensor of the fluid, $\mathbf{e}_2=(0,1)^T$ is the unit vector in the x_2 direction.

The displacement of the structure depends on the vertical component of the stresses exerted by the fluid on the interface (equations 5.1 and 5.41). This cames from the continuity of the stresses across the interface.

The movement of the structure changes the domain where the fluid equations must be solved (equations 5.17 and 5.18). Also, on the interface we have to impose the equality between the fluid and structure velocity (equation 5.24).

The stresses exerted by the fluid $-\sigma^F n$ are defined on the elastic wall Γ_t, while the stresses on the structure η are defined on the horizontal segment $\widehat{\Gamma}$. The factor $\sqrt{1+\left(\frac{\partial u}{\partial x_1}(x_1,t)\right)^2}$ which appears in the equation (5.41) is necessary to have

$$\int_{\Gamma_t} \sigma^F \mathbf{n}\cdot\mathbf{e}_2\, d\gamma = \int_0^L \left(\sigma^F \mathbf{n}\cdot\mathbf{e}_2\right)_{(x_1,H+u(x_1,t))} \sqrt{1+\left(\frac{\partial u}{\partial x_1}(x_1,t)\right)^2}\, dx_1.$$

The displacement u must be admissible or equivalent the elastic wall Γ_t does not touch the bottom boundary Σ_2.

The existence results for the fluid structure interaction can be found for example in [16, 1] for the steady case and in [15, 9, 2, 4] for the unsteady case. We didn't cited here the results concerning the interaction between a fluid and a rigid solid in rotation or in translation.

5.3.2 Identification of the stresses on the interface using the Least Squares Method

We recall that, the most frequently, the fluid-structure interaction problems are solved numerically by partitioned procedures, i.e. the fluid and the structure equations are solved separately. This can be done by using fixed point or Newton like methods. If the starting point is not chosen "sufficiently close" to the solution, these methods diverge.

In the following, the equation (5.41) will be treated by the Least Squares Method and at each time step we have to solve an optimization problem which is less sensitive to the choice of the starting point. This is the main advantage of this approach.

In order to evaluate the cost function, we must call one time the structure solver, to update the mesh and to call one time the fluid solver. We present the details below.

The unknowns of the optimization problem are the stresses on the interface.

Suppose that at the previous time step t_n we know:

- the approximations of the displacement, the velocity and the acceleration of the structure denoted respectively by

$$u_m^n(x_1) = \sum_{i=0}^{m-1} q_i^n \phi_i(x_1), \quad \dot{u}_m^n(x_1) = \sum_{i=0}^{m-1} \dot{q}_i^n \phi_i(x_1), \quad \ddot{u}_m^n(x_1) = \sum_{i=0}^{m-1} \ddot{q}_i^n \phi_i(x_1);$$

- the polygonal approximation of the fluid domain denoted by $\Omega_h^{F,n}$;

- the finite element approximations of the velocity and the pressure of the fluid denoted by $\mathbf{v}_h^n$ and p_h^n respectively.

We seek an approximation of the stresses on the interface at the current time step t_{n+1} of the form $\eta_m^{n+1}(x_1) = \sum_{i=0}^{m-1} \alpha_i^{n+1}\phi_i(x_1)$, where α_i^{n+1}, $i = 0, \ldots, m-1$ are the parameters to be identified.

Let $\boldsymbol{\alpha} = (\alpha_0, \ldots, \alpha_{m-1}) \in \mathbb{R}^m$.

Structure sub-problem

For $i = 0, \ldots, m-1$, knowing q_i^n, $\dot{q}_i^n$, $\ddot{q}_i^n$, find Q_i, $\dot{Q}_i$, $\ddot{Q}_i$ such that:

$$\left(1 + \omega_i^2(\Delta t)^2\theta\right)\ddot{Q}_i = \frac{1}{\rho^S h^S}\alpha_i - \omega_i^2\left[q_i^n + \Delta t\dot{q}_i^n + (\Delta t)^2\left(\frac{1}{2} - \theta\right)\ddot{q}_i^n\right] \tag{5.42}$$

$$\dot{Q}_i = \dot{q}_i^n + \Delta t\left[(1-\delta)\ddot{q}_i^n + \delta\ddot{Q}_i\right], \tag{5.43}$$

$$Q_i = q_i^n + \Delta t\dot{q}_i^n + (\Delta t)^2\left[\left(\frac{1}{2} - \theta\right)\ddot{q}_i^n + \theta\ddot{Q}_i\right] \tag{5.44}$$

The above equations have been obtained from (5.16), (5.13), (5.14) replacing α_i^{n+1}, q_i^{n+1}, $\dot{q}_i^{n+1}$, $\ddot{q}_i^{n+1}$ by α_i, Q_i, $\dot{Q}_i$, $\ddot{Q}_i$ respectively.

Set

$$U(x_1) = \sum_{i=0}^{m-1} Q_i\phi_i(x_1), \quad \dot{U}(x_1) = \sum_{i=0}^{m-1} \dot{Q}_i\phi_i(x_1), \quad \ddot{U}(x_1) = \sum_{i=0}^{m-1} \ddot{Q}_i\phi_i(x_1).$$

Fluid sub-problem

Let $\widehat{\mathcal{T}}_h$ be a mesh with triangular elements of the reference domain $\widehat{\Omega}^F$. We define the mesh with triangular elements $\mathcal{T}_h$ by moving each node of $\widehat{\mathcal{T}}_h$ using the map

$$\mathcal{A}_U\left(\widehat{x}_1, \widehat{x}_2\right) = \left(\widehat{x}_1, \frac{H + U\left(\widehat{x}_1\right)}{H}\widehat{x}_2\right)^T.$$

We denote by Ω_h^F the polygonal domain corresponding to the mesh $\mathcal{T}_h$ and we have $\partial\Omega_h^F = \Sigma_1 \cup \Sigma_2 \cup \Sigma_3 \cup \Gamma_h$ where Γ_h is the top boundary.

Let us introduce the finite dimension spaces

$$\begin{aligned} W_h &= \left\{\mathbf{w}_h \in \left(C^0\left(\overline{\Omega}_h^F\right)\right)^2;\ \forall K \text{ triangle of } \mathcal{T}_h,\ \mathbf{w}_h|_K \in P1 + bubble,\right. \\ &\quad \left.\mathbf{w}_h \times \mathbf{n} = 0 \text{ on } \Sigma_1 \cup \Sigma_3,\ \mathbf{w}_h = 0 \text{ on } \Sigma_2 \cup \Gamma_h\right\}, \\ Q_h &= \left\{q_h \in C^0\left(\overline{\Omega}_h^F\right);\ \forall K \text{ triangle of } \mathcal{T}_h,\ q_h|_K \in P1\right\}. \end{aligned}$$

Remark that the finite element spaces are defined directly on the physical domain. Many authors (see [28, 22, 29]) use a different framework: the test function in the

physical domain is obtained from the one in a reference domain via the ALE map. In this case, we have to pay attention to the quadrature formulas (see [29]).

Find the velocity $\mathbf{v}_h$ satisfies the boundary conditions

$$\begin{aligned} \mathbf{v}_h \times \mathbf{n} &= 0, \text{ on each vertex of } \Sigma_1 \cup \Sigma_3, \\ \mathbf{v}_h &= \mathbf{g}(\cdot, t_{n+1}), \text{ on each vertex of } \Sigma_2, \\ \mathbf{v}_h &= \left(0, \dot{U}\right)^T, \text{ on each vertex of the top boundary } \Gamma_h \end{aligned}$$

and the pressure $p_h \in Q_h$ such that

$$\left\{ \begin{array}{lll} a_F^{n+1}(\mathbf{v}_h, \mathbf{w}_h) + d_F^{n+1}(\mathbf{v}_h, \mathbf{w}_h) + b_F^{n+1}(\mathbf{w}_h, p_h) &= \ell^{n+1}(\mathbf{w}_h), & \forall \mathbf{w}_h \in W_h \\ b_F^{n+1}(\mathbf{v}_h, q_h) &= 0, & \forall q_h \in Q_h \end{array} \right. \tag{5.45}$$

When $\ell^{n+1}(\mathbf{w}_h)$ is evaluated, we have to replace $\mathcal{A}_{t_n} \circ \mathcal{A}_{t_{n+1}}^{-1}$ by $\mathcal{A}_{u_m^n} \circ \mathcal{A}_U^{-1}$ in the definition (5.40).

Definition of the cost function

The right side part of the equation (5.41), which represents the stresses from fluid acting on the interface, will be approached by $\sum_{i=0}^{m-1} \beta_i \phi_i(x_1)$.

Let us define for $i = 0, \ldots, m-1$

$$\beta_i = -\int_0^L \phi_i(x_1) \left(\sigma^F(\mathbf{v}_h, p_h)\, \mathbf{n} \cdot \mathbf{e}_2\right)_{(x_1, H+U(x_1))} \sqrt{1 + \left(\frac{\partial U}{\partial x_1}(x_1)\right)^2}\, dx_1.$$

Since $\mathbf{n} = (n_1, n_2)^T = \frac{1}{\sqrt{1+\left(\frac{\partial U}{\partial x_1}\right)^2}} \left(-\frac{\partial U}{\partial x_1}, 1\right)^T$, we obtain

$$\beta_i = \int_0^L \phi_i(x_1) \left(p_h - \mu \left(\frac{\partial v_{h,1}}{\partial x_2} + \frac{\partial v_{h,2}}{\partial x_1}\right) \left(-\frac{\partial U}{\partial x_1}\right) - 2\mu \frac{\partial v_{h,2}}{\partial x_2}\right)_{(x_1, H+U(x_1))} dx_1.$$

Set the cost function

$$J^{n+1}(\boldsymbol{\alpha}) = \frac{1}{2} \sum_{i=0}^{m-1} (\alpha_i - \beta_i)^2.$$

The terms containing the viscosity can be neglected from the boundary expressions. Consequently, we could use the simpler formula

$$\beta_i = \int_0^L \phi_i(x_1) p_h(x_1, H + U(x_1))\, dx_1, \quad i = 0, \ldots, m-1.$$

We recall that the stresses on the interface at the current time step t_{n+1} will be approached by $\eta_m^{n+1}(x_1) = \sum_{i=0}^{m-1} \alpha_i^{n+1} \phi_i(x_1)$.

The parameters α_i^{n+1} for $0 \leq i \leq m-1$ will be "identified" solving an optimization problem, more precisely

$$\boldsymbol{\alpha}^{n+1} \stackrel{def}{=} \left(\alpha_0^{n+1}, \ldots, \alpha_{m-1}^{n+1}\right) \in \arg\min_{\boldsymbol{\alpha}\in\mathbb{R}^m} J^{n+1}(\boldsymbol{\alpha}).$$

We will see in the following that the above defined cost function is related to the fixed point approach for fluid-structure interaction.

We introduce the structure operator given by $\mathcal{S}(\boldsymbol{\alpha}) = \left(Q, \dot{Q}, \ddot{Q}\right)$ and the fluid operator given by
$\mathcal{F}\left(Q, \dot{Q}, \ddot{Q}\right) = \boldsymbol{\beta}$, where $\left(Q, \dot{Q}, \ddot{Q}\right) = \left(Q_i, \dot{Q}_i, \ddot{Q}_i\right)_{0\leq i\leq m-1}$.

Our approach is to minimize

$$J^{n+1}(\boldsymbol{\alpha}) = \frac{1}{2}\left\|\boldsymbol{\alpha} - \boldsymbol{\beta}\right\|_2^2 = \frac{1}{2}\left\|\boldsymbol{\alpha} - \mathcal{F}\circ\mathcal{S}(\boldsymbol{\alpha})\right\|_2^2$$

where $\|\cdot\|_2$ stands the Euclidean norm of $\mathbb{R}^m$.

The fixed point framework is to solve $\mathcal{F}\circ\mathcal{S}(\boldsymbol{\alpha}) = \boldsymbol{\alpha}$.

Some authors use the displacement of the structure in place of $\boldsymbol{\alpha}$ as a fixed point. In the following we will study the sensitivity of the displacement and velocity of the structure with respect to $\boldsymbol{\alpha}$. This enables us to compare the solution computed minimizing the cost function with the ones presented in [26, 14, 12].

Let

$$\left(dQ, d\dot{Q}, d\ddot{Q}\right) = \mathcal{S}(\boldsymbol{\alpha}) - \mathcal{S}(\boldsymbol{\beta})$$

where $\left(dQ, d\dot{Q}, d\ddot{Q}\right) = \left(dQ_i, d\dot{Q}_i, d\ddot{Q}_i\right)_{0\leq i\leq m-1}$ and set

$$dU(x_1) = \sum_{i=0}^{m-1} dQ_i\,\phi_i(x_1), \quad d\dot{U}(x_1) = \sum_{i=0}^{m-1} d\dot{Q}_i\,\phi_i(x_1).$$

We denote by $\|\cdot\|_{L^2(0,L)}$ the usual norm of the space $L^2(0,L)$.

Proposition 5.1 *We have*

$$\|dU\|_{L^2(0,L)} \leq \frac{(\Delta t)^2\theta}{\rho^S h^S}\sqrt{2J^{n+1}(\boldsymbol{\alpha})} \tag{5.46}$$

$$\left\|d\dot{U}\right\|_{L^2(0,L)} \leq \frac{(\Delta t)\delta}{\rho^S h^S}\sqrt{2J^{n+1}(\boldsymbol{\alpha})}. \tag{5.47}$$

Proof. From the equations (5.42)–(5.44), we obtain that

$$d\ddot{Q}_i = \frac{1}{(1+\omega_i^2(\Delta t)^2\theta)}\frac{1}{\rho^S h^S}(\alpha_i - \beta_i), \quad d\dot{Q}_i = (\Delta t)\delta\, d\ddot{Q}_i, \quad dQ_i = (\Delta t)^2\theta\, d\ddot{Q}_i.$$

Since $\theta > 0$, we have $(1 + \omega_i^2 (\Delta t)^2 \theta) > 1$ and consequently

$$\left| d\ddot{Q}_i \right| \leq \frac{1}{\rho^S h^S} \left| \alpha_i - \beta_i \right|, \quad \left| d\dot{Q}_i \right| \leq \frac{(\Delta t)\delta}{\rho^S h^S} \left| \alpha_i - \beta_i \right|, \quad |dQ_i| \leq \frac{(\Delta t)^2 \theta}{\rho^S h^S} \left| \alpha_i - \beta_i \right|.$$

Using that $\{\phi_i\}_{i \in \mathbb{N}}$ is a orthonormal basis of $L^2(0, L)$, we have

$$\|dU\|^2_{L^2(0,L)} = \sum_{i=0}^{m-1} |dQ_i|^2 \leq \left(\frac{(\Delta t)^2 \theta}{\rho^S h^S} \right)^2 \cdot \sum_{i=0}^{m-1} |\alpha_i - \beta_i|^2 .$$

By definition $2J^{n+1}(\boldsymbol{\alpha}) = \sum_{i=0}^{m-1} |\alpha_i - \beta_i|^2$. Therefore, it follows (5.46).

In the same manner, we can prove (5.47). □

The inequalities (5.46) and (5.47) mean that the difference between the displacements or the velocities of the structure obtained at two consecutive steps of fixed point algorithm is bounded by an expression depending on the cost function.

5.3.3 Coupled fluid-structure algorithm by the BFGS Method

In order to solve at the current time step t_{n+1} the optimization problem $\min J^{n+1}(\boldsymbol{\alpha})$ for $\boldsymbol{\alpha} \in \mathbb{R}^m$, we employ the quasi-Newton iterative method called Broyden, Fletcher, Goldforb, Shano (BFGS) scheme (see for example [6], chap. 9).

Step 0. Choose a starting point $\boldsymbol{\alpha}^{n+1,0} \in \mathbb{R}^m$, an $m \times m$ symmetric positive matrix H_0 and a positive scalar ϵ. Set $k = 0$.

Step 1. Compute $\nabla J^{n+1}(\boldsymbol{\alpha}^{n+1,k})$.

Step 2. If $\left\| \nabla J^{n+1}(\boldsymbol{\alpha}^{n+1,k}) \right\| < \epsilon$ stop.

Step 3. Set $\mathbf{d}^k = -H_k \nabla J^{n+1}(\boldsymbol{\alpha}^{n+1,k})$.

Step 4. Determine $\boldsymbol{\alpha}^{n+1,k+1} = \boldsymbol{\alpha}^{n+1,k} + \theta_k \mathbf{d}^k$, $\theta_k > 0$ by means of an approximate minimization

$$J^{n+1}(\boldsymbol{\alpha}^{n+1,k+1}) \approx \min_{\theta \geq 0} J^{n+1}(\boldsymbol{\alpha}^{n+1,k} + \theta \mathbf{d}^k).$$

Step 5. Compute $\delta_k = \boldsymbol{\alpha}^{n+1,k+1} - \boldsymbol{\alpha}^{n+1,k}$.

Step 6. Compute $\nabla J^{n+1}(\boldsymbol{\alpha}^{n+1,k+1})$ and $\gamma_k = \nabla J^{n+1}(\boldsymbol{\alpha}^{n+1,k+1}) - \nabla J^{n+1}(\boldsymbol{\alpha}^{n+1,k})$.

Step 7. Compute

$$H_{k+1} = H_k + \left(1 + \frac{\gamma_k^T H_k \gamma_k}{\delta_k^T \gamma_k} \right) \frac{\delta_k \delta_k^T}{\delta_k^T \gamma_k} - \frac{\delta_k \gamma_k^T H_k + H_k \gamma_k \delta_k^T}{\delta_k^T \gamma_k}$$

Step 8. Update $k = k + 1$ and go to the **Step 2**.

The matrices H_k approach the inverse of the Hessian of J.

For the inaccurate line search at the **Step 4**, the methods of Goldstein and Armijo were used.

The coupled fluid-structure algorithm is: suppose that at the previous time step t_n we know $u_m^n = \sum_{i=0}^{m-1} q_i^n \phi_i$, $\dot{u}_m^n = \sum_{i=0}^{m-1} \dot{q}_i^n \phi_i$, $\ddot{u}_m^n = \sum_{i=0}^{m-1} \ddot{q}_i^n \phi_i$, $\mathbf{v}_h^n$ and p_h^n, then solve

$$\boldsymbol{\alpha}^{n+1} \in \arg \min_{\boldsymbol{\alpha} \in \mathbb{R}^m} J^{n+1}(\boldsymbol{\alpha})$$

using the BFGS scheme. The solution $\boldsymbol{\alpha}^{n+1}$ is the last term of the suite $\boldsymbol{\alpha}^{n+1,0}$, ... , $\boldsymbol{\alpha}^{n+1,k}$, $\boldsymbol{\alpha}^{n+1,k+1}$, ...

The stresses on the interface at the current time step t_{n+1} are given by

$$\eta_m^{n+1}(x_1) = \sum_{i=0}^{m-1} \alpha_i^{n+1} \phi_i(x_1).$$

At each evaluation of the cost function we have to solve one structure sub-problem, to update the mesh and to solve one fluid sub-problem. We denote by u_m^{n+1}, $\dot{u}_m^{n+1}$, $\ddot{u}_m^{n+1}$ the solution of the structure sub-problem and by $\mathbf{v}_h^{n+1}$ and p_h^{n+1} the solution of the fluid sub-problem when J^{n+1} is evaluated in the point $\boldsymbol{\alpha}^{n+1}$.

In this paper, we compute $\nabla J^{n+1}(\boldsymbol{\alpha})$ by the Finite Differences Method

$$\frac{\partial J^{n+1}}{\partial \alpha_k}(\boldsymbol{\alpha}) \approx \frac{J^{n+1}(\boldsymbol{\alpha} + \Delta\alpha_k \mathbf{e_k}) - J^{n+1}(\boldsymbol{\alpha})}{\Delta\alpha_k}$$

where $\mathbf{e_k}$ is the k-th vector of the canonical base of $\mathbb{R}^m$ and $\Delta\alpha_k > 0$ is the grid spacing.

5.3.4 Fixed point, Newton and BFGS Methods

In this section, we analyze different iterative methods for solving coupled fluid-structure problems.

In the previous section, we have presented the BFGS Method in order to solve the optimization problem

$$\inf_{\boldsymbol{\alpha} \in \mathbb{R}^m} J(\boldsymbol{\alpha}) = \frac{1}{2} \left\| \boldsymbol{\alpha} - \mathcal{F} \circ \mathcal{S}(\boldsymbol{\alpha}) \right\|^2$$

where $\|\cdot\|$ stands the Euclidean norm of $\mathbb{R}^m$.

The fixed point framework is to solve $\mathcal{F} \circ \mathcal{S}(\boldsymbol{\alpha}) = \boldsymbol{\alpha}$.

Let $G : \mathbb{R}^m \to \mathbb{R}^m$ the nonlinear application given by $G(\boldsymbol{\alpha}) = \mathcal{F} \circ \mathcal{S}(\boldsymbol{\alpha})$. In order to approach the fixed point $G(\boldsymbol{\alpha}^*) = \boldsymbol{\alpha}^*$, we could use the following algorithm

$$\boldsymbol{\alpha}^0 \in \mathbb{R}^n, \quad \boldsymbol{\alpha}^{k+1} = G(\boldsymbol{\alpha}^k).$$

If G is a contraction and if the starting point $\boldsymbol{\alpha}^0$ is sufficiently close to the solution, then the sequence $\left\{\boldsymbol{\alpha}^k\right\}$ is linearly convergent to $\boldsymbol{\alpha}^*$.

We can set $F : \mathbb{R}^m \to \mathbb{R}^m$, $F(\boldsymbol{\alpha}) = \boldsymbol{\alpha} - G(\boldsymbol{\alpha})$, then the fixed point problem is equivalent to $F(\boldsymbol{\alpha}) = 0$. The Newton Method can be employed for finding the roots of F:

$$\boldsymbol{\alpha}^0 \in \mathbb{R}^m, \quad \boldsymbol{\alpha}^{k+1} = \boldsymbol{\alpha}^k - \left(\nabla F(\boldsymbol{\alpha}^k)^T\right)^{-1} F(\boldsymbol{\alpha}^k).$$

If the Jacobian matrix $\nabla F(\boldsymbol{\alpha}^*)^T$ is nonsingular and the starting point is sufficiently close to the solution, then the sequence $\left\{\boldsymbol{\alpha}^k\right\}$ is quadratically convergent.

In a general framework, the BFGS Method is designed to find approximation of the local minimizers of J, solutions of the nonlinear system $\nabla J(\boldsymbol{\alpha}) = 0$. Its convergence is superlinarly. In our particular case $J(\boldsymbol{\alpha}) = \frac{1}{2}\left\|F(\boldsymbol{\alpha})\right\|^2$, we get

$$\nabla J(\boldsymbol{\alpha}) = \left(\nabla F(\boldsymbol{\alpha})\right) F(\boldsymbol{\alpha}).$$

Consequently, if $\boldsymbol{\alpha}^*$ is a local minimizer, then $\left(\nabla F(\boldsymbol{\alpha}^*)\right) F(\boldsymbol{\alpha}^*) = 0$. What is most surprising is the fact that if the Jacobian matrix $\nabla F(\boldsymbol{\alpha}^*)^T$ is nonsingular, from the above equality we obtain that $F(\boldsymbol{\alpha}^*) = 0$! In other words, a local minimizer $\boldsymbol{\alpha}^*$, with nonsingular Jacobian matrix $\nabla F(\boldsymbol{\alpha}^*)^T$, is a global minimizer of zero residual, i.e. $J(\boldsymbol{\alpha}^*) = 0$. Only in the case when $\nabla F(\boldsymbol{\alpha}^*)^T$ is singular and $F(\boldsymbol{\alpha}^*) \neq 0$, the solution computed by the BFGS Method is not a solution of the fluid-structure coupled problem.

We have to recall that the Newton method fails if $\nabla F(\boldsymbol{\alpha}^*)^T$ is nonsingular.

Concerning the convergence rate, the fixed point algorithm is slower than the BFGS Method, which is slower than the Newton Method. But, if the starting point is not sufficiently close to the solution, the fixed point and Newton algorithms diverge.

On the contrary, the BFGS Method is less sensitive to the choice of the starting point and, in general, it is convergent to a local minimizer from almost any starting point. This is the main advantage.

At each iteration of the Newton Method we have to solve a linear system of matrix $\nabla F(\boldsymbol{\alpha}^k)^T$, but it is not the case if we employ the BFGS Method, since the matrices H_k approach the inverse of the Hessian. Moreover, if the Jacobian matrix $\nabla F(\boldsymbol{\alpha}^k)^T$ is singular or ill-conditioned, the Newton Method doesn't work.

5.4 Numerical results

5.4.1 Case of an impulsive pressure wave in a higher compliant channel

Input data. We have tested on the 2D benchmark proposed in [13] arising from blood flow in arteries. Our numerical experiments have only an academic purpose. The structure equation (5.1) is not appropriate to model the artery wall. However, the algorithm presented in this paper can be easily adapted to simulate the blood flow in arteries by replacing (5.1) by the one dimensional axisymetric membrane model.

The computation has been made in a domain of length $L = 6\ cm$ and height $H = 1\ cm$. The viscosity of the fluid was taken to be $\mu = 0.035\ \frac{g}{cm \cdot s}$, its density $\rho^F = 1\ \frac{g}{cm^3}$. The thickness of the elastic wall is $h^S = 0.1\ cm$, the Young modulus $E = 0.75 \cdot 10^6\ \frac{g}{cm \cdot s^2}$, the Poisson ratio $\nu = 0.5$, the density $\rho^S = 1.1\ \frac{g}{cm^3}$. The volume force in fluid is $\mathbf{f}^F = (0,0)^T$.

We remark that the structure is light and its density is comparable to the ones of the fluid. For this data, the fixed point algorithm with relaxation can diverge if the relaxation parameter is not carefully chosen [26].

For the boundary conditions we have used:

$$\begin{aligned} P_{in}(\mathbf{x},t) &= \begin{cases} 10^3(1-\cos(2\pi t/0.005)), & \mathbf{x} \in \Sigma_1, 0 \le t \le 0.005 \\ 0, & \mathbf{x} \in \Sigma_1, 0.005 \le t \le T \end{cases} \\ \mathbf{g}(\mathbf{x},t) &= 0, \quad \mathbf{x} \in \Sigma_2, 0 \le t \le T \\ P_{out}(\mathbf{x},t) &= 0, \quad \mathbf{x} \in \Sigma_3, 0 \le t \le T \end{aligned}$$

and for the initial conditions we have taken: $u^0 = 0$, $\dot{u}^0 = 0$, $\ddot{u}^0 = 0$, $\mathbf{v}^0 = 0$.

The maximal pressure imposed at the inflow is $P_{in}(\cdot, 0.0025) = 2000\ \frac{dynes}{cm^2}$ and the time duration of the over-pressure at the inflow is $0.005\ s$.

We have performed the simulation for $N = 500$ time steps with a time step $\Delta t = 0.0005\ s$ which gives a time duration $T = N\Delta t = 0.25\ s$.

The numerical tests have been produced using *freefem++ v1.34* (see [18]).

Only the first 5 modes have been considered for the structure. In order to compute the normal mode shapes, the system (5.6)–(5.9) has been solved using the software *Maple*. For the Newmark algorithm we have used $\delta = 0.6$ and $\theta = 0.5$.

For the approximation of the fluid velocity and pressure we have employed the triangular finite elements $\mathbb{P}_1$+*bubble* and $\mathbb{P}_1$ respectively. We have used three reference meshes of parameters presented in Table 5.1.

Δt	mesh size h	no. triangles	no. vertices
0.0005	$h_1 = 0.25$	196	127
0.0005	$h_2 = 0.17$	226	448
0.0005	$h_3 = 0.10$	1250	696

Table 5.1: Parameters for the three tests with same time step and different mesh sizes

The gradient of the cost function is approached by the Finite Differences Method with the grid spacing $\Delta\alpha_k = 0.001$.

Starting point for the minimization algorithm. In our computations, the stress at the previous time step $\boldsymbol{\alpha}^n$ is used as starting point in the iterative method at the current time step. We remark in the left picture of Figure 5.2 that the starting values of the cost function are huge during the over-pressure imposed at the inflow. This means that

the **starting point is not closed to the solution**, where the cost function reaches the zero value. Also, we observe that the **starting values of the cost function are not very sensitive to the mesh size**.

Stopping criteria and efficiency. At each time step, the optimization problem have been solved by the BFGS algorithm.

We have employed the *freefem++* implementation of the BFGS algorithm which use the stopping criteria: $\|\nabla J\| < \epsilon$ or the number of iterations reaches a maximal value *nbiter*. We have performed the computations with $\epsilon = 10^{-4}$ and $nbiter = 8$. We set to 4 the maximal number of the iterations for the line search. For the Least Squares problems of zero residual, a more useful stopping criteria is $\|J\| < \epsilon$, but it is not implemented yet.

To sum up, at each time step the cost function is called at most

$$\text{maximal number iterations BFGS} \times (m + \text{maximal number iterations line search}).$$

At each evaluation of the cost function we have to solve one structure sub-problem, to update the mesh and to solve one fluid sub-problem.

The final values of the cost function are less than 10^{-3} almost everywhere with very few exceptions (see Figure 5.3).

From the formulas (5.46) and (5.47), it follows:

$$\begin{aligned}
\left\|d\dot{U}\right\|_{L^2(0,L)} &\leq \frac{(\Delta t)\delta}{\rho^S h^S}\sqrt{2J^{n+1}(\boldsymbol{\alpha})} \leq \frac{0.0005 \cdot 0.6}{1.1 \cdot 0.1}\sqrt{2 \cdot 10^{-3}} \approx 1.21 \cdot 10^{-4} \\
\|dU\|_{L^2(0,L)} &\leq \frac{(\Delta t)^2\theta}{\rho^S h^S}\sqrt{2J^{n+1}(\boldsymbol{\alpha})} \leq \frac{(0.0005)^2 \cdot 0.5}{1.1 \cdot 0.1}\sqrt{2 \cdot 10^{-3}} \approx 5.08 \cdot 10^{-8}.
\end{aligned}$$

In [26], at each time step, the coupled fluid-structure problem was solved by fixed point strategy with a relaxation parameter. At the start up of the simulation an important number of iterations (see [26], Figure 4.14, p. 150) is necessary to satisfy the criteria

$$\max\left(\frac{\|dU\|_{L^\infty}}{\|U\|_{L^\infty}}, \frac{\left\|d\dot{U}\right\|_{L^\infty}}{\left\|\dot{U}\right\|_{L^\infty}}\right) \leq 10^{-4}.$$

The convergence of the fixed point algorithm can be accelerated using the Aitken's [14] or transpiration method [7].

Good convergence rate was obtained in [14] where the derivative of the operator was replaced by a much simpler operator. In order to achieve $\|dU\| \leq 10^{-6}$, six iterations of quasi-Newton method are required.

In [12], the block Newton algorithm is used where the jacobian is evaluated exactly. The convergence is obtained in 2-3 iterations, only.

Behavior of the computed solution. The coupled fluid-structure algorithm is numerically stable for $\Delta t = 0.0005\ s$.

The wave starts from the left side (see Figures 5.4, 5.5) and it will be reflected at the right side. The animations including the displacement of the structure and the pressure of the fluid can be visualized on the web page of the author. The pulse speed is about 170 cm/s. In [13, 26], a 3D fluid-structure model is coupled with a 1D reduced model in order to reduce the reflexion due to the inappropriate boundary conditions for the structure and for the fluid on the right side.

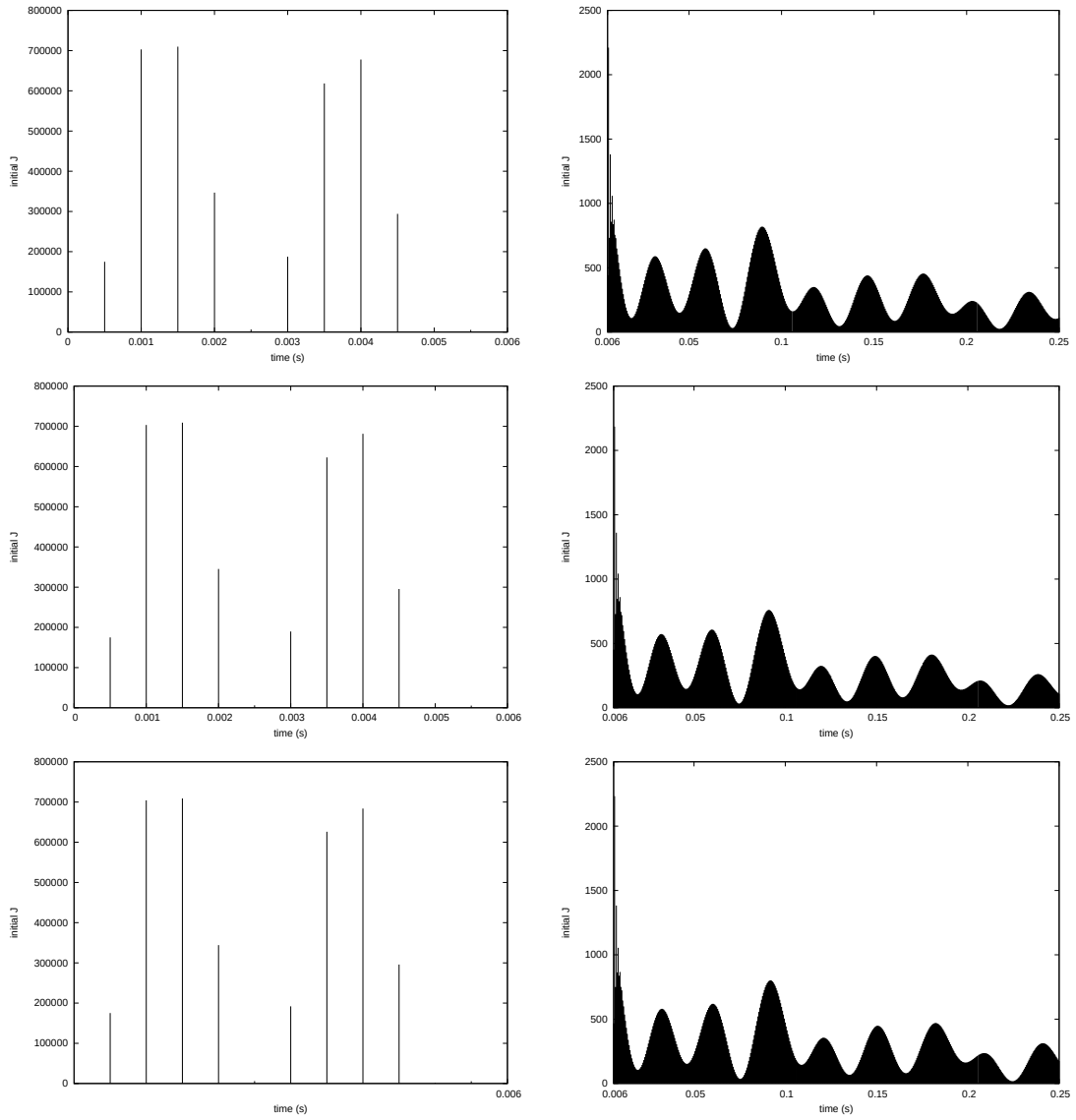

Figure 5.2: Starting values of the cost function during the pressure impulse (at the left) and after (at the right) for the mesh sizes h_1 (top), h_2 (middle), h_3 (bottom).

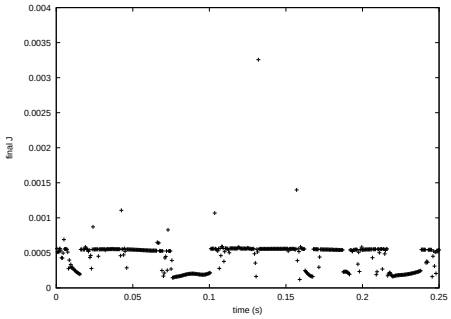

Figure 5.3: Final values of the cost function at each time step for the mesh size h_1.

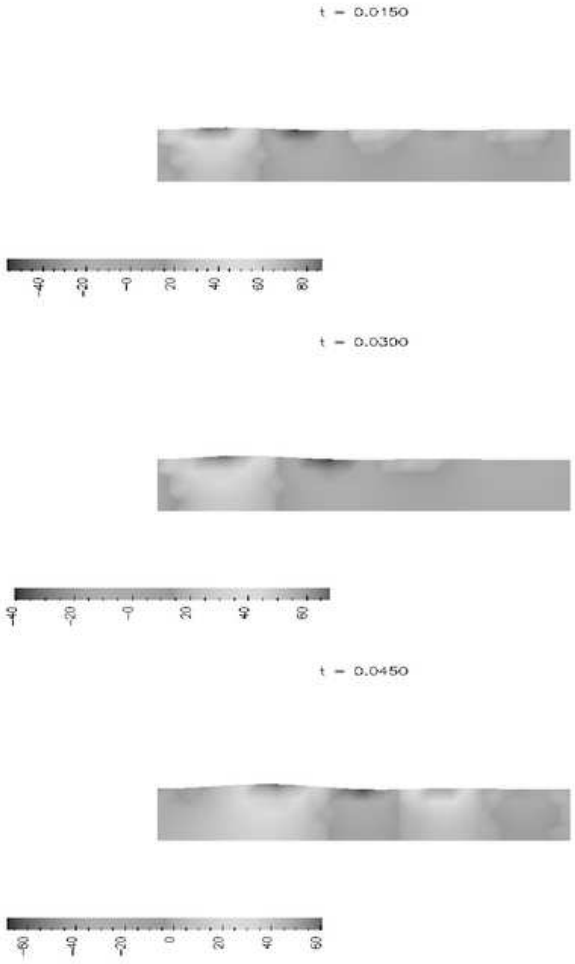

Figure 5.4: Fluid pressure $[\frac{dynes}{cm^2}]$

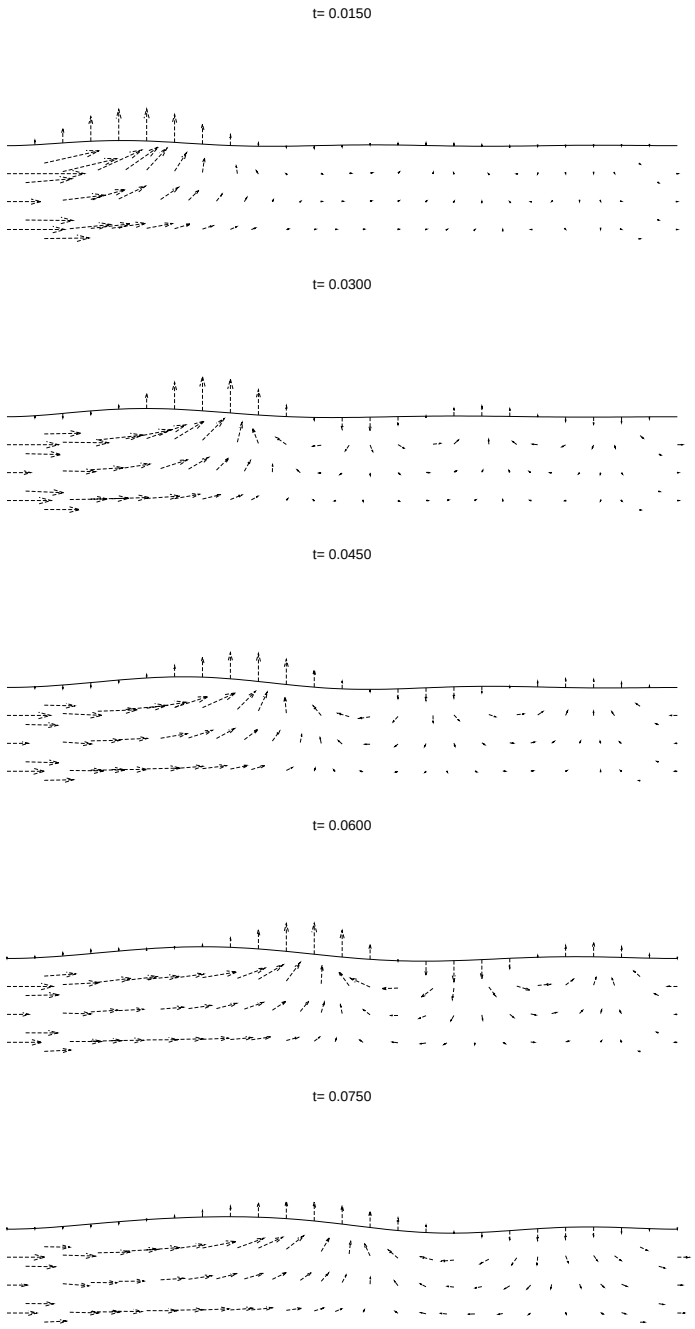

Figure 5.5: Displacements $[cm]$ of the top wall and fluid velocity $[\frac{cm}{s}]$. The arrows were scaled by a factor 0.1

5.4.2 Case of a sine wave of the pressure input in a less compliant channel

We will test now the sensitivity of the computed data by increasing the time step Δt. The BFGS method will be successful from farther starting point.

The simulations were performed for $E = 3 \cdot 10^6 \ \frac{g}{cm \cdot s^2}$ the Young modulus of the structure and for a five times longer over-pressure at the inflow:

$$P_{in}(\mathbf{x},t) = \begin{cases} 10^3(1-\cos(2\pi t/0.025)), & \mathbf{x} \in \Sigma_1, 0 \le t \le 0.025 \\ 0, & \mathbf{x} \in \Sigma_1, 0.025 \le t \le T \end{cases}$$

The other parameters are the same as in the previous test.

For the three numerical tests, we have used the same reference mesh of 448 triangles and 267 vertices.

The time step Δt, the mesh size h, the number of time steps N and $T = N\Delta t$ are reported in Table 5.2.

Δt	h	N	T
0.0005	0.17	200	0.1
0.0010	0.17	100	0.1
0.0025	0.17	40	0.1

Table 5.2: Parameters for the three numerical tests

The stress at the previous time step $\boldsymbol{\alpha}^n$ is used as starting point in the iterative method for solving the minimization problem $\min_{\boldsymbol{\alpha} \in \mathbb{R}^m} J^{n+1}(\boldsymbol{\alpha})$ at the current time step. The starting values of the cost function $J^{n+1}(\boldsymbol{\alpha}^n)$ are showed in the left column of Figure 5.6.

Remark that some values of the cost function in the starting points can reach $1.8 \cdot 10^5$ when $\Delta t = 0.0005$ or $5 \cdot 10^5$ when $\Delta t = 0.0010$ or $1.2 \cdot 10^6$ when $\Delta t = 0.0025$. These great values mean that for some time instants, **the solution at the previous time step is not closed to the solution at the current time step**.

Also, we observe that values of the cost function in the **starting points are very sensitive to** Δt.

At each time step, the BFGS algorithm find efficiently an optimal value of the cost function less than 0.00055 (see the right column of Figure 5.6).

We have performed less than 10 iterations of the BFGS algorithm and less than 5 iterations for the line search at each time step.

Even in the case of important displacements of the structure, the algorithm is successful (see Figure 5.7).

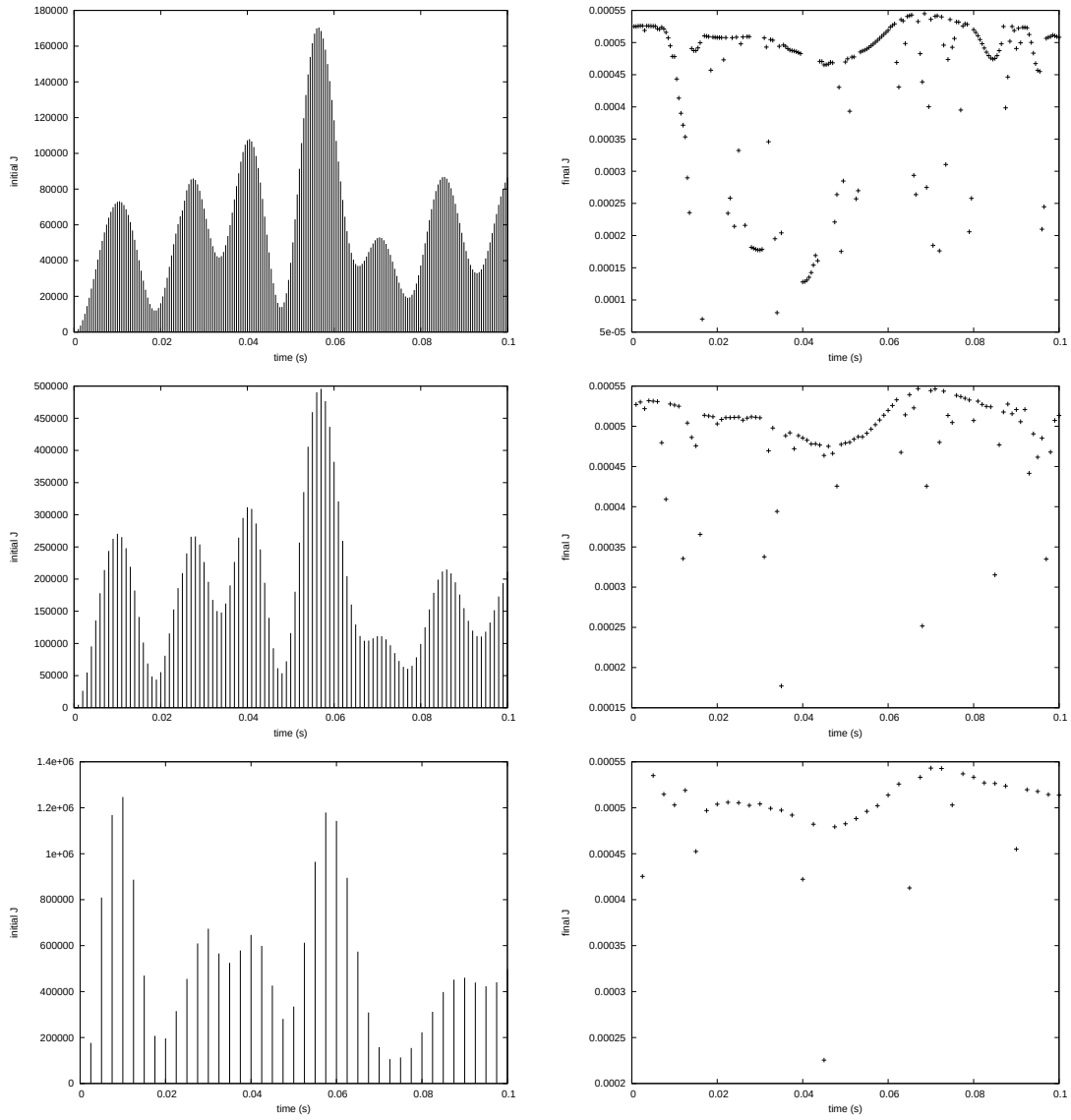

Figure 5.6: Starting (left) and final (right) values of the cost function for $\Delta t = 0.0005$ (top), $\Delta t = 0.0010$ (middle) and $\Delta t = 0.0025$ (bottom)

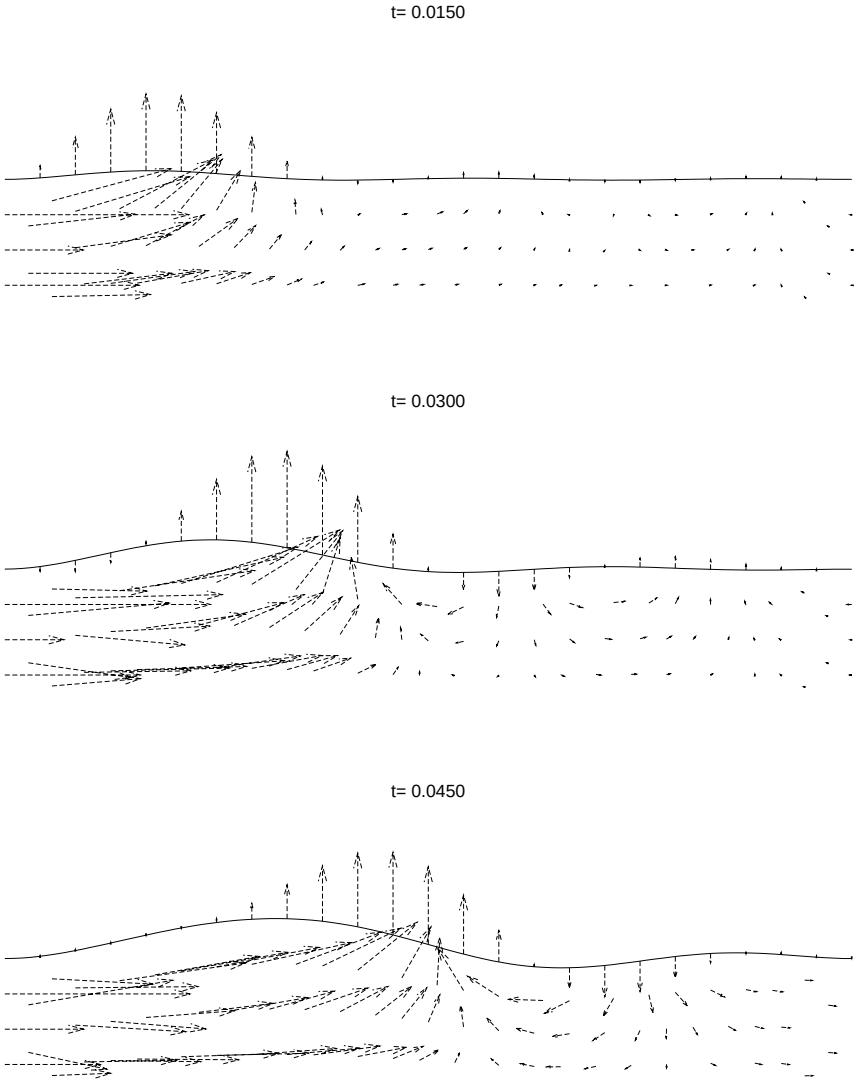

Figure 5.7: Displacements $[cm]$ of the top wall and fluid velocity $[\frac{cm}{s}]$. The arrows were scaled by a factor 0.05

5.4.3 Modified Newton Method

The Modified Newton Method (Newton Method with line search strategies) inherits the fast local convergence of the Newton Method and, in the same time, it is less sensitive to the starting point. We will see that, in some situations, this method can be a better choice than the BFGS Method.

Step 0. Choose a starting point $\boldsymbol{\alpha}^0 \in \mathbb{R}^m$ and a positive scalar ϵ. Set $k = 0$.

Step 1. If $\left\|F(\boldsymbol{\alpha}^k)\right\| < \epsilon$ stop.

Step 2. Set $\mathbf{d}^k = -\left(\left(\nabla F(\boldsymbol{\alpha}^k)\right)^T\right)^{-1} F(\boldsymbol{\alpha}^k)$.

Step 3. Determine $\boldsymbol{\alpha}^{k+1} = \boldsymbol{\alpha}^k + \theta_k \mathbf{d}^k$, $\theta_k > 0$ by means of an approximate minimization

$$\left\|F(\boldsymbol{\alpha}^{k+1})\right\| \approx \min_{\theta \geq 0} \left\|F(\boldsymbol{\alpha}^k + \theta \mathbf{d}^k)\right\|.$$

Step 4. Update $k = k + 1$ and go to the **Step 1**.

In this paper, we make distinction between the *Modified Newton Method* described above and the *Newton Method* where at the Step 3, we always take $\theta_k = 1$.

First, we will employ the *Modified Newton Method* for a nonlinear problem in $\mathbb{R}^2$, then for a fluid-structure interaction problem presented previously.

Validation tests

Let $F : \mathbb{R}^2 \to \mathbb{R}^2$ be defined by

$$F(\boldsymbol{\alpha}) = F(\alpha_1, \alpha_2) = \begin{pmatrix} \alpha_1^2 + \alpha_2^2 - 2 \\ \exp(\alpha_1 - 1) + \alpha_2^2 - 2 \end{pmatrix}$$

which has the roots $(1, 1)^T$ and $(1, -1)^T$. Numerical results obtained by Newton Method for solving $F(\boldsymbol{\alpha}) = (0, 0)^T$ are presented in [19]. The Jacobian of F can be computed analytically by

$$(\nabla F(\boldsymbol{\alpha}))^T = \begin{pmatrix} 2\alpha_1 & 2\alpha_2 \\ \exp(\alpha_1 - 1) & 2\alpha_2 \end{pmatrix}.$$

Observe that the Jacobian is singular for $\alpha_2 = 0$.

We have investigated Newton, BFGS and Modified Newton methods for two initial starting points: $\boldsymbol{\alpha}^0 = (2, 3)^T$ and $\boldsymbol{\alpha}^0 = (3, 5)^T$ using *freefem++* [18]. The line search strategy implemented in *freefem++* starts with the step $\theta = 1$ and then, if it is not acceptable, reduces it using backtracking with cubic interpolation (see [6], Section 6.3.2, pp. 126–129).

We denote by $J(\boldsymbol{\alpha}) = \frac{1}{2}\left\|F(\boldsymbol{\alpha})\right\|^2$, where $\|\cdot\|$ is the Euclidian norm of $\mathbb{R}^2$. The gradient can be computed analytically by $\nabla J(\boldsymbol{\alpha}) = (\nabla F(\boldsymbol{\alpha}))\, F(\boldsymbol{\alpha})$.

The first starting point: $\boldsymbol{\alpha}^0 = (2,3)^T$

Newton Method. Only 4 iterations are needed to the Newton Method in order to satisfy the stopping criteria $\|F(\boldsymbol{\alpha})\| < \epsilon$, where $\epsilon = 10^{-3}$. At the initial iteration we have $\boldsymbol{\alpha}^0 = (2,3)^T$, $J(\boldsymbol{\alpha}^0) = 107.723$. At the final iteration we have obtained: $\boldsymbol{\alpha}^4 = (1,\ 1.00011)^T$, $J(\boldsymbol{\alpha}^4) = 5.01828e-08$ and

$$F(\boldsymbol{\alpha}^4) = (0.000224015,\ 0.000224015)^T.$$

BFGS Method. The stopping criteria $\|\nabla J(\boldsymbol{\alpha})\| < \epsilon$ for $\epsilon = 10^{-3}$ is reached after 25 iterations. The mean number of evaluations of the cost function J is 5.16 for the inaccurate line search. At the final iteration we have obtained: $\boldsymbol{\alpha}^{25} = (1.00015,\ -1.00036)^T$, $J(\boldsymbol{\alpha}^{25}) = 9.05405e-07$ and

$$\nabla J(\boldsymbol{\alpha}^{25}) = (0.000299141,\ -0.000724457)^T.$$

Modified Newton Method. We have performed the computations with the same line search strategy as in the BFGS Method. The stopping criteria $\|F(\boldsymbol{\alpha})\| < \epsilon$ holds after 12 iterations, where $\epsilon = 10^{-3}$. The mean number of evaluations of the cost function J is 4 for the inaccurate line search. At the final iteration we have obtained: $\boldsymbol{\alpha}^{12} = (0.999982,\ 0.999824)^T$, $J(\boldsymbol{\alpha}^{12}) = 1.42877e-07$ and

$$F(\boldsymbol{\alpha}^{12}) = (-0.000386687,\ -0.000369091)^T.$$

Discussions. The Newton method is the faster. The BFGS Method performs 25 iterations, while the Modified Newton Method only 12 to obtain a final cost function of about 10^{-7}. The Newton and Modified Newton Methods approach the root $(1,1)^T$ and the BFGS Method finds the other root $(1,-1)^T$.

The second starting point: $\boldsymbol{\alpha}^0 = (3,5)^T$

The *Newton Method* is divergent for this starting point. The history of the cost function is the following: $J(\boldsymbol{\alpha}^0) = 974.747$, $J(\boldsymbol{\alpha}^1) = 396.045$, $J(\boldsymbol{\alpha}^2) = 1309.35$.

The *Modified Newton Method* will stagnate from the 9th to the 30th iteration near the point
$\boldsymbol{\alpha} = (3.47282,\ 0.000614253)^T$ which is not a solution because $J(\boldsymbol{\alpha}) = 99.1761$ and $F(\boldsymbol{\alpha}) = (10.06,\ 9.85592)^T$. This stagnation is a consequence of the fact that the Jacobian is singular for $\alpha_2 = 0$.

We have performed 30 iterations of the *BFGS Method*. The mean number of evaluations of the cost function J for the inaccurate line search is 4.33. At the final iteration we have obtained: $\boldsymbol{\alpha}^{30} = (0.996168,\ -0.998812)^T$, $J(\boldsymbol{\alpha}^{30}) = 6.9477e-05$ and $\nabla J(\boldsymbol{\alpha}^{30}) = (0.00758799,\ 0.002399)^T$.

Also, we have tested the *BFGS Method* with the starting point
$\boldsymbol{\alpha} = (3.47282,\ 0.000614253)^T$ which is a stagnation point for the *Modified Newton*

Method. After the 21 iterations, the *BFGS Method* finds $\boldsymbol{\alpha} = (-0.47772,\ 1.33111)$, where $J(\boldsymbol{\alpha}) = 3.62384e-09$.

Discussions. If the starting points is not close to the solution, the Newton Method is divergent. Contrary to the Modified Newton Method, the BFGS Method gives satisfaction even in the neighborhood of the points where the Jacobian is singular.

Solving fluid-structure interaction by Modified Newton Method

In Section 5.4.2, we have presented numerical results for solving a fluid-structure interaction problem. At each time step, the BFGS Method was employed to solve $\inf J(\boldsymbol{\alpha}) = \frac{1}{2}\left\|F(\boldsymbol{\alpha})\right\|^2$.

The aim of this section is to compare the performances of the Modified Newton and BFGS methods for solving a particular fluid-structure interaction problem. The stopping criteria for the Modified Newton Method $\|F(\boldsymbol{\alpha})\| < \epsilon$ is not equivalent to the one used by the BFGS Method $\|\nabla J\| = \|(\nabla F(\boldsymbol{\alpha}))\, F(\boldsymbol{\alpha})\| < \epsilon$, so we will proceed in the following manner: at each time step, we perform the same number of iterations of the both methods. We will compare the values of the cost function $J(\boldsymbol{\alpha})$ after 10 iterations. Then we will observe which method gives the smaller values. The same inexact line search strategy will be employed.

Moderate time step

For the time step $\Delta t = 0.0005$, the BFGS methods finds final values of J less than 0.0006. The numerical results obtained by the Modified Newton Method are reported in the right plot of Figure 5.8. The BFGS method wins at each time iteration.

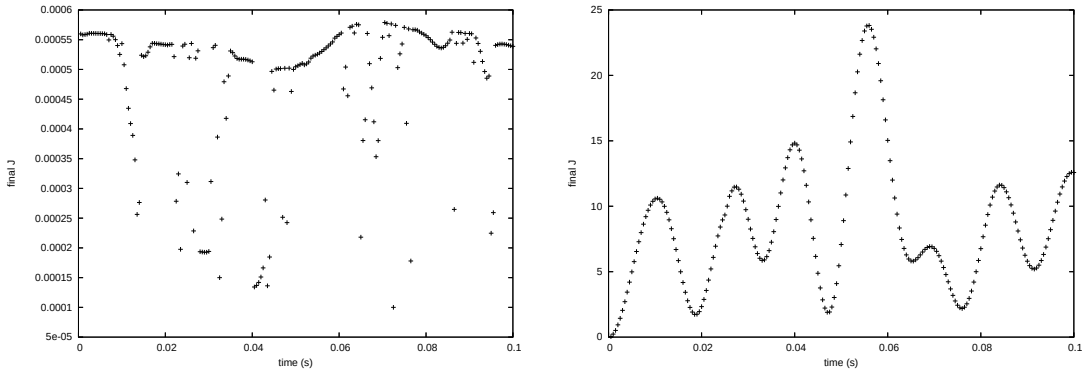

Figure 5.8: Final values of J obtained by the BFGS (left) and Modified Newton Method (right) for $\Delta t = 0.0005$

Concerning the CPU time, in order to perform $N = 200$ time iterations, the BFGS Method needs 2 hours, 30 minutes and 55 seconds while the Modified Newton Method

needs 3 hours, 34 minutes and 38 seconds on a computer with two processors of 3.6 GHz frequency.

The Jacobian of F was computed by the same Finite Differences scheme as for ∇J

$$\frac{\partial F}{\partial \alpha_k}(\boldsymbol{\alpha}) \approx \frac{F(\boldsymbol{\alpha} + \Delta\alpha_k \mathbf{e_k}) - F(\boldsymbol{\alpha})}{\Delta\alpha_k}$$

where $\mathbf{e_k}$ is the k-th vector of the canonical base of $\mathbb{R}^m$ and $\Delta\alpha_k > 0$ is the grid spacing. The columns of the Jacobian are the vectors $\frac{\partial F}{\partial \alpha_k}$. In spite of the fact that the gradient of J is a vector of dimension m and the Jacobian of F is a $m \times m$ matrix, the computation of the both needs the same number of evaluation of F, more precisely $m+1$. Contrary to the BFGS Method, at each iteration the Modified Newton Method requires the solution of a linear system in order to compute the direction $\mathbf{d}^k$.

Also, for the time step $\Delta t = 10^{-4}$, the BFGS methods finds values of J smaller than the Modified Newton Method.

Small time step

We have performed numerical tests for $N = 100$ time iterations with the step $\Delta t = 10^{-5}$. We can see in Figure 5.9, that the Modified Newton Method finds smaller values than the BFGS Method.

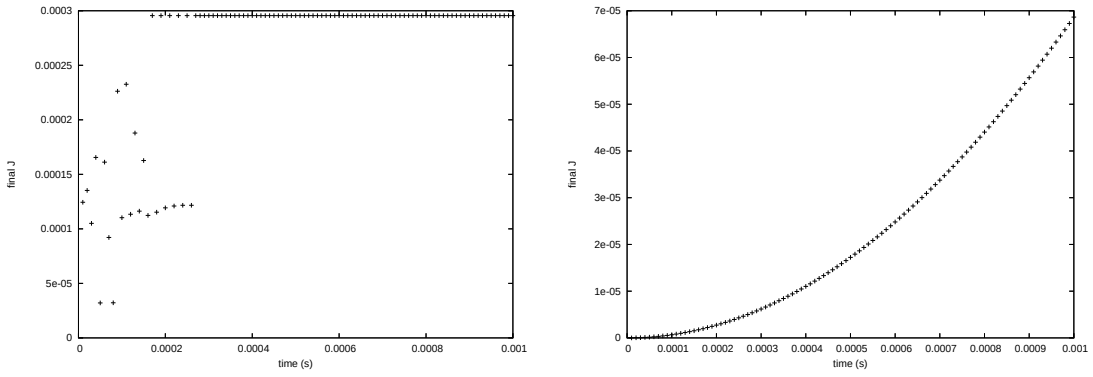

Figure 5.9: Final values of J obtained by the BFGS (left) and Modified Newton Method (right) for $\Delta t = 10^{-5}$

The CPU time is 76 minutes and 9 seconds for the BFGS Method and 107 minutes and 27 seconds for the Modified Newton Method.

After the time instant $t = 0.0003$, the BFGS Method obtains final values of J which have the first digits 0.0002955. The further digits change, but this is not visible on the left plot of Figure 5.9.

Discussions. The numerical results presented in this section suggest to use the Modified Newton Method for small time steps, while the BFGS Method is preferable for moderate time steps.

5.5 Conclusions

In this paper, the continuity of the stresses at the interface was treated by the Least Squares Method. At each time step we have to solve an optimization problem which is less sensitive to the choice of the starting point and it permits us to use moderate time step. This is the main advantage of this approach.

For moderate time step, the solution at the previous time step is not close to the solution at the current time instant. Such phenomena is amplified during the phase when the flow rate increase or decrease rapidly or if we increase the time step. In order to solve the optimization problem, we have employed the BFGS method which is successful from farther starting point. The gradient of the cost function was approached by the Finite Difference Method.

The coupled fluid-structure algorithm has good stability properties.

We conclude with a suggestion from [6]: use Newton like methods for their fast local convergence when ever it seems to be working well, otherwise use a slower method such BFGS but which is designed to converge to the local minimizer from almost any starting point.

Bibliography

[1] G. Bayada, M. Chambat, B. Cid and C. Vazquez, On the existence of solution for a non-homogeneus Stokes-rod coupled problem. *Nonlinear Analysis: Theory, Methods and Applications*, **59** (2004) 1-19.

[2] H. Beirao da Veiga, On the existence of strong solution to a coupled fluid structure evolution problem. *J. Math. Fluid Mech.* **6** (2004) 21–52.

[3] P. Causin, J.F. Gerbeau, F. Nobile, Added-mass effect in the design of partitioned algorithms for fluid-structure problems, *Comput. Methods Appl. Mech. Engrg.*, **194** (2005), no. 42-44, 4506–4527

[4] A. Chambolle, B. Desjardins, M. J. Esteban, C. Grandmont, Existence of weak solutions for an unsteady fluid-plate interaction problem, *J. Math. Fluid Mech.* **7** (2005), no. 3, 368–404.

[5] R. Dautray and J.L. Lions, *Analyse mathématique et calcul numérique pour les sciences et les techniques*, vol. 7, 9, Masson, (1988).

[6] J.E. Dennis Jr. and R.B. Schnabel, Numerical methods for unconstrained optimization and nonlinear equations. Classics in Applied Mathematics, 16. Society for Industrial and Applied Mathematics, Philadelphia, PA, (1996).

[7] S. Deparis, M.A. Fernandez and L. Formaggia, Acceleration of a fixed point algorithm for fluid-structure interaction using transpiration conditions. *Math. Model. Numer. Anal.* **37** (2003) no. 4, 601–616.

[8] S. Deparis, Numerical Analysis of Axisymmetric Flows and Methods for Fluid-Structure Interaction Arising in Blood Flow Simulation, PhD, Ecole Polytechnique Féderale de Lausanne, Switzerland, (2004).

[9] B. Desjardins, M. Esteban, C. Grandmont and P. Le Tallec, Weak solutions for a fluid-elastic structure interaction model. *Rev. Mat. Complut.* **14** (2001), no. 2, 523–538.

[10] G. Duvaut and J.-L. Lions, *Les inéquations en mécanique et en physique*. Dunod, Paris, (1972).

[11] C. Farhat, M. Lesoinne, Two efficient staggered algorithms for the serial and parallel solution of three-dimensional nonlinear transient aeroelastic problems, *Comput. Methods Appl. Mech. Engrg.* **182** (3-4) (2000) 499–515.

[12] M.A. Fernandez and M. Moubachir, A Newton method using exact jacobians for solving fluid-structure coupling. *Comput. & Structures* **83** (2005), no. 2-3, 127–142.

[13] L. Formaggia, J. F. Gerbeau, F. Nobile and A. Quarteroni, On the coupling of 3D and 1D Navier-Stokes equations for flow problems in compliant vessels. *Comput. Methods Appl. Mech. Engrg.* **191** (2001), no. 6-7, 561–582.

[14] J.F. Gerbeau and M. Vidrascu, A quasi-Newton algorithm on a reduced model for fluid - structure interaction problems in blood flows. *Math. Model. Numer. Anal.* **37** (2003), no. 4, 663–680.

[15] C. Grandmont and Y. Maday, Existence for an unsteady fluid-structure interaction problem. *Math. Model. Numer. Anal.* **34** (2000), no. 3, 609–636.

[16] C. Grandmont, Existence for a three-dimensional steady state fluid-structure interaction problem. *J. Math. Fluid Mech.* **4** (2002), no. 1, 76–94.

[17] J.-L. Guermond and L. Quartapelle, On the approximation of the unsteady Navier-Stokes equations by finite element projection methods. *Numer. Math.* **80** (1998) 207–238.

[18] F. Hecht and O. Pironneau, A finite element software for PDE: freefem++, `http://www.freefem.org`.

[19] C.T. Kelley, Solving nonlinear equations with Newton's method. Fundamentals of Algorithms. Society for Industrial and Applied Mathematics (SIAM), Philadelphia, PA, 2003.

[20] H.P. Langtangen, Computational Partial Differential Equations: numerical methods and Diffpack programming, Springer, Berlin, (1999).

[21] P. Le Tallec, Introduction à la dynamique des structures, Cours Ecole Polytechnique, Ellipses, (2000).

[22] P. Le Tallec and J. Mouro, Fluid-structure interaction with large structural displacements. *Comput. Methods Appl. Mech. Engrg.* **190** (2001) no. 24-25, 3039–3067.

[23] Y. Maday, B. Maury, P. Metier, Interaction de fluides potentiels avec une membrane élastique, in *ESAIM Proc.* **10** (1999), Soc. Math. Appl. Indust., Paris, pp. 23–33.

[24] C. Murea, The BFGS algorithm for a nonlinear least squares problem arising from blood flow in arteries. *Comput. Math. Appl.* **49** (2005), 171–186.

[25] C. Murea and C. Vazquez, Sensitivity and approximation of the coupled fluid-structure equations by virtual control method. *Appl. Math. Optim.* **52** (2005), no. 2, 357–371.

[26] F. Nobile, *Numerical approximation of fluid-structure interaction problems with application to haemodynamics*. PhD thesis, EPFL, Lausanne, (2001).

[27] O. Pironneau, Conditions aux limites sur la pression pour les équations de Stokes et Navier-Stokes. *C. R. Acad. Sc. Paris*, **303** (1986), no. 9, 403–406.

[28] A. Quarteroni, M. Tuveri and A. Veneziani, Computational vascular fluid dynamics: problems, models and methods. *Comput. Visual. Sci.* **2** (2000) 163–197.

[29] A. Quarteroni and L. Formaggia, Mathematical Modelling and Numerical Simulation of the Cardiovascular System. Chapter in *Modelling of Living Systems*, N. Ayache Ed., Handbook of Numerical Analysis Series, vol. XII, P.G Ciarlet Ed., Elsevier, Amsterdam, (2004).

[30] J. Steindorf and H.G. Matthies, Partioned but strongly coupled iteration schemes for nonlinear fluid-structure interaction. *Comput. & Structures* **80** (2002) 1991–1999.

Chapter 6

Dynamic meshes generation using the relaxation method with applications to fluid-structure interaction problems

This chapter is based on the paper:

C.M. Murea, Dynamic meshes generation using the relaxation method with applications to fluid-structure interaction problems, *An. Univ. Bucuresti Mat.*, **47** (1998), No. 2, pp. 177–186

6.1 Introduction

The numerical solutions for some partial differential equations in moving boundary domains using the Finite Element Method requires to know a mesh of the domain at each time step.

We assume that the boundary of the domain is known at each instant.

We could generate the mesh of the domain at the instant $t_0 + \triangle t$ ignoring the mesh at the initial instant t_0, but this approach has the following bad points: the mesh generation takes time and we don't own a mesh generator capable to built a mesh for the 3D domains with complex geometry knowing only the "skin" of the mesh.

Consequently, we shall try to adapt the initial mesh to the current boundary.

In [1], the displacement of an interior node is computed iteratively making a mean of the displacements of the neighboring nodes.

In [3, p. 90], the displacement of an interior node is computed making a weight mean of the displacements of the boundary nodes.

In [6], the placement of the interior nodes is obtained minimizing a deformation

energy of an elastic body.

Also, a method based on a minimization of a deformation energy will be employed in this paper in order to generate the dynamic meshes. The all generated meshes will have the same number of nodes as the initial mesh.

6.2 Presentation of the method

Let Ω^0 be a domain in $\mathbb{R}^3$ and $\mathcal{T}_h^0$ his mesh.

Let $\{A_i\}_{1\leq i\leq NBV}$ be the nodes of the mesh.

The coordinates of the nodes are $(x_i^0,\ y_i^0,\ z_i^0)_{1\leq i\leq NBV}$.

Let us consider the following sets of indices:

$$Int = \{i \in \{1,\ldots,NBV\}\,;\ A_i \text{ is an interior node of } \Omega^0\}$$
$$Fr = \{i \in \{1,\ldots,NBV\}\,;\ A_i \text{ is a boundary node of } \Omega^0\}$$

For each node A_i of the mesh, we note J_i the set of the indices of the neighboring nodes, more exactly

$$J_i = \left\{j \in \{1,\ldots,NBV\}\,;\ [A_iA_j] \text{ is an edge of } \mathcal{T}_h^0\right\}$$

The domain Ω^0 moves and we assume that the new coordinates $(\overline{x}_i,\ \overline{y}_i,\ \overline{z}_i)_{i\in Fr}$ of the boundary nodes are known.

The problem is to replace the interior nodes in order to obtain a reasonable mesh for the deformed domain.

Modeling each edge of the mesh by a string, the new coordinates of the interior nodes $(\overline{x}_i,\ \overline{y}_i,\ \overline{z}_i)_{i\in Int}$ will be computed minimizing the following energy:

$$J\left(x_i,\ y_i,\ z_i\ ;\ i \in Int\right) =$$
$$\frac{1}{2}\sum_{\substack{1\leq i<j\leq NBV\\ (i\in Int)\vee(j\in Int)}} \left[(x_i-x_j)^2+(y_i-y_j)^2+(z_i-z_j)^2\right]$$

Proposition 6.1 *The optimization problem without constraints* $\inf J$ *has a unique solution characterized by:*

$$\forall i \in Int$$
$$\overline{x}_i = \frac{1}{card\left(J_i\right)}\sum_{j\in J_i}\overline{x}_j \quad \textit{and the similar relations for } \overline{y}_i,\ \overline{z}_i \tag{6.1}$$

Proof: The application J is two times continuous differentiable and her Hessian is a diagonal matrix.

Since for all i in Int we have $\partial^2 J/\partial x_i^2 = card\left(J_i\right)$ and the similar relations for y_i and z_i, it follows that J is elliptic (see [2], for example).

Using the standard optimization results, we obtain that the optimization problem without constraints $\inf J$ has a unique solution characterized by the relations (6.1). □

6.3 Approximation using the relaxation method

In order to solve numerically the linear system (6.1), we could use a lot of algorithms. We have prefered a relaxation like method for her efficiency (only 3-4 iterations are sufficient for obtaining a reasonable mesh) and which can be easily implemented.

The algorithm

Step 1 We know:
$(x_i^0,\ y_i^0,\ z_i^0)_{1\leq i\leq NBV}$ the coordinates of the nodes of the initial mesh;
$(\overline{x}_i,\ \overline{y}_i,\ \overline{z}_i)_{i\in Fr}$ the coordinates of the boundary nodes of the moved mesh;
$\omega \in \mathbb{R}$ the relaxation parameter;
$k \leftarrow 0$ the iterations counter;

Step 2 For all $i \in Int$ we compute:

$$x_i^{k+1} = (1-\omega)\, x_i^k + \frac{\omega}{card\,(J_i)} \left(\sum_{j\in J_i \cap Int} x_j^k + \sum_{j\in J_i \cap Fr} \overline{x}_j \right)$$

We compute y_i^{k+1} and z_i^{k+1} similarly.

Step 3 We set $k \leftarrow k+1$ and go to Step 2

In the following, a convergence result will be proved.

Theorem 6.1 *For any* $(x_i^0,\ y_i^0,\ z_i^0)_{1\leq i\leq NBV}$ *and* $(\overline{x}_i,\ \overline{y}_i,\ \overline{z}_i)_{i\in Fr}$, *if* $\omega \in (0,1]$ *then the above algorithm is convergent to the unique solution of the optimization problem* $\inf J$.

Proof: The algorithm has the form $X^{k+1} = BX^k + c$, where

$$B = (b_{ij})_{i,j\in Int}\,, \quad b_{ij} = \begin{cases} 1-\omega & \text{if } i=j \\ \frac{\omega}{card(J_i)} & \text{if } j \in J_i \cap Int \\ 0 & \text{otherwise} \end{cases}$$

It is known that X^k is convergent if and only if $\rho\,(B) < 1$.
We have

$$\rho\,(B) \leq \|B\|_\infty = \max_{i\in Int} \left(\sum_{j\in J_i} |b_{ij}| \right)$$
$$\leq \max_{i\in Int} \left(1 - \omega + \omega \frac{card\,(J_i \cap Int)}{card\,(J_i)} \right) \leq 1$$

but we have to prove the strict inequality.

We proceed by contradiction: let λ be an eigenvalue of B such that $|\lambda| = 1$.

First, we prove the following inequalities:

$$\forall i \in Int, \quad |\lambda - b_{ii}| \geq \sum_{\substack{j \in Int \\ j \neq i}} |b_{ij}| \tag{6.2}$$

For all $i \in Int$ we have $|\lambda| - |b_{ii}| \leq |\lambda - b_{ii}|$.

If there exists i in Int such that

$$|\lambda - b_{ii}| < \sum_{\substack{j \in Int \\ j \neq i}} |b_{ij}|$$

then

$$|\lambda| < \sum_{j \in Int} |b_{ij}| .$$

Since $\omega \in (0, 1]$ and using the values of b_{ij}, it follows

$$1 < 1 - \omega + \omega \frac{card\,(J_i \cap Int)}{card\,(J_i)} \leq 1$$

which is a contradiction, consequently the inequalities (6.2) hold.

The matrix B is evidently symmetric.

We shall prove that it is irreductible, too. It is known that a matrix is irreductible if and only if his associated graph is strongly connex (see [5, vol. 1, p. 35, Lemma 27]). The associated graph of the matrix B is in fact the mesh $\mathcal{T}_h^0$ after we have eliminated the boundary nodes and all edge that have as an end point a boundary node. Therefore B is irreductible.

Knowing that the matrix B is symmetric and irreductible, from the inequalities (6.2) and according to a Gerschgörin - Hadamard theorem (see [5, vol. 1, p. 57, Theorem 57]), we have

$$\forall i \in Int, \quad |\lambda - b_{ii}| = \sum_{\substack{j \in Int \\ j \neq i}} |b_{ij}|$$

It follows

$$\forall i \in Int, \quad |\lambda| - |b_{ii}| \leq \sum_{\substack{j \in Int \\ j \neq i}} |b_{ij}| \Rightarrow$$

$$\forall i \in Int, \quad 1 \leq 1 - \omega + \omega \frac{card\,(J_i \cap Int)}{card\,(J_i)}$$

But there exists $i \in Int$ such that

$$card\,(J_i \cap Int) < card\,(J_i)$$

therefore

$$\exists i \in Int, \quad 1 \leq 1 - \omega + \omega \frac{card\,(J_i \cap Int)}{card\,(J_i)} < 1$$

We have get a contradiction, consequently the theorem is proved. □

6.4 Some numerical results

In order to made the mesh of the domain at the initial instant, we have used the 3D mesh generators MODULEF [7]. The mesh has: 74 boundary nodes, 29 interior nodes, 336 tetrahedron. All adapted meshes will have the same characteristics.

The domain moves and we can see in the Appendix A how the algorithm adapts the initial mesh to the current boundaries. Only 3-4 iterations are sufficient for obtaining the adapted meshes.

We have used NSP1B3 [4] in order to see the nodes of the mesh in a vertical section of the domain. The nodes lie at the points of the little arrows.

The initial and the current boundaries are not homothetical, therefore we can't use the homothetical transformation in order to generate the adapted meshes.

6.5 Applications to a fluid structure interaction problem

A three dimensional fluid structure interaction problem is studied under the following hypotheses: the fluid is incompressible and limited by an elastic structure, the all interior cavity of the structure is filled by the fluid, the structure is thick. A part of the external boundary of the structure is fixed.

We suppose that the structure is governed by the time-dependent linear elasticity equations and the fluid is governed by the time-dependent Stokes equations.

6.5.1 Mathematical model

Under the hypotheses above, a variational formulation is proposed in [9]. The key of this model is a Lagrange multiplier used to treat one of the problem's constraints: the equality of the fluid's and structure's velocities at the contact surface. This Lagrange multiplier has the physical signification of the density of the forces at the contact surface and it permits to decouple the problem. Knowing the density of the forces at the contact surface, we solve independently the fluid's and structure's problems and we obtain the velocity and the pressure of the fluid from the fluid's problem and the displacement and the velocity of the structure from the structure's problem.

The problem is to find the density of the forces at the contact surface such that the fluid's and structure's velocities are equal at the contact surface. The existence and the uniqueness of the solution of this three-dimensional problem are proved in [10].

6.5.2 Numerical aspects

In order to approximate the solution, first we had discretized in time using Finite Difference Method, after that we used Mixed-Hybrid Finite Element Method.

Discrete time problem

The time discretization corresponds to the implicit Euler method for the fluid's problem and Newmark method for the structure's problem.

In [9] it is proved that the time discrete problem is well posed. Also the stability of the semidiscrete algorithm is proved.

Finite Element approximation

In [8] it's presented the choice of the mixed-hybrid finite elements such that the fully discretized problem is well posed.

The numerical procedure proposed in the same work solves at each time step a symmetrical linear system by an iterative method. At each iteration, two decoupled problems are solved: one for the fluid and the other for the structure. The both problems have as control the density of the forces at the contact surface and the iterative method finds the "good" control such that the fluid's and structure's velocities are equal at the contact surface. The iterative method is convergent.

The stability in time of the algorithm is proved, too.

Implementation of the adapted mesh algorithm

Let us suppose that we have solved numerically the coupled fluid structure problem up to the n^{th} time step.

Interpoling the structure velocity computed at the first n time steps, we can obtain the structure displacement at the $(n+1)^{th}$ time step.

Supposing that the all interior cavity of the structure is filled by the fluid, the new shape of the fluid domain is well established by the structure displacement. Now we adapt the initial mesh to the current boundary using the relaxation like algorithm presented in this paper and then we recompute all matrices which depend upon the new mesh of the fluid domain.

The coupled fluid structure problem at the $(n+1)^{th}$ time step was solved using the algorithm presented in [8, p. 116].

The main program calls subroutines from [4] in order to solve the fluid's problem and from [7] in order to solve the structure's problem.

In Appendix B are presented the computed velocities of the coupled fluid structure problem at two different instants. We can see that the algorithm finds the "good" density of the forces at the contact surface such that the fluid's and structure's velocities are equal at the contact surface.

6.6 Appendix A

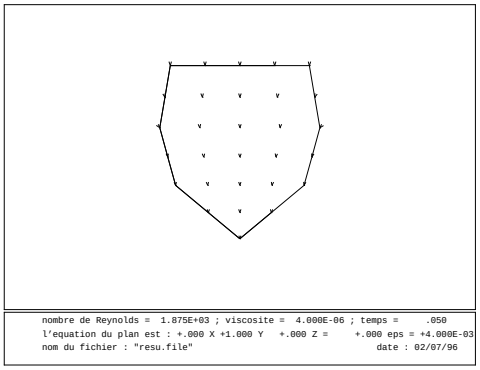

a) A vertical section of the initial mesh

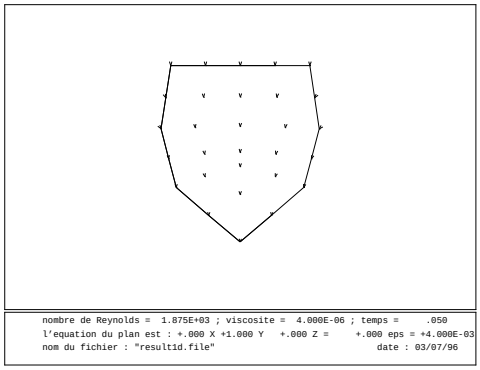

b) Displacements magnitude: 2.2%

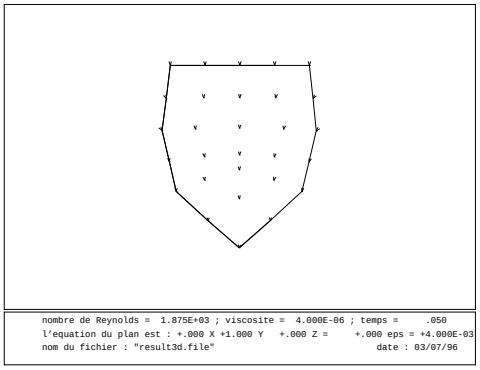

c) Displacements magnitude: 5.5%

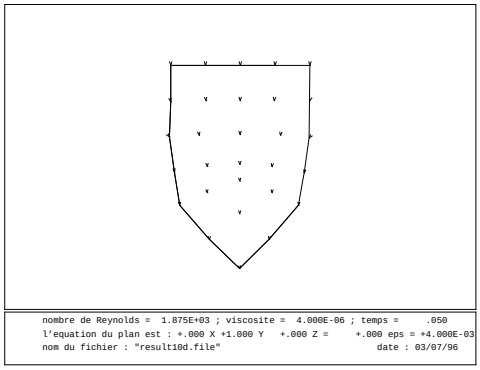

d) Displacements magnitude: 16.5%

Figure 6.1: The initial a) and the adapted meshes b), c), d)

6.7 Appendix B

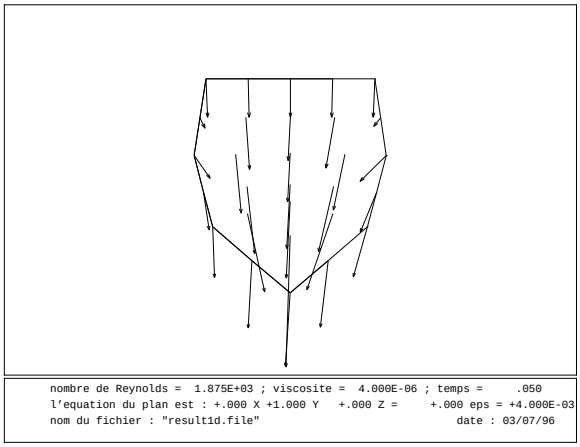

a) Computed fluid velocity

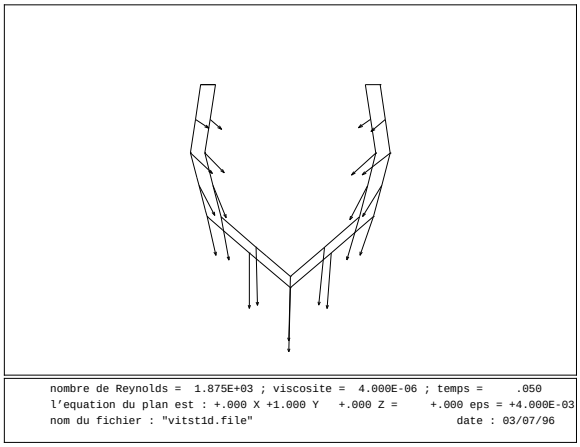

b) Computed structure velocity

Figure 6.2: A coupled fluid structure problem. Magnitude of the displacements: 2.2%

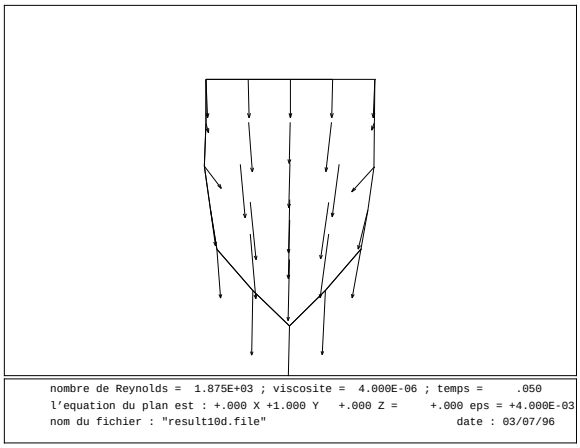

a) Computed fluid velocity

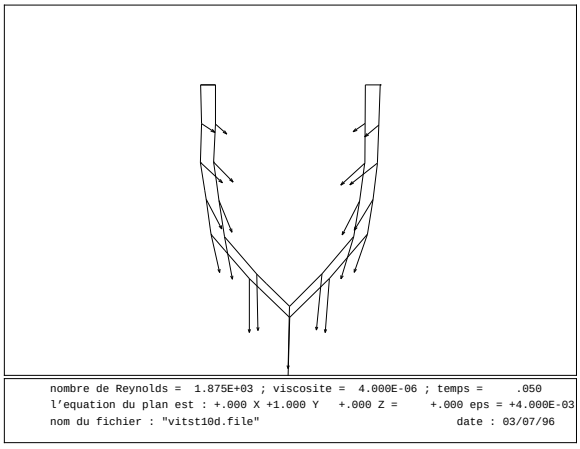

b) Computed structure velocity

Figure 6.3: A coupled fluid structure problem. Magnitude of the displacements: 16.5%

Acknowledgments

The author would like to thank: Prof. Yvon MADAY from the University Paris 6, for his attention to this work and fruitful discussions, Mr. Frederic HECHT, Senior Research Scientist at INRIA, for providing *"NSP1B3: a software to solve 3D incompressible Navier Stokes equations"*, Prof. Olivier PIRONNEAU from the University Paris 6, for giving to the author the possibility to present this work at the Conference *"Optimization Algorithms for Shape Design in Engineering"*, June 24-26, 1996, Orsay, France.

The author expresses his gratitude to the European Science Foundation - Free Boundary Problems Committee for financial support during April-September 1996.

Also, the author would like to thank members of ASCI Laboratory, Orsay for their help.

Bibliography

[1] J.T. BATINA - *Unsteady Euler Airfoil Solutions Using Unstructured Dynamic Meshes*, AIAA Journal, vol. 28, no. 8, pp. 1381-1388, 1990

[2] P.G. CIARLET - *Introduction à l'analyse numérique matricielle et à l'optimisation*, Masson, 1988

[3] P.L. GEORGE - *Génération automatique de maillages, applications aux méthodes d'éléments finis*, Masson, 1991

[4] F. HECHT & C. PARÉS - *NSP1B3 un logiciel pour résoudre les équations de Navier-Stokes incompressible 3D*, Raport de Recherche 1449, INRIA, 1991

[5] P. LASCAUX & R. THEODOR - *Analyse numérique matricielle appliquée à l'art de l'ingineur*, 2e édition, vol. 1, Masson, 1993

[6] P. LE TALLEC, G. GALLICE & C. MARTIN - *Maillages adaptifs pour la résolution numérique des équations de Navier-Stokes*, 25e Congrès National d'Analyse Numérique, Giens, France, 1993

[7] MODULEF 1994 Une bibliothèque modulaire d'éléments finis, BERNADOU (M.), GEORGE (P.L.), HASSIM (A.), JOLY (P.), MULLER (B.), PERRONNET (A.), SALTER (E.), STERR (D.), VANDERBORCK (G.), VIDRASCU (M.)

[8] C.M. MUREA - *Modélisation mathématique et numérique d'un problème tridimensionnel d'interaction entre un fluide incompressible et une structure élastique*, Thèse de doctorat, Université de Franche-Comté, juin 1995

[9] C.M. MUREA & J.-M. CROLET - *A stable algorithm for a fluid structure interaction problem in 3D*, in Contact Mechanics II, Computational Techniques, M.H. Aliabadi & C. Alessandri (eds.), pp. 325-332, Computational Mechanics Publications, Southampton, Boston, 1995

[10] C.M. MUREA & J.-M. CROLET - *Hybrid formulation for a fluid structure interaction problem*, to appear

Chapter 7

Finite element methods for investigating the moving boundary problem in biological development

This chapter is based on the paper:

C.M. Murea, G. Hentschel, Finite element methods for investigating the moving boundary problem in biological development, *Progress in Nonlinear Differential Equations and Their Applications*, Vol. 64, 357–371, Birkhauser Verlag, Basel, 2005

Abstract. We describe two finite element algorithms which can be used to study organogenesis or organ development during biological development. Such growth can often be reduced to a free boundary problem with similarities to two-fluid flow in the presence of surface tension, though material is added at a constant growth rate to the developing organ. We use the specific case of avian limb development to discuss our algorithms.

7.1 Introduction

Biological development involves both growth and changes of form which can often involves free moving boundaries [22]. Such moving boundary problems are similar in some respects to two fluid flow interfaces such as the Hele-Shaw problem with surface tension also called Mullins-Sekerka problem. In general, however, in contrast to incompressible flows, growth due to mitosis and nutrients ensure that material is constantly being added (and sometimes removed when cell death or apoptosis occurs). In addition, specific boundary conditions (in general different for each organ or cell type considered) will result in a more complex boundary value problem than those studied in Hele Shaw cells. In this paper to be specific we shall consider avian limb development, though

we believe that similar finite element algorithms described here will be useful for other problems of organogenesis or organ morphogenesis and biological development.

In this paper we will consider the evolution of two dimensional moving domains. The more realistic but more complex case of three dimensional domains separated by two dimensional interfaces will be described in a future publication. In the case of the avian limb, the ventral-dorsal length scale (back of limb to palm) is normally small compared to the proximal-distal (tip of finger to point at which the limb joins the main body of the organism) or the posterior-anterior distance (from thumb to little finger) and therefore two dimensional simulations are quite informative. In addition, at the developmental stage we are interested in, namely the embryo the whole limb which is only of a millimeter in scale, has approximately the shape of an ellipse with boundary $\Gamma_1(t)$ and a boundary $\Gamma_2(t)$ grafted to the trunk of the organism. In general only the growth velocity of $\Gamma_1(t)$ parallel to the gradient of a pressure, while the growth of $\Gamma_2(t)$ can be described by the motion of the joining vertex with the main trunck (in the more complex three dimensional case this single point becomes a closed one dimensional contour). The pressure in the limb whose gradient describes the rate of growth of the limb is the solution of a Poisson problem with Dirichlet boundary conditions depending on the curvature of the boundary.

In Section 7.2 we give a brief description of some relevant aspects of avian limb development. Then in Section 7.3 we present a mathematical formulation of the resulting free boundary problem.

In Section 7.4 two algorithms are described to solve numerically integrate the resulting equations of motion and find the dynamical evolution of the interface.

In the first algorithm the boundary of the domain is approached by a polygon and the pressure is computed by a Finite Element Method. The computed pressure is a piecewise linear function, globally continuous. The curvature is computed as the inverse of the ray of the circle passing through three consecutive vertices of the boundary. The gradient of the pressure is then computed in a vertex of the mesh, as a weighted mean of the gradients in the neighborhood triangles. For the time discretization, we use the forward finite difference Euler's scheme. A dynamic mesh technique is used in order to generate a triangular mesh at each time step. Starting from the mesh at the precedent time step and knowing the boundary at the current time step, we generate a mesh by redistributing the interior vertices using an optimization algorithm. The number of the interior vertices are constant. Also the connections of all meshes are the same, i.e. if i, j, k are the vertices of a triangle in the mesh at the precedent time step, these points are the vertices of a triangle in the current mesh.

While in the second algorithm, the boundary is approached by cubic spline interpolation which gives a curve twice continuously differentiable. The curvature is computed using the parametrization of the splines. Again at each time step, a new mesh is generated, but this time, the generation of the current mesh is independent from the previous one.

In Section 7.5 we describe the numerical tests of our algorithms. Finally in Section 7.6, we give a brief discussion of the potential of these approaches for studies of organogenesis and biological development.

7.2 Early Avian Limb Development

Early avian limb development presents a beautiful example of organogenesis and biological pattern formation: Well-defined developmental axes exist which need to be understood. Limb growth changes the size and shape of internal domains in which biochemical processes occur. Cartilege formation via mesenchymal cell condensation occurs which will later differentiate into bone and form the skeletal limb. Many of these features appear to be robust: if comparisons are made anatomically with such an apparently different vertabrates as chicken and mouse, it is remarkable the extent to which the gross features of patterning observed during development are conserved by evolution. All of which suggests that universal physical mechanisms controlling development exist.

The embryo produces the raw materials (e.g. proteins, polysaccharides, RNAs) for its development from the available nutrients, according to rules embodied in the genetic code; diffusion, spreading, differential adhesion and chemotaxis transport these materials to specific regions of the organism. The mechanical or chemical changes which may take place in the course of the transport (change of concentration, cell shape, adhesiveness and cohesiveness) are signals that often affect the production of the building material itself, that is, gene activity.

In the course of these events cells differentiate and become more specialized. Differentiation involves regulated gene expression, but elaborate interactions among cells determine where and when new genes are expressed. In addition, morphogenetic changes require coordinated cell movement. The formation of the avian limb requires the establishment of proximal-distal positional gradients and transverse periodic modulations of morphogens to control the formation of individual and multiple parallel skeletal elements. These morphogen patterns act on limb mesenchyme to promote the formation of precartilage condensations, and ultimately the chondrocytes that will give rise to the cartilaginous primordia of the limb skeleton, which ultimately are replaced by bone.

In this paper we wish to investigate only one aspect of this morphogenesis. Namely what type of overall shape is to be expected as a result of growth of the developing embryonic limb. To investigate this problem we consider a minimal model which incorporates the key features of this biological growth. Key is the addition of material at a rate S to the extracellular matrix in which the cells move (more generally the rate of growth will be $S(\mathbf{x}, t)$ as it could be both spatially varying and have a temporal dependence due to genetic switching mechanisms). This means that that the material flow in the limb will obey

$$\nabla \cdot \mathbf{v} = S. \tag{7.1}$$

We treat growth of the limb as due to a creeping flow because of the very low Reynolds numbers involved [8]. Therefore we can expect the flow to obey Darcy's Law

$$\mathbf{v} = -\alpha \nabla p \tag{7.2}$$

where p is a pseudo pressure field, which obeys $\Delta p = -S/\alpha$ in the limb domain.

Finally we need biologically reasonable boundary conditions. As it appear there is no flow of material into the main body of the organism at $\Gamma_2(t)$ we shall take slip boundary condition here

$$\mathbf{v} \cdot \nu = 0, \tag{7.3}$$

where ν is the outer unit normal vector to the boundary, while the elastic properties of the epithelial layer of cells forming the skin layer at $\Gamma_1(t)$ will result a pressure at this boundary obeying

$$p = \gamma \kappa, \tag{7.4}$$

where γ is the effective surface tension of the limb [9] while κ is the limb curvature.

The equation of the normal velocity of the boundary $\Gamma_1(t)$ is

$$V_\nu = \mathbf{v} \cdot \nu. \tag{7.5}$$

The above condition requires that the boundary $\Gamma_1(t)$ moves with the fluid.

It is the integration of this free boundary value problem that we study below. This mathematical model agrees favorably with the analysis presented in [3] based on biological experiments where the limb is considered as a homogeneous and highly hydrated core embedded in an dense envelope.

7.3 The free boundary problem

We study the evolution of a bounded connected open domain $\Omega(t)$ of $\mathbb{R}^2$ with boundary $\partial\Omega(t) = \Gamma_1(t) \cup \Gamma_2(t)$, where $\Gamma_1(t)$ and $\Gamma_2(t)$ are two non empty subsets of $\partial\Omega(t)$. Here $t \geq 0$ is the time. We assume that $\Gamma_1(t)$ is a non closed curve of class $\mathcal{C}^2$ and its ends evolve on the Oy ax. The boundary $\Gamma_2(t)$ is the segment which has the same ends as $\Gamma_1(t)$. Let ν denote the outer unit normal vector to the boundary.

From the equations (7.1)–(7.5), we can eliminate $\mathbf{v}$ and we obtain a system in p only. In the moving domain $\Omega(t)$, we have to find the pressure $p(x, y, t) : \Omega(t) \to \mathbb{R}$, such that

$$\left\{ \begin{array}{rcll} -\Delta p & = & S/\alpha & \text{in } \Omega(t) \\ p & = & \gamma\kappa & \text{on } \Gamma_1(t) \\ \dfrac{\partial p}{\partial \nu} & = & 0 & \text{on } \Gamma_2(t) \end{array} \right. \tag{7.6}$$

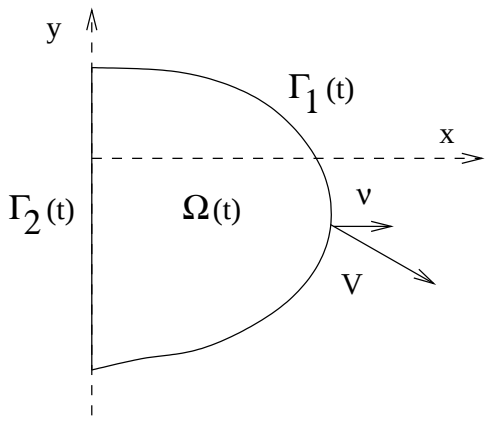

Figure 7.1: Schematic illustration of the free boundary problem

where α, γ, S are positive real constants and κ is the curvature of $\Gamma_1(t)$. We use the sign convention that convex domains have positive curvature of the boundary.

The boundary $\Gamma_1(t)$ evolves according to the law

$$V_\nu = -\alpha \frac{\partial p}{\partial \nu} \tag{7.7}$$

where V_ν is the normal velocity of $\Gamma_1(t)$.

We know the initial domain

$$\Omega(0) = \Omega^0. \tag{7.8}$$

We consider the problem (7.6)–(7.8) of determining the evolution of $\Omega(t)$ and to find the pressure $p(x, y, t)$ for $t \in [0, T]$, where $T > 0$ is a given real constant.

This problem is similar to the Hele-Shaw problem with surface tension, but in our case the pressure is no longer harmonic ($\Delta p \neq 0$).

Let $\overline{p}(x, y, t) = \frac{S}{4\alpha}(x^2 + y^2)$. We set $P = p + \overline{p}$ and we obtain from (7.6)–(7.7) the following problem : in the moving domain $\Omega(t)$, we have to find the pressure $P(x, y, t) : \Omega(t) \to \mathbb{R}$, such that

$$\left\{ \begin{array}{rcll} \Delta P & = & 0 & \text{in } \Omega(t) \\ P & = & \gamma\kappa + \overline{p} & \text{on } \Gamma_1(t) \\ \dfrac{\partial P}{\partial \nu} & = & 0 & \text{on } \Gamma_2(t) \end{array} \right. \tag{7.9}$$

and the normal velocity of the boundary $\Gamma_1(t)$ is

$$V_\nu = -\alpha \left(\frac{\partial P}{\partial \nu} - \frac{\partial \overline{p}}{\partial \nu} \right). \tag{7.10}$$

Though we cannot prove the existence and uniqueness of our solution, the existence and uniqueness of classical solution for the Hele-Shaw with surface tension problem was

proved in [7], suggests that this is the case here also. It is possible that, in order to obtain the existence and uniqueness of solution, we have to prescribe the angles between the boundaries $\Gamma_1(t)$ and $\Gamma_2(t)$. The problem of existence and uniqueness is now under active investigation by G. Simonett.

As it was shown in [12], the shape of the moving domain is determined solely by its normal velocity. In other words, if the velocity of $\Gamma_1(t)$ has the form

$$\mathbf{V} = V_\nu \cdot \nu + V_\tau \cdot \tau$$

where τ is the unit tangent vector to the boundary and V_ν is given by (7.7), then the movement of the domain and the pressure are the same as in the case $V_\tau = 0$. We set $V_\tau = -\alpha\left(\nabla p \cdot \tau\right)$ and then $\mathbf{V} = -\alpha \nabla p$. The advantage of this choice is that we do not need to evaluate the normal vector to the boundary when we compute the velocity of the boundary.

It is convenient to describe the curve $\Gamma_1(t)$ by the parametric coordinates

$$\begin{array}{rcll} x & = & r_1(\theta,t), & \\ y & = & r_2(\theta,t), & \theta \in [a,b]\,. \end{array}$$

Let us introduce the following generalized cylinder:

$$\Omega_T = \bigcup_{t\in]0,T[} \left(\Omega(t) \times \{t\}\right).$$

The problem (7.6), (7.7) and (7.8) is equivalent to the following:
find $r = (r_1, r_2) : [a,b] \times [0,T] \to \mathbb{R}^2$ and $p : \overline{\Omega}_T \to \mathbb{R}$, such that

$$\begin{array}{rcll} \dfrac{\partial r_1}{\partial t}(\theta,t) & = & -\alpha \dfrac{\partial p}{\partial x}\left(r_1(\theta,t), r_2(\theta,t), t\right), & \forall \theta \in [a,b], \forall t \in]0,T[\\ \dfrac{\partial r_2}{\partial t}(\theta,t) & = & -\alpha \dfrac{\partial p}{\partial y}\left(r_1(\theta,t), r_2(\theta,t), t\right), & \forall \theta \in [a,b], \forall t \in]0,T[\\ r(\theta,0) & = & \left(r_1^0(\theta), r_2^0(\theta)\right), & \forall \theta \in [a,b] \end{array}$$

where $r^0 = (r_1^0, r_2^0)$ is a parametric representation of $\Gamma_1(0)$ and $p(x,y,t)$ is the solution of (7.6).

Since $\frac{\partial p}{\partial \nu} = 0$ and $\nu = (-1,0)^T$ on $\Gamma_2(t)$, we have $\frac{\partial p}{\partial x} = 0$ on $\Gamma_2(t)$. If we suppose that $p \in \mathcal{C}^2\left(\Omega(t)\right) \cap \mathcal{C}^1\left(\overline{\Omega}(t)\right)$, we obtain that $\frac{\partial p}{\partial x} = 0$ at the ends of $\Gamma_2(t)$, also

$$\begin{array}{l} \frac{\partial p}{\partial x}\left(r_1(a,t), r_2(a,t), t\right) = 0, \forall t \in]0,T[\\ \frac{\partial p}{\partial x}\left(r_1(b,t), r_2(b,t), t\right) = 0, \forall t \in]0,T[. \end{array}$$

Then $\frac{\partial r_1}{\partial t}(a,t) = \frac{\partial r_1}{\partial t}(b,t) = 0$ and consequently $r_1(a,t) = r_1(b,t) = 0$, $\forall t \in]0,T[$.

The boundary could be parametrized in multiple ways, but the solution must be independent of parametrization.

7.4 Numerical methods

The free boundary problem (7.6)–(7.8) is similar to the Hele-Shaw problem with surface tension also called Mullins-Sekerka problem.

To solve numerically the Hele-Shaw problem with surface tension, there exists an efficient approach named $\theta - L$ introduced in [12]. The variables are the tangent angle θ to the moving boundary and its arc length L. This framework makes the application of an implicit method for time integration easy and it permits to study the problem in a long time interval [13], [4]. In this approach a Fredholm like boundary integral has solved and the integral representation of a harmonic function is used. This is specific to some linear problems with constant coefficients. This method is not appropriate if we replace the linear Darcy's law (7.2) by the non-linear Navier-Stokes equation with a volume source located at a certain point in the domain

$$\rho_0 \left(\frac{\partial \mathbf{v}}{\partial t} + (\mathbf{v} \cdot \nabla) \mathbf{v} \right) - \mu \Delta \mathbf{v} + \nabla p = \mathbf{f} + \frac{\mu}{3} \nabla (\nabla \cdot \mathbf{v})$$

where $\rho_0 > 0$ is the density of the fluid and $\mu > 0$ its viscosity.

A frequented framework used for Navier-Stokes equation in moving domain is Arbitrary Lagrangian Eulerian together with the Finite Element Method [14].

Other approaches are Time-Space Finite Elements [1], Level Set Method [21] and Immersed Boundary Methods [17]. The last one was employed to study the avian limb development in [6]. One of the disadvantage of the continuum models is the complex implementation required to handle the moving boundary of the domain where we have to solve a system of PDEs.

In [15] the software *CompuCell* is presented, where a purely continuum approach for morphogenesis is used in combination with a discrete cellular automata. One of the part of *CompuCell* is based on the cellular Potts model (CMP). A criticism of this formalism is that it neglects simple force balance between cells.

In this paper we present two algorithms which belong to the general framework called "front-tracking methods" [5]. The numerical results were produced for the Darcy's law, but these algorithms could be used for the steady Navier-Stokes equation also.

7.4.1 The first algorithm

For the time discretization, we use the forward finite differences Euler's scheme. We denote by Δt the time step and by $N = T/\Delta t$ the number of time steps. We approximate $\Gamma_1(n\Delta t)$ by a polygonal line Γ_1^n of vertices (x_i^n, y_i^n) for $i = 0, \ldots, M$. We have $x_0^n = x_M^n = 0$, for all n. We denote by Ω^n the polygonal domain bounded by Γ_1^n and the Oy ax. For each vertex (x_i, y_i) of Γ_1^n, we compute the discrete curvature $\kappa^n(x_i, y_i)$ as the inverse of the ray of the circle passing through the three points (x_{i-1}^n, y_{i-1}^n), (x_i^n, y_i^n) and (x_{i+1}^n, y_{i+1}^n).

The problem (7.6) is solved numerically by the Finite Element Method. The computed pressure p^n is approached by P_1 function, globally continuous. We follow [18] for computing the discrete gradient of p^n. Let A be a vertex of Γ_1^n. We denote by $star(A)$ the set of all triangles T of the mesh such that A is a vertex of T. We compute the discrete gradient of p^n at the point A as following:

$$\frac{\sum_{T\in star(A)} Area(T)\cdot \nabla p^n{}_{|T}}{\sum_{T\in star(A)} Area(T)},$$

where $p^n{}_{|T}$ is the linear function representing the restriction of the function p^n on the triangle T.

Algorithm 1

Generate a triangular mesh for Ω^0 using **freefem+** [2].
for each n **from** 0 **to** $N-1$ **do**

Step 1: Compute the discrete curvature $\kappa^n(x_i,y_i)$ at each vertex (x_i,y_i) of Γ_1^n.

Step 2: Compute p^n by the Finite Element Method

$$\begin{cases} -\Delta p^n(x,y) &=& S/\alpha, & \text{in } \Omega^n \\ p^n(x_i,y_i) &=& \gamma\,\kappa^n(x_i,y_i), & \forall\,(x_i,y_i) \text{ vertex of } \Gamma_1^n \\ \dfrac{\partial p^n}{\partial \nu}(x,y) &=& 0, & \text{on } \Gamma_2^n. \end{cases}$$

Step 3: Compute the discrete gradient of p^n at each vertex of Γ_1^n.

Step 4: Compute the vertices of Γ_1^{n+1}

$$\begin{aligned} x_i^{n+1} &= x_i^n - \alpha\Delta t\frac{\partial p^n}{\partial x}(x_i^n,y_i^n) \\ y_i^{n+1} &= y_i^n - \alpha\Delta t\frac{\partial p^n}{\partial y}(x_i^n,y_i^n) \end{aligned}$$

for each vertex $(x_i^n,y_i^n)\in\Gamma_1^n$, $i=0,1,\ldots,M$, then set $x_0^{n+1}=x_M^{n+1}=0$.

Step 5: The boundary Γ_2^{n+1} is the segment of ends $\left(x_M^{n+1},y_M^{n+1}\right)$ and $\left(x_0^{n+1},y_0^{n+1}\right)$.

Step 6: Compute a triangular dynamic mesh for Ω^{n+1}, where $\partial\Omega^{n+1}=\Gamma_1^{n+1}\cup\Gamma_2^{n+1}$ using the algorithm [16].

endfor;

At the **Step 6**, we start from the mesh at the precedent time step and knowing the boundary at the current time step, we generate a mesh by redistributing the interior vertices using an optimization algorithm. The number of the interior vertices are constant. Also, the connections of all meshes are the same, i.e. if i, j, k are the vertices of a triangle in the mesh at the precedent time step, these points are the vertices of a triangle in the current mesh.

7.4.2 The second algorithm

Let (x_i^n, y_i^n) for $i = 0, \ldots, M$ be points on $\Gamma_1(n\Delta t)$. Let $\{a = s_0 < s_1 < \cdots < s_M = b\}$ be a partition of an interval $[a, b]$. We will compute the interpolating cubic spline functions $\Gamma_1^n = \{(x(s), y(s)),\ s \in [a, b]\}$ with the properties:

- $x(s)$ and $y(s)$ are twice continuously differentiable on $[a, b]$,
- $x(s)$ and $y(s)$ coincide on every subinterval $[s_i, s_{i+1}]$, $i = 0, \ldots, M-1$ with polynomials of degree three,
- $x(s_i) = x_i^n$ and $y(s_i) = y_i^n$ for $i = 0, \ldots, M$,
- $x''(a) = x''(b) = 0$ and $y'(a) = y'(b) = 0$.

For the numerical tests, we have chosen $s_i = i$, for $i = 0, \ldots, M$.
In order to prevent the oscilations, we could choose $a = 0$ and

$$s_{i+1} - s_i = \sqrt{\left(x_i^n - x_{i+1}^n\right)^2 + \left(y_i^n - y_{i+1}^n\right)^2}.$$

The curve $(x(s), y(s))$, $s \in [a, b]$ has a continuous curvature given by

$$k(s) = \frac{x'(s)y''(s) - x''(s)y'(s)}{\left((x'(s))^2 + (y'(s))^2\right)^{3/2}}. \tag{7.11}$$

Algorithm 2

Let (x_i^0, y_i^0) for $i = 0, \ldots, M$ be points on $\Gamma_1(0)$.
for each n **from** 0 **to** $N-1$ **do**

Step 1: Compute the cubic spline functions

$$\Gamma_1^n = \{(x(s), y(s)),\ s \in [a, b]\}$$

Step 2: Compute the curvature $\kappa^n(x_i, y_i)$ at each vertex (x_i^n, y_i^n) using (7.11).

Step 3: Generate a triangular mesh for Ω^n using **freefem+** [2], where $\partial\Omega^n = \Gamma_1^n \cup \Gamma_2^n$ and Γ_2^n is the segment of ends (x_M^n, y_M^n) and (x_0^n, y_0^n).

Step 4: Step 5: Step 6: Compute p^n, ∇p^n and (x_i^{n+1}, y_i^{n+1}) as in the Algorithm 1.

endfor;

At he step **Step 3**, the generation of the current mesh is independent from the previous one.

We shall now describe some numerical tests of the efficacy of these algorithms in studies of organogenesis.

7.5 Numerical tests

7.5.1 The initial domain is a semicircle

First let consider the case where the initial domain is a semicircle of ray R_0. Then, if we set the parametric representation of $\Gamma_1(0)$ as

$$\begin{array}{rcl} r_1^0(\theta) & = & R_0\cos(\theta), \\ r_2^0(\theta) & = & R_0\sin(\theta), \end{array} \qquad \theta\in\left[-\frac{\pi}{2},\frac{\pi}{2}\right]$$

the evolution of the boundary $\Gamma_1(t)$ is described by

$$\begin{array}{rcl} r_1(\theta,t) & = & R_0\, e^{\frac{St}{2}}\cos(\theta), \\ r_2(\theta,t) & = & R_0\, e^{\frac{St}{2}}\sin(\theta), \end{array} \qquad \theta\in\left[-\frac{\pi}{2},\frac{\pi}{2}\right],\quad t>0.$$

The pressure has the form

$$p\,(x,y,t)=\frac{S}{4\alpha}\left(R_0^2\,e^{St}-x^2-y^2\right)+\frac{\gamma}{R_0\,e^{\frac{St}{2}}}.$$

The algorithms have been implemented using the programming language C++ and the Finite Element classes of F. Hecht [10]. The numerical results were displayed using `gnuplot`.

The first simulation was performed using the **Algorithm 1** for $R_0=1$, $S=2$, $\gamma=1$, $\alpha=0.5$, $\Delta t=0.05$. The number of time steps is $N=10$.

A dynamic mesh technique is used in order to generate a triangular mesh at each time step. We have used the algorithm described in [16] for the mesh generation. The initial mesh has: 208 vertices, 362 triangles, $M=32$ (the number of vertices on the boundary Γ_1), $h=0.155178$ (the mesh size).

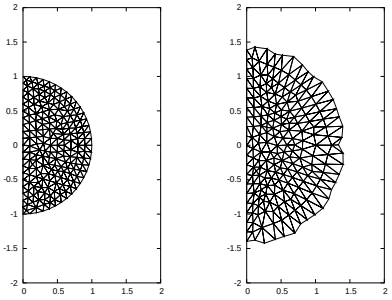

Figure 7.2: The initial mesh (left) and the mesh after 10 time steps (right)

The number of vertices, triangles, boundary edges are the same for the first 10 meshes. In the below table, we see the evolution of the mesh size h.

Time step (n)	1	2	3	4	5
Mesh size (h)	0.155	0.171	0.187	0.202	0.216

Time step (n)	6	7	8	9	10
Mesh size (h)	0.231	0.244	0.256	0.266	0.276

After 10 time steps, the domain might be a semicircle of ray $e^{0.5} \approx 1.648721$.

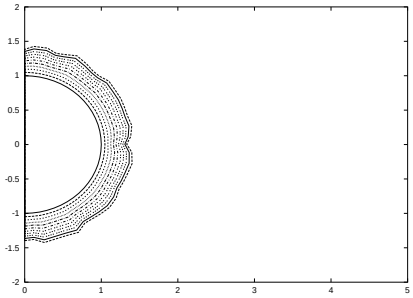

Figure 7.3: The evolution of the moving boundary (0–10 time steps)

The second simulation was performed using the **Algorithm 2** for $\Delta t = 0.0005$ and $N = 1000$ (the number of time steps). The others parameters are the same as in the first simulation.

The software `freefem+` [2] was used to generate a triangular mesh at each time step. The numbers of the vertices and of the triangles are not the same for the all meshes. For example, the mesh after 1000 time steps has 205 vertices and 356 triangles.

After 1000 time steps, the domain might be a semicircle of ray $e^{0.5} \approx 1.648721$.

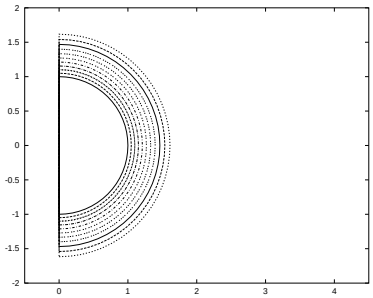

Figure 7.4: The boundary after 0, 100, ..., 1000 time steps

7.5.2 A non-convex initial domain

Let now consider a case when the initial domain is no-convex as in Figure 5. The boundary $\Gamma_1(0)$ has two flat parts on the bottom, on the top and three semicircles of rays $r1 = 0.6$, $r2 = 0.2$ and $r3 = 0.2$ respectively.

The simulations ware performed for: $S = 2$, $\alpha = 0.5$, $\gamma = 0.5$, $\Delta t = 0.0001$ and $N = 180$ (the number of time steps).

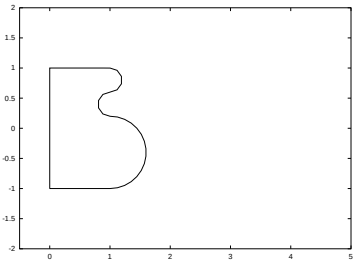

Figure 7.5: The initial domain

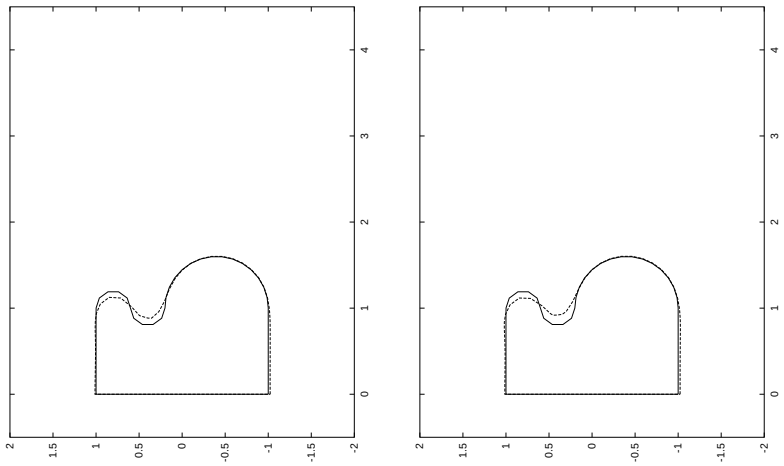

Figure 7.6: The initial (continuous) and the final (dashed) boundaries. Algorithms 1 (left) and 2 (right)

We have observed that the pressure is almost constant near the two flat parts of $\Gamma_1(t)$ and near the largest semicircle. Consequently, these parts of boundary don't move.

We obtain boundary with self-intersection (like the 8) after 182 time steps using the Algorithm 2 and after 230 time steps using the Algorithm 1.

7.5.3 Concluding remarks

The second algorithm is superior to the first one due in principal to a better approximation of the curvature and a better mesh. We can improve the results by moving the boundary along the normal velocity which preserves a reasonable distribution of the vertices on the boundary. The velocity of the boundary could be computed more accurate by using P2 Finite Element for the pressure. Also adapting mesh techniques could be employed for improving the quality of the mesh.

In the first numerical test, we have solved the free boundary problem until time $t = 0.5$ and in the second, until $t = 0.018$.

We have to use implicit in time algorithms in order to study this kind of free boundary problem in a long time interval. The Arbitrary Lagrangian Eulerian framework together with the Finite Element Method will be employed in a future paper. These methods could be employed for the Navier-Stokes equation with surface tension.

7.6 Discussion

The algorithms described above could form the basis for many important investigations of organogenesis and biological development in general. Of course they will need to be extended in several directions to give a quantitative picture of how growth and form develops. Obviously highly computationaly intensive three dimensional simulations are necessary. While genetic switching mechanisms will need to be incorporated in order to understand the temporal properties of biological development. But in addition to these questions many other lines of investigation need to be developed.

For example we know that cell condensation and bone development depend on reaction diffusion mechanisms in a progress zone of undifferentiated cells at the tip of the limb. The size of this progress zone can be expected to have a significant impact on the resulting prepattern created in the limb [19, 20, 11]. This is because even at the most basic level the number of standing waves of a heterogeneous distribution of a chemical species formed by a reaction-diffusion mechanism depends both on the scale of the basic pattern (set by the magnitude of the biological parameters) and on the space available for this pattern to develop (set by the domain size). Thus a very question is how the size of this progress zone changes with time? In order to answer this question studies of limb growth will form a vital ingredient.

Another question involves how the skeletal elements themselves, once formed, would influence growth of the developing limb? Fairly significant changes in internal domain organisation occur between early development when the stylopod and zeugopod are created, and later on when the digits appear. This question will require the development of algorithms for complex connected domains in which the skeletal elements create internal boundaries to growth. In addition, the existence of such internal domains will in turn influence reaction-diffusion mechanisms in the interdigital regions. Such reaction-

diffusion mechanisms might be relevant to properly controlled cell death leading ultimately to digit formation. The influence will be very dependent on the relative scale of the patterning compared to the size of the interdigital domains.

Clearly these algorithms need to be developed in several directions for studies of biological development and these will be reported in future publications.

Acknowledgments

The authors are very grateful to Professor Stuart A. Newman from the New York Medical College whose questions and comments have contributed to improve the contents of this paper.

Bibliography

[1] Bansch E., Finite element discretization of the Navier-Stokes equations with a free capillary surface. *Numer. Math.* **88** (2001) no. 2, 203–235.

[2] Bernardi D., Hecht F., Ohtsuka K., Pironneau O., A finite element software for PDE: freefem+.
`http://www-rocq.inria.fr/Frederic.Hecht`

[3] Borkhvardt V.G., Growth and Shaping of the Fin and Limb Buds. *Russian Journal of Developmental Biology*, **31** (2000) no. 3, 154–161.

[4] Ceniceros H. D., Hou T. Y., Si H., Numerical study of Hele-Shaw flow with suction. *Phys. Fluids* **11** (1999) no. 9, 2471–2486.

[5] Crank J., Free and moving boundary problems. The Clarendon Press, Oxford University Press, New York, 1987.

[6] Dillon R., Othmer H.G., A mathematical Model for outgrowth and spatial pattering of the vertebrate limb bud. *J. Theor. Biol.*, **197** (1999) 295–330.

[7] Escher J., Simonett G., Classical solutions for Hele-Shaw models with surface tension. *Adv. Differential Equations* **2** (1997) no. 4, 619–642.

[8] Forgacs G., Foty R.A., Shafrir Y., Steinberg M.S., Viscoelastic properties of living tissues: a quantitative study. *Biophysical Journal* **74** (1998) 2227–2234.

[9] Foty R.A., Pfleger C.M., Forgacs G., Steinberg M.S., Surface tensions of embryonic tissues predict their mutual envelopment behavior. *Development* **122** (1996) 1611–1620.

[10] Hecht F., C++ et Eléments Finis, Cours DEA, Université Paris VI,
`http://www-rocq.inria.fr/Frederic.Hecht`

[11] Hentschel H.G.E., Glimm T., Glazier J.A., Newman S.A., Dynamical Mechanisms for Skeletal Pattern Formation in the Avian Limb, *Proc Royal Soc B.* **271** (2004) 1713-1722.

[12] Hou T.Y., Lowengrub J.S., Shelley M.J., Removing the stiffness from interfacial flows with surface tension. *J. Comput. Phys.* **114** (1994) 312–328.

[13] Hou T. Y., Lowengrub J. S., Shelley M. J., The long-time motion of vortex sheets with surface tension. *Phys. Fluids* **9** (1997) no. 7, 1933–1954.

[14] Hughes T.J.R., Liu W.K., Zimmermann T.K., Lagrangian-Eulerian finite element formulation for incompressible viscous flows. *Comput. Methods Appl. Mech. Engrg.* **29** (1981) no. 3, 329–349.

[15] Izaguirre J.A., Chaturvedi R., Huang C., Cickovski T., Cof J., Thomas G., Forgac G., Alber M., Hentschel G., Newman S.A., Glazier J.A., COMPUCELL, a multi-model framework for simulation of morphogenesis, *Bioinformatics* **20** (2004) no. 7, 1129–1137.

[16] Murea C.M., Dynamic meshes generation using the relaxation method with applications to fluid-structure interaction problems. *An. Univ. Bucuresti Mat.* **47** (1998) no. 2, 177–186.

[17] Peskin C.S., The immersed boundary method. *Acta Numer.* **11** (2002), 479–517.

[18] Pironneau O., Hecht F., Introduction au Calcul Scientifique en C++, Cours Matrîse de Mathématiques, Ingénierie Mathématique. Université Paris VI, 2000. `http://www-rocq.inria.fr/Frederic.Hecht`

[19] Newman S.A., Frisch H.L., Dynamics of skeletal pattern formation in developing chick limb. *Science* **205** (1979), 662–668.

[20] Newman S.A., Frisch H.L., Percus J.K. On the stationary state analysis of reaction-diffusion mechanisms for biological pattern formation. *J. Theor. Biol.* **134**, (1988) 183–197.

[21] Sethian J. A., *Level set methods: evolving interfaces in geometry, fluid mechanics, computer vision and material science*, Cambridge University Press, 1996.

[22] Wolpert L., Beddington R., Brockes J., Jessell T., Lawrence P., Meyerowitz E., *Principles of Development*. Oxford, New York, Tokyo. Oxford University Press, 1998.

Chapter 8

A Finite Element Method for Growth in Biological Development

This chapter is based on the paper:

C.M. Murea, G. Hentschel, A Finite Element Method for Growth in Biological Development, *Math. Biosci. Eng.* **4** (2007) 2, 339-353

Abstract. We describe finite element simulations of limb growth based on Stokes flow models with a non zero divergence representing growth due to nutrients in the early stages of limb bud development. We introduce a "tissue pressure" whose spatial derivatives yield the growth velocity in the limb and our explicit time advancing algorithm for such tissue flows is described in detail. The limb boundary is approached by spline functions in order to compute the curvature and the unit outward normal vector. At each time step, a mixed-hybrid finite element problem is solved, where the condition that the velocity is strictly normal to the limb boundary is treated by a Lagrange multiplier technique. Numerical results are presented.

8.1 Introduction

The subject of limb development has generated much recent interest in the Biology and Physics communities. The reason for this interest is both because of its importance as an example of well defined organogenesis during embryological development and because the biological and physical process underlying skeletogenesis are still far from clear. Among the many open questions that exist are those related to how the overall limb shape develops. There exits a vast literature on the molecular biology involved in limb development [19], [21], [26], [27], [4], but how this molecular biology translates into patterning and growth is less clear. New experiments, however, suggest that the time is now ripe to investigate computationally how overall limb shape develops during

vertebrate limb growth. As we are dealing with a complex free boundary problem, we will need to develop new algorithmic approaches to biological fluid flows in non convex domains, and this paper is a contribution to this area of biocomplexity. Such work is not only important from a conceptual viewpoint. Its health implications are significant as this research can be expected to impact several pharmacutical and bioengineering technologies.

In Section II we describe the basic biology required to understand how the overall limb develops its complex asymmetric form. This is a rich source of biocomplexity, for concurrent with the development of overall growth and form, internal spatiotemporal distributions of morphogens, activators, inhibitors and associated gene products occur that both depend on and control limb growth and form.

In Section III we describe the types of free boundary problems associated with creeping flows in non convex growing domains that occur during organogenesis. Specifically, in such developing domains, we need to solve for the growth velocity in the limb using a Stokes flow with a non zero divergence representing local nutrients generating the observed growth. We introduce a "tissue pressure" whose gradient yields the growth velocity and calculate the resultant scalar field using biologically plausible boundary conditions including expressions for the tissue pressure at the limb boundary formulated in terms of the instantaneous limb curvature, and the imposition on the internal epithelial surface of the limb the biologically plausible boundary condition that the tangential velocity field is zero. At the boundary joining the limb with the main trunk of the vertebrate embryo we impose a less restrictive slip condition for the growth velocity. The growth rate of the limb is then given by the normal velocity of the fluid at this moving boundary.

In Section IV we describe in detail a new finite element algorithm for studying such flows. Mathematically, several general frameworks for solving Stokes equations in moving domain have been developed. These include the Arbitrary Lagrangian Eulerian together with the Finite Element Method [16], the Level Set Method [25], the Immersed Boundary Method [22], and the Particle Method [5], [17]. The approach we develop here is an explicit time advancing scheme belongs to the framework called "front-tracking methods".

In Section V we apply our algorithm to track the free boundary and internal growth velocity field in both initially semicircular (in the very early vertebrate embryo the limb bud is approximately semicircular, see Figure 8.1), and in non convex domains. Finally we discuss our results in Section VI.

8.2 Biology underlying vertebrate limb development

Studies of limb development involve many interconnected questions from what are the mechanisms controlling overall limb shape to how does internal structure in the growing

limb bud develop. There exits a large literature on the molecular biology involved in limb development [19], [21], [26], [27], [4], but how this molecular biology translates into growth and form is less clear. An examination of limb physiology shows that this is a complex process. Clearly defined axes exist–proximal-distal, anterior-posterior, and dorsal-ventral. Different sizes and shapes for the stylopod (one bone in the upper arm or thigh), zeugopod (two bones in the forearm or calf) and autopod (different numbers of nonidentical segmented digits) are observed in the tetrapod limb. From a computational viewpoint the situation is equally challenging. We need to understand both how the overall limb develops its complex asymmetric form, and concurrent with this process how internal asymmetric spatiotemporal distributions of morphogens, activators, inhibitors and associated gene products result in the skeletal limb forms created by evolution.

Recently there have been new insights into skeletal development. Thus, much recent evidence suggests that the early stages of skeletal pattern formation in the developing vertebrate limb depend on complex dynamics involving several growth factors and differentiation of cells with receptors that allow response to these factors. We have shown that this biology is indeed sufficient to generate the basic patterning of the generic vertebrate limb [14]. Computational work in three dimensions [18], [2] has both confirmed and extended this mechanism [14]. It incorporates a core set of cellular-biochemical processes known to occur in limb bud mesenchyme and is capable of generating both wrist and ankle spot-like elements [1] in addition to the longer stripe-like bone elements.

But nearly all studies described above were carried out in growing rectangular or parallelpiped domains. Real biological development, however, involves both growth and changes of form of free moving boundaries [29]. This is certainly the case of the limb bud (see Figure 8.1).

Therefore in this paper we describe tissue flows and their associated algorithmic implementation that both help shape the embryonic limb and help convect internal morphogens and gene products vital to the development of internal form. As we are concentrating on external epithelial domain grown and form we suppose it can be described mathematically as a free moving boundary problem controlled by internal Stokes flow due to internal tissue growth fed by a continuous source of nutrients $S(\mathbf{x})$. This boundary value problem is similar in some respects to other two-fluid flow interfaces in Hele-Shaw cells with surface tension. Such flows are known to give rise to nontrivial interfacial structure due to the existence of the Mullins-Sekerka instability. More generally they fall into the general category of creeping flows in the presence of moving boundaries. The fact that creeping flows are involved can easily be seen by estimating the associated growth Reynolds number. As the typical length scales in the developing limb are $L \sim 10^{-1} cm$, while typical convective velocites induced by growth are $V \sim 10^{-6} cm/sec$, while the kinematic viscosity of water $\nu \sim 10^{-2} cm^2/sec$, the resulting flows typically have Reynolds numbers in the range $Re = LV/\nu \sim 10^{-5}$. As mesodermal cellular flows will have effective viscosities significantly larger than water, then the Reynolds numbers will be even smaller [8]. Another similarity is that at least in the

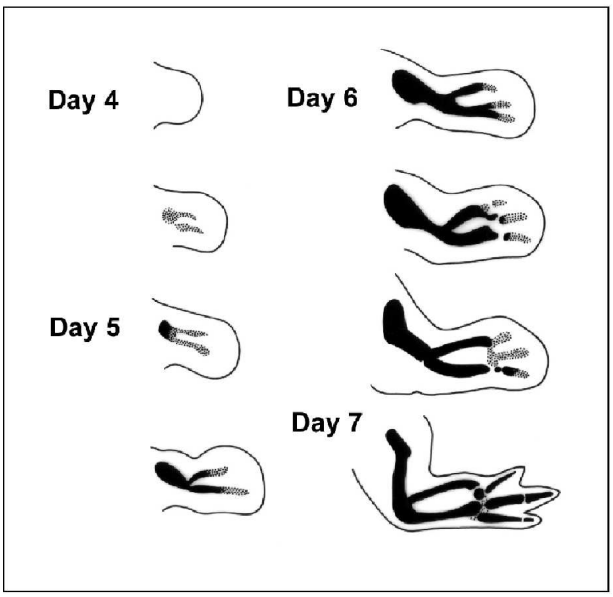

Figure 8.1: A schematic drawing of the early stages of both external and internal growth of the embryonic verebrate limb bud.

first approximation growth is two-dimensional. In the developing limb fibres connect the dorsal and ventral walls of the limb bud [3] leading to two-dimensional flows. Also the phenomenon of convergent extension [28], in which flattened cells tend to develop in the two-dimensional plane defined by the proximal-distal (shoulder to digit tip) and anterior-posterior (thumb to little finger) axes will help justify a growth description in terms of two dimensional flows.

There are, however, several differences from the usually studied incompressible Stokes flows. As mentioned above, growth due to mitosis and nutrients ensure that material is constantly being added (and sometimes removed when cell death or apoptosis occurs). In addition, the surface tension in the developing limb embryo is heterogeneous due to the fact that the epithelial cell layer is weaker near the AER, and consequently boundary conditions will result in a more complex boundary value problem than those studied in Hele Shaw cells.

There exists a previous integration of the influence of growth on form in the context of the avian limb bud [6]. There it was assumed that the flow was a Navier-Stokes flow in the presence of homogeneous boundary conditions. In addition, the growth was assumed to be strongly dependent on the local FGF concentration released by the apical ectodermal ridge (AER) near the tip of the limb bud. More recent evidence suggests, that mitosis and therefore growth is not strongly influenced by the local FGF concentration, but rather its main influence is on cell differentiation.

The need to develop general methods for integrating creeping flows in biology have motivated our search to develop finite element algorithms for creeping flows in the context of avian limb development. We also believe that similar finite element algorithms will be useful in the more general context of organogenesis.

8.3 Mathematical model

8.3.1 The Basic Ingredients

We consider, therefore the following minimal model which incorporates the key features of this biological growth. Addition of material occurs everywhere either at a constant rate S or more generally the rate of growth can be assumed to be $S(\mathbf{x}, t)$ as addition of material could be both spatially varying and have a temporal dependence due to genetic switching mechanisms. This means that that the tissue flow in the limb will include a continuous distribution of sources and therefore obey

$$\nabla \cdot \mathbf{v} = S, \tag{8.1}$$

where $\mathbf{v}$ is the fluid velocity.

We treat growth of the limb as due to a creeping flow because of the very low Reynolds numbers involved [8]. Therefore we can expect the flow to obey the Stokes equation with volume source

$$-\mu \Delta \mathbf{v} + \nabla p = \mathbf{f} + \frac{\mu}{3} \nabla S \tag{8.2}$$

where p is a pseudo pressure field defined by $p = P - p_{air}$, where P is the pressure of the fluid and μ is the viscosity of the fluid.

Finally we need boundary conditions. As it appears there is no flow of material into the main body of the organism we shall take slip boundary conditions at the boundary of the limb connected to the main body

$$\mathbf{v} \cdot \boldsymbol{\nu} = 0, \tag{8.3}$$

where $\boldsymbol{\nu}$ is the outer unit normal vector to the boundary, while the elastic properties of the epithelial layer of cells forming the skin layer will result a pressure at the free growing boundary that obeying

$$p(s) = P(s) - p_{air} = \gamma(s)\kappa(s), \tag{8.4}$$

where $\gamma(s)$ is the effective surface tension of the limb at a point s on the free boundary [9] while $\kappa(s)$ is the limb curvature at point s.

The equation of the normal velocity of the free boundary is

$$V_n(s, t) = \mathbf{v}(s, t) \cdot \boldsymbol{\nu}. \tag{8.5}$$

8.3.2 Detailed Structure of the Dynamics

We now describe in detail the structure of the creeping flow dynamics we wish to integrate. We study the evolution of a bounded connected open domain $\Omega(t)$ of $\mathbb{R}^2$ with boundary $\partial\Omega(t) = \Gamma_1(t) \cup \Gamma_2(t)$, where $\Gamma_1(t)$ and $\Gamma_2(t)$ are two non empty subsets of $\partial\Omega(t)$. Here $t \geq 0$ is the time. We assume that $\Gamma_1(t)$ is a non closed curve of class $\mathcal{C}^2$ and its ends evolve on the Oy axis (see Figure 8.2). The boundary $\Gamma_2(t)$ is the segment which has the same ends as $\Gamma_1(t)$. Let $\boldsymbol{\nu} = (\nu_1, \nu_2)$ denote the unit outward normal vector and by $\boldsymbol{\tau} = (-\nu_2, \nu_1)$ the unit tangential vector to the boundary.

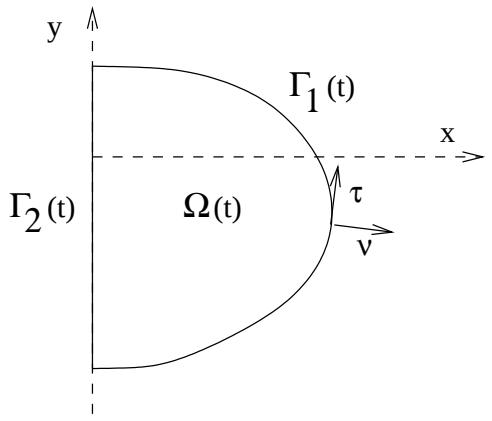

Figure 8.2: Schematic illustration of the free boundary problem

In the moving domain $\Omega(t)$, we have to find:
the velocity $\mathbf{v}(x, y, t) = (v_1(x, y, t), v_2(x, y, t)) : \Omega(t) \to \mathbb{R}^2$
the pressure $p(x, y, t) : \Omega(t) \to \mathbb{R}$ of the fluid, such that

$$-\mu\Delta\mathbf{v} + \nabla p = \mathbf{f} + \frac{\mu}{3}\nabla S, \quad \text{in } \Omega(t) \tag{8.6}$$

$$\nabla \cdot \mathbf{v} = S, \quad \text{in } \Omega(t) \tag{8.7}$$

$$\mathbf{v} \cdot \boldsymbol{\tau} = 0, \quad \text{on } \Gamma_1(t) \tag{8.8}$$

$$p = \gamma\kappa, \quad \text{on } \Gamma_1(t) \tag{8.9}$$

$$\mathbf{v} \cdot \boldsymbol{\nu} = 0, \quad \text{on } \Gamma_2(t) \tag{8.10}$$

$$\frac{\partial v_2}{\partial x} - \frac{\partial v_1}{\partial y} = 0, \quad \text{on } \Gamma_2(t) \tag{8.11}$$

where $\mu > 0$ is the viscosity of the fluid, $\mathbf{f} = (f_1, f_2)$ are the applied volume forces, $S > 0$ is the rate of growth, $\gamma > 0$ is the effective surface tension and κ is the curvature of $\Gamma_1(t)$. We use the sign convention that convex domains have positive curvature of the boundary.

Remark 8.1 *In a previous work [20], we have studied a similar problem, where the fluid velocity was not necessarily normal to the boundary $\Gamma_1(t)$. In [15], it is suggested the importance to prescribe either the normal or the tangential component of the fluid velocity, in order to enforce the stability of the finite element approximations. In the present paper, the fluid velocity is supposed to be normal to the boundary $\Gamma_1(t)$ (see equation (8.8)). Even if the actual assumption concerning the fluid velocity on free boundary is not the most appropriate from the biological point of view [7], this constraint is required by the boundary condition concerning the pressure (8.9).*

The equation (8.11) is a natural boundary condition associated to the essential boundary condition (8.10).

The boundary $\Gamma_1(t)$ evolves according to the law

$$V_\nu = \mathbf{v} \cdot \boldsymbol{\nu} \tag{8.12}$$

where V_ν is the normal velocity of $\Gamma_1(t)$.

The combination of (8.8) and (8.10) requires that the the boundaries $\Gamma_1(t)$ and $\Gamma_2(t)$ are normal at the intersections, more precisely

$$\boldsymbol{\nu}_{|\Gamma_1(t)} \cdot \boldsymbol{\nu}_{|\Gamma_2(t)} = 0, \quad \text{in the two corners} \tag{8.13}$$

where $\boldsymbol{\nu}_{|\Gamma_1(t)}$ and $\boldsymbol{\nu}_{|\Gamma_2(t)}$ are the outer unit normal vectors to $\Gamma_1(t)$ and $\Gamma_2(t)$, respectively. Without this condition, the fluid velocity will not be continuous in the two corners. This requirement is biologically plausible in terms of flow, though of course the boundaries of real limb domains are not exactly normal to each other in geometrically.

We know the initial domain

$$\Omega(0) = \Omega^0. \tag{8.14}$$

We consider the problem (8.6)–(8.14) of determining the evolution of $\Omega(t)$ and to find the velocity $\mathbf{v}(x, y, t)$ and the pressure $p(x, y, t)$ for $t \in [0, T]$, where $T > 0$ is a given real constant.

8.4 The Finite Element Algorithm

We develop a key algorithm to study such creeping flows in the presence of moving boundary conditions.

In order to evaluate the curvature terms, the boundary is approached by cubic spline interpolation which gives a curve twice continuously differentiable. The curvature is computed using the parametrization of the splines.

At each time step, a new mesh is generated, but the generation of the current mesh is independent from the previous one.

To numerically solve these equations we use finite element methods. We introduce for each $t \in [0,T]$ the following Hilbert spaces:

$$\mathbf{W}(t) = \left\{ \mathbf{w} = (w_1, w_2) \in \left(H^1(\Omega(t))\right)^2;\ w_1 = 0 \text{ on } \Gamma_2(t) \right\}, \tag{8.15}$$

$$Q(t) = L^2(\Omega(t)), \tag{8.16}$$

$$\Lambda(t) = H^{1/2}(\Gamma_1(t)) \tag{8.17}$$

The weak form of the problem (8.6)–(8.11) is to find $\mathbf{v}(t) \in \mathbf{W}(t)$, $p(t) \in Q(t)$ and $\omega(t) \in \Lambda(t)$ such that

$$a(\mathbf{v}(t), \mathbf{w}) + b(\mathbf{w}, p(t)) + c(\mathbf{w}, \omega(t)) = \ell(\mathbf{w}),\ \forall \mathbf{w} \in W(t) \tag{8.18}$$

$$b(\mathbf{v}(t), q) = g(q),\ \forall q \in Q(t) \tag{8.19}$$

$$c(\mathbf{v}(t), \lambda) = 0,\ \forall \lambda \in \Lambda(t) \tag{8.20}$$

where

$$a(\mathbf{v}, \mathbf{w}) = \mu \int_{\Omega(t)} \left(\frac{\partial v_2}{\partial x} - \frac{\partial v_1}{\partial y} \right) \left(\frac{\partial w_2}{\partial x} - \frac{\partial w_1}{\partial y} \right) d\mathbf{x} + \mu \int_{\Omega(t)} (\nabla \cdot \mathbf{v})(\nabla \cdot \mathbf{w})\, d\mathbf{x} \tag{8.21}$$

$$b(\mathbf{w}, q) = -\int_{\Omega(t)} (\nabla \cdot \mathbf{w})\, q\, d\mathbf{x} \tag{8.22}$$

$$c(\mathbf{w}, \lambda) = \mu \int_{\Gamma_1(t)} (w_1 \nu_2 - w_2 \nu_1)\, \lambda\, ds \tag{8.23}$$

$$\ell(\mathbf{w}) = \int_{\Omega(t)} \left(\mathbf{f} + \frac{\mu}{3} \nabla S \right) \cdot \mathbf{w}\, d\mathbf{x} + \mu \int_{\Gamma_1(t)} S(\mathbf{w} \cdot \boldsymbol{\nu})\, ds - \int_{\Gamma_1(t)} \gamma \kappa (\mathbf{w} \cdot \boldsymbol{\nu})\, ds \tag{8.24}$$

$$g(q) = -\int_{\Omega(t)} S\, q\, d\mathbf{x} \tag{8.25}$$

Remark 8.2 *Some authors use the notations* $\mathbf{v} \times \boldsymbol{\nu} = v_1 \nu_2 - v_2 \nu_1$ *and* $\nabla \times \mathbf{v} = \frac{\partial v_2}{\partial x} - \frac{\partial v_1}{\partial y}$ *for two dimensional vectors. We have to note that, in this case,* $\mathbf{v} \times \boldsymbol{\nu}$ *and* $\nabla \times \mathbf{v}$ *are scalars, not two dimensional vectors. The bilinear applications (8.21) and (8.23) could be rewritten more concisely as:*

$$a(\mathbf{v}, \mathbf{w}) = \mu \int_{\Omega(t)} (\nabla \times \mathbf{v})(\nabla \times \mathbf{w})\, d\mathbf{x} + \mu \int_{\Omega(t)} (\nabla \cdot \mathbf{v})(\nabla \cdot \mathbf{w})\, d\mathbf{x}$$

$$c(\mathbf{w}, \lambda) = \mu \int_{\Gamma_1(t)} (\mathbf{w} \times \boldsymbol{\nu})\, \lambda\, ds.$$

For the weak form of Stokes equations with Dirichlet boundary condition on the velocity, the standard bilinear form is

$$a(\mathbf{v},\mathbf{w}) = \mu \int_{\Omega(t)} \nabla\mathbf{v} : \nabla\mathbf{w}\, d\mathbf{x}.$$

The boundary condition on the pressure requires the use of the alternative bilinear form (8.21).

From the Green's formula and the following identity

$$\begin{aligned}\int_{\Omega(t)} \nabla\mathbf{v} : \nabla\mathbf{w}\, d\mathbf{x} &= \int_{\Omega(t)} \left(\frac{\partial v_2}{\partial x} - \frac{\partial v_1}{\partial y}\right)\left(\frac{\partial w_2}{\partial x} - \frac{\partial w_1}{\partial y}\right) d\mathbf{x} \\ + \int_{\Omega(t)} (\nabla\cdot\mathbf{v})\,(\nabla\cdot\mathbf{w})\; d\mathbf{x} &+ \int_{\partial\Omega(t)} \left(\frac{\partial v_2}{\partial x} - \frac{\partial v_1}{\partial y}\right)(w_1\nu_2 - w_2\nu_1)\; ds \\ - \int_{\partial\Omega(t)} (\nabla\cdot\mathbf{v})(\mathbf{w}\cdot\mathbf{n})\, ds &+ \int_{\partial\Omega(t)} \frac{\partial\mathbf{v}}{\partial\mathbf{n}}\cdot\mathbf{w}\, ds,\end{aligned}$$

we can prove that if $\mathbf{v}$, p is a strong solution of (8.6)–(8.11), then $\mathbf{v}$, p, $\omega = \nabla\times\mathbf{v}$ is a solution of (8.18)–(8.20).

The system (8.18)–(8.20) is a mixed-hybrid like problem in that the trial spaces $\mathbf{W}(t)$, $Q(t)$ and $\Lambda(t)$ are independent and some trial functions are defined on the physical domain, while other ones are defined only on the boundary. The main advantage of this framework is the treatment of the constraints (8.7) and (8.8) by the Lagrange multiplier technique, consequently, we are not forced to use finite elements which verify (8.7) and (8.8).

The finite element approximation of Stokes equation with boundary condition on the pressure was studied in [23],[24] and [12], but the condition (8.8) was treated in a strong way.

We denote by Δt the time step and by $N = T/\Delta t$ the number of time steps.

We approximate $\Gamma_1(n\Delta t)$ by a polygonal line

$$\Gamma^n_{1,h} = [A^n_0, A^n_1, \ldots, A^n_M]$$

where the vertices A^n_i have the coordinates (x^n_i, y^n_i) for $i = 0,\ldots,M$. It is assumed that $x^n_0 = x^n_M = 0$, for all n which implies that A^n_0 and A^n_M evolve on the Oy axis.

We denote by Ω^n_h the polygonal domain bounded by $\Gamma^n_{1,h}$ and the segment $[A^n_M, A^n_0]$. Let $\mathcal{T}^n_h$ a triangular mesh of Ω^n_h.

For the approximation of the fluid velocity $\mathbf{v}$, we have been used the triangular finite elements $\mathbb{P}_1$ + *bubble* also refereed to as MINI elements introduced by Arnold, Brezzi and Fortin (see the general reference [10]), for the fluid pressure p the triangular finite elements $\mathbb{P}_1$ and for the Lagrange multiplier ω, the segment finite elements $\mathbb{P}_1$.

We denote by $\mathbf{v}^n_h$, p^n_h, ω^n_h the finite element approximation of $\mathbf{v}(n\Delta t)$, $p(n\Delta t)$, $\omega(n\Delta t)$, respectively.

Let $\boldsymbol{\nu}_h^n$ the unit outward normal vector to the boundary $\Gamma_{1,h}^n$, which is constant on each edge $\left[A_i^n, A_{i+1}^n\right]$.

In order to compute in (8.23) the integral term containing $\boldsymbol{\nu}$, we have used the approximation

$$\int_{\Gamma_1(t)} (\mathbf{w} \times \boldsymbol{\nu})\, \lambda\, ds \approx \int_{\Gamma_{1,h}^n} (\mathbf{w}_h^n \times \boldsymbol{\nu}_h^n)\, \lambda_h^n\, ds = \sum_{i=0}^{M-1} \int_{\left[A_i^n, A_{i+1}^n\right]} (\mathbf{w}_h^n \times \boldsymbol{\nu}_h^n)\, \lambda_h^n\, ds.$$

In a similar way, we can approximate in (8.24) the term $\int_{\Gamma_1(t)} S\,(\mathbf{w} \cdot \boldsymbol{\nu})\, ds$.

8.4.1 Treatment of the curvature terms

The treatment of the curvature terms requires particular care. We proceed as follows. Let $\{0 = \xi_0 < \xi_1 < \cdots < \xi_M = L\}$ be a partition of an interval $[0, L]$. We will compute the interpolating cubic spline functions $\mathcal{S}^n = \{(x(\xi), y(\xi)),\ \xi \in [0, L]\}$ with the properties:

- $x(\xi)$ and $y(\xi)$ are twice continuously differentiable on $[0, L]$,
- $x(\xi)$ and $y(\xi)$ coincide on every subinterval $[\xi_i, \xi_{i+1}]$, $i = 0, \ldots, M-1$ with polynomials of degree three,
- $x(\xi_i) = x_i^n$ and $y(\xi_i) = y_i^n$ for $i = 0, \ldots, M$,
- $x''(0) = x''(L) = 0$ and $y'(0) = y'(L) = 0$.

For the numerical tests, we have chosen $h = L/M$, $\xi_i = ih$, for $i = 0, \ldots, M$ and $L = 1$.

We have for $i = 0, \ldots, M-1$

$$x(\xi) = m_i^x \frac{(\xi_{i+1} - \xi)^3}{6h} + m_{i+1}^x \frac{(\xi - \xi_i)^3}{6h} + u_i^x\,(\xi - \xi_i) + v_i^x, \quad \forall \xi \in [\xi_i, \xi_{i+1}]$$

where

$$\begin{aligned} u_i^x &= \left(x_{i+1}^n - x_i^n\right)\frac{1}{h} - \left(m_{i+1}^x - m_i^x\right)\frac{h}{6} \\ v_i^x &= x_i^n - m_i^x \frac{h^2}{6}. \end{aligned}$$

We set $m_0^x = m_M^x = 0$ and $\left(m_1^x, \ldots, m_{M-1}^x\right)$ is the solution of the linear system

$$\begin{pmatrix} 4 & 1 & & & 0 \\ 1 & \ddots & \ddots & & \\ & \ddots & \ddots & \ddots & \\ & & \ddots & \ddots & 1 \\ 0 & & & 1 & 4 \end{pmatrix} \begin{pmatrix} m_1^x \\ \vdots \\ \vdots \\ \vdots \\ m_{M-1}^x \end{pmatrix} = \begin{pmatrix} \frac{6}{h^2}\left(x_0^n - 2x_1^n + x_2^n\right) \\ \vdots \\ \frac{6}{h^2}\left(x_{i-1}^n - 2x_i^n + x_{i+1}^n\right) \\ \vdots \\ \frac{6}{h^2}\left(x_{M-2}^n - 2x_{M-1}^n + x_M^n\right) \end{pmatrix}$$

For $y(\xi)$, we have similar formulas. For $i = 0, \ldots, M-1$

$$y(\xi) = m_i^y \frac{(\xi_{i+1} - \xi)^3}{6h} + m_{i+1}^y \frac{(\xi - \xi_i)^3}{6h} + u_i^y (\xi - \xi_i) + v_i^y, \quad \forall \xi \in [\xi_i, \xi_{i+1}]$$

where

$$\begin{aligned} u_i^y &= \left(y_{i+1}^n - y_i^n\right) \frac{1}{h} - \left(m_{i+1}^y - m_i^y\right) \frac{h}{6} \\ v_i^y &= y_i^n - m_i^y \frac{h^2}{6}. \end{aligned}$$

The linear system to solve is:

$$\begin{pmatrix} 2 & 1 & & & 0 \\ 1 & 4 & \ddots & & \\ & \ddots & \ddots & \ddots & \\ & & \ddots & 4 & 1 \\ 0 & & & 1 & 2 \end{pmatrix} \begin{pmatrix} m_0^y \\ \vdots \\ \vdots \\ \vdots \\ m_M^y \end{pmatrix} = \begin{pmatrix} \frac{6}{h^2}\left(y_1^n - y_0^n\right) \\ \vdots \\ \frac{6}{h^2}\left(y_{i-1}^n - 2y_i^n + y_{i+1}^n\right) \\ \vdots \\ \frac{6}{h^2}\left(y_{M-1}^n - y_M^n\right) \end{pmatrix}$$

The curve $\mathcal{S}^n$ has a continuous curvature given by

$$\kappa(\xi) = \frac{x'(\xi)y''(\xi) - x''(\xi)y'(\xi)}{\left((x'(\xi))^2 + (y'(\xi))^2\right)^{3/2}}. \tag{8.26}$$

In the sequel, $\kappa_i^n = \kappa(\xi_i)$ stands for the curvature in the vertex A_i^n using the spline functions.

In order to compute in (8.24) the integral term containing the curvature, we have used the approximation

$$\int_{\Gamma_1(t)} \gamma\kappa \left(\mathbf{w} \cdot \boldsymbol{\nu}\right) ds \approx \sum_{i=0}^{M-1} \int_{\left[A_i^n, A_{i+1}^n\right]} \gamma\kappa_i^n \left(\mathbf{w}_h \cdot \boldsymbol{\nu}_h^n\right) ds.$$

8.4.2 An explicit time-advancing scheme

From (8.12), a point on the boundary $\Gamma_1(t)$ moves along the normal to the boundary with the velocity $\mathbf{v} \cdot \boldsymbol{\nu}$.

In a previous section, we have introduced $\boldsymbol{\nu}_h^n$ the unit outward normal vector to the boundary $\Gamma_{1,h}^n$, constant on each edge $\left[A_i^n, A_{i+1}^n\right]$, but which is not well defined on the vertices A_i^n.

In order to compute the position of the vertices A_i^{n+1} of the polygonal line $\Gamma_{1,h}^{n+1}$, we will use the normal to the spline function $\mathcal{S}^n$ given by

$$\boldsymbol{\nu}_S^n(\xi) = \frac{1}{\sqrt{(x'(\xi))^2 + (y'(\xi))^2}} \left(y'(\xi), -x'(\xi)\right)^T.$$

More precisely, we set

$$\begin{pmatrix} x_i^{n+1} \\ y_i^{n+1} \end{pmatrix} = \begin{pmatrix} x_i^n \\ y_i^n \end{pmatrix} + \Delta t\, \boldsymbol{\nu}_S^n(\xi_i)\left(\mathbf{v}_h^n(x_i^n, y_i^n) \cdot \boldsymbol{\nu}_S^n(\xi_i)\right) \tag{8.27}$$

which is forward Euler's scheme for the numerical approximation of (8.12).

Algorithm

Let A_i^0 of coordinates (x_i^0, y_i^0), $i = 0, \ldots, M$ be vertices of the polygonal line $\Gamma_{1,h}^0$.

for each n **from** 0 **to** $N-1$ **do**

Step 1 Generate $\mathcal{T}_h^n$ a triangular mesh of Ω_h^n. Knowing the boundary points A_i^n, $i = 0, \ldots, M$, the mesh can be generated automatically, using *FreeFem++* [13].

Step 2 Compute the spline function $\mathcal{S}^n = \{(x(\xi), y(\xi)),\ \xi \in [0,1]\}$ passing throw A_i^n, $i = 0, \ldots, M$. The details were presented in the sub-section **Treatment of the curvature terms**.

Step 3 Compute $\kappa_i^n = \kappa(\xi_i)$ the curvature at each vertex A_i^n using the formula (8.26).

Step 4 Find $\mathbf{v}_h^n$, p_h^n, ω_h^n the finite element solution of (8.18)–(8.20). After the finite element discretization, the problem to solve is a symmetric linear system, not positive defined, of the form

$$\begin{pmatrix} A & B^T & C^T \\ B & 0 & 0 \\ C & 0 & 0 \end{pmatrix} \begin{pmatrix} \mathbf{V}^n \\ \mathbf{P}^n \\ \boldsymbol{\Omega}^n \end{pmatrix} = \begin{pmatrix} \mathbf{L}^n \\ \mathbf{G}^n \\ 0 \end{pmatrix}$$

Step 5 Compute $\boldsymbol{\nu}_S^n$ the unit outward normal vector to the spline function $\mathcal{S}^n$ using the formula

$$\boldsymbol{\nu}_S^n(\xi) = \frac{1}{\sqrt{(x'(\xi))^2 + (y'(\xi))^2}} \left(y'(\xi), -x'(\xi)\right)^T.$$

Step 6 Move the vertices of the boundary using the forward schema (8.27).

endfor;

8.5 Numerical tests

We have tested the algorithm presented in this paper for two kind of geometrical shapes: a semicircle and a non convex domain. The both examples were also discussed in [20] using Darcy's law for the fluid flow, while the actual model is based on the Stokes equations with volume source.

8.5.1 The initial domain is a semicircle

First let consider the academic case where the initial domain is a semicircle of ray R_0. We assume that the rate of growth S, the surface tension γ are constants and we set the applied volume forces $\mathbf{f} = (0, 0)$. Of course, these assumptions are not biological reasonable, but in this case, we know an exact solution of the free boundary problem (8.6)–(8.14).

If we set the parametric representation of $\Gamma_1(0)$ as

$$\left\{x(\theta) = R_0 \cos(\theta),\ y(\theta) = R_0 \sin(\theta), \quad \theta \in \left[-\frac{\pi}{2}, \frac{\pi}{2}\right]\right\},$$

the evolution of the boundary $\Gamma_1(t)$ is described by

$$\left\{x(\theta) = R_0\, e^{\frac{St}{2}} \cos(\theta),\ y(\theta) = R_0\, e^{\frac{St}{2}} \sin(\theta), \quad \theta \in \left[-\frac{\pi}{2}, \frac{\pi}{2}\right]\right\}.$$

The velocity and the pressure have the form

$$\mathbf{v}\,(x, y, t) = (S\,x/2, S\,y/2), \quad p\,(x, y, t) = \frac{\gamma}{R_0\, e^{\frac{St}{2}}}.$$

The algorithm has been implemented using the language *FreeFem++* [13] and the numerical results were displayed using `gnuplot` [11].

The simulation was performed for $R_0 = 1$, $\mu = 1$, $\mathbf{f} = (0, 0)$, $S = 2$, $\gamma = 1$, $T = 0.5$. The time step is $\Delta t = 0.005$ while the number of time steps is $N = 100$.

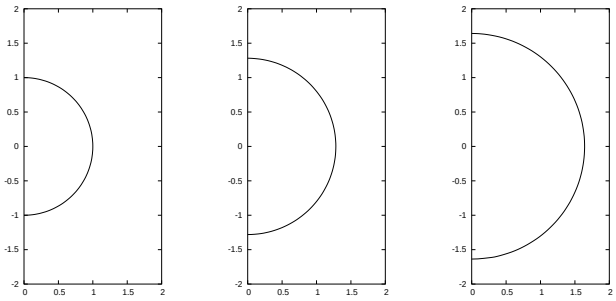

Figure 8.3: Spline approximation of the initial boundary (left), after 50 time steps (middle) and after 100 time steps (right)

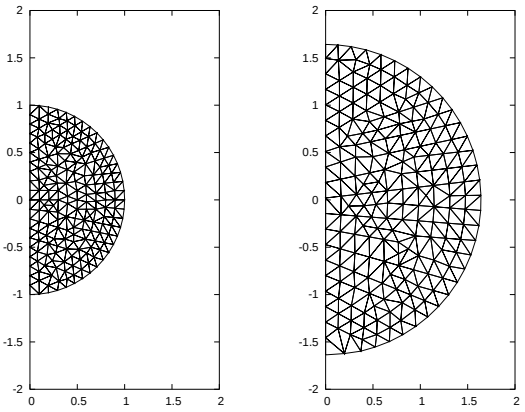

Figure 8.4: The initial mesh (left) and the mesh after 100 time steps (right).

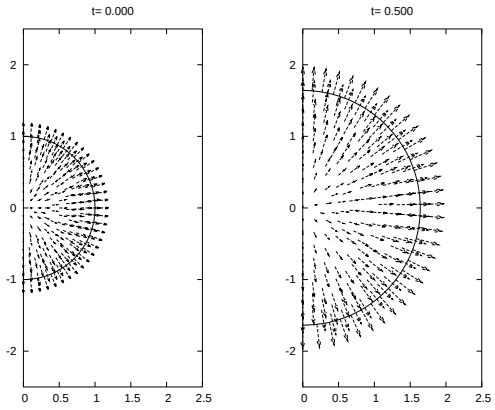

Figure 8.5: The initial velocity (left) and after 100 time steps (right). The scaling factor is 0.2.

At the time instant $t = 0.5$, the domain $\Omega(t)$ might be a semicircle of ray $e^{0.5} \approx 1.648721$. Numericaly, at the time instant $t = N\Delta t = 0.5$, we obtain a semicircle like domain where the ends of the polygonal line $\Gamma_{1,h}^n$ have the coordinates $(0, -1.63703)$ and $(0, 1.64173)$ (see Figure 8.3).

The number of the segments of the polygonal line $\Gamma_{1,h}^n$ is $M = 32$ and the number of edges on the vertical boundary $[A_M^n, A_0^n]$ is 20 for all n.

The initial mesh has 200 vertices, 346 triangles and after 100 time steps we use a mesh of 207 vertices, 360 triangles (see Figure 8.4).

The computed velocity (see Figure 8.5) is radial as the theoretical solution.

8.5.2 A non-convex initial domain

Let now consider a case when the initial domain is non-convex. The boundary $\Gamma_1(0)$ has two flat parts on the bottom, on the top and three semicircles of rays $r1 = 0.6$, $r2 = 0.2$ and $r3 = 0.2$ respectively.

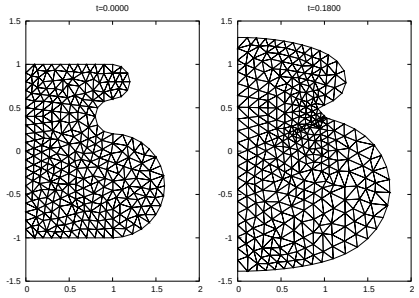

Figure 8.6: The initial mesh (left) and the mesh after 1800 time steps (right).

The simulation was performed for: $\mu = 1$, $\mathbf{f} = (0, 0)$, $S = 2$, $\gamma = 0.5$, $\Delta t = 0.0001$ and $N = 1800$.

The number of the segments of the polygonal line $\Gamma_{1,h}^n$ is $M = 48$ and the number of edges on the vertical boundary $[A_M^n, A_0^n]$ is 20 for all n.

The initial mesh has 302 vertices and 534 triangles (see Figure 8.6). In [20], the flat parts of the boundary $\Gamma_1(0)$ don't move, consequently the growth is only in the Ox direction. As we see in Figures 8.8 and 8.7, the domain growths also along the Oy axis.

In view of Figure 8.8, we can suppose that the domain will evolve to a domain with a cut, while in [20] the same domain seems to evolve to a convex domain.

Using the same time step $\Delta t = 0.0001$, we have performed more than 1800 iterations, while in [20] we have obtained self intersecting moving boundary after 182 iterations.

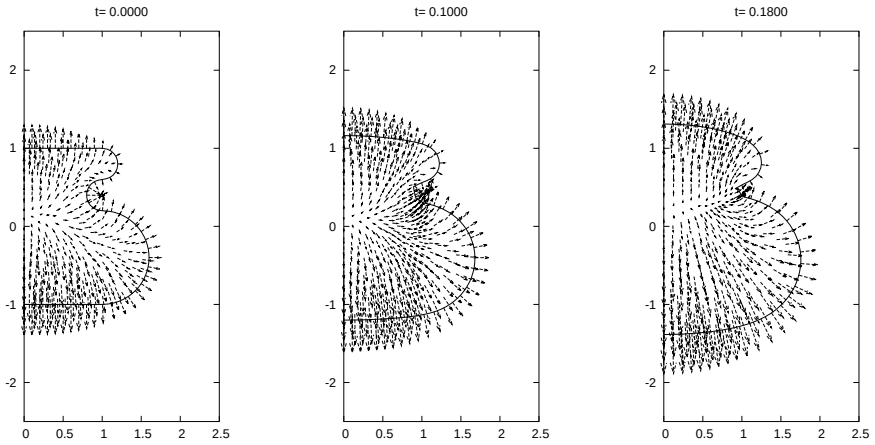

Figure 8.7: The velocity at different time steps. The scaling factor is 0.2.

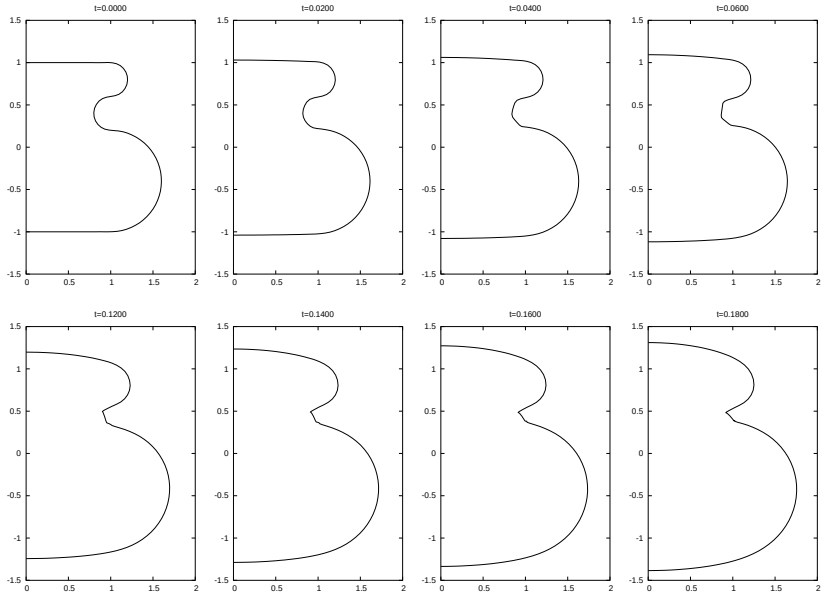

Figure 8.8: Spline approximation of the boundary at different time steps

8.6 Discussion

The finite element algorithm described above contain the basic ingredients required for the study of the development of biological form as a consequence of growth via creeping flows due to nutrient addition to a closed bounded domain surrounded by epithelial cell walls. Perhaps the most interesting results of these simulations can be seen in Figure 8.7. The internal growth velocity field is clearly developed a nontrivial spatial and temporal structure that will effect not only the external shape of the limb bud but also internal processes such as the spatiotemporal distribution of gene products, and consequently the development of internal structure.

Our approach of course represents a minimal model in that it incorporates many crucial biological processes, but at the same time leaves out many critical elements that need to be considered in future algorithms. Such critical elements include internal domains created by skeletal elements that can both channel and hinder fluid flow. Also there exist a core set of cellular-biochemical processes known to occur in limb bud mesenchyme that will further sculpt the developing form of the organism. For example nonuniformly distributed gene products such as Sonic hedgehog and Hox and Wnt proteins, may alter the spatiotemporal distribution of nutrient release $S(\mathbf{x}, t)$ and consequently growth and form with time. This could lead to both positive and negative feedback phenomena with important biological consequence for development.

Finally, of course, explicit three dimensional simulations need to be undertaken in order to investigate how spatially varying surface tension due to heterogeneous epithelial properties effect growth and form. This is more complex algorithmically since in the two dimensional case powerful tools exist that can automatically generate moving meshes when the parametric description of the boundary is provided. We are now studying the three dimensional version of these algorithms and are especially interested in how heterogeneous properties of the epithelial layer will affect growth and form.

We believe, however, that all such considerations can be incorporated into developments of the basic algorithm proposed here and need to be studied further.

Bibliography

[1] M. S. Alber, T. Glimm, H.G.E. Hentschel, B. Kazmierczak, S.A. Newman, Stability of n-dimensional patterns in a generalized Turing system: implications for biological pattern formation, Nonlinearity 18 (2004) 125–138.

[2] K. Aras, T. Cickovski, D. Cieslak, C. Huang, Simulation of Chicken Limb Growth With Irregular Domain Shape, (preprint, 2005)

[3] V.G. Borkhvardt, Growth and Shaping of the Fin and Limb Buds. Russian Journal of Developmental Biology, 31 (2000) no. 3, 154–161.

[4] J. Capdevila, J.C.I. Belmonte, Patterning Mechanisms Controlling Limb Development. Ann. Rev. Cell. Dev. Biol. 17 (2001) 87-132.

[5] G.-H. Cottet, Particle methods for CFD, Lecture notes for Summer school "Advances for CFD for industrial and geophysical turbulence", Autrans, 2003.

[6] R. Dillon, H.G. Othmer, A mathematical model for outgrowth and spatial pattering of the vertebrate limb bud. J. Theor. Biol., 197 (1999) 295–330.

[7] Drossopoulou G, Lewis KE, Sanz-Ezquerro JJ, Nikbakht N, McMahon AP, Hofmann C, Tickle C., A model for anteroposterior patterning of the vertebrate limb based on sequential long- and short-range Shh signalling and Bmp signalling. Development. 127 (7) (2000), 1337-48.

[8] G. Forgacs, R.A. Foty, Y. Shafrir, M.S. Steinberg, Viscoelastic properties of living tissues: a quantitative study. Biophysical Journal 74 (1998) 2227–2234.

[9] R.A. Foty, C.M. Pfleger, G. Forgacs, M.S. Steinberg, Surface tensions of embryonic tissues predict their mutual envelopment behavior. Development 122 (1996) 1611–1620.

[10] V. Girault, P.A. Raviart, Finite Element Methods for Navier-Stokes Equations. Theory and Algorithms, Springer Verlag, 1986.

[11] http://www.gnuplot.org

[12] F. Hecht, C. Pares, NSP1B3 : un logiciel pour resoudre les equations de Navier Stokes incompressible 3D, Rapport de recherche de l'INRIA-Rocquencourt, 1991.

[13] F. Hecht, O. Pironneau, A finite element software for PDE: freefem++, http://www.ann.jussieu.fr/~hecht/freefem++.htm.

[14] H.G.E. Hentschel, T. Glimm, J.A. Glazier, S.A. Newman, Dynamical mechanisms for skeletal pattern formation in the vertebrate limb. Proc. R. Soc. B 271 (2004) 1713–1722.

[15] J.-L. Guermond and L. Quartapelle, On the approximation of the unsteady Navier-Stokes equations by finite element projection methods. Numer. Math. 80 (1998) 207–238.

[16] T.J.R. Hughes, W.K. Liu, T.K. Zimmermann, Lagrangian-Eulerian finite element formulation for incompressible viscous flows. Comput. Methods Appl. Mech. Engrg. 29 (1981) no. 3, 329–349.

[17] S.R. Idelsohn, E. Onate, F. Del Pin, N. Calvo, Fluid-structure interaction using the particle finite element method. Comput. Methods Appl. Mech. Engrg. 195 (2006), no. 17-18, 2100–2123

[18] J.A. Izaguirre, R. Chaturvedi, C. Huang, T. Cickovski, J. Coffland, G. Thomas, G. Forgacs, M. Alber, H.G.E. Hentschel, S.A. Newman, J.A. Glazier, COMPUCELL, a multi-model framework for the simulation of morphogenesis. Bioimformatics 20 (2004) 1129–1137.

[19] F. V. Mariani, G. R. Martin, Deciphering skeletal patterning: clues from the limb. Nature 423 (2003) 319–25.

[20] C.M. Murea, H.G.E. Hentschel, Finite element methods for investigating the moving boundary problem in biological development, in: Progress in Nonlinear Differential Equations and Their Applications, Vol. 64, 357–371, Birkhauser Verlag, Basel, 2005.

[21] S. Newman, J. Tomasek, in: Morphogenesis of connective tissues, Harwood Academic Publishers, Reading, U.K., 1996, pp. 335–369.

[22] C.S. Peskin, The immersed boundary method. Acta Numer. 11 (2002) 479–517.

[23] O. Pironneau, Conditions aux limites sur la pression pour les équations de Stokes et de Navier-Stokes. C. R. Acad. Sci. Paris Sér. I Math. 303 (1986) no. 9, 403–406.

[24] O. Pironneau, Finite element methods for fluids. Translated from the French. John Wiley & Sons, Ltd., Chichester; Masson, Paris, 1989.

[25] J. A. Sethian, Level set methods: evolving interfaces in geometry, fluid mechanics, computer vision and material science, Cambridge University Press, 1996.

[26] C. Tickle, Limb development: an international model for vertabrate pattern formation. Int. J. Dev. Biol. 44 (2000) 101-108.

[27] C. Tickle, Patterning systems-from one end of the limb to the other. Dev. Cell. 4 (2003) 449–58.

[28] M. Zajac, G.L. Jones, J.A. Glazier, Model of Convergent Extension in Animal Morphogenesis, Phys. Rev. Lett. 85 (2000) 2022–2025.

[29] L. Wolpert, R. Beddington, J. Brockes, T. Jessell, P. Lawrence, E. Meyerowitz, Principles of Development. Oxford, New York, Tokyo. Oxford University Press, 1998.

Part III

Annexe

Formation

Fonctions et établissement actuel : Maître de Conférences titulaire, Université de Haute-Alsace, Laboratoire de Mathématiques, Informatique et Applications

Adresse professionnelle : Laboratoire de Mathématiques, Informatique et Applications, Université de Haute-Alsace, 4, rue des Frères Lumière, 68093 MULHOUSE Cedex

Numéro de téléphone : 03.89.33.60.34, fax : 03.89.33.66.53

Adresse électronique : `cornel.murea@uha.fr`

Internet : `http://www.edp.uha.fr/murea/`

Titres universitaires :

• **Doctorat**, Spécialisation : *Mathématiques et Applications*
Titre de la thèse : Modélisation mathématique et numérique d'un problème tridimensionnel d'interaction entre un fluide incompressible et une structure élastique
Date et lieu de soutenance : 28 Juin 1995, Université de Franche-Comté, Besançon
Directeur de thèse : J.M. Crolet, Professeur à l'Université de Franche-Comté
Jury de thèse : M. P. Lesaint - Président du jury, Mme D. Cioranescu - Rapporteur, M. J.M. Thomas - Rapporteur, M. A. Halanay - Examinateur, M. F. Hecht - Examinateur, J.M. Crolet - Directeur de thèse.

• **Diplôme d'Etudes Approfondies** de *Mathématiques et Applications*, Juin 1992, Université de Franche-Comté, France

• **Maîtrise de Mathématiques**, Spécialisation *Informatique*, Novembre 1992, Université de Bucarest, Faculté de Mathématiques, Roumanie, **major** avec la moyenne générale sur cinq années **10/10**

Expérience professionnelle

- à partir de septembre 2000, Université de Haute-Alsace, Laboratoire de Mathématiques et Applications, fonction : Maître de Conférences
- octobre 1999 - août 2000, Université de Franche-Comté, Besançon, Equipe de Mathématiques et Laboratoire de Physique Moléculaire, fonction : Ingénieur de Recherche
- octobre 1996 - septembre 1999, Université de Bucarest, Faculté de Mathématiques, fonction : Assistant
- octobre 1993 - septembre 1996, Université de Bucarest, Faculté de Mathématiques, fonction : Préparateur

Publications dans des revues internationales ou nationales avec comité de lecture

1. C.M. Murea, Sur la convergence d'un algorithme pour la résolution découplée d'un système de type Kuhn-Tucker, *An. Univ. Bucureşti Mat.*, **46** (1997), No. 1, pp. 35–40, Zbl 894.65027

2. C.M. Murea, Dynamic meshes generation using the relaxation method with applications to fluid-structure interaction problems, *An. Univ. Bucureşti Mat.*, **47** (1998), No. 2, pp. 177–186

3. C.M. Murea, Domain decomposition method for a flow through two porous media, *Bull. Math. Soc. Sc. Math. Roumaine*, **41** (1998), No. 4, pp. 257-265, MR1880365 (2002j:65121)

4. C.M. Murea, Optimization of satellite antenna, *An. Univ. Bucureşti Mat.*, **48** (1999), pp. 207–216

5. C.M. Murea, J.-M. Crolet, Formulation hybride pour un problème d'interaction fluide structure, *Rev. Roumaine Mat. Pure App.*, **44** (1999), No. 3, pp. 435–445, MR1839512 (2002d:74021)

6. C.M. Murea, La méthode du lagrangien augmenté pour un problème d'interaction fluide-structure, *Rev. Anal. Numér. Théor. Approx.*, **29** (2002), No. 1, pp. 49–56

7. C.M. Murea, The BFGS algorithm for a nonlinear least squares problem arising from blood flow in arteries, *Comput. Math. Appl.*, **49** (2005), pp. 171–186, MR2123400 (2006b:76084)

8. C.M. Murea, C. Vazquez, Sensitivity and approximation of coupled fluid-structure equations by virtual control method, *Appl. Math. Optim.*, **52** (2005), no. 2, pp. 183–218, MR2157200 (2007a:74032)

9. C.M. Murea, Numerical simulation of a pulsatile flow through a flexible channel, *ESAIM: Math. Model. Numer. Anal.* **40** (2006), no 6, 1101-1125

10. C.M. Murea, G. Hentschel, A Finite Element Method for Growth in Biological Development, *Math. Biosci. Eng.* **4** (2007) 2, 339–353

Toutes les revues où j'ai publié sont indexées par Mathematical Reviews et Zentralblatt fur Mathematik. Les articles 1 respectivement 3, 5, 7, 8, 16 ont fait l'objet d'un rapport en Zentralblatt fur Mathematik respectivement Mathematical Reviews.

Colloques internationaux avec comité de lecture et actes à large diffusion

11. C.M. Murea, J.-M. Crolet, A stable algorithm for a fluid-structure interaction problem in 3D, in *Contact Mechanics II, Computational Techniques*, M.H. Aliabadi, C. Alessandri (eds.), pp. 325–332, Computational Mechanics Publications, Southampton, Boston, 1995

12. C.M. Murea, J.-M. Crolet, Etude d'un problème parabolique avec multiplicateur de Lagrange, *Proceedings of the anual meeting of the Romanian Society of Mathematical Sciences 97*, pp. 237–242, Bucharest, 1998

13. C.M. Murea, J.-M. Crolet, Optimal control approach for a flow in unsaturated porous media, dans *Computational Methods for Flow and Transport in Porous Media*, J.-M. Crolet (ed.), Kluwer Academic Publishers, pp. 107–114, 2000

14. C.M. Murea, Optimal control approach for the fluid-structure interaction problems, *Proceedings of the Fourth European Conference on Elliptic and Parabolic Problems*, Rolduc and Gaeta, 2001, J. Bemelmans et al (eds.), World Scientific Publishing Co. Pte. Ltd., pp. 442–450, 2002

15. C.M. Murea, G. Hentschel, Finite element methods for investigating the moving boundary problem in biological development, *Progress in Nonlinear Differential Equations and Their Applications*, Vol. 64, 357–371, Birkhauser Verlag, Basel, 2005

16. Th. Hangan, C. Murea, Elastic helices, *Rev. Roumaine Mat. Pure App.* **50** (2005), no. 5-6, 527–531, MR2204141 (2006i:58019)

17. C.M. Murea, C. Vazquez, Numerical control of normal velocity by normal stress for interaction between an incompressible fluid and an elastic curved arch, *Proceedings (CDROM) ECCOMAS CFD 2006*, P. Wesseling, E. Onate, J. Périaux (Eds), September 5-8, 2006, Egmond aan Zee, The Netherlands

Rapports de recherche

18. C.M. Murea, Some numerical methods for three-dimensional fluid structure interaction problem with free boundary, *Free Boundary Problems News*, No. 12, pp. 31-32, 1996

19. C.M. Murea, Y. Maday, Existence of an optimal control for a nonlinear fluid-cable interaction problem, Rapport de recherche CEMRACS 96, Interaction fluide-structure, Luminy, 1996

20. C.M. Murea, J.-M. Crolet, Mixed-Hybrid Finite Element for a three-dimensional fluid-structure interaction problem, 2000

Pré-publications

21. I. Mbaye, C. Murea, Numerical procedure with analytic derivative for unsteady fluid-structure interaction

22. I. Mbaye, C. Murea, Approximation par la méthode des moindres carrés d'un problème bidimensionnel stationnaire d'interaction fluide-structure

Logiciels développés

- Logiciel pour résoudre l'interaction Navier-Stokes et poutre en 2D. Langage : freefem++, OpenDx, 2003-2004

- L'approximation par la méthode d'éléments finis d'un problème dans un domaine en mouvement où la vitesse de la frontière dépend de la courbure. Langage : C++ (2002), freefem++ (2005)

- Génération automatique des maillages dynamiques. Langage : C++, 2001

- Un algorithme de type EM pour l'estimation de mélange. Langage : Mathematica, 2001, en collaboration avec Dr. Florin VAIDA de l'Université de Harvard

- Logiciel pour résoudre numérique les équations du câble pour un problème d'interaction fluide câble en 3D. Langage : C/C++, 1996

- Logiciel pour résoudre l'interaction fluide (Navier-Stokes) structure (élasticité linéaire) en 3D. Langage : FORTRAN, 1993-1995

Communications orales à des conférences ou colloques

2006

C.M. Murea, Simulation numérique d'un écoulement pulsatif dans un tube flexible, Séminaire du Laboratoire de Modélisation et Calcul, IMAG, Grenoble, le 12 janvier 2006

C.M. Murea, Simulation numérique des problèmes d'interaction fluide-structure et applications, Journée Mathématiques et Industrie, le 7 avril 2006, Mulhouse

C.M. Murea, C. Vazquez, Numerical control of normal velocity by normal stress for interaction between an incompressible fluid and an elastic curved arch, accepté pour ECCOMAS CFD 2006, September 5-8, 2006, Egmond aan Zee, The Netherlands

C.M. Murea, Numerical approximation of the interaction between a pulsatile incompressible fluid and an elastic wall, accepté pour ECCOMAS CFD 2006, September 5-8, 2006, Egmond aan Zee, The Netherlands

C.M. Murea, Simulation numérique d'une problème d'interaction entre un fluide pulsatif et une structure élastique, séminaire du Laboratoire de Mécanique de Lille, le 12 octobre 2006

C.M. Murea, La Méthode du Lagrangian Augmenté pour un problème d'interaction fluide-structure, colloque Fluides et Structures, 7-8 décembre 2006, Mulhouse

2005

C.M. Murea, Numerical approximation of a pulsatile flow through an flexible pipe, Journées de Metz 2005, Problèmes de valeurs propres et applications, 8 avril 2005, Metz

C.M. Murea, Numerical approximation of a pulsatile flow through an flexible pipe, 2ème Congrès National de Mathématiques Appliquées et Industrielles, 23 - 27 mai 2005, VVF "Lac et Montagne", Evian

C. Murea, Numerical control of normal velocities by normal stress in a fluid-structure interaction problem, exposé dans le cadre du colloque Fluides et structures, 17-18 novembre 2005, Mulhouse

2004

C.M. Murea, Finite element methods for investigating the moving boundary problem in biological development, Journées de Metz 2004, Problèmes à frontières libres, interfaces en mouvement: Méthodes mathématiques, Algorithmes et simulations, Applications, 28-30 avril 2004, Metz

C.M. Murea, The BFGS algorithm for a nonlinear least squares problem arising from blood flow in arteries, 36ème Congrès national d'Analyse Numérique, 31 mai - 4 juin 2004, Obernai, France

C.M. Murea , G. Hentschel, Finite element methods for investigating the moving boundary problem in biological development, Nonlinear Elliptic and Parabolic Problems: A Special Tribute to the Work of Herbert Amann, June 28-30, 2004, Zurich

C.M. Murea, Numerical approximation of a pulsatile flow through an elastic pipe, CEMRACS 2004, 2 aout 2004, Luminy

C.M. Murea, Simulation numérique de l'écoulement sanguine dans les artères, Séminaire Calcul Scientifique - Analyse Numérique, Besancon, le 21 octobre 2004

C.M. Murea, Simulation numérique d'un écoulement pulsatif dans un tube flexible, Workshop Fluides et Structures 18-19 novembre 2004, Mulhouse, France

2003

C.M. Murea, Fluid structure interaction with a reduced number of parameters, Applied Mathematics and Applications of Mathematics, February 10-13, 2003, Nice

C.M. Murea, Numerical method for a two dimensional steady incompressible fluid - beam interaction, Journées de Metz 2003, Développements récents de la Méthode des Eléments Finis, Analyse, Mise en oeuvre, Applications, 02-04 avril 2003, Metz

C. Murea, Sensitivity and approximation of fluid-structure equations coupled by virtual control method, Workshop on Fluid-structure coupled problems and nonlinear Partial Differential Equations, October 9-10, 2003, Mulhouse

C. Murea, Sensitivity and approximation of fluid-structure equations coupled by virtual control method, Seminaire Département de Mathématiques Metz, 6 novembre 2003

2002

C.M. Murea , G. Hentschel, Finite element approximation of a moving boundary problem with curvature dependent speed, Free Boundary Problems: Theory and Applications, Trento, Italy, June 4-9

2001

C.M. Murea - *Optimal control approach for the fluid-structure interaction problems*, The Fourth European Conference on Elliptic and Parabolic Problems: Theory-Applications, Gaeta, Italy, 24-28 septembre 2001

Dans le cadre du groupe de travail Mathématiques Appliquées, Laboratoire de Mathématiques et Applications, Université de Haute-Alsace, j'ai exposé 5 fois sur les sujets :

- Interaction fluide - structure,
- L'approximation d'un problème dans un domaine en mouvement où la vitesse de la frontière dépend de la courbure,
- Un algorithme de type EM pour l'estimation de mélange.

2000

C.M. Murea - *Modèle de type contrôle optimal pour des problèmes aux frontières libres*, Séminaire du Laboratoire de Mathématiques, Université de Haute-Alsace, Mulhouse, 21 janvier 2000

C.M. Murea - *Modélisation mathématique et numérique des écoulements externes*, Séminaire du Laboratoire de Mathématiques, Université de Franche-Comté, Besançon, 27 janvier 2000

C.M. Murea - *Modèle de type contrôle optimal pour des problèmes aux frontières libres*, Séminaire du Laboratoire de Modélisation et Calcul, IMAG, Grenoble, 17 février 2000

1998

C.M. Murea, P. Mader - *Optimization of satellite antenna*, Journées ASCI, Université Paris Sud, Orsay, France, 23-27 février 1998

C.M. Murea, Y. Maday - *Existence of an optimal control for a nonlinear fluid-cable interaction problem*, Workshop on *Control of Fluids and Structures*, Institute "Henri Poincaré", Paris, France, March 9-13, 1998

C.M. Murea, C. Vázquez Cendón - *Shape Sensitivity of the Stokes Equations. Application to the Fluid-Structure Interaction Problems*, Workshop on *Control of Fluids and Structures*, Institute "Henri Poincaré", Paris, France, March 9-13, 1998

C.M. Murea - *Algorithms for MinMax problems. Applications to the satellite antenna*, Conference of the Faculty of Mathematics, University of Bucharest, Romania, May 8-9, 1998

C.M. Murea - *Sensitivity Analysis for a variational system with shape prameter*, Conference on "Ordered Topological Linear Spaces", Sinaia, Romania, June 16-18, 1998

C.M. Murea, J.-M. Crolet - *Mixed-Hybrid Finite Element for a three-dimensional fluid-structure interaction problem*, Conference in "Computational Mechanics and Numerical Methods", Miskolc, Hungary, August 24-27, 1998

C.M. Murea - *La méthode du lagrangien augmenté pour un problème d'interaction fluide-structure*, The 4th Franco-Romanian Conference in Mathematics, Metz, France, August 31 - September 4, 1998

C.M. Murea, J.-M. Crolet - *Optimal control approach for a flow in unsaturated porous media*, International Symposium on Computer Methods for Engineering in Porous Media. Flow and Transport, Giens, France, Sept. 28 - Oct. 2, 1998

C.M. Murea, C. Vázquez - *Computation of the gradient for a nonlinear fluid-structure interaction problem*, Conference at the University La Coruña, Spain, Decembre 11, 1998

C.M. Murea - *Optimization of satellite antenna*, Conference at the University La Coruña, Spain, Decembre 18, 1998

1997

C.M. Murea, Y. Maday - *Existence of an optimal control for a nonlinear fluid-cable interaction problem*, Journées ASCI, Université Paris Sud, 4-7 mars 1997, Orsay, France

C.M. Murea, G. Abdoulaev - *Approximation of a 3D nonlinear fluid-cable interaction problem via partitioned procedures*, Journées ASCI, Université Paris Sud, 4-7 mars 1997, Orsay, France

C.M. Murea - *La méthode du lagrangien augmenté pour un problème d'interaction fluide-structure*, Conference of the Romanian Society of Operational Recherche, May 9-10, 1997, Bucharest, Romania

C.M. Murea, J.-M. Crolet - *Etude d'un problème parabolique avec multiplicateur de Lagrange*, The annual meeting of the Romanian Society of Mathematical Sciences, May 29 - June 1, 1997, Bucharest, Romania

C.M. Murea - *Optimal control approach for the fluid-structure interaction problems*, International Congress on *Free Boundary Problems, Theory and Applications*, June 8-14, 1997, Herakleion, Crete, Greece

C.M. Murea, P. Mader - *Optimization of satellite antenna*, CEMRACS 97 on *Shape Optimization*, August 28, 1997, C.I.R.M. Luminy, France

C.M. Murea - *Optimal allocation of the resources in the Romanian Army*, Conference on *Modelling and Simulation in the Romanian Army*, November 27-28, 1997, Military Academy, Bucharest, Romania

C.M. Murea - *Optimal control approach for the fluid-structure interaction problems*, Conference at the University La Coruna, Department of Mathematics, Spain, December 2, 1997

C.M. Murea - *Mixed-Hybrid Methods for fluid-structure interaction problems*, Conference at the University La Coruna, Dept. of Mathematics, Spain, December 2, 1997

1996

C.M. Murea - *Modélisation mathématique et numérique d'une interaction 3D fluide structure*, Séminaire du Laboratoire Applications Scientifiques pour le Calcul Intensif, CNRS UPR 9029, 18 avril 1996, Université Paris Sud, Orsay, France

C.M. Murea - *Dynamic meshes generation using the relaxation method with applications to fluid-structure interaction problems*, International Workshop on *Optimal Algorithms for Shape Design In Engineering*, June 24-26, 1996, Laboratoiry ASCI, University Paris Sud, Orsay, France

C.M. Murea, J.-M. Crolet - *Formulation hybride pour un problème d'interaction fluide structure*, 3ème Colloque franco-roumain de Mathématiques, 23-27 sept. 1996, Cluj-Napoca, Roumanie

C.M. Murea, Y. Maday- *Some numerical methods for three-dimensional fluid structure interaction problem with free boundary*, 3ème Colloque franco-roumain de Mathématiques, 23-27 sept. 1996, Cluj-Napoca, Roumanie

C.M. Murea - *Design optimal et problèmes aux frontières libres*, 28-30 novembre. 1996, Session de communications de la Faculté de Mathématiques, Université de Bucarest, Roumanie

1995

C.M. Murea, J.-M. Crolet - *A stable algorithm for a fluid-structure interaction problem in 3D*, The Second International Conference in Contact Mechanics, July 11-13, 1995, Ferrara, Italy

C.M. Murea - *Uzawa like algorithm for a fluid structure interaction problem*, ECMI Workshop on Applied Mathematics and Industrial Problems, September 14-16, 1995, Romanian Academy, Bucharest, Romania

C.M. Murea - *Modélisation mathématique et numérique du coeur humain*, The 18th Romanian Conference in Medical Informatics, 3-5 novembre. 1995, l'Académie Roumaine, Bucarest, Roumanie

1994

C.M. Murea, J.-M. Crolet - *Etude d'un problème d'interaction fluide incompressible-structure élastique*, 2ème Colloque franco-roumain de Mathématiques Pures et Appliquées, 2-6 mai 1994, E.N.S. Rue d'Ulm, Paris, France

C.M. Murea, V. Preda - *Présentation d'un algorithme d'adaptation des maillages pour les domaines en mouvement*, Session spéciale de l'Académie Roumaine, 25 novembre. 1994, Bucarest, Roumanie

1993

C.M. Murea - *Utilisation des multiplicateurs de Lagrange dans les problèmes d'optimisation infiniment dimensionnels*, Session de communications de la Faculté de Mathématiques, Université de Bucarest, 15-17 novembre. 1993, Bucarest, Roumanie

Animation scientifique

- Co-organisateur du colloque : Fluides et structures, 7-8 décembre 2006, Mulhouse, *Conférenciers* : V. Milisik, F. Flori, C. Murea, B. Di Martino.
- Co-organisateur du colloque : Fluides et structures, Applications en biomécanique, 17-18 novembre 2005, Mulhouse *Conférenciers* : Z. Belhachimi, B. Mauroy, E. Maitre, S. Akesbi, C. Murea, N. Dos Santos, M. Belhadj.
- Co-organisateur du colloque : Fluides et structures, 18-19 novembre 2004, Mulhouse *Conférenciers* : Benoit Roman, Miguel Fernandez, Fabio Nobile, Adel Blouza, Laurent Dumas, Cornel Murea, Mohamed Belhadj.
- Co-organisateur du colloque : Fluid-structure coupled problems and nonlinear Partial Differential Equations, 9-10 octobre 2003, Mulhouse *Conférenciers* : E. Maitre, C. Grandmont, S. Piperno, J.-F. Gerbeau, J. Cagnol, C. Murea.
- J'ai fait un exposé dans le cadre de la formation continue des professeurs de l'enseignement secondaire. "A la rencontre des mathématiques", le 25 janvier 2006, Mulhouse
- J'ai fait des exposés en avril 2006 et 2005 pour les élèves du Lycée Jeanne d'Arc, Mulhouse sur le métier d'enseignant-chercheur.

Rayonnement

- Rapporteur *Mathematical Reviews* depuis novembre 2005
- Rapporteur pour un article soumis au *Numerische Mathematik* en 2004
- Invitation dans des conférences : Mathematics and Applications in Biology and Medicine, 2 août 2004, Luminy et "Professeur invité" à l'Université La Coruña, Espagne, décembre 1998
- "Chairman" de session au European Simposium of Vascular Biomaterials, 13-15 décembre 2003
- "Chairman" de la session *Flow control and optimization*, European Conference on the Computational fluid Dynamics, September 5-8, 2006, Egmond aan Zee, The Netherlands
- Membre CSE Sections 25-26, Université de Haute-Alsace
- Prime d'encadrement doctorale à partir d'octobre 2006

Encadrement

Nom du diplomé : M. Ibrahima MBAYE, Diplome : thèse, Titre : Étude mathématique et numérique de quelques problèmes d'interaction fluide structure.
Date début : le 15 novembre 2002, date fin : le 20 juin 2006
Nom et % officiel de co-directeurs : C. Murea (50%) et S. Akesbi (50%)

Nom du diplomé : M. Thomas BELAT. Mémoire en M1 Pro Mathématiques, Titre : Poutre mince soumise à des efforts de flexion,
Date début : novembre 2005, date fin : juin 2006

Nom du diplomé : M. Souibou SY, bourse de l'Université de Haute-Alsace, Diplome : thèse, Sujet : Résolution numérique des problèmes d'interaction fluide-structure.
Date début : octobre 2006
Nom et % officiel de co-directeurs : C. Murea (80%) et B. Brighi (20%)

Activités administratives

- Membre du Conseil d'Administration du Laboratoire de Mathématiques, Informatique et Applications (LMIA), Mulhouse
- Responsable du reseau informatiques du LMIA
- Responsable des achats : fournitures et équipement informatique pour le LMIA.
- Responsable du site web du LMIA.